Study Program for

Canadian Domestic Communications Satellite

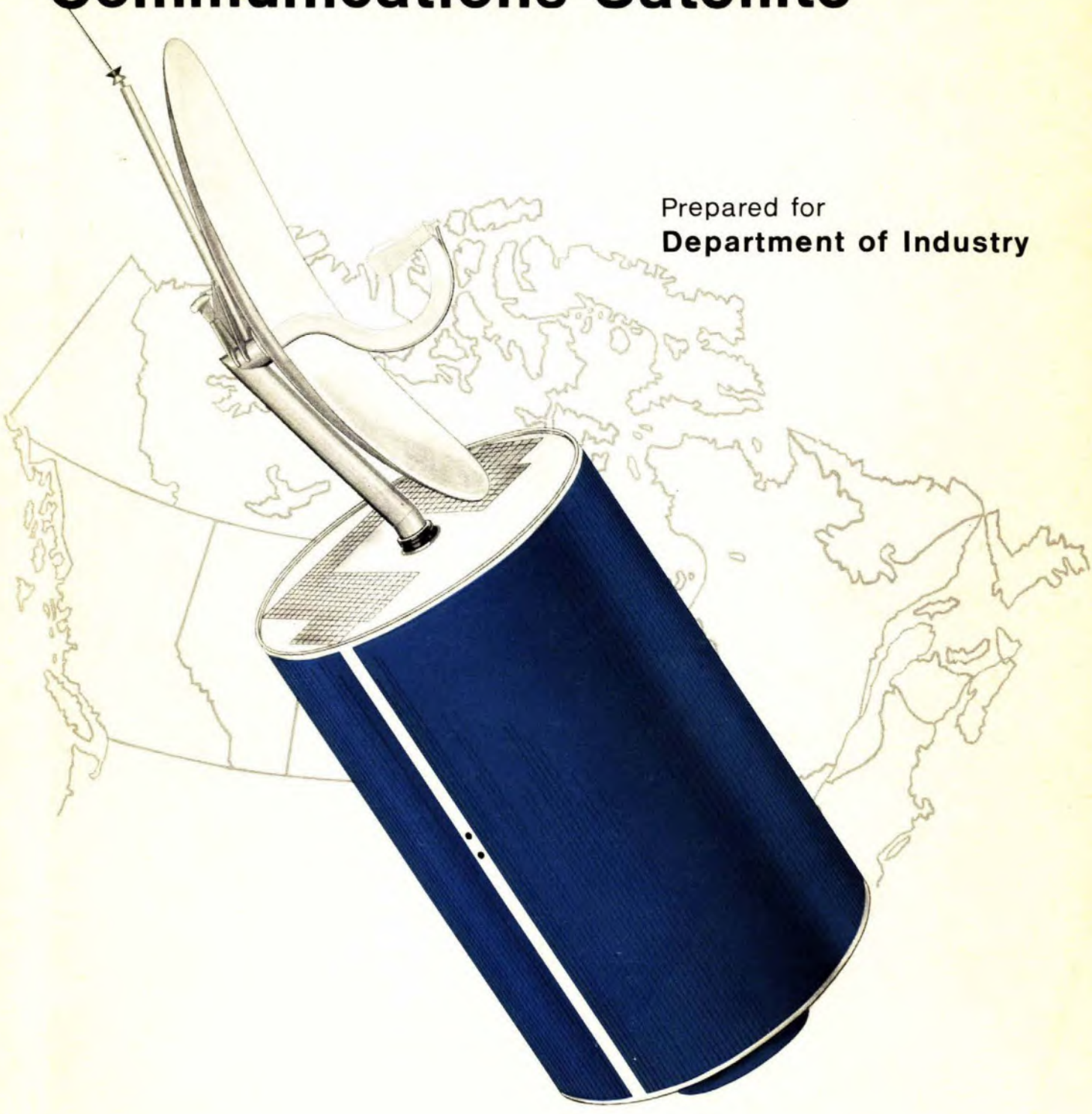

Prepared for
Department of Industry

Final Report
Volume Two - Part One - Spacecraft Design - Electrical

RCA Space Systems

Copy No. 46

STUDY PROGRAM

for the

DESIGN, DEVELOPMENT AND SUPPLY

of a

DOMESTIC SATELLITE COMMUNICATIONS SYSTEM

FINAL REPORT
VOLUME 2a, SPACECRAFT DESIGN, ELECTRICAL

Prepared for

DEPARTMENT OF INDUSTRY

by

RCA LIMITED, Space Systems
1001 Lenoir Street, Montreal

PROPOSITION No. 2220-I

NOVEMBER 25th, 1968

PREFACE

This report is submitted by RCA Limited to the Department of Industry in compliance with Section 4.2 of the Statement of Work forming part of D.O.I. Contract, File No. IRA. 9122-03-4.

The report is in six volumes, namely:

Volume 1	Design Considerations
Volume 2(a)	Spacecraft Design - Electrical
Volume 2(b)	Spacecraft Design - Mechanical
Volume 3	Technical Appendices
Volume 4	Program Plan
Volume 5	Program Costs

The information contained in the report is supplied to Her Majesty for use solely in connection with the design, development, manufacture, operation, repair, maintenance and testing of a Canadian Domestic Satellite Communication System.

1. TRANSPONDER

1.1 INTRODUCTION

The transponder, for the purpose of this report, is defined as the electronics package which accepts signals from the rotary joint in the frequency band 5925 - 6425 MHz and delivers amplified signals to the rotary joint in the frequency band 3900 - 4200 MHz. It therefore excludes components associated with the antenna, viz, the polarizer, the orthogonal coupler or the duplexer and the rotary joint itself.

The transponder consists basically of an amplifying chain with some means of translating the 6 gHz band to the 4 gHz band. With the proposed scheme the transponder amplifies only the communications signals and is devoid of any function in the command and telemetry area.

1.2 MINIMUM INPUT CARRIER & FLUX DENSITY

The uplink carrier to noise temperature or C/T ratios were calculated in Vol.1 S.1-3 on the basis of an idealized noise budget and provide the C/T required at the input of the transponder. The system is proposed to operate in Mode 'B', requiring a medium gain - medium level transponder. Assuming an effective noise temperature for the satellite to be about 1830°K, composed of an antenna contribution of 290°K and a transponder noise figure of 8 dB, the power received per carrier can be computed.

Type of Service	C/T dBW/°K	Carrier (T=1830°K) dBW	Flux Density at Satellite Antenna: Beam Center dBW/M^2	Flux Density at Satellite Antenna: Beam Edge dBW/M^2
60 channels	-135.1	-102.5	-95.7	-91.1
600 channels	-123.2	- 90.6	-83.8	-79.2
1200 channels	-121.5	- 88.9	-82.9	-77.5
1500 channels	-117.6	- 85.0	-78.2	-73.6
TV	-125.0	- 92.4	-85.6	-81.0

The last two columns give the r.f. flux density required to produce the minimum carrier power and are based on an effective antenna gain of 30.4 dB and 25.8 dB at beam center and edge respectively. The antenna gain is referred to the output of the rotary joint in the spinning section and is computed at 6.175 MHz.

1.3 THE INTERMOD PROBLEM INMULTICARRIER OPERATION

The complexity of transponder design depends on how early in the amplifier chain the carriers have to be separated. This is related to the mode of system operation (Figure 1-1)since each mode imposes a different penalty in terms of increase in intermod noise.

To help understand this problem, Figure 1-1 has been drawn up to indicate the relative increase in intermodulation products for the five modes of operation discussed in the Volume 1. The multicarrier wideband portion of the transponder is treated here as a unit. The discussion is quite general and is independent of the internal configuration of the transponder. The simplest mode (E) utilizing a high but fixed gain transponder is used as reference. A lower but fixed gain transponder (Mode D) would have a larger C/T at the input and require a correspondingly larger C/I to maintain the ratio of thermal to intermod noise. By controlling the gain within the wideband section, the penalty in intermod can be held low.

In mixed traffic modes requiring variable gain transponders, the amount of intermod generated is controlled by the larger carriers. This leads to a small C/I ratio for the smaller carriers used for TV traffic.

The increase in intermod is a function of the number of large carriers present and of the difference in level of the carriers as shown in Figure 1-2. For example a transponder designed to operate in Mode A has to be able to accomodate a 30 lb. increase in intermod in the presence of 4 telephone carriers relative to the intermod level produced if the transponder was used for TV traffic only.

To reduce the burden on the transponder, it is possible to tradeoff either the range of carrier levels at transponder input or the number of large carriers. The former is tied in closely with the Earth Station G/T ratios and transmitter powers while the latter depends on the utilization of the Satellite Communications System.

For the purpose of this report, it is assumed that the system will operate in mode (B) and that the maximum number of large telephone message carriers will be restricted to three (3). Since the telephone carriers are more sensitive to intermod, a scheme in which the larger amounts of intermodulation do not fall on the telephone carriers is used. This scheme allows the location of one or two telephone carriers anywhere in the band but excludes alternate or adjacent channel allocations when three large carriers are present. This scheme permits the use of 14 out of 20 possible combinations of 3 carriers located in 6 channels.

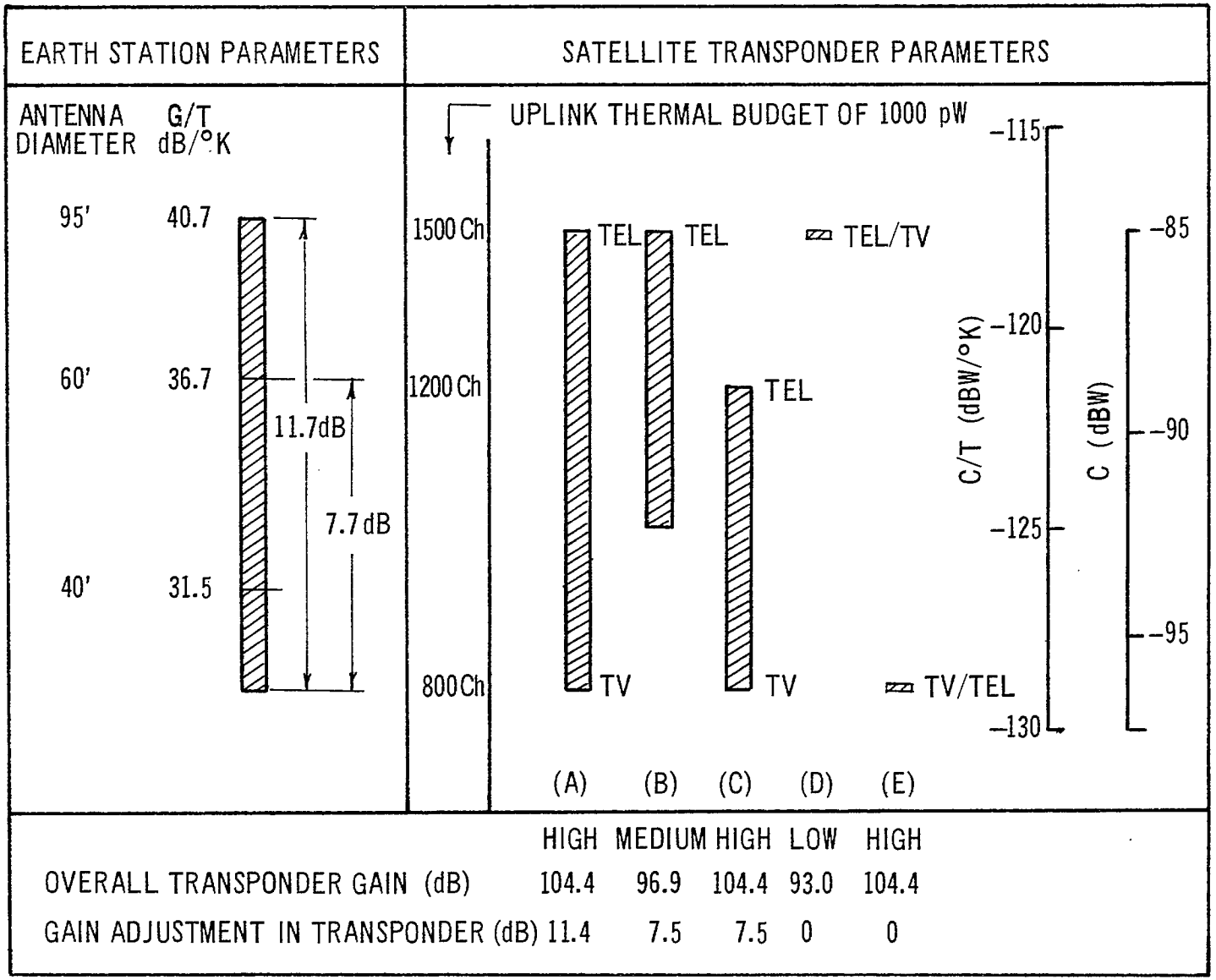

Figure 1-1 Modes of Satellite Communication Operation

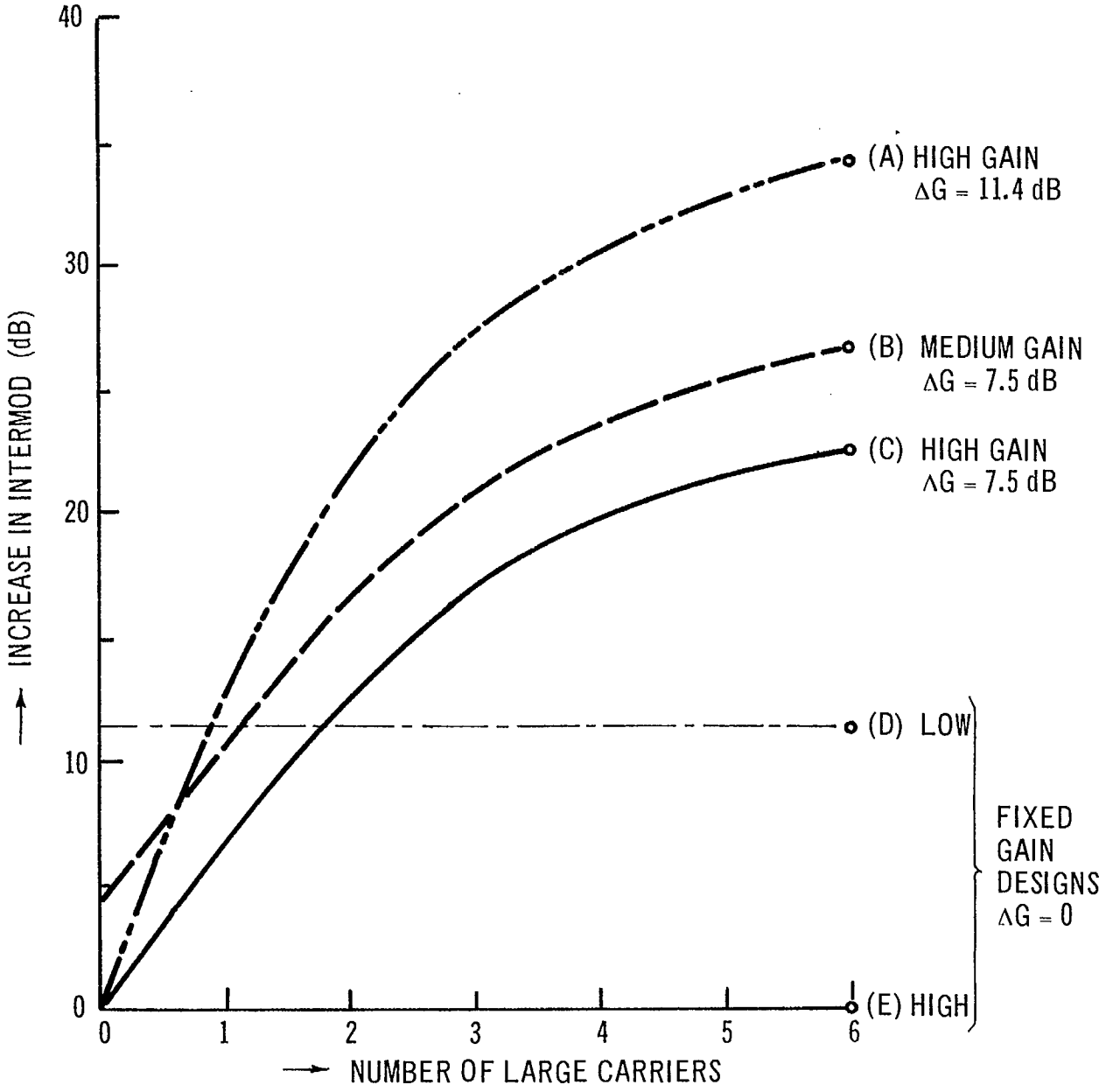

x = Ratio of large to small carrier level in dB

Figure 1–2 Intermod Requirements

1.4 MULTICARRIER OPERATION WITHIN A SINGLE CHANNEL

One of the RF channels will be utilized for Northern communications. Up to six small carriers each one loaded with a maximum of 60 telephone messages can be handled by one transponder. The output TWT is backed off 2.7 dB for this operation leaving 1.5 dBW (1.4W) per carrier. This corresponds to a beam edge ERP of 26.5 dBW. The carrier to total intermod products level will exceed 15 dB for six equispaced carriers. Since only 27 MH_Z out of the total of 36 MH_Z BW is occupied a certain amount of flexibility, in spacing the carriers to avoid intermodulation products, is retained.

1.5 SELECTION OF PREAMPLIFIER

A Tunnel Diode Amplifier (TDA) has been chosen as the preamplifier for its low noise capability and its essential simplicity. A noise figure of 5 dB can be achieved with a 6 gHz TDA. The TDA therefore bridges the gap between the very low noise parametric amplifiers (NF: 1-3 dB) and transistors when they become available.

The need to keep the level of intermod level small forces low level operation of the preamplifier section. The subsequent amplying devices therefore contribute substantially to the overall transponder noise figure, and no large advantage is associated with the use of a first amplifier with the lowest noise figure.

1.6 TRANSPONDER OUTPUT

The output capability of the transponder may also be derived from system considerations. Based on tradeoff studies described elsewhere it appears that an antenna with beamwidths of 8.5° East-West and 3.25° North-South and an effective beam-edge gain of approximately 26 to 27 dB will be used. The effective gain, which is adjusted for the losses in the antenna circuitry and the rotary joint, is referred to the bottom end of the latter.

Assuming that the ERP directed towards the beam edge stations will be +34 dBW, the output of the transponder will have to be +8 dBW (ERP-gain) maximum. The circuit loss between the final amplifier of the transponder and the input to the antenna would be approximately 1.2 dB consisting mostly of the output multiplexer loss. The final amplifier output would therefore have to be +9 dBW or 8 watts.

Selection of Output Amplifier

The main criteria for the selection of the output amplifier is the DC to RF power conversion efficiency. The obvious condidate therefore is a Travelling Wave Tube (TWT) amplifier which has an overall efficiency of about 28% including power supply and other losses. Space qualified TWT's with 8 watts output and a saturated gain of 42-48 dB are available.

1.7 INTERSTAGE AMPLIFICATION RF vs IF

With a broadband TDA as the 6 gHz multicarrier amplifier and a saturated TWT as the 4 gHz single carrier output amplifier, there are three functions to be performed by the interstage amplifiers.

i) translating the 6 gHz band to the 4 gHz band
ii) separation of the 36 MHz wide channels for individual amplification by the TWT output stage
iii) additional amplification

All three functions can be provided with either a scheme utilizing Intermediate Frequency (IF) amplifiers or with RF amplifiers as shown in Figure 1-3.

The main advantage of the IF scheme is that amplification is easily available and hence losses in the branching network are of no consequence. As a result filters with very steep skirt selectivities can be built in reasonable volume and weight. The same applies to group delay and loss equalizers. The disadvantages are that a high IF (> 500 MHz) has to be used if preselection at 6 gHz is to be avoided, the number of local oscillator sources is large, and most important of all a high level upconvertor is needed to provide sufficient drive for the output TWT. This creates a serious spurious and intermodulation problem.

The main advantage of the RF scheme is its simplicity and a lower parts count and the requirement of a single translating L.O. source. Wideband amplifiers are also easily available. The main disadvantage is the size and weight of the branching network, this being dictated by the amount of loss which can be tolerated.

1.8 DRIVERS FOR THE POWER AMPLIFIERS

Three types of drivers were considered.

i) Tunnel Diode Limiter-Amplifiers (TDLA):
An overdriven TDA acts as a saturating amplifier and can be made to deliver outputs of the order of -10 dBM. With

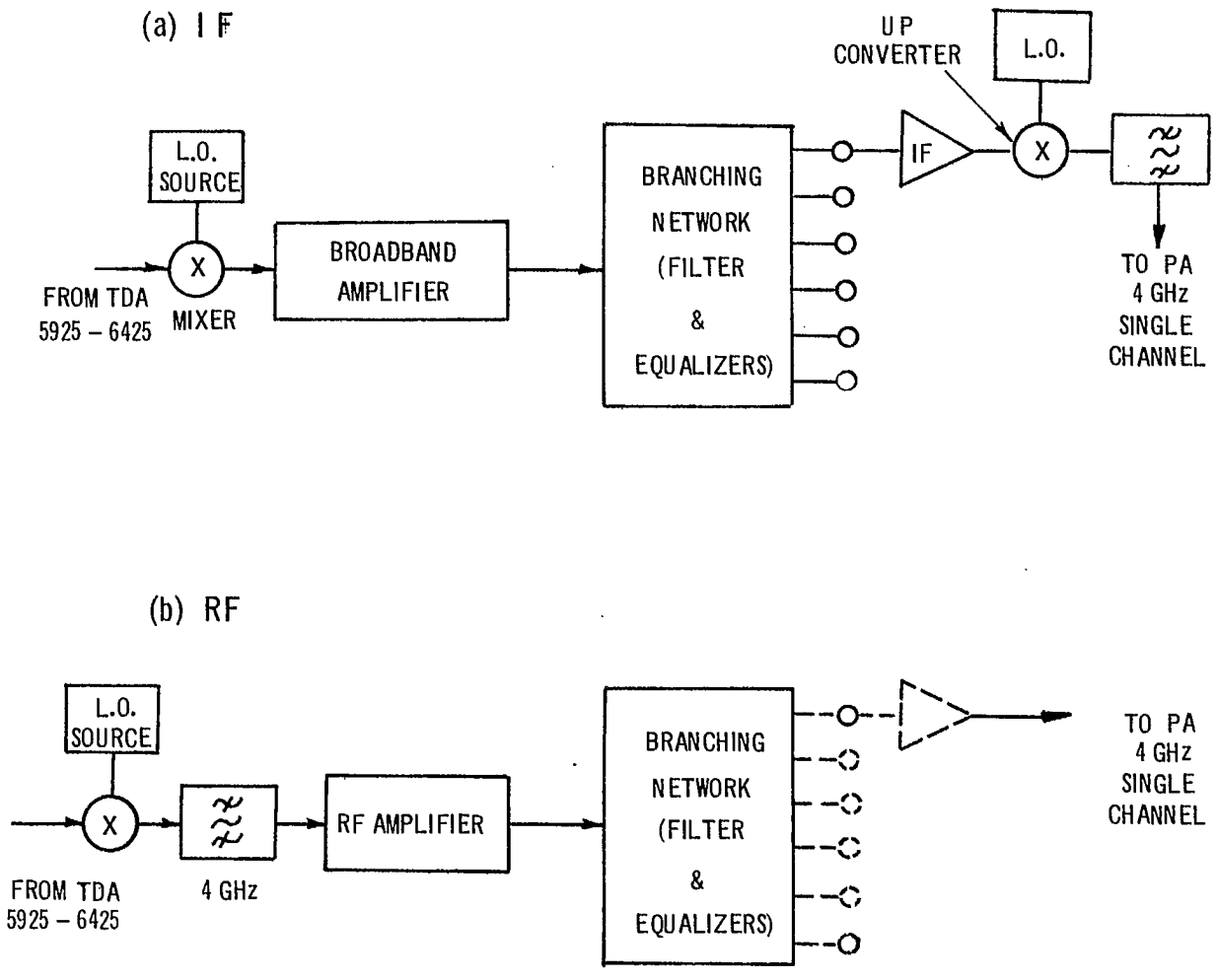

Figure 1-3 Interstage Amplification

balanced configurations and better diodes this output limit can perhaps be raised a few dB. The use of TDLA's would therefore require i) increase in the power amplifier gain and ii) separate drivers for each PA. TDAL's are only suitable for channels dedicated to single carrier operation (e.g. trunk message) and hence would not be suitable for a mixed traffic satellite.

ii) Transistor Amplifiers:

The transistor amplifiers appear very attractive as drivers because of their wide dynamic range - low noise figures combined with high outputs - and the inherent wide bandwidths. They would be ideal to bridge the gap between the usable TDA outputs (-20 to -30 dBM) and the required drive level for PA's. An added advantage could be increased reliability associated with solid state circuits and an overall reduction in amplifier - power supply weight.

Presently the commercially available transistor amplifiers (class A, linear operation) have an output of +5 dBM and a top frequency of 3.5 gHz. During this study discussions were held with the manufacturers of these units. Most of the development effort in this area has been confined to low noise figure-wideband devices. In our particular requirement, on the other hand, a higher noise figure and a 500 MHz band centered on 3.95 gHz would suffice. At least one manufacturer felt hopeful that a 20 dB gain amplifier with a noise figure of 15 - 17 dB with a restricted bandwidth could be produced for evaluation.

Insufficient data on electrical performance and on reliability have forced us to exclude the transistor amplifier as the first choice. However, further evaluation on a development model will be carried out.

iii) TWT Driver Amplifiers:

TWT amplifiers, with noise figures of 20 - 23 dB and saturated outputs of 100 to 500 mw , suitable for driver applications are available in space qualified configurations. The main disadvantages of the TWT amplifiers are the weight and the generation of intermodulation products. Intermodulation problems can be avoided either by the use of a larger power tube for multicarrier wideband operation or by the use of two or more drivers with suitable channel selection.

A weight vs number of TWT drivers trade off curve has been generated (Figure 1-4). It includes the weight of the branching

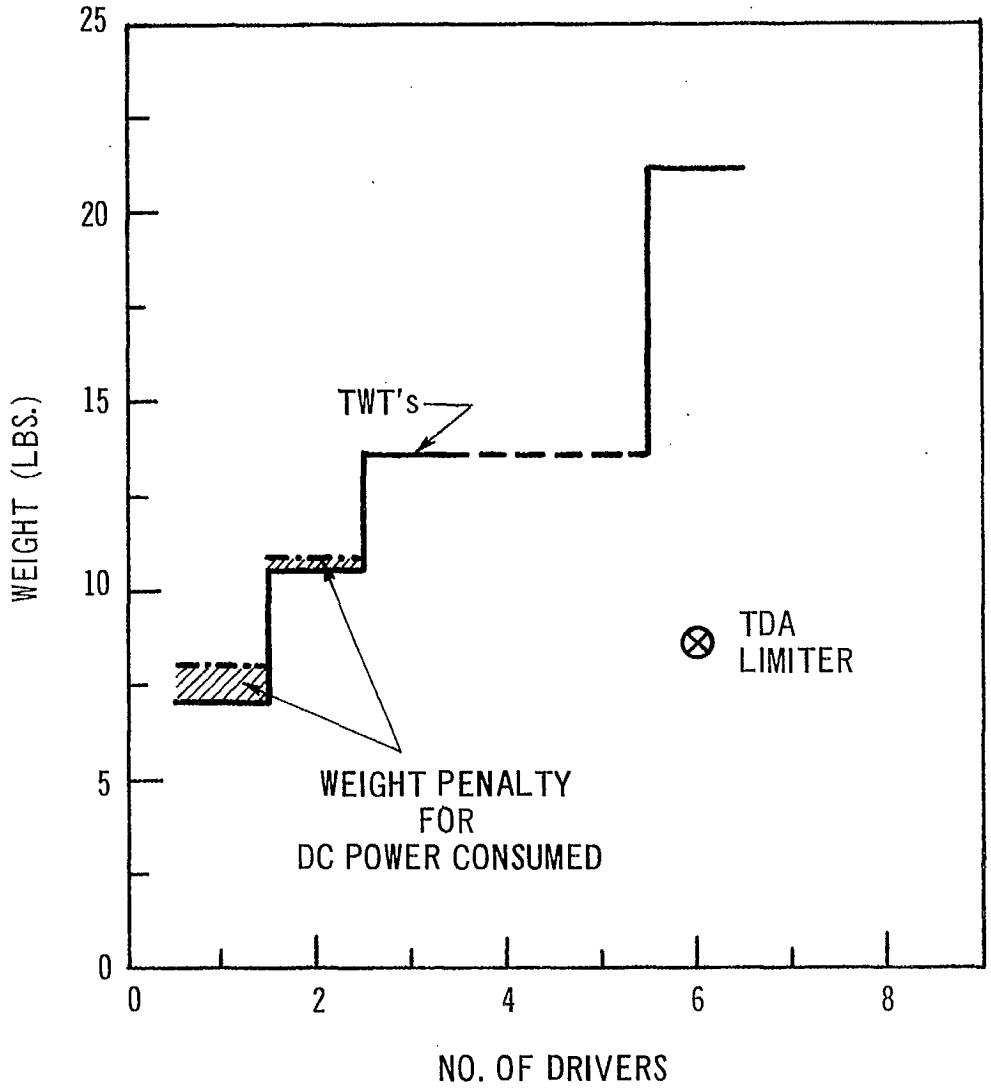

Figure 1–4 Weight Tradeoff for Driver Stage + Branching Networks

network required for that configuration, the weight of the TWT power - supply(s), but not the redundant drivers. The weight trade-off also includes a penalty for DC power consumption. Individual TDAL's are also indicated on the diagram for 6 driver configuration as a comparison.

The trade-off indicates that the single driver configuration is the least weight solution.

1.9 OVERALL TRANSPONDER DESIGN

Amplifier Chain

The proposed transponder, shown in Figure 1-5, utilizes redundant wide-band amplifying chains up to the output stage. The output stage consists of an individual travelling wave tube (TWT) power amplifier for each of the six channels used in the satellite.

Redundancy at the output stage is provided by a one spare for two active amplifier arrangement. The spare amplifier can be switched into either of two adjacent transponders by ground command.

There are four stages of amplification, all at microwave frequencies, and one frequency translation. The preamplifier is a low-noise Tunnel Diode Amplifier, followed by a Translator (pumped by a L.O. at 2225 MHz) which shifts the uplink 6 gHz common carrier frequency band to the 4 gHz downlink band. Another TDA (4gHz) completes the pre-amplifier chain. The preamplifier chain has a redundant spare which can be switched into the circuit by ground command. The preamplifier chain is fully 500 MHz wide and has no filtering functions except those associated with the frequency translator.

A single wideband TWT, with a redundant switchable spare, is proposed as a driver amplifier for all six output stages, since this is the least weight solution. Schemes utilizing two TWT drivers and proper selection of channels have been studied to circumvent the intermod problem. Since there is a weight penalty associated with two drivers, the present preference is for the proposed single driver scheme. Experimental verification of the intermodulation predictions would be made before a final design is arrived at.

Another attractive possibility is individual transistor drivers for the six output TWTs. If such units become available in the near future, the transponder design can be adapted without too much modification.

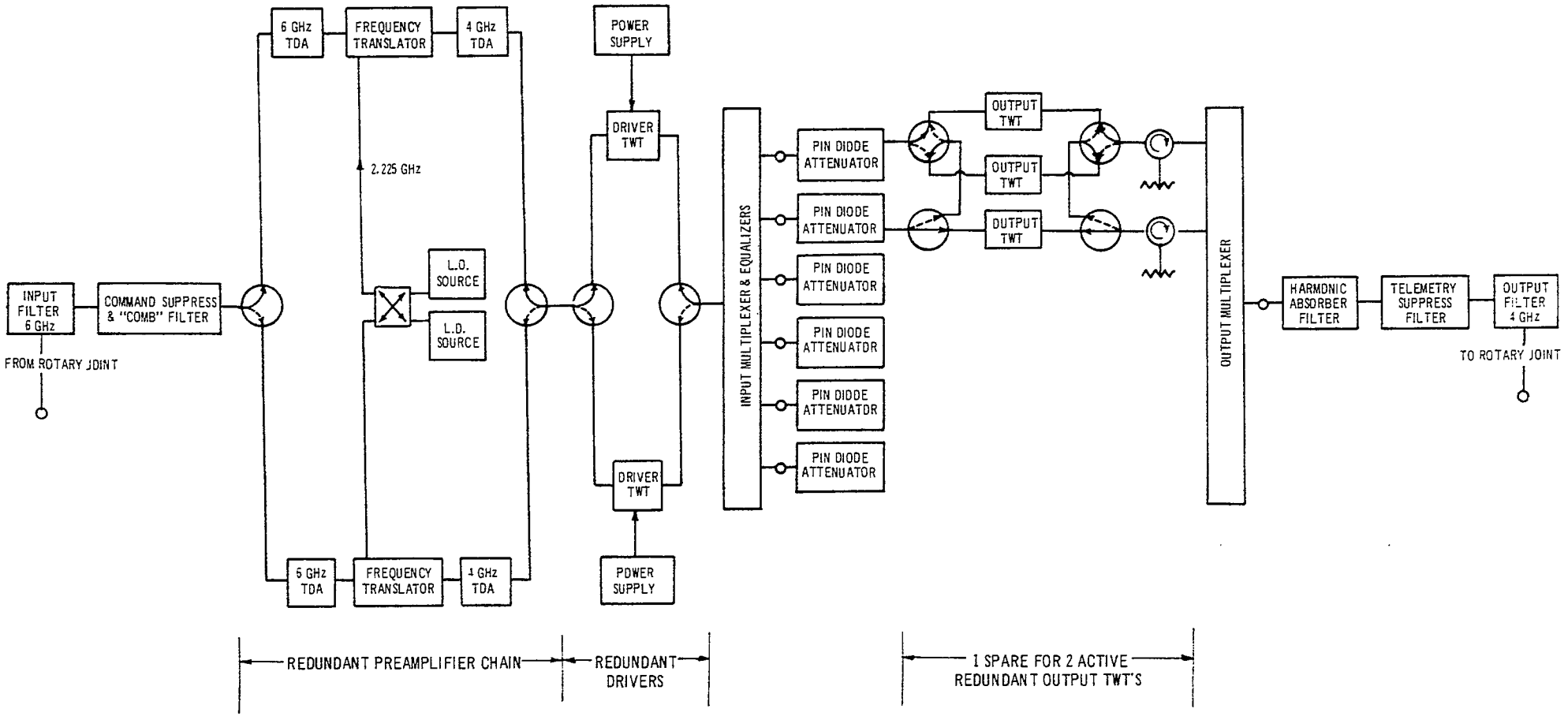

Figure 1-5 Block Schematic of Transponder

The output power amplifier stage uses high-efficiency TWT's with a saturated output of 8 watts. Pin diode attenuators, with an adjustment range of 9 dB, are used to reduce the drive level to the PA as required. For TV traffic the attenuators are set to minimum and the maximum transponder gain is available. For telephone trunking carriers which arrive at a higher level or for small capacity carriers in the same r.f. channel which require TWT backoff the attenuators are used to adjust the drive level.

Filtering

Besides the amplifier chain, the transponder also has a large number of passive filtering devices which serve various functions.

i) Input and Output Bandpass Filters

The main function of these filters is to prevent the 4 gHz output signal and its spurii (in the 6 and 8 gHz band) from re-entering the amplifier chain. Subsidiary functions for the input filter are to exclude out of band signals from Earth from reaching the preamplifier and for the output filter to reduce radiation of spurious signals.

ii) Command and Telemetry Suppression Filters:

Since the transponder is devoid of any T & T function, these filters are utilized to prevent the command signal entering the transponder and to suppress any radiation from the transponder in the telemetry band.

iii) "Comb" filter:

The satellite will be using either the even or the odd channels in 12 channel frequency plan covering 500 MHz. For an odd channel satellite the only isolation for even channels is due to polarization discrimination and this may be limited to 12 - 15 dB.

It may be necessary to reduce the power in the even channels even further in order to keep the intermodulation low. It is therefore proposed to use a filter consisting of notches tuned to the even channel frequencies which will pass the required channels.

iv) Input Multiplexer:

Functionally the input multiplexer is a one input, six output device which selects the appropriate 36 MHz wide RF channel and diverts it to the proper output amplifier. Since it is the main frequency selective element in the transponder it must also provide sufficient isolation for the adjacent channels. Because of this narrow band filtering, the

multiplexer will introduce large parabolic group delay component in each channel. It is intended, therefore, to provide a single section RF equalizer on each channel to partially compensate the group delay.

v) Output Multiplexer:
The output multiplexer will combine the six outputs from the power amplifiers into one port. Since the channels are 36 MHz wide but spaced 80 MHz apart the output filters can be made fairly wide and hence would have low group delay.

vi) Harmonic Suppression Filter:
This filter will suppress the radiation of 8 GHz, the 2nd harmonic frequency, from the output TWT.

1.10 THERMAL NOISE & INTERMODULATION IN THE TRANSPONDER

The thermal noise & intermodulation contributions of the various stages in the transponder are summarized in Table 1.1. In the table the active devices are characterized by gain, noise figure and intercept point. To compute excess noise temperature of the transponder, the individual noise temperatures of the components are referred to the input as shown in column 6 (ratio Te/To). The system noise temperature or figure are derived by summing noise contributions from all components including the antenna. The C/T ratios at the inputs to the various amplifiers are also shown in the table.

The overall system noise figure, for this configuration, is 7.2 dB which leaves a margin of 0.8 dB from the originally assumed 8.0 dB.

The intercept point is a measure of the 3rd order nonlinearity and of low level AM to PM conversion which produce intermod products of the type $2f_1 - f_2$ & $f_1 + f_2 - f_3$ . . It is defined on the basis of measurements carried out with two equal carriers by the equation;

$$\frac{C}{I} = \frac{\overline{P}^2}{C^2}$$

where: I = output intermod power at $2f_1 - f_2$
C = output carrier power at f_1 or f_2
$\overline{P}$ = intercept point.

The derivation and the application of this formula is limited to the quasi-linear region as shown in Fig. 1-6. For multicarrier operation the total intermod products produced by 'N' equally spaced carriers and falling in channel 'i' is given by;

$$I = \frac{C^3}{\overline{P}^2} \cdot f_1(n) \cdot f_i\ (x, j, k \ldots.)$$

Table 1.1
Table of Thermal Noise & Intermod Contributions

TV Carrier, Input Level -92.4 dBW

Items	Gain dB	Noise Figure dB	Intercept Point dBW	Thermal C/T dBW/ok	Noise Ratio Te/To	Carrier/Intermod 6 TV carriers	3 TV & 3 TEL
Input Filters	- 1.2			-110.8	0.24		
6 gHz TDA	+18.0	5 dB	-36.5	-121.6	2.88	63.6	46.6
Translator	- 6.0		-33.0			86.6	69.6
4 gHz TDA	+18.0	5 dB	-36.5	-113.9	0.49	48.2	31.2
Driver TWT	+33.0	21 dB	+ 0.0	-114.5	0.56	57.2	40.2
Output	+48.0	33 dB					
Other contributions				-107.0	0.10		
					4.27		
			Overall	C/T	-124.2	C/I	30.5

Excess noise temp. of transponder: 4.27 x 290° = 1220°K
Antenna noise temp. = 290°
Referred to transponder input
System noise temp. = 1510°K
System noise figure = 7.2 dB
System noise margin = 0.8 dB

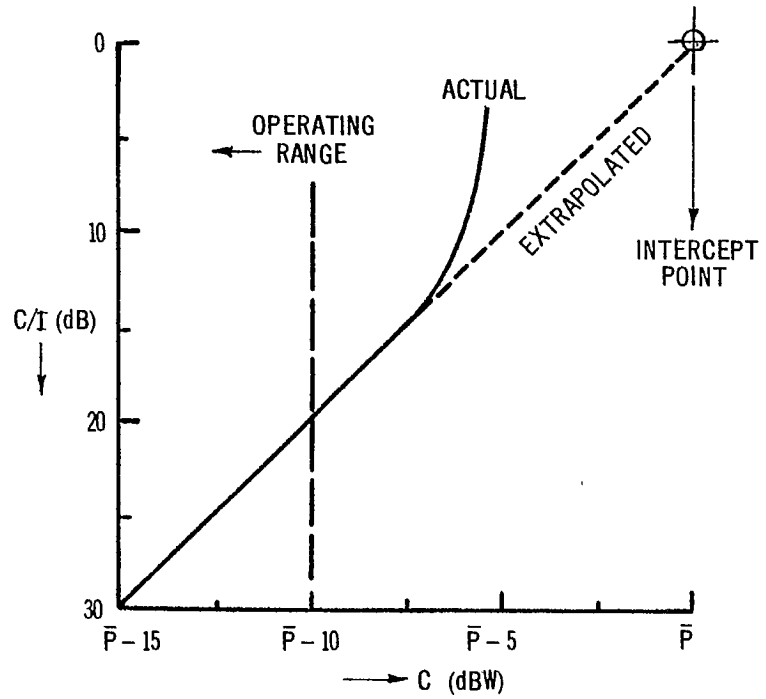

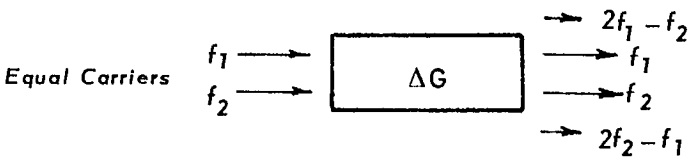

C = *Output Power Level at Frequency* f_1 *&* f_2

I = *Output Power Level at Frequency* $2f_1 - f_2$ *&* $2f_2 - f_1$

$\bar{P}$ = *Intercept Point*

$C/\bar{P}$ = *Normalized Operating Level*

Figure 1–6 The Intercept point of an Amplifier

where

$f_i(n)$ = intermod products weighting factor for channel 'i' with equal carriers.
$f_i(x, jk)$ = weighting factor for channel 'i' with larger carriers located in ch j, k etc.
x = ratio of power in larger carrier to smaller carrier.

Tables of $f_i(n)$ and $f_i(x, jk)$ have been prepared to evaluate the total intermod generated in any channel. In the mode of operation chosen, the worst case intermod occurs for larger carriers in ch 2, 3 & 5 with smaller carriers in ch 1, 4 & 6.

For this case;

$f_i(n) = f_4(6) = 30$ or 14.8 dB

$f_i(xjkL) = f_4(x.235) = 50$ or 17 dB for x = 7.5 dB

It can be seen from the form of the intermod equation that the carrier to intermod at the output of any amplifier for a given mode of system operation, is proportional to $(\overline{P}/C)^2$ only. The term $(C/\overline{P})$ is designated the "normalized operating point" of an amplifier and represents a backoff from the intercept point. To reduce intermod a lower operating point is chosen, either by decreasing the carrier level or by increasing the intercept point.

The intercept point for the TDA's, derived from state of the art units presently in use for earth station applications, is -36.5 dBW and is not easily amenable to any increase. On the other hand the intercept points for the translator and the driver TWT can be adjusted upwards by increasing the L.O. drive to former and by using a larger power tube for the latter.

In a TWT specially designed for driver applications and operated at lower helix voltages, the intercept point $\overline{P}$ can be made 7 to 10 dB higher than the maximum saturated output P_s. However, it is rather pointless to talk about the saturated output of a tube which is deliberately utilized at low efficiency and low outputs. The driver TWT is therefore specified directly in terms of the intercept point.

At the output of the driver TWT we have chosen to reduce the intermod by using both a high intercept point of 0 dBW and a low (single TV) carrier level of -36 dBW. The latter is achieved by utilizing a high gain (48 dB) output TWT.

Contrary to the expectations, the 4 gHz TDA - driver TWT interface turns out to be the critical point. On one hand the intercept point of the TDA cannot be raised while on the other hand the carrier level cannot be decreased without increasing the thermal noise contribution of the driver.

A compromise level has been used which gives an adequate C/I ratio of 31.2 dB.

The third order intermod coming out of the 6 gHz TDA and the translator is quite small but in the latter case spurii produced by the higher harmonics of the L.O. beating with higher harmonics of the signals will also be present. On the basis of measurements on similar units built for earth stations, the spurii are expected to be more than 60 dB below the carrier at the operating levels used.

1.11 Advanced Development Program

RCA Ltd has started a company funded advanced development program to prove out some of the design concepts used in the proposed transponder and to develop some of the components which are not presently available. The effort will be concentrated in two critical areas: Intermodulation and Crosstalk in multicarrier multi-level operation and group delay and amplitude response distortion produced by the filtering devices.

A simple but systematic theory of 3rd order intermod generation has been evolved and used in the transponder synthesis. The development program will be designed to prove out the theory. For this purpose a breadboard model of the transponder will be built with a wideband preamplifier section but only one output TWT. Multicarrier operation will be simulated and each amplifying device checked for intermod and crosstalk. The overall transponder performance will be related to simple device parameters such as intercept points and a parametric method will be evolved to choose device parameters and operating points to minimize the transponder intermod and crosstalk.

The major component of the group delay in the transponder is produced by the input multiplexer filters. A promising approach, which will be pursued during this development program, appears to be the use of Inverse Tchebychev filters. The group delay response of these filters is second only to Elliptic function filters and far superior to Butterworth or Tchebychev filters. (Narrowband Elliptic Function filters, unfortunately, cannot be synthesized at present at microwave frequencies).

Group delay equalization within the satellite calls for RF equalizers operating at 4 GHz. Linear and parabolic equalizer appear to be within the state of the art. However, most filters have a predominantly tri-quadratic (4th order) group delay at the edges of the passband. One of the objects of the development program therefore is the synthesis of 2nd and 4th order group delay equalizers. Optimum cavity loading techniques, to compensate the amplitude response of the filters with that of the equalizers, will also be investigated.

2. ANTENNA SUBSYSTEM

2.1 COMMUNICATION ANTENNA

2.1.1 Illumination Control

The requirement for the antenna on the Cansat satellite is to exceed a minimum specified power level over the surface of Canada. It must do this in a manner which is most economical in terms of satellite weight and power requirements. This is somewhat different than normal antenna designs where maximum gain on axis is required and the optimum configuration must be determined.

The actual antenna gain is given by the expression $G = \varepsilon \frac{4\pi A}{\lambda^2}$ which becomes:

$$G = \frac{\pi^2 \varepsilon \ a \ b}{\lambda^2} \text{ for an elliptical aperture and}$$

$$G = \frac{4\pi \ \varepsilon^2 a \ b}{\lambda^2} \text{ for a rectangular aperture.}$$

Where ε is aperture efficiency

a is the major dimension and

b is the minor dimension of the aperture

The 3 dB beam widths are $\theta_{a3} = \frac{K\lambda}{a}$, $\theta_{b3} = \frac{K\lambda}{b}$

in the directions of the major and minor axis respectively where the proportionality constant K is the same in the two directions but differ from rectangular to circular and for different illumination tapers.

Eliminating a and b the gain becomes

$$G = \frac{\pi^2 \ \varepsilon \ K^2}{\theta_{a3}\theta_{b3}} \text{ elliptical and}$$

$$G = \frac{4\pi \ \varepsilon^2 K^2}{\theta_{a3}\theta_{b3}} \text{ rectangular}$$

Since θ_{a3} and θ_{b3} are fixed by geometrical considerations it is necessary only maximize the product $G\theta_{a3}\theta_{b3}$ which can be considered a figure of merit for antennas of this type.

Using published* values of gain and beam width for different illumination tapers, the products $G\theta_{a3}\theta_{b3}$ have been calculated and plotted in Figure 2-1 as a function of the first side lobe level. The figure of merit varies from a low of 9.7 for uniform illumination to a high of 12.4 for $(\text{Cos}\frac{\pi x}{2})^4$ illumination with side lobe levels ranging between 13.2 dB for uniform to 48 dB for $(\text{Cos}\frac{\pi x}{2})^4$. This graph stresses the fact that the less energy radiated into the side lobes the more will be available for the main lobe and every effort should be directed towards reducing the level of the side lobes, and preventing loss due to spill over. While a rectangular aperture with $(\text{Cos}\frac{\pi x}{2})^4$ illumination is the best it would require the antenna to be made so perfectly that the 48 dB side lobe levels are maintained. It is preferable to aim at side lobe levels between 20 and 25 dB which are more easily attainable. Two tapers look reasonable, a circular aperture with $1-\rho^2$ taper and $\text{Cos}\frac{\pi x}{2}$ taper with a rectangular aperture.

In addition to finding the optimum illumination taper for the aperture it is necessary to determine the antenna size to give maximum gain at the edge of the required coverage. In this way the required transmitter power is a minimum. The minimum beam widths required to adequately cover Canada have been determined by a series of computer calculations described in Volume I. These minimum angles are 3.25 degrees N-S and 8.5 degrees E-W.

For a circular aperture with $1-\rho^2$ illumination the maximum gain at the edge of the coverage occurs when the field strength is 4.03 dB below the maximum. For a rectangular aperture with $\text{Cos}\frac{\pi x}{2}$ illumination the corresponding figure is 4.00 dB below the beam peak. The following table summarizes the results for these two illumination tapers.

Table 2.1 Beam edge gain for two different illumination tapers

	Circular	Rectangular
U at edge of coverage	2.29	$.682\pi$
Aperture width for 3.25° beam (inches)	76.8	71.9
Aperture width for 8.5° beam (inches)	29.4	27.5
Theoretical gain (dB)	33.97	34.44
Efficiency loss (dB)	1.25	1.83
Net gain (dB)	32.72	32.61
Beam edge below peak (dB)	-4.03	-4.00
Gain at edge of coverage (dB)	28.69	28.61

*Silver S. Microwave Antenna Theory and Design Volume 12, Radiation Laboratory Series

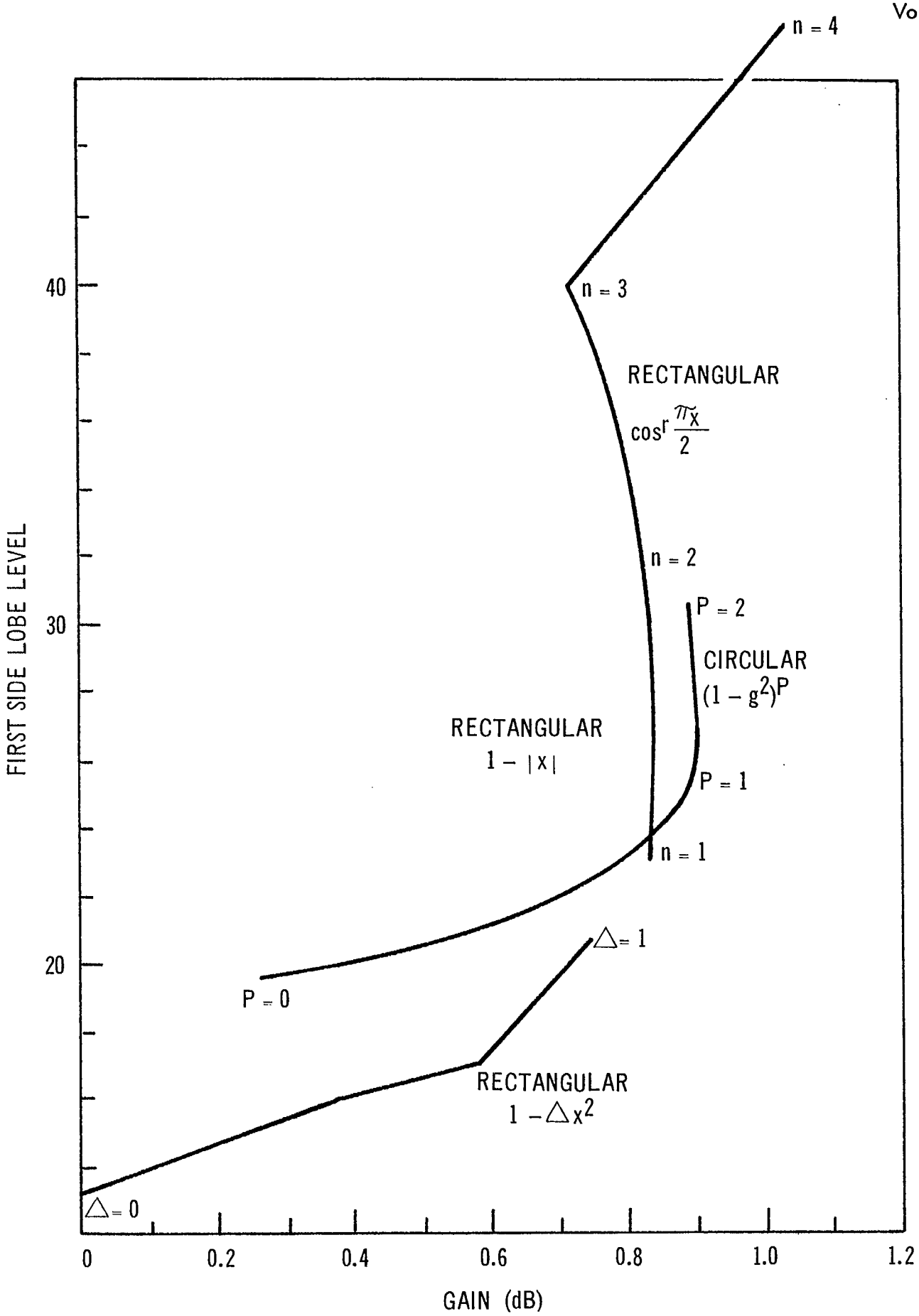

Figure 2.–1 Gain improvement compared to a rectangular aperture with uniform illumination over a specified angular coverage

The circular aperture illumination has a slight margin of superiority in gain at the expense of a slightly higher antenna. However, the lack of the square corners may make it easier to fit within the shroud. The final dimensions of the antenna may be adjusted depending upon the illumination taper actually obtained.

Three antenna configurations have been investigated in detail. The structure, support feed and feed line have been designed for each and the antennas are compared on the basis of total weight and net loss. The three antenna configurations are 1) offset segment of a parabola of revolution. 2) Center fed parabola of revolution, 3) double reflector antenna system. These configurations are described in more detail in the following paragraphs.

2.1.2 Antenna Configurations

(a) Offset segment of a parabola of revolution

This has a number of attractive features as well as some difficult design problems. The antenna has no aperture blockage because the feed horn is outside the aperture area. In addition the feed line from the satellite is minimum resulting in lowest losses: Undesirable electrical features are the assymetric aperture illumination and the poorer cross polarization performance compared to a symmetically fed parabola of revolution. This configuration presents some difficult mounting problems. A focal length of 42 inches is about optimum. With a shorter focal length the upper tip interferes with the shroud and with a longer focal length very little space is available behind the reflector for support structure. In addition the configuration presents difficult thermal design problems to prevent excessive thermal distortions due to temperature differences between different parts of the support structure. Additional weight would be necessary to balance the despun platform.

(b) Center fed parabola of revolution

This configuration offers adequate space to design a rigid light weight and thermally stable support structure. In addition, because a shorter focal length can be used, the antenna can be positioned so that no additional weights are required for balancing purposes. The antenna has good cross polarization characteristics but has larger losses due to the long feed line and some blockage.

(c) Double reflector antenna

A standard cassegrain utilizing a parabola and hyperbola of revolution is difficult to design for this application,

both because of the large beam widths involved and the large aspect ratios in aperture dimensions. It has the same attractive features as the second configuration with a slightly shorter feed line.

The subreflector blockage is greater than the blockage of the horn in antenna two. It is however possible to shape the subreflector to accomplish illumination control. In this way it is possible to radiate the energy normally blocked by the subreflector and to control the illumination taper for optimum performance. In this way much of the loss due to blockage can be eliminated. Some loss remains due to the degradation in pattern because of the hole in the illumination.

2.1.3 Bandwidth

The satellite communication band is a full 500 MHz between 3.7 and 4.2 GHz for the down link and between 5.925 and 6.425 GHz for the up link. The antenna and feed system must handle the full 500 MHz band at both up and down frequencies. In addition, a duplexer must be provided to isolate the receiver from the transmitter signal. The 500 MHz band is divided into twelve 40 MHz bands. A plan for allocating these bands is described in section 3 Volume I. As described in that section one satellite would transmit channels 1,3,5----11. With the up link polarized at right angles to the down link while a second satellite at the same location in space would transmit channels 2,4, -- 12 with the up and down links polarized in the same direction. Thus on one satellite a polarizer is used to isolate the up and down link while in the second satellite a diplexer is used.

2.1.4 Polarization

The preferred polarization from the antenna stand point is E-W for the 4 GHz down link and either N-S or E-W for the 6 GHz up link. This preference is slight and the alternate polarization for the 4 GHz down link could be used. However, the horn and duplexer are designed on the assumption that the 4 GHz down link is polarized E-W.

2.1.5 Feed Methods

The various methods by which the up and down links can be taken through the rotary joint are presented in section 3 Volume I. The two preferred configurations for the two satellites carrying the even and odd frequency bands respectively are reproduced in figure 2-2.

The orthocoupler or polarizer is located directly behind the horn. The 4 GHz transmitter is connected to the horn by means of waveguide after passing through a coaxial rotary coupler and a waveguide to coax transition.

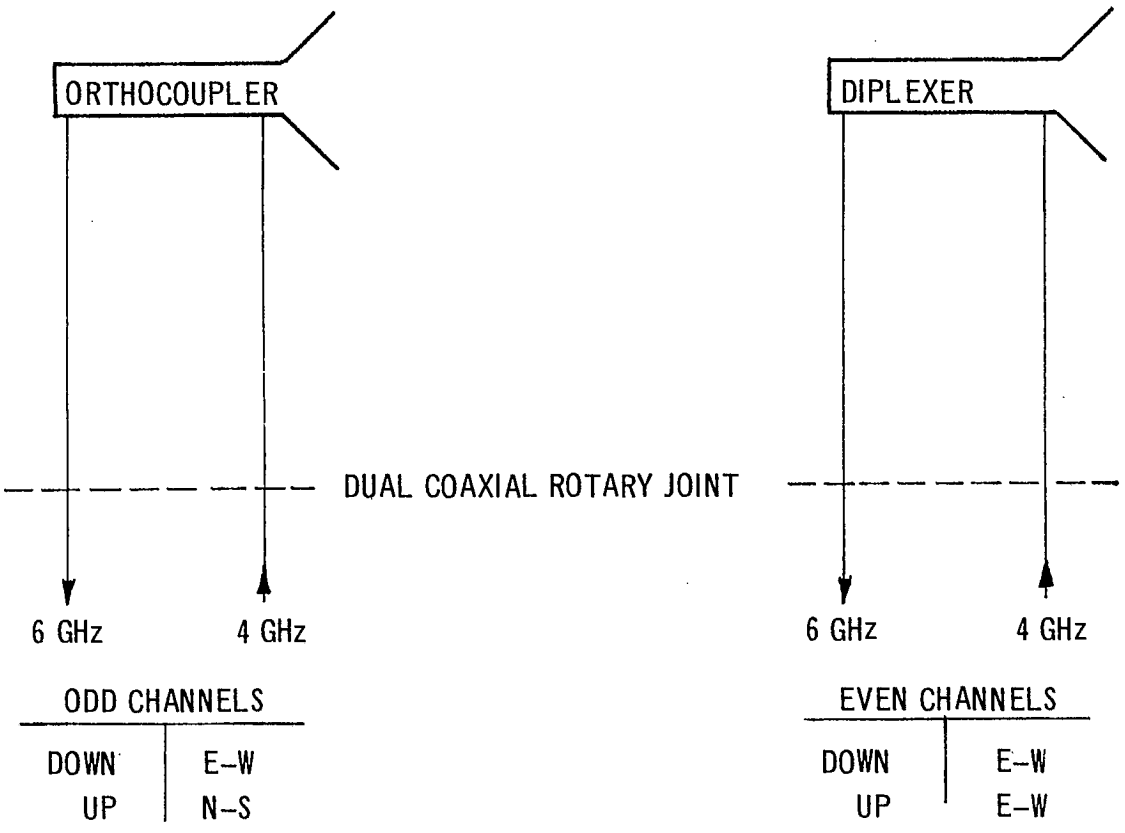

Figure 2–2 Preferred duplexer configurations of linerar polarization systems

The 6 GHz received signal is coupled directly into coax at the polarizer and connected to the receiver through a separate coax and coaxial rotary coupler. The use of two feedlines instead of one for the cross polarized satellite is considered necessary because of the coupling between modes in a curved multimode waveguide.

For the alternate satellite design using the same polarization for the up and the down link a single mode broadband waveguide can be used. In this case the diplexer separating the transmit and receive frequencies will be placed inside the antenna mast just above the coaxial rotary joint. The two signals pass through the rotary joint on separate lines.

2.1.6 Feed Horn

The beam shape and beam widths of the antenna are required to be the same for both 4 and 6 GHz and the same when the 6 GHz beam is cross polarized. A feed horn which would fulfill these requirements has been built previously. This horn is a fin loaded type to equalize, as much as possible, the E-plane and H-plane illumination distributions across the mouth of the horn. The measured far field pattern of a square horn is presented in figure 2-3. It is seen that the beam widths in the E and H-plane are almost exactly the same at the higher frequency and very nearly the same at the lower frequency. It is also seen that the beam width at the higher frequency is narrower than at the lower frequency. For this reason the area of the reflector illuminated at the higher frequency is smaller than at the lower frequency. The reduction in illuminated area is very close to that required to maintain the beam widths and ground coverage at the upper frequency equal to that at the lower frequency. As seen from Figure 2-3 this horn was not quite square at both frequencies. In the event that this assymetry existed in the final antenna design the horn would be optimized for the down link and a slight degradation in beam coverage tolerated for the up link.

2.1.7 Efficiency

The theoretical gain of the antenna given by $\frac{4\pi A^2}{\lambda^2}$ is reduced by the efficiency of the aperture distribution and a number of other losses which must be evaluated. The first loss is spillover loss, i.e., that part of the feed horn pattern which is not intercepted by the reflector surface. This includes back lobe energy from the horn. If a subreflector is used some of this loss occurs at the subreflector, but an additional amount occurs at the main reflector. If any obstruction occurs within the aperture then an additional loss of energy occurs. This is divided into two parts, the loss due to the reduction in radiated energy and the loss in gain due to pattern degradation.

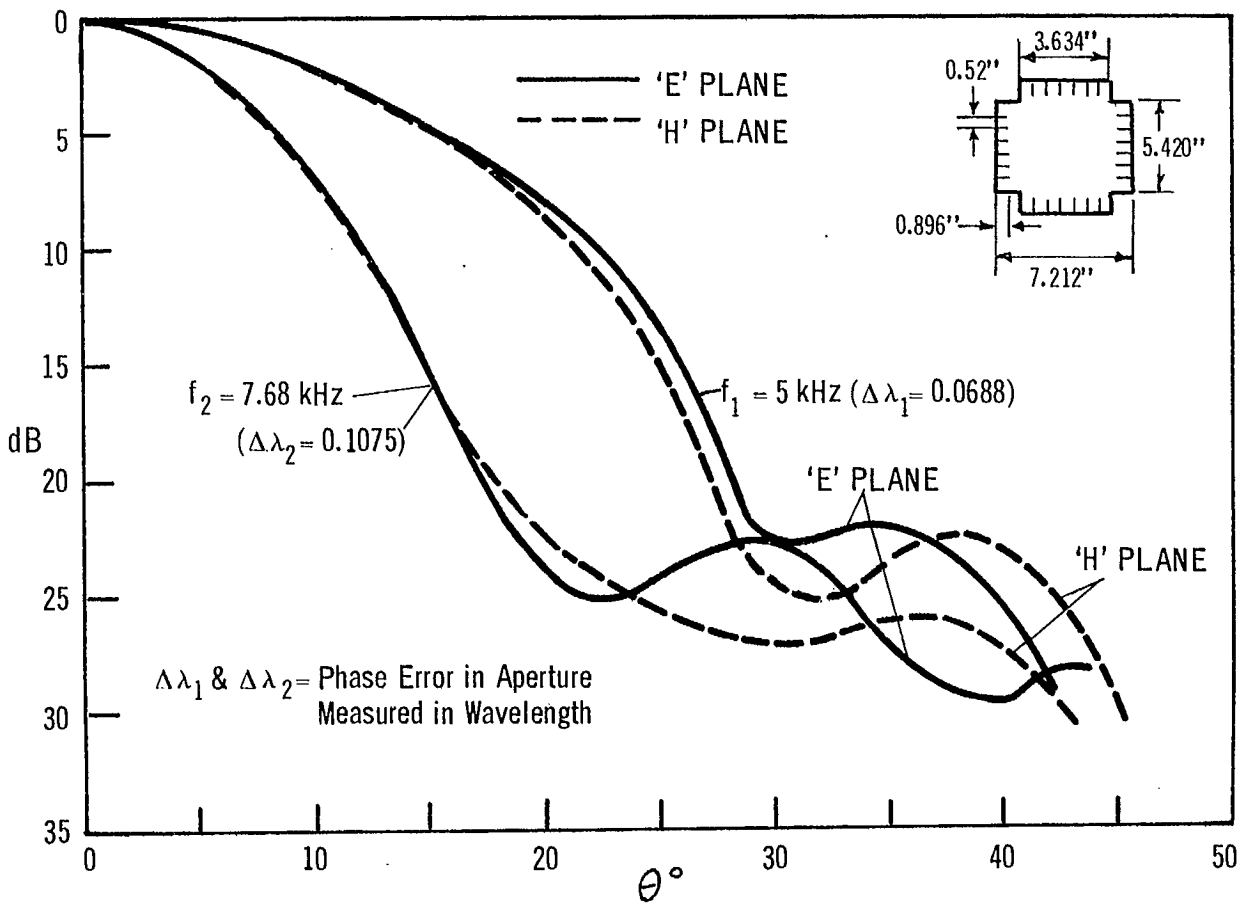

Figure 2–3 Characteristics of the X-band fin-loaded horn

The first part is recoverable by properly shaping the subreflector, the second part is not recoverable. The support structure for the horn or subreflector contributes the blockage loss. Random deviations in surface contours cause a loss in gain due to scattering into the side lobes. Loss in gain also occurs due to phasing errors caused by the phase center of the horn being of finite size. The above losses are caused by geometrical errors and are associated with the antenna gain. The remaining losses are associated with the feed line, including mismatch loss in the feed horn, absorption loss in the horn, ortho coupler or duplexer loss, waveguide loss, waveguide to coax transition loss, and finally the rotary joint loss.

2.1.8 Antenna Gain

The antenna gain calculations at both 4 GHz and 6 GHz have been based on the measured patterns for a square horn shown in figure 2-3. It has been shown that the illumination should approximate a $1-\rho^2$ taper which means a low edge illumination. On the other hand at 6 GHz only a minimum amount of the first side lobe can be allowed to fall on the reflector as this energy is out of phase with the main lobe. The edge of the reflector was placed at 25 degrees on the radiation pattern in figure 2-3 and the horn scaled to the correct frequency and beam width. Using this information the spillover loss, the illumination efficiency and the blockage loss can be calculated.

The results of these calculations for 4 GHz are presented in table 2.2 and for 6 GHz in table 2.3. The antenna would be optimized for operation at 4 GHz and any slight degradation in performance at 6 GHz would be compensated by a slight increase in the transmitter power at the ground station. The antenna losses at 4 GHz have been calculated for three antenna configurations. The offset feed horn has the lowest loss but presents some severe mounting problems resulting in increased weight and beam twisting due to thermal distortions. The center feed horn has slightly higher loss but has minimum mounting and thermal distortion problems. The third configuration, that of a shaped subreflector is estimated to have still higher loss and is otherwise less well defined as the required shape of the subreflector has not been worked out. For this reason the simple horn fed parabola of revolution is considered the preferred solution at this point in time. The losses at 6 GHz have been calculated only for this configuration.

At the up link frequency the reflector is much larger than the area illuminated by the horn. The technique used to calculate the antenna gain was to define the edge of the beam at the 20 dB level and determine the reflector area within this contour. The theoretical gain

Table 2.2

Antenna Gain at 3.95 GHz, Elliptical Aperture 73.9 x 28.3 inches

	Offset Feed Center	Feed Horn	Shaped Subreflector
Distribution Efficiency	1.00	0.90	0.90
Spill over - main	0.40	0.30	0.30
Spill over - sub	-	-	0.30
Energy blockage	-	0.15	-
Pattern degradation	-	0.07	0.55
Support blockage	-	0.20	-
Surface Inaccuracy sd = .033"	0.10	0.10	0.20
Phase center errors	0.10	0.10	0.10
Total Antenna Losses dB	1.60	1.82	2.35
Reflection loss in feed	0.04	0.04	0.04
Absorption loss in feed	0.03	0.03	0.03
Line length (inches)	30	80	50
Line loss (waveguide)	0.05	0.11	0.07
Rotary Joint loss	0.35	0.35	0.35
WG to coax transition	0.04	0.04	0.04
Orthocoupler or diplexer	0.10	0.10	0.10
Total feed loss dB	.61	.67	.63
Total loss dB	2.21	2.49	2.98
Theoretical Antenna gain dB	33.64	33.64	33.64
Net Antenna gain dB	31.43	31.15	30.66
Net gain at beam edge dB (-4.11 dB) Referred to transmitter side of rotary joint	27.32	27.04	26.55

Table 2.3

Antenna Gain at 6.175 GHz, Illuminated Area 55" x 22"

	Center Feed Horn
Distribution Efficiency	2.14
Spill over-main	0.40
Spill over-sub	-
Energy Blockage	0.14
Pattern Degradation	0.07
Support Blockage	0.20
Surface Inaccuracy Sd = 0.035"	0.15
Phase Center errors	0.15
Total Antenna Loss dB	3.25
Reflection Loss in Horn	0.04
Absorption Loss in Horn	0.04
Line Length (inches)	80
Line Loss (coax)	0.67
Rotary Joint	0.50
WG to Coax	0.05
Ortho Coupler	0.15
Total Feed Loss dB	1.45
Total Loss dB	4.70
Theoretical Antenna Gain dB (Illuminated area 55 x 22 inches)	35.15
Net Antenna gain	30.45
Gain at Beam edge E-W (-4.60) dB	25.85
Gain at Beam edge N-S (-4.23) dB (Referred to receiver side of rotary joint)	26.22

is based on this area and the distribution efficiency and spillover are based on an illumination taper with a 20dB pedestal. The beam widths at 6 GHz are slightly narrower than at 4 GHz with the east west beam width decreasing slightly more than the north south beam widths. It is seen from tables 2.2 and 2.3 that the E-W beam edge gain at 6 GHz is only 1.19 dB less than at 4 GHz while the 6 GHz N-S edge gain is only 0.82 dB less than at 4 GHz. The exact performance of the antenna at 6 GHz depends upon the performance of the horn at this frequency and exactly how the properties scale to the larger divergence angles required for the space craft antenna.

2.1.9 Support

The antenna support structure must fulfil a number of rather stringent requirements. It must maintain the antenna dimensions and pointing accuracy, have minimum weight, withstand the launch environment, and not interfere with the shroud during launch. In addition, the despun platform must be balanced about the axis of the spacecraft, and finally it must be thermally stable so that temperature differentials do not distort the antenna or change the beam direction excessively.

A detailed description of the mechanical and thermal aspects of the antenna support are given in section 11on structures and in section 10 on the thermal subsystem.

2.1.10 Further Investigation

While the simple horn fed parabola of revolution appears to be the optimum compromise solution, other areas of approach may present some advantage. These areas, being investigated under a company sponsored program already started, include the following:- utilizing increased reflector width to accomplish far field beam shaping, modeling a feed horn for a parabola of revolution with elliptical cross section, and investigating the shaping required for the sub and main reflector for the third configuration presented here.

2.2 TELEMETRY AND COMMAND ANTENNAS

2.2.1 Bicone

The telemetry and command function is needed during the transfer orbit and the positioning maneuvers. Because the main communication antenna is disoriented during this period a second antenna with a near isotropic pattern is required. In addition, since the spacecraft is spinning a pattern with cylindrical symmetry is desirable. A coaxially fed bicone with a 40° beam angle has been selected for this application. It provides the field pattern and large frequency band required in a simple light weight structure. It is located on the axis of symmetry of the spacecraft on the despun platform above the communication antenna reflector.

2.2.2 Beacon Antenna

A short whip antenna is added to the bicone to radiate the 136 MHz beacon signal. The whip is a loaded quarter wave length radiator with the upper half of the bicone forming part of the radiating structure. The 136 MHz signal would be carried on the same coax as the 4 GHz and 6 GHz signals. The 136 MHz is separated from the 4 and 6 GHz on the antenna side of the rotary joint. The 136 GHz is passed through the rotary joint on one section and the 4 and 6 GHz on a second section. Some difficulty is expected in designing an efficient radiating structure for all three frequencies. However, it is anticipated that the structure can be optimized at 4 and 6 GHz and then optimization at 136 MHz can be accomplished by loading the whip and tuning the line in locations where only 136 MHz energy is present.

2.2.3 Polarization

The telemetry and command antenna and the beacon whip are linearly polarized along the spacecraft axis. Contact with the ground station can be maintained, independent of direction of polarization if the ground station is circularly polarized. A constant 3 dB loss is experienced with this arrangement. Detailed systems considerations are presented in section 3.

2.3 RF COAXIAL ROTARY JOINT

2.3.1 Introduction

The RF coaxial Rotary Joint proposed for this mission utilizes known microwave techniques combined with straight forward mechanical design. A similar rotary joint has been developed for the Communications Satellite Corporation as an efficient means of transferring multiple

RF signals from a spinning satellite to a set of mechanically despun antennas.

Several alternatives were studied and the final choice rests on a coaxial system with all four channels being concentric. At the cross-section where the fixed and the rotating sections meet, the RF signals are in a true coaxial TEM Mode and RF coupling is provided by air dielectric choke sections in the walls of the coaxial lines.

This particular approach was selected because it separates the problem of coupling RF energy across a rotary joint from the problem of exciting the correct mode in the transmission lines. The outer three transmission paths therefore consist of three items:

1) a multipoint feeder to excite the TEM mode without exciting the higher order modes in the large diameter coax lines

2) a coaxial transmission line - rotary joint with choke coupling and

3) a multipoint feeder again.

In the center channel a simple connector to coax transition suffices as a feeder.

The overall expected performance is summarized in the following table.

Table 2.4
Performance Parameters for each channel of a
Four Channel Coaxial Rotary Joint

Type	Used for	Electrical Performance					
		VSWR (Max)		Insertion Loss dB		Isolation dB	Power Handling Watts
		Steady State	WOW	Steady State	WOW		
Ch 1 Straight Coax	Uplink 6 GHz	1.2	1.05	0.5	.05	40	5
Ch 2 Multipoint Feeder - Coax - Multipoint Feeder	Command & Telemetry 6 & 4 GHz	1.2	1.05	0.5	.05	40	5
Ch 3 "	Downlink 4 GHz	1.2	1.05	0.35	.03	40	50
Ch 4 "	Telemetry Beacon 136 MHz	1.5	1.2	1.0	0.1	40	5

(1) All rotating joints are non-contacting choke type
(2) Estimated total weight 3.5 lbs max.
(3) Estimated life time 5 years min.

2.3.2 Principle of Operation

(a) Choke Coupled Rotary Joint

The choke coupled rotary joint has the advantage over the spring contact version, that no friction is produced. For narrow band operation, a single stub choke section is normally adequate. However, in multiple concentric lines, where adjacent channels might carry signals in widely separated frequency band,a multiple stub choke would be required. The two versions are shown schematically in figure 2-4.

The principle of operation can be understood by reference to Figure 2-5 a & b in which the electrical equivalent networks of the joints are also drawn. The high impedance short-circuited line 'Zo_4' is made resonant at the center of the required band and reflects an open circuit in the leakage path $Zo_3 - Zo_5$. As a result no coupling can exist between ch 1 & ch 2 at this frequency. The open circuit at the interface of Zo_3 and Zo_5 is reflected as a series short circuit in Zo_1 and Zo_2 and hence provides a low loss path for the main channels.

At a frequency away from the design center frequency the isolation provided is controlled by the ratio of the impedances Zo_4/Zo_3 and Zo_1/Zo_3.

However, mechanical consideration put limits on how small Zo_3 or how large Zo_4 can be made. A spacing of .025" between the sections of rotary joints is sufficient to provide more than 45 dB isolation over a 500 MHz band centered on 4 GHz.

For dual frequency operation a double stub choke design is used, as shown in Figure 2-5 (b) with its electrical equivalent. The stubs Zo_6 and Zo_4 are made resonant at 6 and 4 GHz respectively. The rest of the operation can be understood by an extension of the rationale given above.

The assignments of channels in table 2.5 is based on minimizing the complexity of the choke joints required on the rotary coupler.

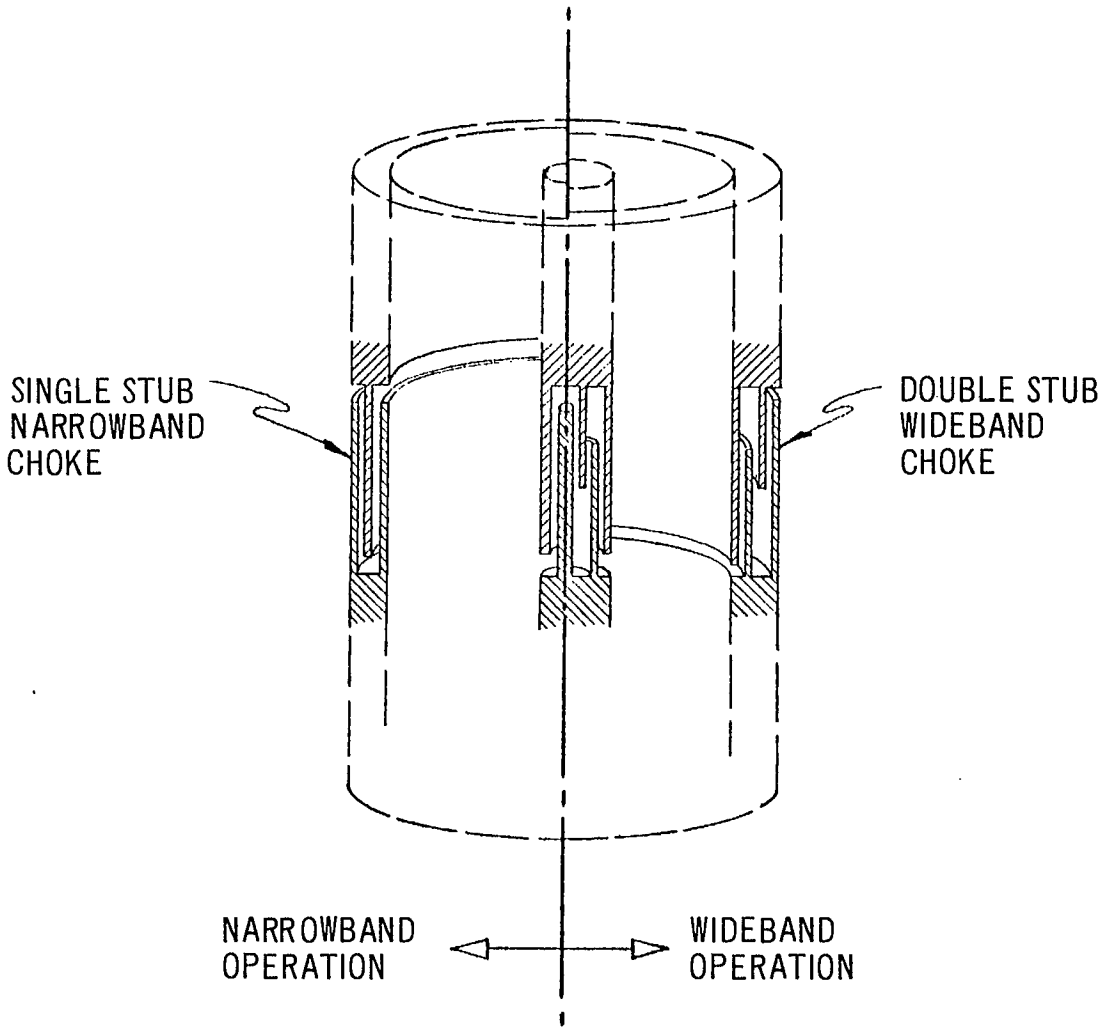

Figure 2–4 Schematic of a Coaxial Rotary Joint

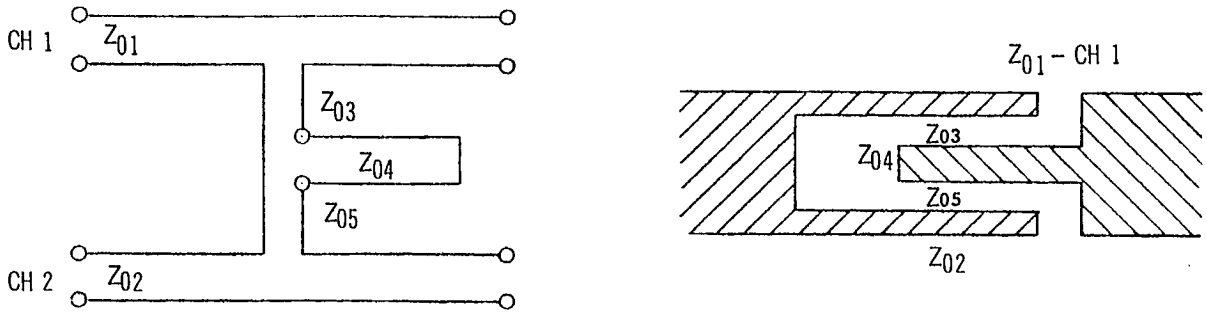

Figure 2–5 (a) Single stub choke joint and its electrical network

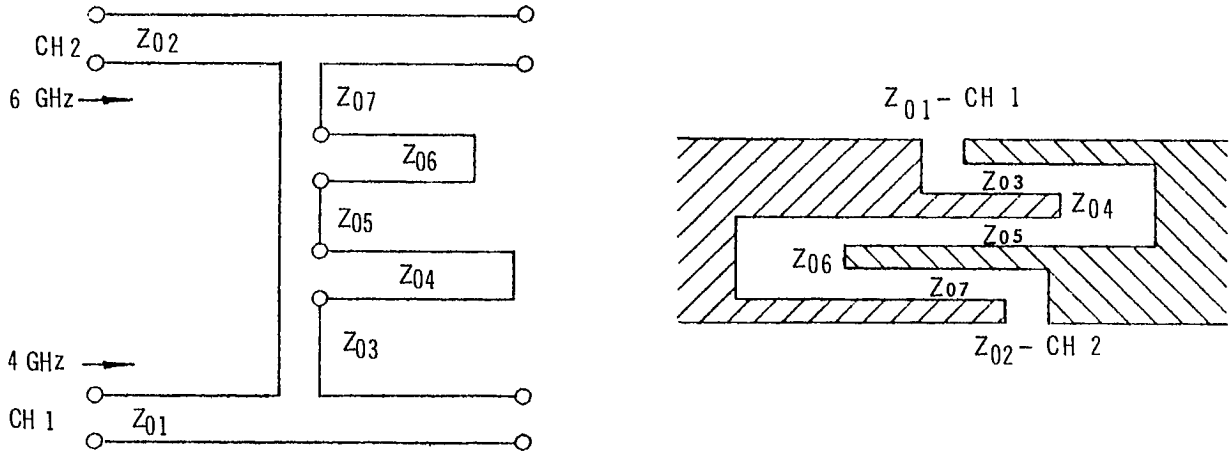

Figure 2–5 (b) Double stub choke joint and its electrical equivalent network

Table 2.5 Channel Allocation

Conductor	Channel	Choke Joints
Center Conductor	6 GHz	single stub 6 GHz
2nd Conductor	6 & 4 GHz	double stub 6 inside 4 outside
3rd Conductor	4 GHz	double stub 6 inside 4 outside
4th Conductor	136 MHz	single stub 4 GHz
5th Conductor		single stub (corregated) 136 MHz

A 136 MHz choke joint cannot be produced in the length available. This channel would therefore act as a series capacitance coupled joint. By putting it on the outermost transmission line allows the largest circumferential capacitance. This also provides access to the outermost choke joint which can now be made corrugated to provide larger capacitance.

b) Multipoint Feeders

As the diameter of the coaxial line increases higher order modes can be propagated. To suppress the generation of these modes requires a feeder system which equalizes the rf potential along the peripheri of the transmission line. One method is to use a large number of probes around the peripheri and excite them in the same rf phase as shown in Figure 2-6. For mechanical reasons it is usually more convenient to conver the coaxial line into a radial line and then insert the probes along a circle in this line. This is best seen in the cross-section of the proposed rotary joint, Figure 2-7.

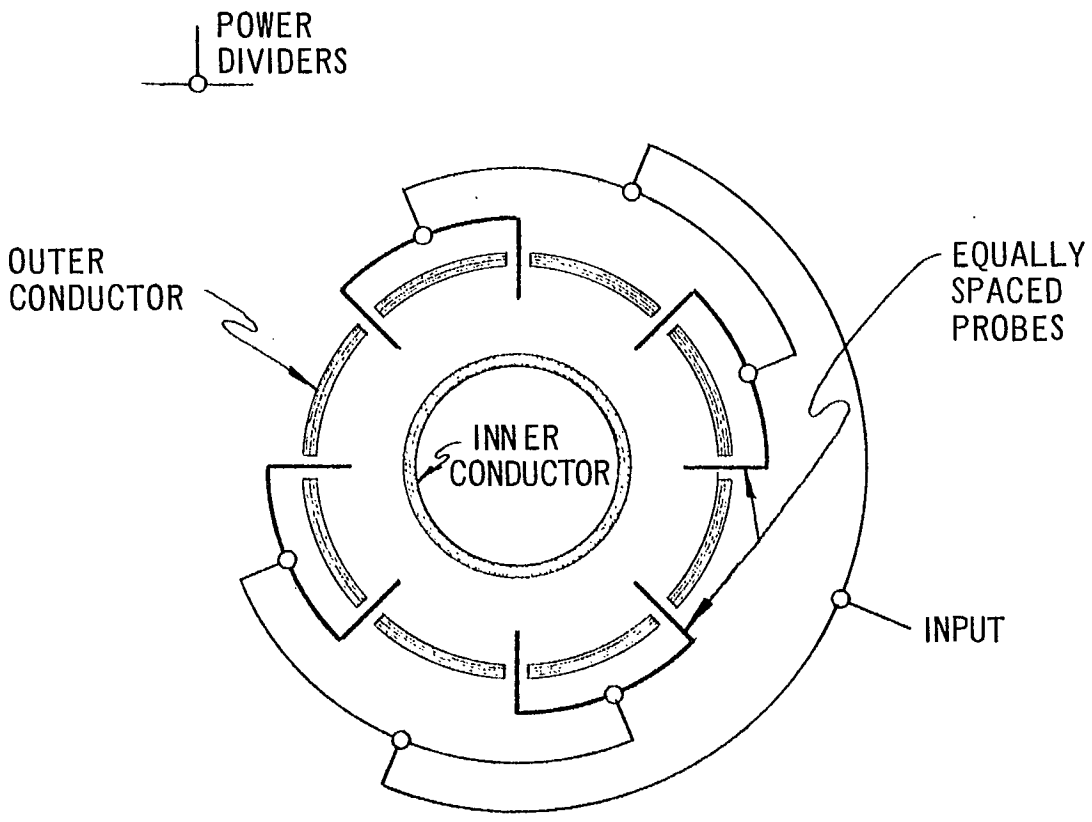

Figure 2-6 Principle of Multipoint Feeder

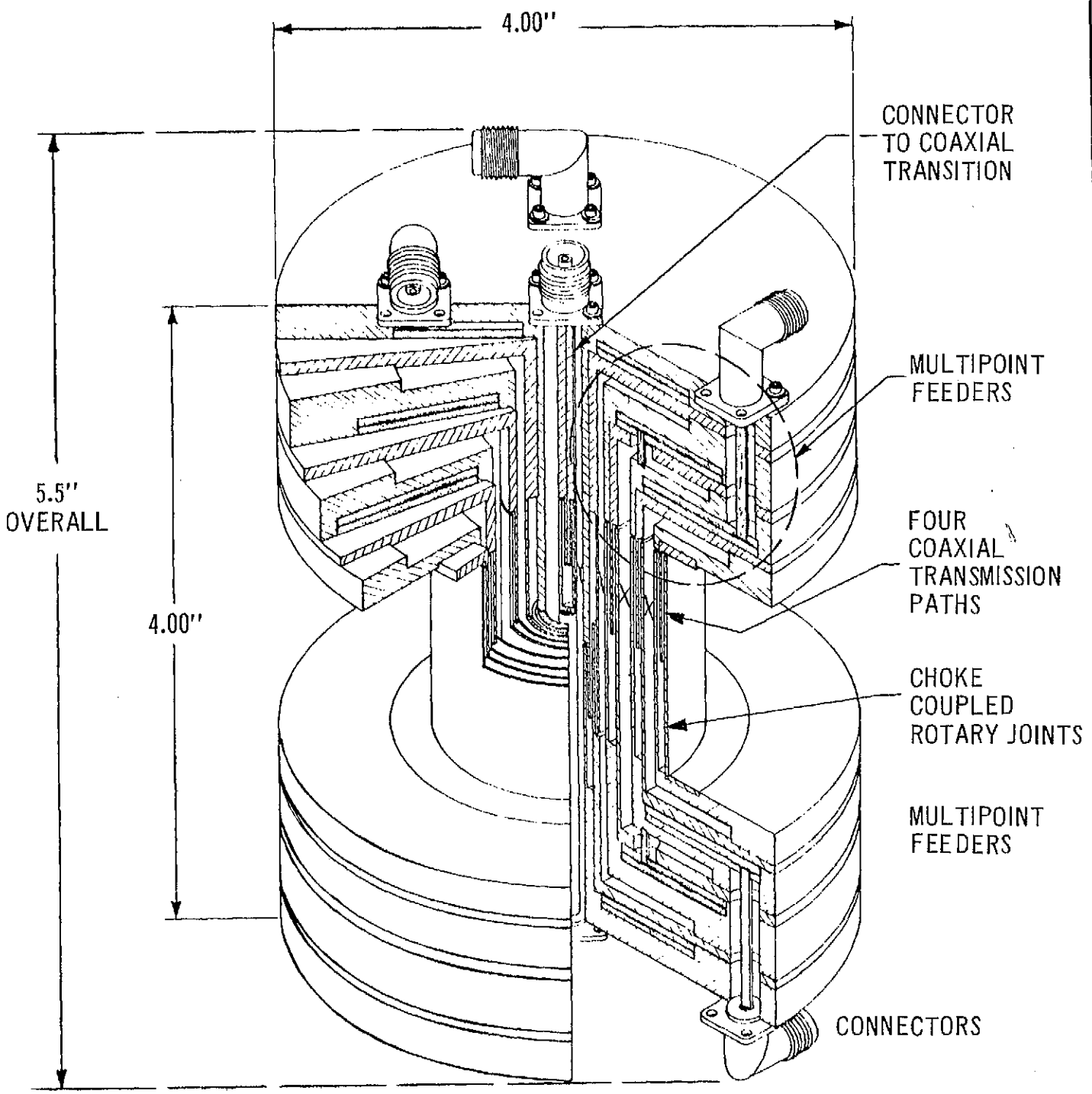

Figure 2-7 Four Channel Rotary Joint

3. TELEMETRY AND COMMAND

3.1 BASIC SYSTEMS CONSIDERATIONS

3.1.1 Introduction

The basic Telemetry and Command Subsystem requirements for a Canadian Communications Satellite system has been studied in detail, and in this section we present a model of a working system to satisfy these requirements. Because of the many aspects to be considered in arriving at the complete system, we have subdivided this section into four major subsections with the following headings:

a) Basic Subsystem Considerations
b) Command System
c) Telemetry System
d) Equipment

In this subsection we consider the basic subsystem to establish the frequencies, modulation characteristics, major operational requirements and so forth.

The Command and Telemetry Systems, and the equipments are covered in the following three subsystems.

3.1.2 General

The concept of the Telemetry and Command System has been evolved from consideration of

a) reliability and continuity of equipment operations
b) accuracy of command execution
c) relatively slow telemetry data rate requirements
d) use of telemetry and command during the transfer orbit, and to-station manoeuvering of the spacecraft
e) freedom from interference
f) standardization of techniques and equipments
g) freedom from intermodulation problems with the communications system
h) simplicity of equipment and operational procedures
i) provision of a tracking carrier thereby permitting precision angle tracking

These concepts are in line with the requirements of the "Provisional Work Statement" for the "Preliminary Study for the Design and Development of a Domestic Communications Satellite" issued by the Department of Industry.

In following this section, we must bear in mind that, while the general specifications insofar as spectrum requirements, transmitter powers , and so forth may be taken as reasonably firm, the exact baseband formats of the signals (particularly for the time multiplexed signals) can be considerably varied. This is an important consideration, for it means that until designs are finally frozen, considerable adjustments can be made in the data formats without upsetting power, weight, or overall system parameters. Why changes? Because the format used has a considerable bearing on protection, operator efficiency, diagnostic ability and general routine capabilities. And these aspects in turn depends upon overall requirements which must encompass ground activities heavily and are therefore beyond the scope of this study.

As to the requirement for hardware, the basic concept is conventional. The minimal equipment required for telemetry and command is

a) a command receiver for recovering the transmitted command signal baseband from the received RF command transmission

b) a command decoder for identifying the specific command from the baseband

c) a telemetry encoder for multiplexing all the monitor signals onto a single telemetry baseband

d) a telemetry transmitter for converting the telemetry baseband to an RF signal of required frequency and power

e) an antenna and feed system for proper radiation and receiving of the RF telemetry and command signals.

A block diagram of the Telemetry and Command Subsystem is shown in Figure 3-1. Note that redundant equipments are added, an aspect that we will discuss later in this section.

3.1.3 Transmission and Frequency Considerations

The Work Statement calls for a beacon transmission, during orbit manoeuvers, at a frequency in the VHF band. We will assume that for practical purposes, the beacon frequency is in the 136 MHz or 137 MHz Telemetry Band. After orbital manoeuvers are completed, the transmissions will be transferred to the 4 GHz band for operational purposes.

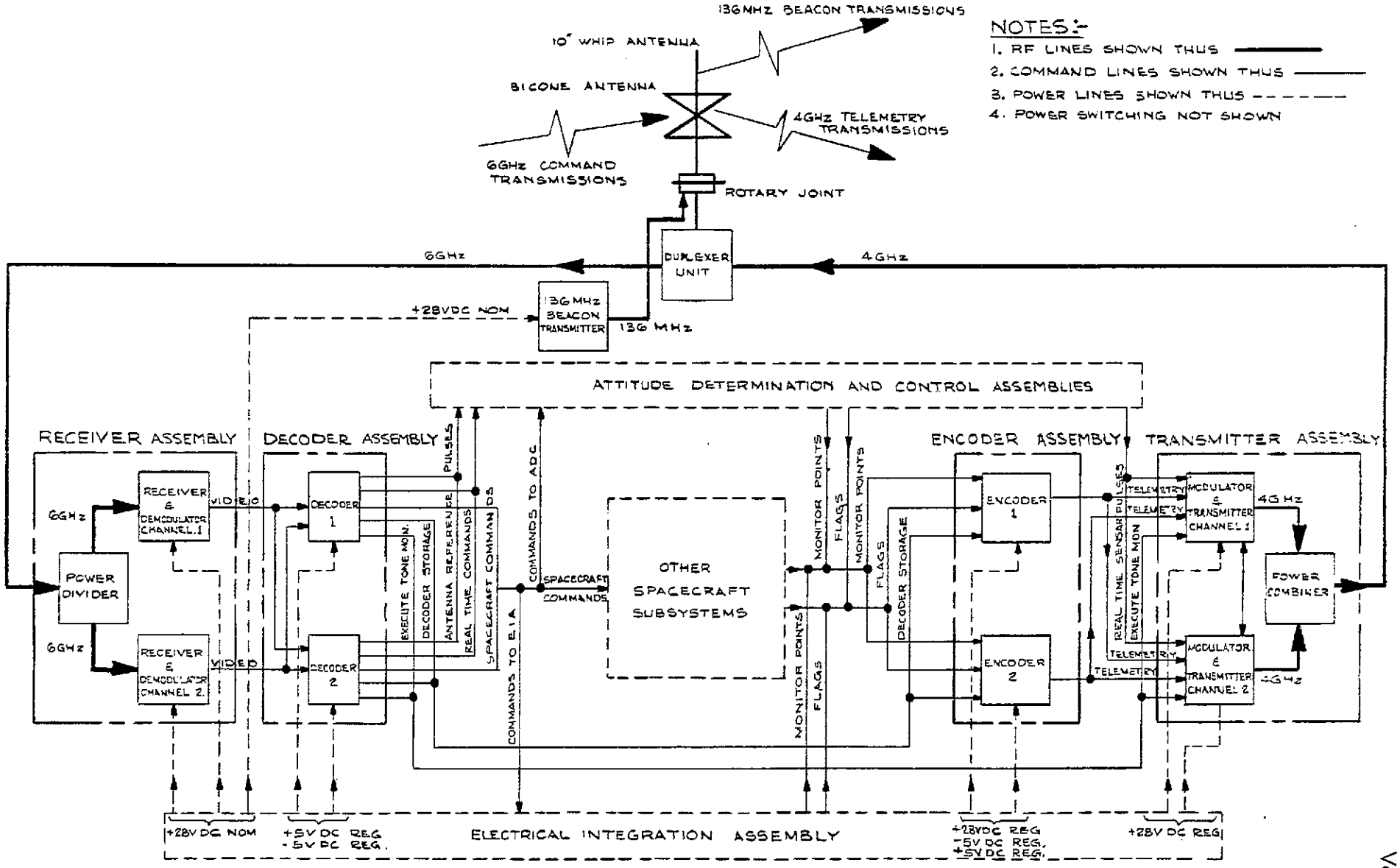

Figure 3–1 Block Diagram Telemetry and Command Sub System

In studying the case for beacon transmissions at two frequencies, we note that VHF is primarily required for safety reasons during the initial phases of the launch operations. VHF transmissions ensure

a) relatively simple initial aquisition following launch and

b) continuous tracking in the parking or transfer orbits

using the NASA STADAN or Minitrack networks. Aquisition and tracking capabilities do not exist in the 4 GHz bands at these stations.

Whether telemetry data should be placed on the VHF carrier, however, requires some further consideration. Telemetry during the initial orbital phases is required to first check out the "state-of-health" of the satellite and from then on to provide continuous monitor information of the sensor outputs and operational status.

The attitude of the spacecraft is determined from the telemetered sensor data, and from this the orbital manoeuvering control requirements are established. Thus telemetry must be available somewhat in advance of the orbital manoeuver events.

Since orbital manoeuvering requires control, and hence command capability, let us consider the command signal. The Work Statement provides no guidelines on the choice of Command frequencies. However, for the foregoing discussions on Beacons and Telemetry, we may consider that potential assignments for the Command signals would lie in the 148 MHz band or in the 6 GHz band, or both.

Command capability at 148 MHz permits commanding via NASA facilities in principle, subject to the condition that NASA Command Standards be followed. This, of course, would not only permit complete freedom in command timing, but would also

a) allow command capability outside of Canada by other than Canadian Authrotities, and

b) be susceptible to stray commands

since the 148 MHz system is relatively heavily loaded. Thus, in principle, we should avoid the 148 MHz band and only consider the 6 GHz band.

The 6 GHz common carrier band is a protected band, but since there is no CommandStandard established for use in this band, we can develop our own system for maximum protection and for optimum complexity as long as our RF transmissions do not contravene the CCIR recommended characteristics.

The earth based antenna used for command transmissions may be assumed to be either the communications antenna, or one of equivalent dimensions. Its beam width is narrow therefore accurate aquisition is necessary before command capability is available. We conclude that aquisition by the 4 GHz antenna must be an accomplished fact before commanding.

We now visualize that the telemetry signals necessary for monitoring before orbital manoeuvers are begun can be transmitted via the 4 GHz link rather than via the 136 MHz link. The 136 MHz link may thus be relegated to a simple beacon function. In view of this we will call the 136 MHz transmission the Beacon and the 4 GHz transmission the Telemetry Signal.

With regard to the locations of the Telemetry and Command signals in the 4 and 6 GHz communications bands, we assume no restrictions so as to permit any channelling plan to be used. However, a recommended channelling plan for the subject system has been proposed (see Section 1) in which the Telemetry and Command signals are placed very near the band edges.

3.1.4 Carrier Modulation

Conventional Frequency Modulation (FM) techniques are the most suitable for the Command link since FM

a) provides a power advantage
b) provides some protection against the effect of spurious interfering signals, and
c) FM theory is well known.

However, Phase Modulation (PM) techniques are used for the Telemetry because in addition to the above, PM

d) provides a residual carrier for tracking.

Other modulation techniques such as SSBFM, while being more efficient with respect to information transmission vs transmitter power, are more complex than FM thereby posing a possible reliability hazard.

3.1.5 Redundancy

A failure in the Command or Telemetry equipment in the spacecraft would seriously impair the spacecraft usefulness. To improve the reliability of this subsystem, therefore, we must provide parallel redundancy of the major units. Thus, for command:

a) The two command receivers, each driven by half of the available received command power, are available and always powered. Failure of one receiver will not affect the operation of the other.

b) The two command decoders supplied will each be driven by the output from both receivers. The loss of one receiver will not affect the decoder operation. Either receiver can then drive either decoder. The decoders will both be always powered.

c) The decoder outputs will be paralleled. Loss of one decoder will not affect command capability.

and for telemetry:

a) Two separate but identical encoders will be provided, but only one will be on at a time, selectable on command.

b) The transmitter will be a dual channel phased system so that the RF signal outputs can be added to boost the output power by almost 3 dB. Dual capacity will be used during launch and tracking and telemetry for "to-station" manoeuvering.

c) Either of the transmitters can be turned off to conserve power. The 3 dB power loss resulting will be subtracted from margin only, therefore, the specified performance should still be available most of the time.

d) At least one transmitter will be on to ensure that a tracking beacon is available at all times. Automatic transfer from one channel to the other in the event of failure should be provided.

3.1.6 Command Concept

Faulty commands can occur either because the command has been corrupted during transmission by natural causes (e.g. noise) or because it was incorrectly transmitted in the first place (e.g. operator error). For this reason we select a command procedure whereby the command consists of two instructions:

a) A command instruction is transmitted and stored in the spacecraft decoder, then the contents of the store are telemetered to earth

b) After verification of the telemetered command instruction, an execute instruction (tone) is transmitted to cause the spacecraft to effect that instruction.

This procedure, while it does not reduce the probability of incorrect command instructions, does help to improve operational reliability by permitting identification and correction of incorrect command instructions before they are executed.

While command verification is suggested as the normal operational procedure, it does not preclude transmission of the execute instruction. Thus, in the unlikely event of a telemetry system failure, either in the spacecraft or in the ground equipment, resulting in the inability to receive command verification, we could still execute the command normally, trusting that the command has been received. This is an important consideration.

3.1.7 Telemetry Concept

The complexity of the spacecraft with respect to communications and the requirement for rather exacting station-keeping performance imposes a necessity for monitoring both sampled and real time data. Telemetry transmission of the sampled data is relatively easily achieved using a time division multiplex technique such as PAM or PCM (See section 3.3.4).

The real time data may be either transmitted in real time, or processed "on board" for transmission in a coded format which would fit in with the sampled data. The advantage of "on board" processing is that a very considerable reduction in required signal bandwidth over that needed for direct real time transmission can be achieved. The disadvantage is that more equipment complexity is necessary because of the processing.

Since we are primarily interested in simplicity, we favor the more direct real time transmission of real time data, even though it involves a loss of information efficiency. Subsequent calculations show that the required telemetry transmitter power is not too excessive, nor does it place an undue burden on the power capability of the spacecraft.

To handle several real time signals we make use of frequency division multiplex using conventional sub-carrier techniques. The composite time division multiplexed signal may then be treated as one of real time signals.

In general, IRIG standards are applied to sub-carrier parameters. However, a non-IRIG sub-carrier is used for the Telemetry signal because of spacecraft equipment simplicity and the possibility of using coherent detection for recovery of the signal at the earth terminal.

3.1.8 Ranging

In ranging, continuous tones are transmitted to the spacecraft and returned to earth via a transponder in the spacecraft. The recovered signals are then phase compared with the transmitted signals, and the measured phase differences are used to compute range. Several tones must be used to resolve range ambiguities which might otherwise discredit the results. Figure 3-2 is a block diagram of the ranging system. The ranging system can thus be seen to be similar to radar in that the signal must travel a distance 2R to determine the range R.

The ranging accuracy required is not specified in the work statement. We have assumed that a basic uncertainty of $\pm$ 150 meters (at the 3 σ error level) is adequate and have established the requirements for ranging tone frequencies and signal-to-noise ratio requirements, accordingly. The calculations are given in Appendix A to Volume 3. Here we shall state the results.

Four ranging tones at a S/N ratio not exceeding 30 dB are required to resolve range ambiguities to 1000 kilometers (we assume that we always know range to at least this value) with a basic accuracy of $\pm$ 150 meters. The tone frequencies are

$$fr_1 = 100 \text{ Hz}$$
$$fr_2 = 800 \text{ Hz}$$
$$fr_3 = 6{,}400 \text{ Hz}$$
$$fr_4 = 50{,}000 \text{ Hz}$$

The two lower frequencies are too close to the carrier frequency for convenient demodulating. They will therefore be upconverted using the 6400 Hz and transmitted at 6300 and 5600 Hz respectively.

The received tones will be recovered on the ground and after phase locking, the 100 Hz and the 800 Hz signals will be recovered by mixing both the 6300 Hz and 5600 Hz tones with the 6400 Hz tones.

3.1.9 Artificial Earth Pulse Operation

Failure of one of the two earth sensors on board the spacecraft leaves the earth "lock-on" capability for the communications antenna susceptible to interference by the sun and the moon as these heavenly

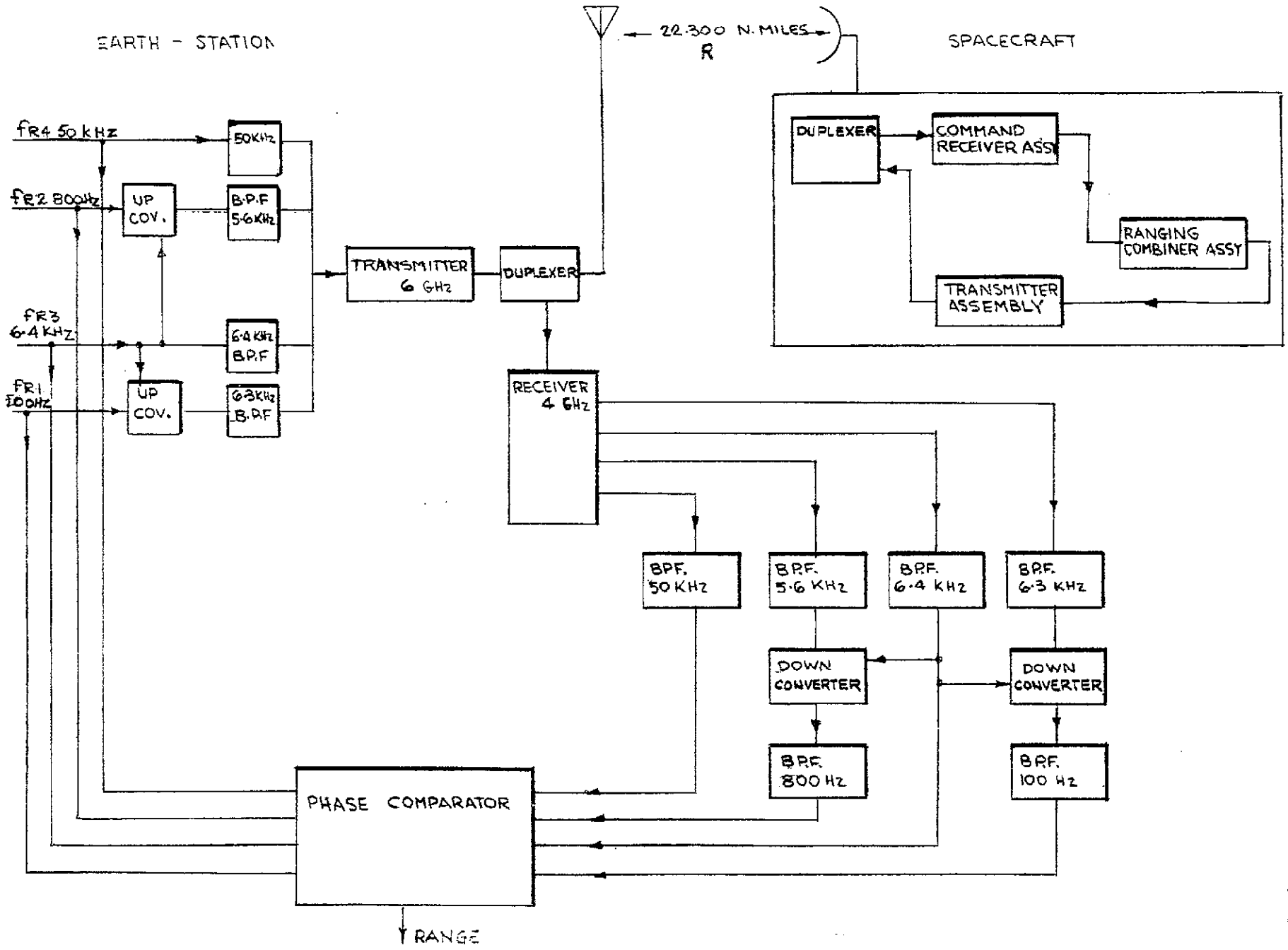

Figure 3–2 Ranging System Block Diagram

bodies become eclipsed by the earth as seen from the satellite. Failure of both earth sensors, of course, results in complete loss of automatic "lock-on". It is the function of the artificial earth pulses to restore lock capability, as the title applies, in an artificial manner. A detailed description of the operation is given in section 5.

From the straight command and telemetry point of view, all that we are required to do is to ensure that the transmitted pulses from the earth are received by the spacecraft without being significantly corrupted by noise or altered by bandwidth limitations.

Since the pulses are intended to replace the regular earth generated pulses we must ensure that they are of at least equivalent quality. As far as pulse shape is concerned, we should reasonably assume that as long as the shape is reasonably pulse-like, and neglecting jitter, then the pulse-timing can be adjusted to cancel out slight differences which may arise due to variations between the pulse shapes of the real and artificial pulses.

In normal operation, a peak-signal-to-rms-noise value of 30 dB is sufficient for satisfactory station keeping performance and is therefore applicable to the artificial earth pulse as well. Since the artificial earth pulses are derived from telemetered sensor and antenna pulse data we must apportion the S/N ratios between the up and the down paths.

If we are to maintain spacecraft telemetry transmitter power to as low a level as practical, we must allow more noise in the down link than the up link. We therefore assume that down link noise is 10 dB less than up link noise. Thus, the rms-signal-to-rms-noise ratio requirements for the transmission of artificial earth pulses to the satellite is

$$S/N = 37 \text{ dB}$$

3.1.10 System Configuration and General Specification

From these basic considerations we may now establish the concept for telemetry and command. The system block diagram has already been given (Figure 3-1) and shows how it interfaces with the remainder of the spacecraft.

We may now summarize the parameters established for the Telemetry and Command Subsystem on the general basis developed thus far. This is given in Table 3.1.

Table 3.1

Provisional General Subsystem Specification		
Parameter	Area	Comment
Operating Frequency	Command Telemetry Beacon	In the 5.925 to 6.425 GHz band In the 3.7 to 4.2 GHz band In the 130 to 137 MHz band
Carrier Modulation	Command Telemetry	FM PM
Redundancy	General	All units except Beacon redundant
Command Concept	Command	Verify before execute
Telemetry Concept	Telemetry	FDM for real time channels TDM for sampled channels
Ranging	General	4 Tone CW
Ranging tone frequencies	General	100 Hz 800 Hz 6400 Hz 50,000 Hz
Artificial Earth Pulse	Command	Real Time Subcarrier FM modulated
Subcarriers	General	IRIG Channels except for telemetry

3.2 COMMAND SYSTEM

3.2.1 General

The command system is required to permit operational changes to the operating state of the spacecraft as desired. It must be capable of achieving this safely and securely, without operational difficulty, and without interfering with the other systems. We begin the discussion with the requirements for command protection.

3.2.2 Command Protection

We may visualize an operational satellite communications system as consisting of a number of orbiting satellite terminals coupling into a grid of communications-satellite earth stations. For efficient and reliable service, we require that the satellites be under strict control, both electrical and orbital, by one or perhaps two earth stations in the grid. We further require that the control be both flexible and secure.

At the outset we should define our terminology. Flexibility, as used in the context of this study, means;

a) The ability to set up a spacecraft into any or all of its operational configurations.
b) The ability to correctly position the spacecraft as required by station-keeping considerations.
c) The ability to control all of the orbiting spacecraft comprising the system, and
d) The provision of sufficient redundancy to allow at least restricted performance should certain key circuits fail.

When we come to "security", we must comment that we do not mean security in the Military sense wherein it includes the freedom and protection against deliberate interference by an adversary. We mean security in the narrower sense of;

a) Rejecting incorrectly transmitted commands.
b) Rejecting commands corrupted by random noise.
c) Protection against interfering carriers.
d) Protection against the effect of equipment failures.
e) Protection against gross operator errors.
f) Protection against commanding the wrong spacecraft.

In short, we do not assume malicious intent.

Let us also define several more terms:

Missed Command or address	- A correctly transmitted command or address rejected by the spacecraft due to noise corruption, reduced antenna gain or other causes.
False Command	- A correctly transmitted command corrupted by noise or other causes, but accepted by the spacecraft.
Incorrect Command	- A wrong command due to either operator error or ground equipment failing.
False Address	- A correctly transmitted address corrupted by noise or other causes, but accepted by the wrong spacecraft.
Incorrect Address	- A correctly transmitted address corrupted by noise or by other causes and rightly rejected by the spacecraft.

Of the above unwanted situations we may say that as long as the number of missed commands or addresses is not too great, they should not cause great concern inasmuch as precise timing of commands is not essential and we usually will have ample time to retransmit the command.

On the other hand, a false command, which may cause an unwanted action to occur in the spacecraft, is clearly undesirable and we must therefore take steps to prevent its occurence.

Even worse, a falsely addressed command which causes an action to occur in an unwanted spacecraft may result in considerable operator confusion which can impair service for substantial periods of time before the unwanted action can be identified and cleared.

Therefore in terms of the probabilities of occurence the order of security must be;

a) Security against false addresses.
b) Security against false commands.
c) Security against missed addresses or commands.

3.2.3 Command System Standards

In selecting an appropriate command system, we may first examine some of the systems currently standardized and in use in space endeavors. The most advanced and practical of the standards is probably the Aerospace Data Systems Standards, NASA Document X-560-63-2 issued by Goddard Space Flight Center. For Command purposes, the Aerospace Standards list three systems. These are;

a) Tone Command Standard, latest issue 11 Aug/66.
b) Tone Digital Command Standard, latest issue 15 Jan/63.
c) PCM Command Data System Standard, latest issue 23 April/68.

We shall very briefly outline the major features of each standard.

a) Tone Command System

In this system, the commands are identified by a specific assembly of discrete audio tones. Usually, the tones are sounded in serial time sequence and the command is identified by the frequency and the order of tones. The possible number of commands is given by M^N where M is the number of tones in a given command, and N is the overall number of different tones. Some degree of protection is given by requiring that no tone be sounded more than once in a given command. In this case the possible number of commands is given by M!/N!.

A second set of tones, different from the above tones (which are called the execute tones), is reserved for addressing. Each orbiting spacecraft is assigned a unique address tone and, in order that that spacecraft, but no other, respond to a transmitted command, the execute tones are preceded by the address tone.

The tone command thus consists of an address tone followed by several execute tones.

b) Tone Digital Command System

The Tone Digital System makes use of a digital code to identify the command. The coded command then 100% modulates a carrier tone to produce tone bursts.

PDM coding is used. A digital "1" is represented by a tone burst lasting 1/2 bit period whilst a digital "0" is represented by a tone burst lasting 1/4 bit period.

A complete tone digital command consists of a synch tone burst followed by a command text (comprised of an address and a command) and then a blank interval. The basic format must be complete and in the correct sequence before a command can be accepted. Further protection may be obtained by requiring that the address and the command text be sent twice and compared for agreement before acceptance.

c) PCM Command System

The PCM Command System is used where a high capacity command is required. The commands are coded in a PCM format, and the resulting binary signal is used to "frequency shift key" an SCO so that one frequency represents a "0" and the other represents a "1". A clocking signal is transmitted as an AM modulation of the sub-carrier produced by the SCO.

The command is preceded by 13 "0", a "1", and a 7 bit command address. The command text can be up to 64 bits duration.

Protection can be provided by requiring that both the address and the test be transmitted twice and compared for agreement before acceptance.

3.2.4 Command System Selection

The tone digital system is the least desirable system for a communications satellite. The requirement of one filter per tone means that seven or eight tone filters would be required in each command decoder to provide the address and command capability necessary for the system.

The tone digital system has the merit of simplicity in that only one tone frequency is required. However, as is shown in Appendix C , the use of a PDM code to establish binary "1"s and "0"s gets a penalty of almost 3 dB in signal-to-noise ratio.

The PCM command system is the most flexible and has been selected for use in the subject command system, even though two tones are required for commands. We have not followed the NASA standard, however, with respect to the clocking signal. In the NASA standards, the clock is an AM signal superimposed on the command subcarrier while the command itself is transmitted in NRz form. We have, however, used an Rz form for command transmission which is a self clocking code thereby not requiring a separate clock transmission.

The use of Rz coding results in a simplified command decoding concept.

A practical PCM basic command text for the Canadian communications spacecraft is one consisting of 12 bits transmitted in serial form. The first 5 bits are reserved for the address instruction while the remaining 7 are reserved for the command instruction.

The use of 5 bits for address allows 32 different addresses. The 7 bits in command instruction permits a capability of 128 commands, which, as will be seen later, is more than adequate.

3.2.5 Error Rates

If we say that we can tolerate one command error every second year on the basis of transmission of 100 commands per day (highly improbable), our bit error rate (assuming equally likely '1' and '0' errors) would be about 1 every 10^6 bits. On this basis we would have an address error about once every 2 years.

If there were as many spacecraft as there are 5 bit combinations in the address (32) then the consequence of an address error would be commanding the wrong spacecraft. This, of course, assumes that there is no discrimination by spatial means (such as command antenna pointing) between the spacecraft.* A false address is most definitely an undesirable event, hence we must minimize the probability of its occurence. One of the simplest ways of achieving this is to require the transmission of an address twice and reject the command if the two transmitted addresses are not exactly alike. We have now protected ourself from acceptance of an incorrect address but have doubled its probability.

The probability of exactly identical errors in the two address texts is insignificant over the spacecraft's lifetime. However, a complement of 16 spacecraft seems sufficient, which will allow us to use one of the five address bits as a parity bit. For false address this would require an error of two bits in five. The probability of this event occuring is negligible, hence we have further reduced the probability of false address.

Therefore, with a bit error rate of 1 in 10^6 bits, we will have probabily of missed command only once per year at a rate of 100 commands per year, and a negligible probability of false address or command, due to purely random processes.

3.2.6 Command Classification

The basic command principle that is recommended is to "verify before execute". This requires that the instruction portion of the command be transmitted and stored in the spacecraft's decoder command register but not otherwise immediately acted upon. The contents of the register are telemetered to earth at a relatively fast rate to enable the operator to verify that the command has been correctly transmitted and stored. At that point the operator can then transmit the execute portion of the command and cause the spacecraft to respond to the command instruction accordingly.

The relative flexibility and complexity of the subject spacecraft implies that many commands would be required. Further we may assume that not all commands are of a similar nature. We should therefore make some attempt at a classification, and to assist us here we use the designations type S, type B, type R and Type A.

a) Type S Commands

Most operational commands to the spacecraft simply require that the equipment on board be switched into a particular configuration. Thus, for example, the number of communications TWT's in operation at a given time is determined by commanding individually the required TWT "on".

* We shall maintain this pessimistic assumption for the sake of being conservative.

The transmitted command is identified in the spacecraft decoder. Once identified, accepted and executed, the command appears as a discrete pulse on the appropriate output terminal of the decoder. Since this pulse Sets the spacecraft into a specific configuration, it is designated as a type S pulse. It may be used to set a mechanical latching relay, or a flip-flop, as necessary.

b) Type R Commands

During those times in which orbit maneuvering or station-keeping operations are in progress, the command system must be used to operate on-board thrusters in real time which in turn operate on the spacecraft orbital or attitude characteristics. (See section 4 for a more detailed discussion of attitude control operation).

The commands to fire thrusters may be in the form of a continuous tones, lasting as little as 30 milli-seconds or as long as several minutes, or may be intermittent occuring for short intervals of time synchronized with the spacecraft spin.

These commands, being sent in Real time, are designated as Type R.

Note that in order for a Type R command to be accepted, a Type S command must first be transmitted to set the spacecraft into a configuration so that the Type R command will operate the correct thruster.

c) Type A Commands

A specific set of commands are reserved for Adjustment of the attenuator settings of the output TWT's of the communications system, and for adjustment of the bias setting of the despin motor system for station-keeping. The command code here is the digital coding for the value to which the TWT attenuator or the bias setting is to be adjusted. This command must be preceded by the type S command which selects the device requiring adjustment.

d) Type C Command

One specific failure involving earth sensors, coupled with the interference of the sun with the operation of the other earth sensor, requires the replacement of the earth sensor pulse signal by an artificial earth pulse (AEP) generated by earth-based equipment at the command location.

These artificial earth pulses must be transmitted Continuously as long as the sun interference is present, a type C command.

As in the case of type R commands, this type C command requires prior transmission of the appropriate type S command to set the spacecraft into the proper configuration.

e) Listings of Commands

A tentative listings of commands for the spacecraft is given in Appendix B. Table 3.2 'sumarizes these lists with respect to spacecraft subsystem and command type.

Table 3.2

Summary of Command System Provisional Listing					
Ref. Table	Subsystem	Type			
		S	R	C	A
B.1	Command and Telemetry	10	-	-	-
B.2	Spacecraft Control	12	4	1	1
B.3	Communication	38	-	-	5
B.4	Power	9	-	-	-
	TOTALS	69	4	1	6

3.2.7 Command and Execute Texts

At the end of section 3.2.5, we have seen that the basic 12 bit command text suggested is required to be transmitted twice and compared before acceptance. We must now consider the beginning and end periods of transmission. We have, however, one further point to establish. When commands are not transmitted, the decoder should be "set" into a quiescent mode wherein the receiver output is gated to prevent noise from possibly influencing the command register contents.

A synchronizing tone pulse of 2 1/2 bits duration, preceding the command instruction in a 1/2 bit interval, is added to the transmitted command signal to "set" the decoder. The tone frequency for this pulse is the same as that used for a "1" transmission. A filter circuit at the decoder input will recognize the synchronizing tone and cause the gate circuit to open permitting the command text to pass into the decoding circuitry. The relatively wide synchronizing pulse width allows the use of a comparatively narrow band filter thereby increasing the signal-to-noise ratio requirements for "setting" the decoder and thus provides a greater noise immunity against false command.

The gate will remain open as long as the command text bits are passing through. When no bits occur for a time duration of three bits, the gate will close. Thus the end of transmission is indicated by a three bit "silent" interval during which no tones are transmitted.

Thus a complete command transmission will require a 30 bit time duration as shown in Figure 3.3. The execute part of a command cannot begin until the end of the three bit silent interval.

We will not require transmission of an execute instruction twice. Further, the format of the execute text will differ slightly depending upon the preceding command classification. If the command instruction was a type S or a type A, then the execute instruction would consist of a synchronizing pulse, a 5 bit address, a one bit gap and the execute tone for a duration of 6 bits. A three bit duration gap at the end of the text would indicate completion of the entire command and would reset the decoder.

However, if the command instruction was a type R command, then the execute tone sequence would be variable both in duration and number since the execute tones are used to operate on-board equipment on real time. The decoder would not reset until a specific RESET command instruction is transmitted.*

The execute instruction texts are shown in figure 3.4.

3.2.8 Command Performance Requirements

Earlier it has been shown that the most appropriate command system for our requirements is the tone digital system. In this system two techniques stand out for simplicity:

1) Pulse duration modulation (P.D.M.)
2) Frequency shift key system (F.S.K.)

A comparison of these two systems, as discussed in Appendix C, shows that for the F.S.K. system, the signal-to-noise ratio is 2.7 dB less than for the P.D.M. system: Also, the distinction between "1" and "0" is achieved by using two tones in the F.S.K. system while a pulse width detector would be required for the same purpose in the P.D.M. system.

Clearly, the F.S.K. system has distinct advantages over the P.D.M. system and hence it is chosen for the command system.

3.2.9 Command Receiver Bandwidth and Signal Deviation Considerations

The command system consists of the following signals:

1) Two tones for the operational commands to the spacecraft.
2) Execute tone.
3) 4 Ranging tones.
4) A sub-carrier modulated by artificial earth pulses.

* The RESET command will not require execution. The command text itself is sufficient for the resetting action to occur.

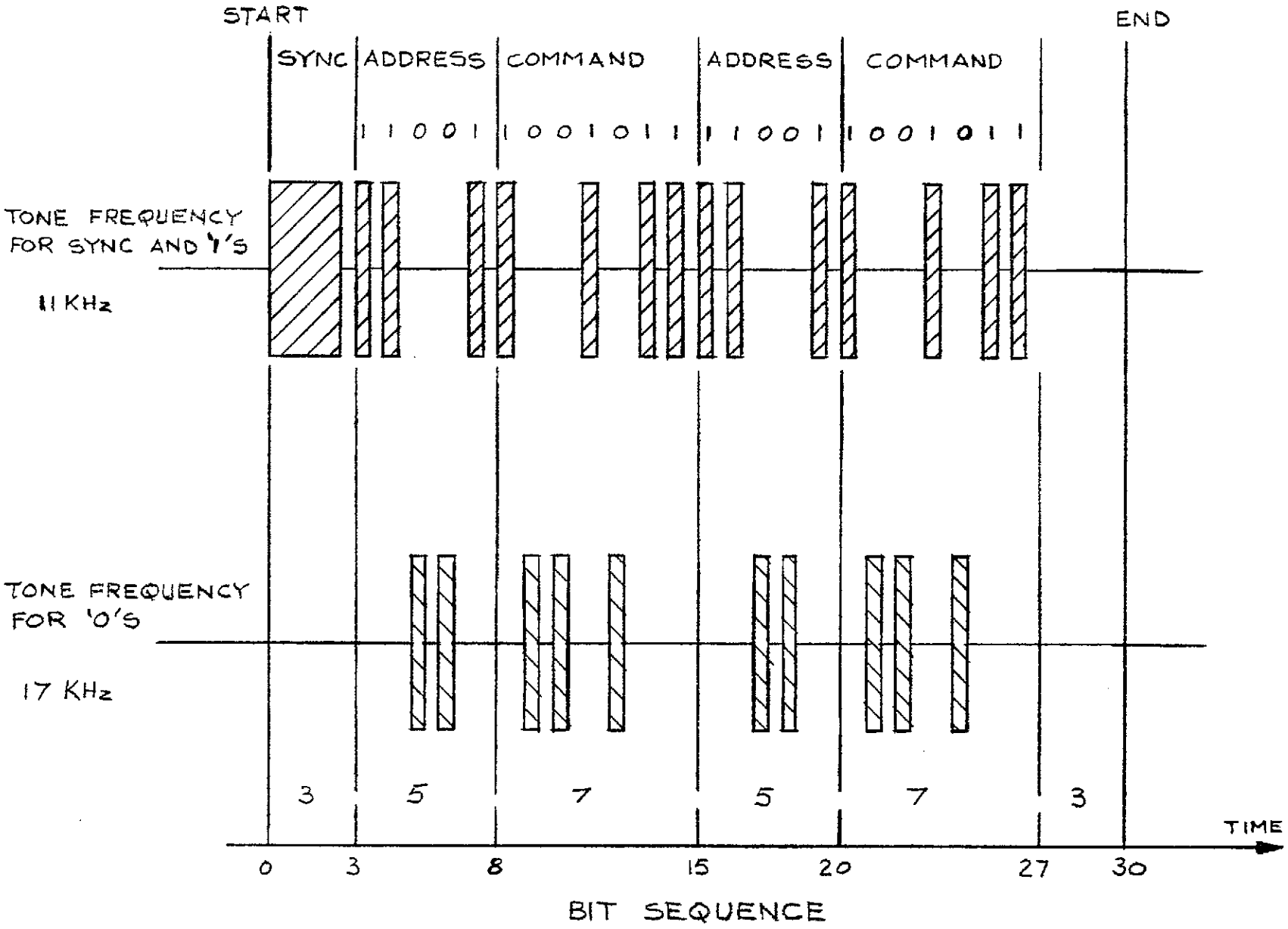

Figure 3–3 Command Instruction Text

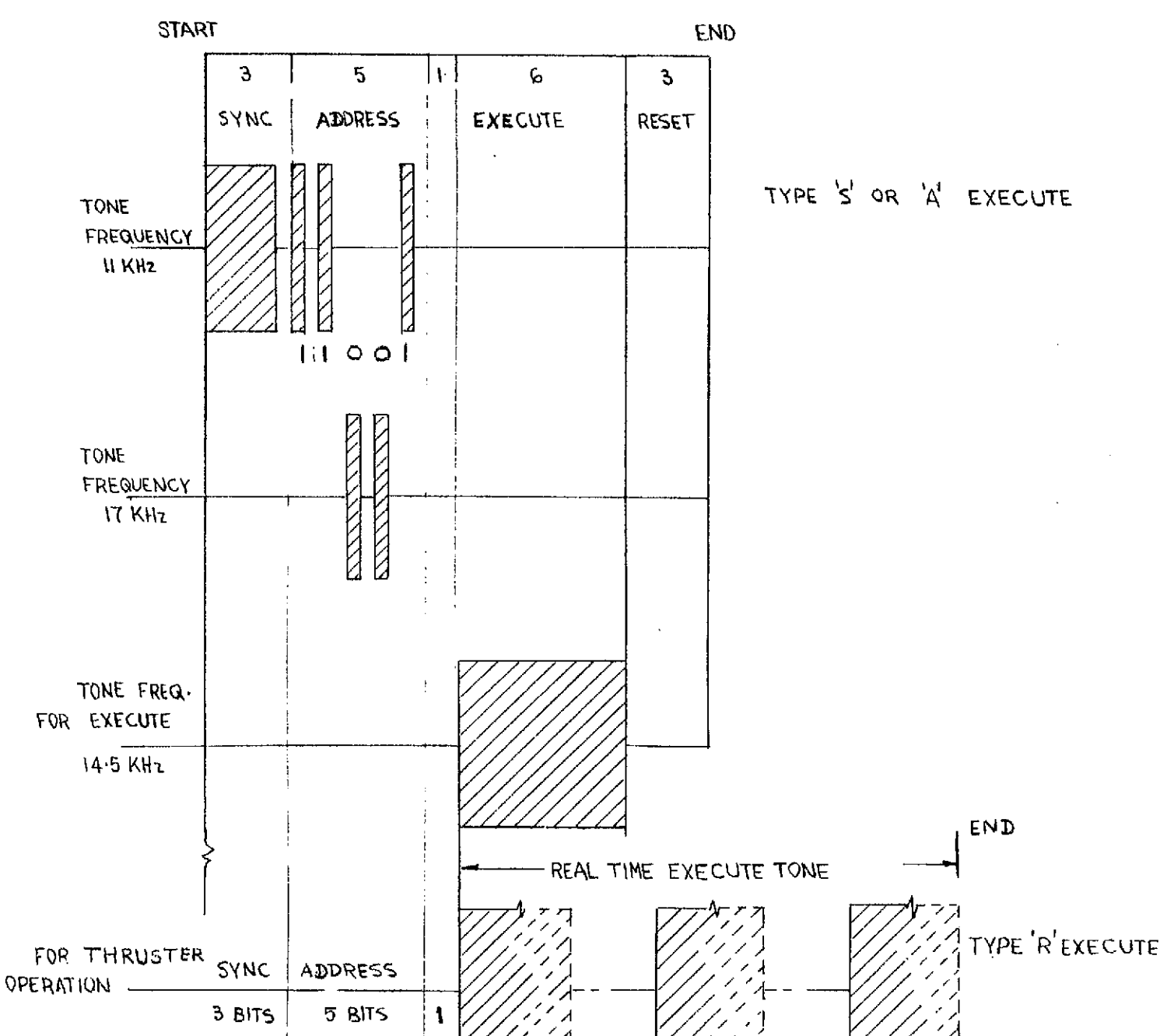

Figure 3–4 Execute Instruction Tests

Only one of the operational command tones or the execute tone is present at one time. This tone, however, can be present with any or all of the ranging tones and the sub-carrier recognizing these facts, optimum carrier deviations were calculated and used to establish the receiver noise bandwidth of 431 kHz. (See Appendix D) For these calculations, the receiver threshold is taken at a 10 dB carrier-to-noise ratio operating point.

3.2.10 Command System RF Link

The basic Command System RF link is shown in Fig. 3.5. The transmitter power required is calculated using the RF equation as follows:

$$Pc = Pr - Gc - Gr + Lp + Pa$$

where:

Pr = Minimum carrier power required
Gc = Transmitting antenna gain (60 ft. parabola)
Gr = Receiving antenna gain
Lp = Path loss
Pa = Atmospheric loss

The values for these constants, as derived in Appendix D, are as follows:

Pr = -112.7 dBW	for receiver noise figure of 15 dB and receiver noise bandwidth of 431 kHz
Gc = 59.0 dB	at 6.425 GHz and antenna efficiency of 50%
Gr = 0 dB	
Lp = 200.7 dB	for a slant range of 22,300 n miles
Pa = 1.0 dB	

Thus:

$$Pc = -112.0 - 59.0 - 0 + 200.7 + 1 \text{ dBW}$$
$$= +30.7 \text{ dBW}$$
$$= 1 \text{ KW}$$

is the required transmitter power measured at the earth station antenna terminals.

3.2.11 Command Signal Baseband

The frequencies of various baseband signals are so chosen as to have minimum harmonic interference with each other. The ranging tones frequencies have been specified already (see Appendix A and Section 3.1.7) and are 50 kHz, 6.4 kHz, 800 Hz and 100 Hz. To improve the performance the lower two tones are up converted using 6.4 kHz to give transmitted baseband frequencies of 50 kHz, 6.4 kHz, 6.3 kHz, and 5.6 kHz.

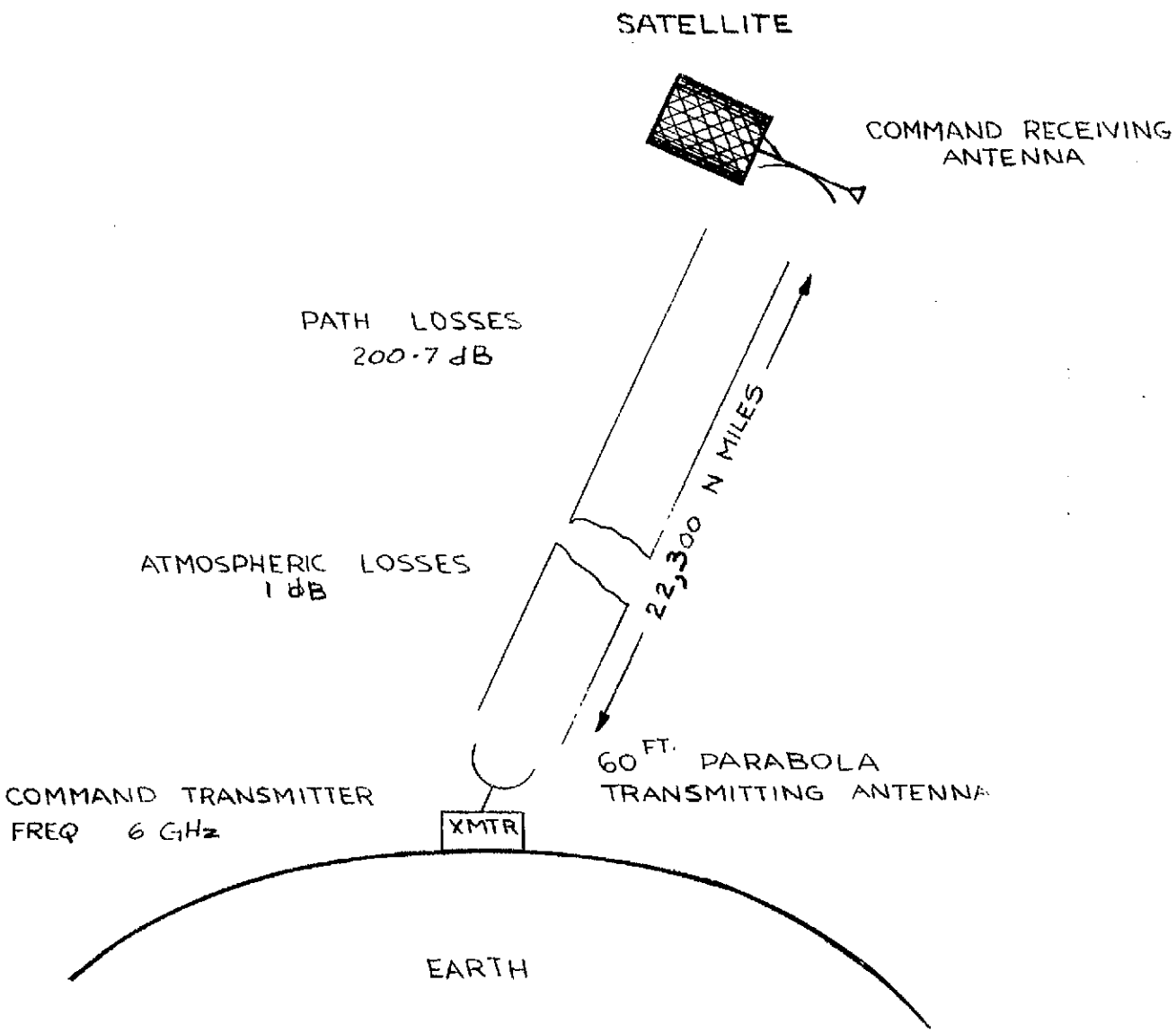

Figure 3–5 Command System RF Link

The artificial earth pulse sub-carrier frequency is chosen from the I.R.I.G. standard frequencies. For a modulation index of 4.8 and signal bandwidth 250 Hz, a 22 kHz sub-carrier frequency is the lowest that can be used and was therefore selected.

The operational tones may now be chosen. A reasonable frequency choice for these tones is 13.0 kHz for the "1"s and the synchronizing tone, 17 kHz for the "0"s tone and 14.5 kHz for the execute tone. Note that among the three operational command tones only one is present at any one time.

The command baseband system is shown in Figure 3.6.

3.2.12 Tentative Command Specifications

Table 3.3 lists the overall specifications for the command system developed in the previous pages.

Table 3.3

Summary of Tentative Command System Specifications

Instructions	Address, Command, Execute
Type	Verify Before Execute
Address Instruction	5 bits (1 bit parity)
Command Instruction	7 bits
Redundancy	Command Transmitted Twice
Bit Error Rate (thermal)	1×10^{-6} @ 10 dB C/N
Command Synch Tone	13 kHz
Command "1" Tone	13 kHz
Command "0" Tone	17 kHz
Execute Tone	14.5 kHz
Address Capacity	16 spacecraft
Command Capacity	128 commands/spacecraft
Command Classification	Types S, A, R, C
Type S	Set Command
Type A	Adjust Commands
Type R	Real Time Commands
Type C	Continuous Artificial Earth Pulses
Ranging Up Link	4 Tones: 100 Hz upconverted to 6.3 kHz 800 Hz upconverted to 5.6 kHz 6.4 kHz 50 kHz
Modulation	FM
RF Frequency Power (Nominal)	in 6 GHz Common Carrier Band 1 KW into 60' parabolic antenna terminals.

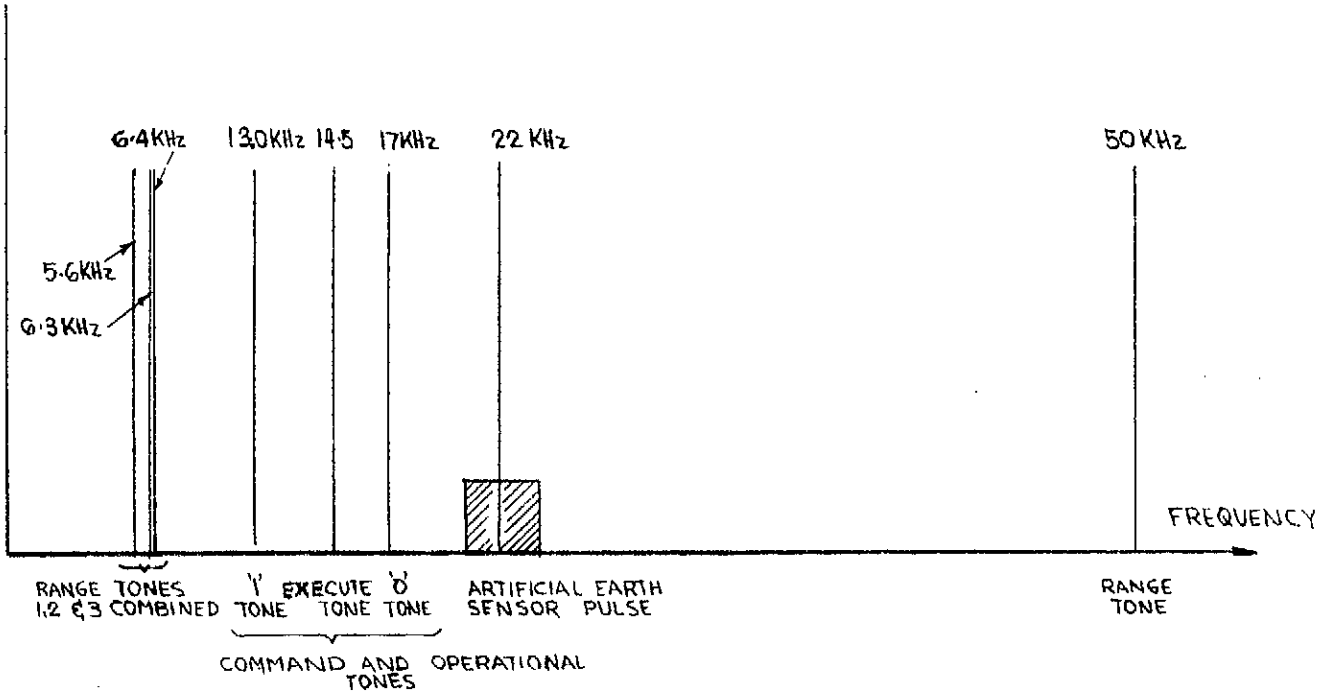

NOTE: ONLY ONE OF THE THREE COMMAND OPERATIONAL TONES IS PRESENT AT A GIVEN TIME.

Figure 3–6 Command Base Band Spectrum

3.3 TELEMETRY SYSTEM

3.3.1 General

The spacecraft telemetry system must provide the ground operator with information relating to the general "health" of the satellite, the operational set-up in use, the return ranging signals, and so forth. This information is quite diverse in its characteristics, as we shall see, therefore we must expect that the telemetry signal requirements be somewhat complex. We begin the development of this signal by first examining the basic types of information that must be telemetered. Table 3.4 lists the types. We shall now discuss them.

3.3.2 Basic Telemetered Signals

a) Housekeeping Signals

The operating conditions and environment of the spacecraft will be assessed from sample measurements performed on the major electrical, thermal, etc., parameters of the spacecraft. The sample rate need not be too high, as variations of these parameters will ordinarily not occur very rapidly. However, there must be a sufficient number of parameters sampled so that a proper diagnosis of the spacecraft state (not status!) can be made.

b) Flags

The indicated flexibility of the spacecraft will permit selection of many configurations. For proper operational control, therefore, some type of "quick-look" facility should be provided to give operators an immediate appreciation of the configuration. This is an important consideration particularly during eclipse.

For that reason, status information indicating on/off or connected/disconnected status by means of a single binary digit will be provided. These indicators will be called "flags".

c) Spacecraft Signature

As the number of emitting spacecraft increases, the requirement for identification of each spacecraft becomes more important. Each spacecraft is therefore assumed to have, in some specific portion of the telemetry channel assignment, a unique "signature" consisting of a binary number, or other format. The signature will be transmitted at least once per sub-frame.

Signal	Characteristic	Data	Use	Note
Housekeeping	Analogue	Sampled	Diagnostic & Monitoring	Sample Rate Relatively Slow
Flags	Digital Bit	Sampled	Operational Monitoring	
Spacecraft Signature	Coded	Sampled	Monitoring	
Command Verification	Coded	Sampled	Operational Monitoring	Sample Rate Relatively Fast
Execute Monitoring	Analogue	Real Time	Operational Monitoring	
Earth Sensor I, Pulses	Analogue	Real Time	Operational Monitoring	Note
Earth Sensor II, Pulses	Analogue	Real Time	Operational Monitoring	Note
Antenna Reference Pulse	Analogue	Real Time	Operational Monitoring	
Sun Sensor Pulses	Analogue	Real Time	Operational Monitoring	Used primarily during Launch phase
Ranging Tones	Analogue	Real Time	Operation	Determines Range

Note (1) Earth Sensor Pulses are normally used for monitoring purposes only, but are required for operational control in a specific case wherein use of artificially generated Earth pulses are used. See Section 4.

Table 3.4 Basic Telemetered Signals

d) Command Verification

The present command concept is that a command instruction received by the spacecraft will not immediately be executed but will be stored in the command decoder. The contents of the store will be telemetered back to the ground station to permit the operator to verify that the command has been understood correctly by the spacecraft's decoder. After such verification the operator can then instruct the spacecraft to execute the stored command.

Command verification thus becomes an important part of the telemetry system and will be transmitted at rates reasonable for good operational practices.

e) Execute Monitoring

Following the verification all commands require specific execute instruction before they are acted on. Most commands simply require that an execute tone lasting about 47 msec be transmitted. If the execute tone is accepted, thereby permitting the command to be effected, then an execute monitor tone is transmitted via telemetry to the ground station thereby informing the operator that the command has been effected. If the execute monitor tone is not received via telemetry, there has been an incorrect transmission.

f) Earth Sensors I and II (Pulses)

The despin system required to keep the communications antenna "locked on" to the earth is described elsewhere (see section 4). Here we are only concerned with the requirements to monitor the pulses generated by the two optical earth sensor units of the despin system. These pulses are produced wherever the field-of-view of the sensor moves from deep space to the earth's disc, or vice versa. A positive pulse followed shortly after by a negative pulse is produced as the sensor's field-of-view crosses the earth.

g) Antenna Reference Pulse

The despin antenna platform is oriented so that the communication antenna points always to the earth. A magnetic sensor in the despin motor generates a pulse at the moment that the earth sensors field-of-view cross the earth's N-S axis line*, therefore the antenna reference pulse occurs in time midway between the earth sensor pulses. With the antenna reference pulses telemetered to earth, the ground operators can monitor the performance of the despin system.

* This, of course, assumes that successful earth lock has been achieved.

h) Sun Sensor Pulses

During the post-launch, but before the satellite is placed "on-station" the attitude of the spacecraft relative to the earth must be determined and monitored during the subsequent maneuvering in order that it be oriented correctly in space for firing of the apogee motor, and later for normal operation. Earth sensors cannot be used for this since their overall fields-of-view are too restrictive.

The sun sensor mounted on the spacecraft has a much greater operating field and view, but in order to provide unambiguous information as to the direction of the sun relative to the spacecraft, three pulses must be generated. The first pulse establishes a reference "longitude", the second establishes whether the sun-satellite direction vector is north or south of the satellite's equatorial plane* and the third pulse establishes the angle of the direction vector from the satellite's equatorial plane.

These three pulses, then,provide information from which the sun-satellite direction vector, using the satellite's co-ordinate system, can be extablished. Normal tracking measurements establish the earth-satellite direction vector and the earth-sun direction vector, hence satellite orientation with respect to the earth may be established (see Section 4).

i) Ranging Tones

These are the recovered form signal tones transmitted via the command system. Transmission of these tones is independent of any other consideration.

3.3.3 Multiplexing of Real Time Signals

We now must combine the various signals into one telemetry signal baseband. We will treat the sampled signals separately from the real time signals. Let us consider the latter first.

The real time signals such as the ranging tones and the execute tone differ in frequency, and this will permit separation of the signals by simple filtering. However, the four sensor pulse train signals are not so easily handled since they occupy essentially the same frequency bands. The most direct way of overcoming this problem is to modulate subcarriers of different frequencies with each of the signals. Separation of the sub-carriers after transmission is thereby simply achieved, again by direct filtering.

---

* Here we refer to the northern portion of the satellite as containing the antennas, whilst the southern portions contain the apogee motor.

Four signals require four subcarriers if complete separation is required. However, we should examine these signals first to see if some of them could be combined before modulation thereby reducing the number of subcarriers. This is not possible for the two earth sensor signals since the pulses occur at the same times for each. We also cannot add the sun sensor pulses to the earth sensor pulses, since there will be times when both will be in time coincidence causing interference. And it is at these times that the resolution between pulse trains will be needed most.

This leaves the antenna reference pulse train. During "locked-on" operation, these pulses occur midway between the positive and the negative earth sensor pulses, hence we can add the antenna and earth sensor pulses directly. If, however, "locked-on" is not achieved, then the antenna reference pulse will occur arbitrarily and so could interfere with the earth pulses. However, this should not prove to be a serious problem because "locked-on" is achieved automatically on board the spacecraft and does not require the telemetry link. Further, during artificial earth pulse operation, the control of the timing of the earth pulse is from the ground, and these would ordinarily be timed so that the antenna reference pulse fell midway between them.

We therefore assume that the real time signals are composed of a frequency multiplexed system consisting of;

a) ranging tones
b) execute tone
c) sub-carrier carrying earth sensor I and antenna reference pulses
d) sub-carrier carrying earth sensor II and antenna reference pulses
e) sub-carrier carrying sun sensor pulses.

Note that we have added the antenna reference pulse train to both earth sensor pulse trains for redundancy.

3.3.4 Multiplexing of Sampled Signals

We may now consider the sampled signals. These, we may recall, are made up of;

a) Housekeeping signals (analogue)
b) Flags (bit)
c) Spacecraft signature (coded)
d) Command verification (coded)

Since these are all sampled signals we may entertain the use of time multiplexing. The choice of multiplexing scheme must now be considered.

We find it convenient to make use of one or more of the basic time division multiplex schemes, PAM, PDM or PCM being the most common. PPM, DELTA modulation, and other schemes exist but offer little or no advantage over the basic ones so we will not consider them. A comparison of the PAM, PDM and PCM schemes for the sampled signals is given in Appendix E. There we have shown that of the three, PCM satisfies the telemetry requirements best hence we selected it for the coding scheme.

A basic 6 bit PCM word provides quantization accuracy better than 98% which is considered satisfactory for the analogue requirements as presently understood. The overall accuracy, including the effect of bit errors due to noise, is estimated to be about 95%. An improved accuracy would be obtained by reducing quantization error through the use of a 6 bit word. Such a move would result in an overall accuracy of about 3% assuming that the other parameters remained constant. The bit error rate would not be greatly affected since the increase in bit rate would only apply to analogue sampling.

A tentative listing of all the sampled channel to be telemetered is given in Appendix F. These are summarized and listed here in table 3.5 A suitable PCM format which combines these signals is given in Fig. 3.7. The PCM words are arranged for convenience into an 8 x 6 matrix.

Table 3.5

Summary of Sampled Telemetry Channel Listings

Ref. Table	Subsystem	Sample Types			
		Analogue	Flag	Verify	Signature
F.1	Command & Telemetry	8	6	14	5
F.2	Spacecraft Controls	10	4		
F.3	Communications	61	59		
F.4	Power	9	5		
	TOTALS	88	73	14	5
	Sample Transmission Rate (Seconds)	32	4	1	4-

WORD 1	2	3	4	5	6	7	8
SYNCHRONIZING PULSES		SUB FRAME IDENTIFICATION	ANALOGUE SAMPLES	COMMAND VERIFICATION		S/C SIGNATURE	ANALOGUE SAMPLES
9							16
FLAG SAMPLES	COMMAND VERIFICATION		ANALOGUE SAMPLES	FLAG SAMPLES			ANALOGUE SAMPLES
17							24
COMMAND VERIFICATION		FLAG SAMPLES	ANALOGUE SAMPLES	FLAG SAMPLES	COMMAND VERIFICATION		ANALOGUE SAMPLES
25							32
FLAG SAMPLES			ANALOGUE SAMPLES	COMMAND VERIFICATION		FLAG SAMPLES	ANALOGUE SAMPLES
33							40
FLAG SAMPLES	COMMAND VERIFICATION		ANALOGUE SAMPLES	FLAG SAMPLES			ANALOGUE SAMPLES
41						WORD	48
COMMAND VERIFICATION		FLAG SAMPLES	ANALOGUE SAMPLES	FLAG SAMPLES	COMMAND VERIFICATION		ANALOGUE SAMPLES

NOTES:
SUB FRAME DURATION 4 SEC.
WORD RATE - 12 WORDS/SEC
BITS/WORD - 6
BIT RATE - 72 BITS/SEC.

Figure 3–7 Typical Telemetry Sub Frame 48-Word Format

3.3.5 VHF Beacon Performance

We will assume that VHF tracking capabilities may be required for the spacecraft in the transfer orbit up to and including synchronous altitude. Under this assumption, and considering that a NASA minitrack station is involved, then we find that the Beacon Transmitter power output of 5 watts is required (See Appendix G).

If, however, tracking is performed by a STADAN station with a 9 element Yagi antenna, the required transmitter power may be reduced to 2.4 watts.

At this point, we recommend that a 5 watt beacon transmitter be specified since the added weight of a 5 watt transmitter over a 2 watt transmitter is not significant (both are "off-the-shelf") and the increased input power requirements is not a major consideration as the beacon usefulness will be over before the communications equipment is turned on operationally.

3.3.6 Telemetry Carrier Deviation

The telemetered signals received at the ground station would show in its baseband three sub-carriers modulated by real time sensor signals, one sub-carrier modulated by telemetry coded signals, one execute monitor and four ranging tones. The signal-to-noise ratio requirement for the component baseband signals are 13.3 dB for the telemetry signal (see Appendix E) yielding an error rate of 1 in 10^5 with a non-coherent system, a 250 Hz bandwidth, 27 dB for real time sensor signals having 17.2 dB for execute monitor tone to yield a bit error rate of 1 in 10^6 and 30dB for the ranging tones. In appendix H, we show that the total peak carrier deviation for these requirements is 3.95 radians.

3.3.7 Telemetry System RF Link

In paragraph 3.3.6 and Appendix H it has been established that the signal level requirement at the ground station receiver is -153.0 dBW allowing a 6 dB margin for fading, the nominal input power requirement at the receiver becomes -147.0 dBW.

From the RF Equation we have;

$$P_r = P_t - L_p + G_t + G_r - P_p$$

where:

P_r = Required power at the receiver
P_t = Required power of the transmitter
G_t = Gain of the transmitting antenna
G_r = Gain of the receiving antenna
P_p = Passive losses in the telemetry harness.
L_p = Free space path attenuation

Gain of the transmitting antenna, G_t, has been assumed 0 dB.
Gain of the receiving antenna, G_r is 55.6 dB at 4200 MHz (50% efficiency)
Free space path loss, L_p = 197.3 dB at 4,200 MHz
Passive losses in the harness, P_p = 2.6 dB

Substituting;

$$-147.0 = P_t - 197.3 + 0 + 55.6 - 2.6$$

Hence;

$$P_t = -147.0 + 197.3 - 0 - 55.6 + 2.6 \text{ dBW}$$
$$= -2.7 \text{ dBW}$$
$$= 537 \text{ Milliwatts}$$

Therefore the required telemetry transmitter power is 537 milliwatts.

The telemetry transmitter will also be used for tracking,and detailed calculations (in Appendix H) show that that carrier-to-noise ratio available for acquisition is 12.8 dB on the basis that 30% of the received signal is available for tracking. The minimum carrier-to-noise required for acquisition may be taken to be 3 dB, hence a safety margin of 9.8 dB exists. This permits the use of a wider loop bandwidth for acquisition than for tracking.

3.3.8 Baseband Frequency Considerations

The required bandwidth for subcarrier-oscillators is 1650 Hz. The lowest recommended I.R.I.G. standard subcarrier frequency for this bandwidth is 22 kHz. Hence we will choose 22.0 kHz, 30.0 kHz and 40.0 kHz as the center frequencies for the three S.C.O.'s required for real time signals.

The telemetry signal subcarrier must be an exact multiple of the bit rate for the PCM data (72 bits/sec). We shall choose 8.640 kHz (=120 x 72). The four range tone requirements are discussed in section 3.1.6 and in Appendix A. The frequencies selected are 100 Hz, 800 Hz, 6.4 kHz and 50 kHz. However for transmission the two lowest frequency tones are mixed with the 6.4 kHz tone to produce 6.3 kHz and 5.6 kHz. The transmitter range tones are therefore 5.6 kHz, 6.3 kHz, 6.4 kHz and 50 kHz.

The execute monitor tone frequency is chosen to be 14.5 kHz to minimize intermodulation possibilities.

The telemetry base band spectrum is shown in Fig. 3.8.

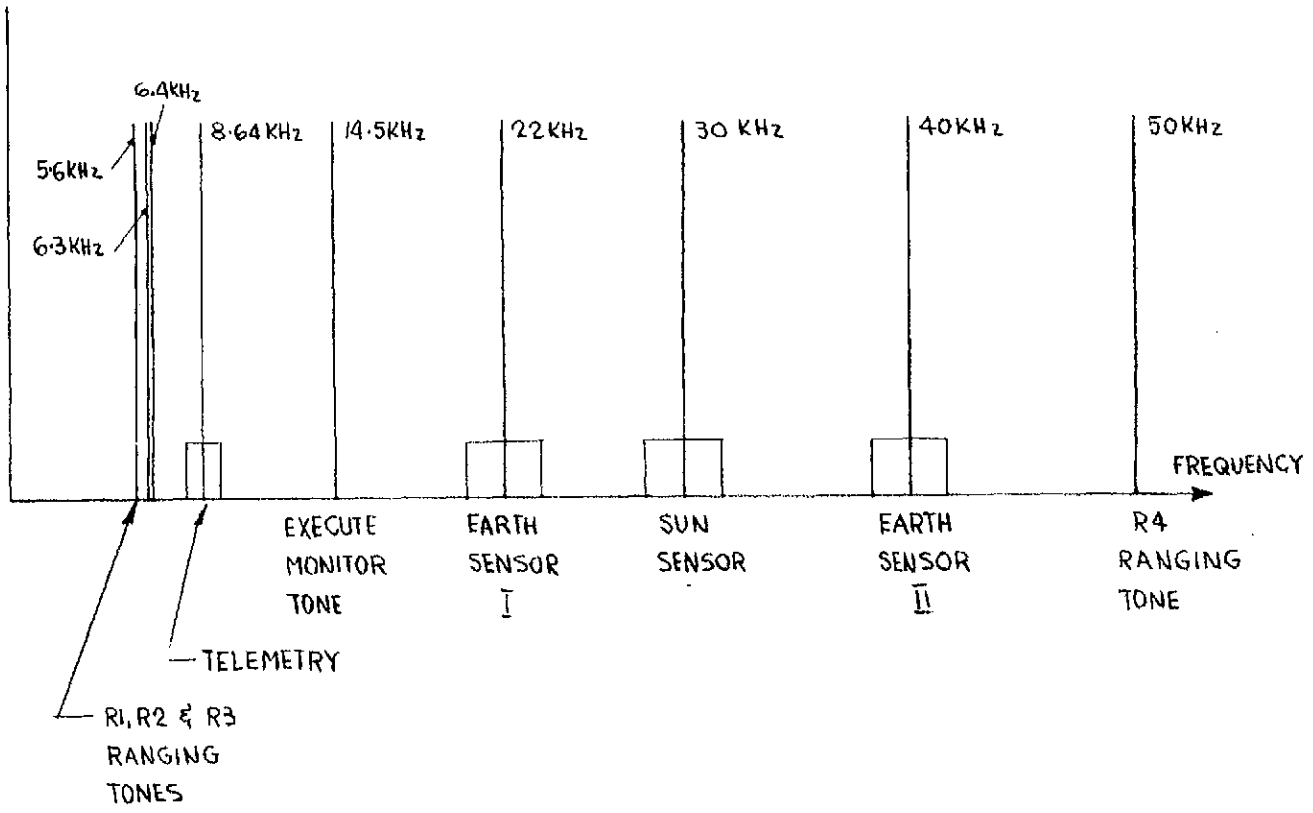

Figure 3.8 Telemetry Base-Band Spectrum

3.3.9 Tentative Performance Specification

We may now summarize the basic performance specification for the telemetry system as developed in the preceding pages. The summary is shown in Table 3.6.

Table 3.6

Tentative Telemetry System Performance Specifications		
Baseband:	:	4 Subcarriers, Ranging Tones, Execute Monitor
Subcarrier 1:	:	8.640 kHz Telemetry
2 (IRIG)	:	22 kHz Earth Sensor I and ARP*
3 (IRIG)	:	30 kHz Sun Sensor Pulses
4 (IRIG)	:	40 kHz Earth sensor and ARP*
Ranging Tones	:	4 Tones: 100 Hz upconverted to 6.3 kHz 800 Hz upconverted to 5.6 kHz 6.4 kHz 50 kHz
Execute Monitor	:	Real Time Execute Monitor 14.5 kHz
Telemetry Signal	:	6 Bit/Word PCM
Word Rate	:	12 Words/Second (72 bits/second)
Words/Subframe	:	48
Subframes/Main Frame	:	8
Subframe Rate	:	4 seconds
Main Frame Rate	:	32 seconds
Analogue Channel capacity	:	96 channels per main frame, subcommutated to 12 words per subframe
Digital Channel (Flag) capacity	:	120 bits per subframe occupying 20 words per subframe
Verification Channels	:	24 bits supercommutated four times per subframe, occupying 16 words per subframe
Modulation	:	Subcarrier 1 (Telemetry) - FSK Subcarriers 2, 3, 4 - FM Main carrier - PM
RF Frequency	:	In 4 GHz Common Carrier Band
Output RF Power (Tx)	:	537 milliwatts

* ARP = Antenna Reference Pulses

3.4 TELEMETRY AND COMMAND EQUIPMENT

3.4.1 General

This section deals with a practical concept for the hardware required to satisfy the performance requirements. All the techniques considered for the development of this hardware exist therefore the only questions that remain are to determine, in some cases, the "best" of the several possible ways of achieving the desired result.

We have carefully considered the possibility of using existing equipments, but the development of space hardware for the 4 and 6 GHz common carrier bands has not progressed very far, particularly in the fields of telemetry and command. Suitable "off-the-shelf" receivers and transmitters have not been found.

As for the digital decoding and encoding equipments, it is usually preferable to develop these for the systems concerned since each system requires unique combinations of functions.

For that reason, we assume that all of the telemetry and command equipment, save for the beacon transmitter, must be newly developed to meet the rather strict requirements of efficiency and weight. It is only in the case of the beacon transmitter which operates in the widely used 136 MHz band that use of existing equipment is practical.

3.4.2 ANTENNA SYSTEM

Introduction

The antenna system consists basically of a radiating structure, a duplexer, a power combiner, and associated interconnection coaxial harnesses, as shown in Figure 3.9. The requirements and possible configurations of these will now be considered. The effective passive losses for each system will also be estimated.

Radiating Sturcture

a) Telemetry Antenna

We desire that the radiating structure be a wideband unit to combine the functions of transmitting 4 GHz telemetry signals and receiving 6 GHz commands signals. This structure should be mechanically rugged, light, and electrically simple. Its radiation characteristic should be as quasi-isotropic.

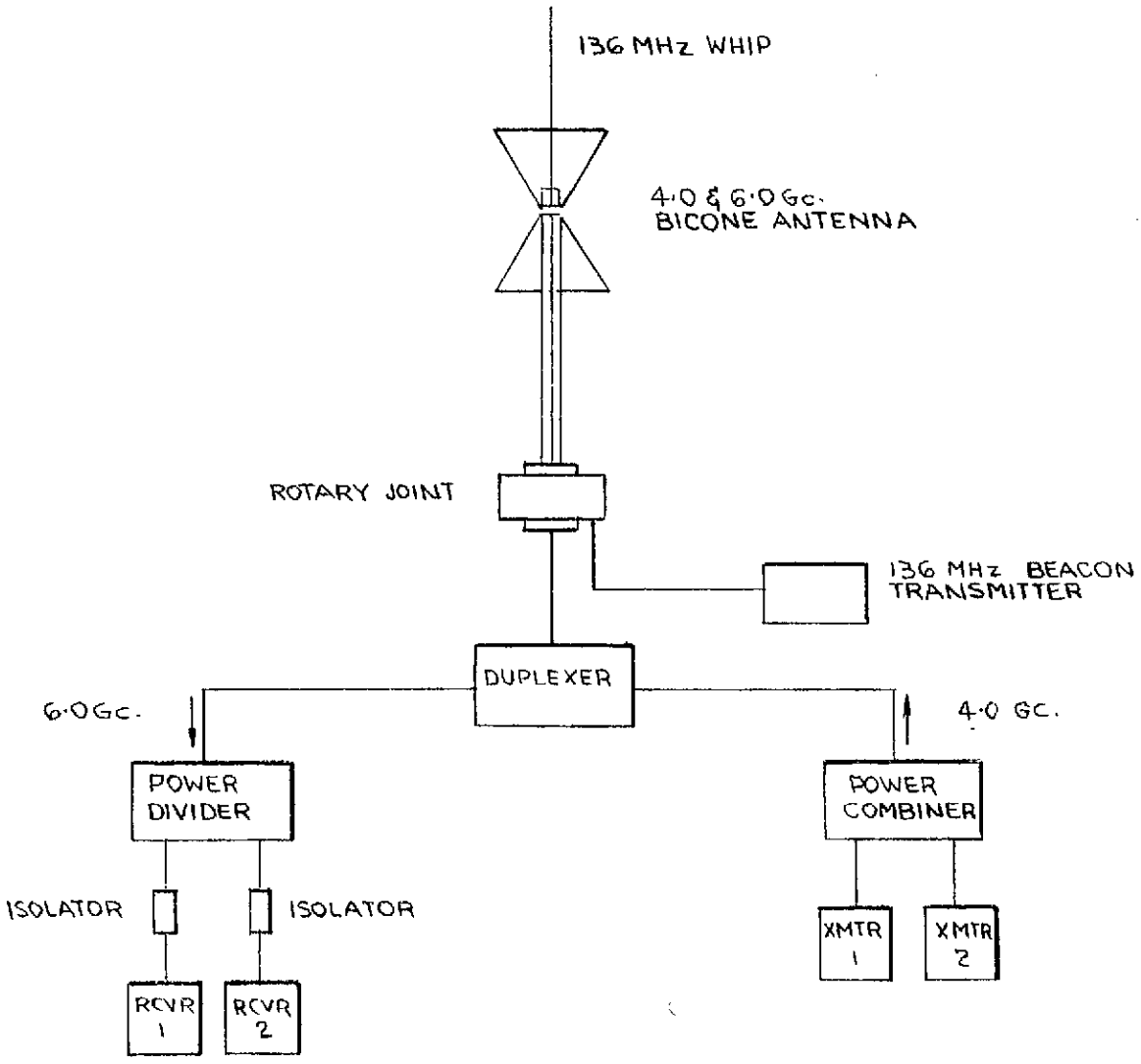

Figure 3--9 Block Diagram Antenna System

A bicone antenna designed at the centre frequency of 5 GHz would meet such requirements. It is basically a wideband antenna which produces a toroidal pattern whose azimuth pattern is omni-directional and elevation pattern is of the figure "8" type. The latter's directivity is easily controlled by altering the slant length, L (See Fig.3-10).

Maximum directivity and gain are realized when L is of the order of 6. However, for the present consideration a low gain and broad elevation pattern is desired, and with L approaching a wave-length, a 40° beamwidth would be obtained in the elevation plane. The structure would thus be small and light.

The input impedance of such antenna is given by

$$Zin = 120 \log_e \cot(\theta/2)$$

and a suitable choice of θ will produce an input impedance of 50 ohms. Thus a 50 ohm semi-flexible coaxial cable can be used to excite the antenna, with the inner connected to the upper half and the outer connected to the lower half. The spacing 'd' between the two apeces is small and is experimentally derived. The resulting polarization is vertical (parallel to axis of symmetry).

b) Beacon Antenna

A 136 MHz Beacon Antenna in the form of a quarter wavelength "whip" may be mounted on top of the bicone and fed directly by a flexible coaxial cable, mounted through the inside of the inner conductor or the bicone feed cable, as shown in Figure 3.10. At the rotary joint separate output ports are available for the VHF Beacon and the microwave telemetry signals.

The VHF signal is connected directly to a coaxial cable which carries the signal to the whip antenna. This cable forms the central part of a larger coaxial structure which carries the microwave signals. A network is used to couple the microwave signals from the rotary joint to the coaxial structure. A possible method of achieving this is shown in Figure 3-11.

c) Duplexer

The use of one common antenna to transmit and receive requires that the two signals be duplexed in common antanna port, as shown in the system block diagram, Figure 3.9. Such a duplexer should provide a coupling for the 4 GHz transmitter power to the antenna and for the 6 GHz received signals from the antenna port to the receiver port, with low dissipation loss and adequate isolation between transmit and receiver ports.

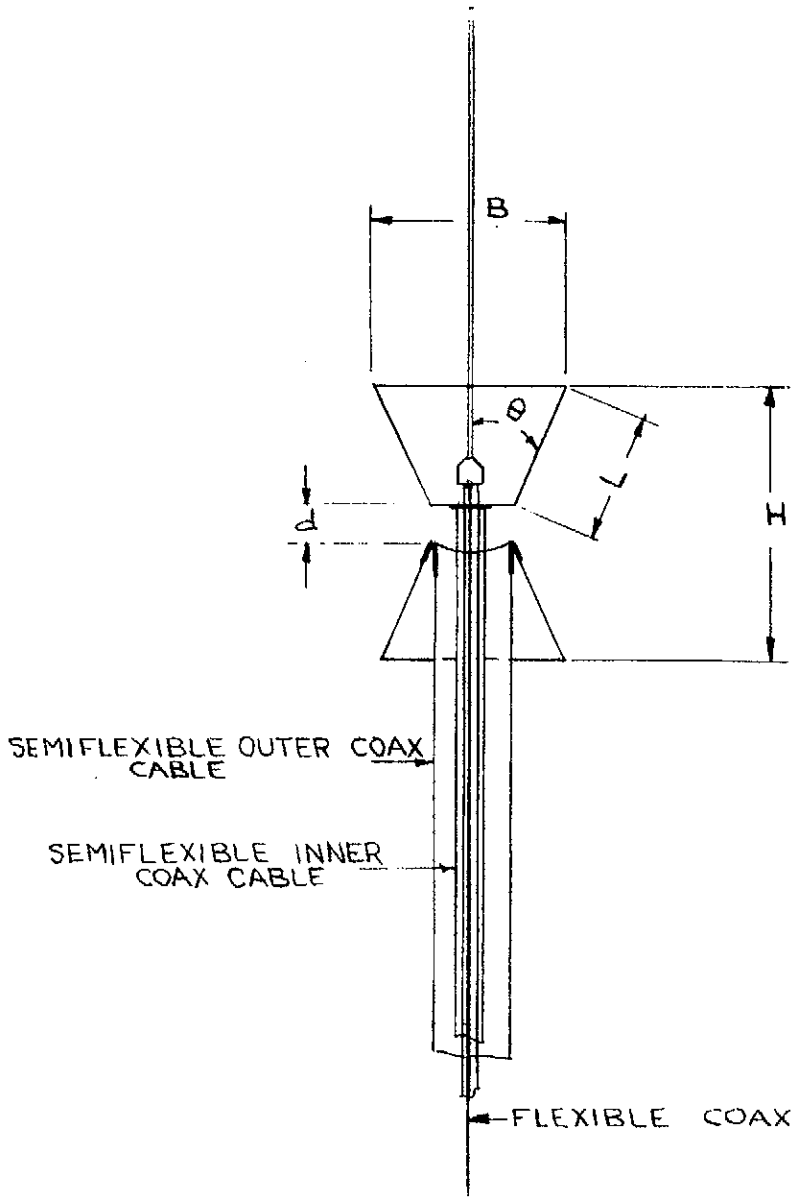

APPROXIMATE DIMENSIONS FOR BICONE DESIGNED AT 5.0 GC.

$L = 1\lambda$ (6 cm.)

$\theta = 65°$

$H = 2L \cos\theta = .82\lambda$

$B = 2L \sin\theta = 1.82\lambda$

WEIGHT = 4 oz.

Figure 3-10 Bicone Antenna

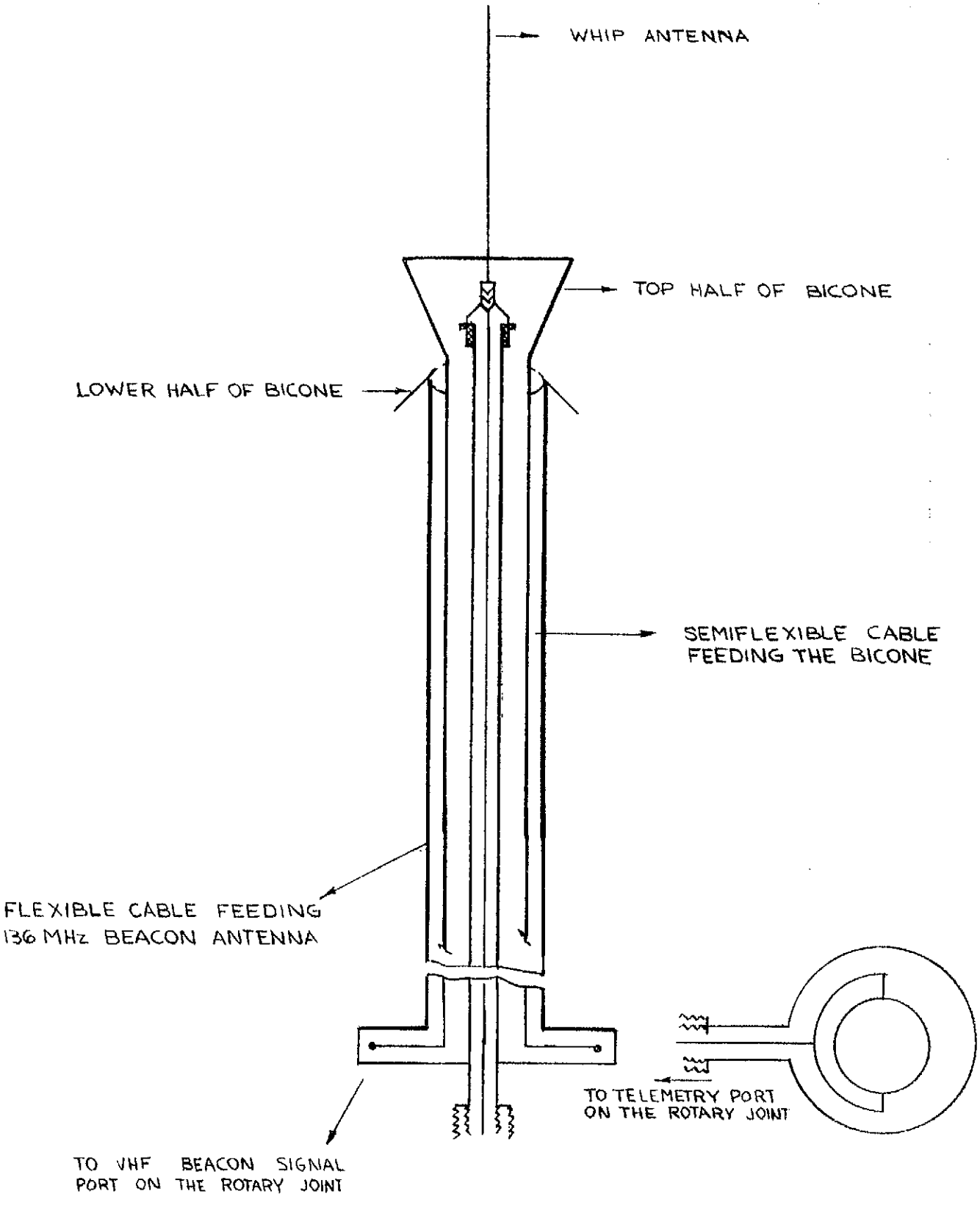

Figure 3–11 Antenna Feed System

It must also be recognized that the telemetry frequency is close to the communications band and consideration must be given to reception of communication signals into the command receiver through the bicone antenna.

The maximum total communications signal power produced at the bicone antenna terminals as a result of such coupling is estimated to be not more than -50 dbm. Performance of a typical command receiver would not be affected if the level of such interfering signals were not to exceed -60 dbm at its input. Thus the duplexer need only provide an isolation of about 10 db at this interferring frequency approximately 30 MHz higher than the telemetry receive frequency. The proposed design of the command receiver indicates that a cavity filter will be included at the input and will provide this degree of isolation for the communication signals from reaching the receiver input.

A possible duplexer configuration is shown in Figure 3-12. The 4.0 GHz telemetry transmit signals are coupled to the antenna port via a 4 GHz interdigital filter and circulator. The 6 GHz command signals are coupled to the command receiver via the circulator and 6 GHz interdigital filter. The response characteristics of this filter would be dictated by choice of local oscillater frequency. Provisionally this is set at 300 MHz below the command signal frequency and hence any leakage of the local oscillater will not interfere with communications signals.

d) Power Divider

This unit is required to split the incoming 6 GHz telemetry signals to feed the two command receivers. It can be either a 3 dB coupler or a T divider network with a $\lambda/4$ transformer. Inclusion of isolators, one in each branch, would maintain the signal level constant at the input of one receiver even if the other one failed partially or completely (in open or short circuit).

The insertion loss of such a device would be approximately 0.5 dB. The connecting leads could be totally eliminated by assembling the power divider and the isolators in one unit, and connection it to the receiver through receptacle connectors on the receiver. It would weigh approximately 6 oz.

e) Power Combiner

It is proposed to include a standby redundant telemetry transmitter to achieve high reliability. Thus in the event of failure of one transmitter, the standby transmitter could be commanded 'on' and switched into the common output. However, the availability of two transmitters on board

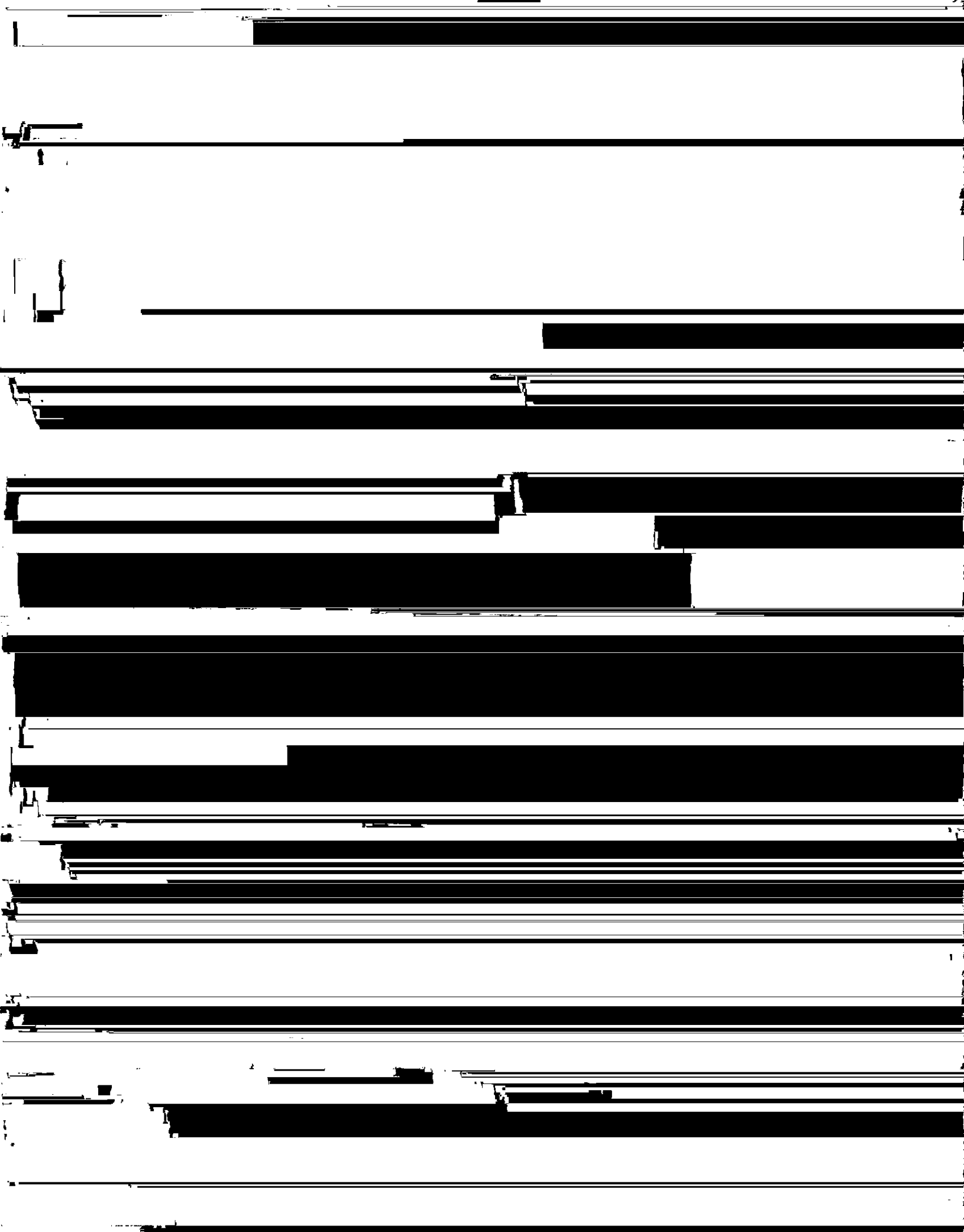

can be utilized to boost the available power by 3 dB. In the initial launch phase, when the antenna pattern might be modified unpredicably by the presence of gantry and boosters, such increase in EIRP would be valuable. As shown in Figure 3.13, a power combiner consisting of a switch and a T-network would enable selection of the transmitters or both transmitters, when required.

By closing the switch A or B, output of transmitter 1 or 2 could be coupled to the antenna through the T network and the $\lambda/4$ transformer. The discontinuity introduced by the $\lambda/4$ transformer would be cancelled by the discontinuity introduced by the length l, which would behave like an open circuit stub.

When both transmitters are operated simultaneously, switches A and B are closed. The T divider and the transformer match the combined impedances of the transmitters to the load and total power will be increased by 3 dB, (assuming the ampitude and phase of the two transmitters are maintained constant at a specified value). Isolators at the output of each transmitter may be provided for protection. The power combiner consisting of two isolators, switches and the T network including the transformer could be assembled in one unit weighing 5 oz. Dissipation loss when only one transmitter is operating will be approximately 0.4 db.

PASSIVE LOSSES

a) Receiving System

The total estimated passive losses of the 6 GHz command system are given in Table 3.7.

Antenna to 6 GHz filter feeder	0.8 dB
Rotary joint	0.5 dB
Circulator	0.4 dB
6 GHz Filter	1.3 dB
Power Divider	0.2 dB
Split Loss	3.0 dB
Total Passive Losses (6 GHz)	6.2 dB

Table 3.7

b) Transmitting System

The total estimated losses of the 4 GHz Telemetry transmit system are given in table 3.8

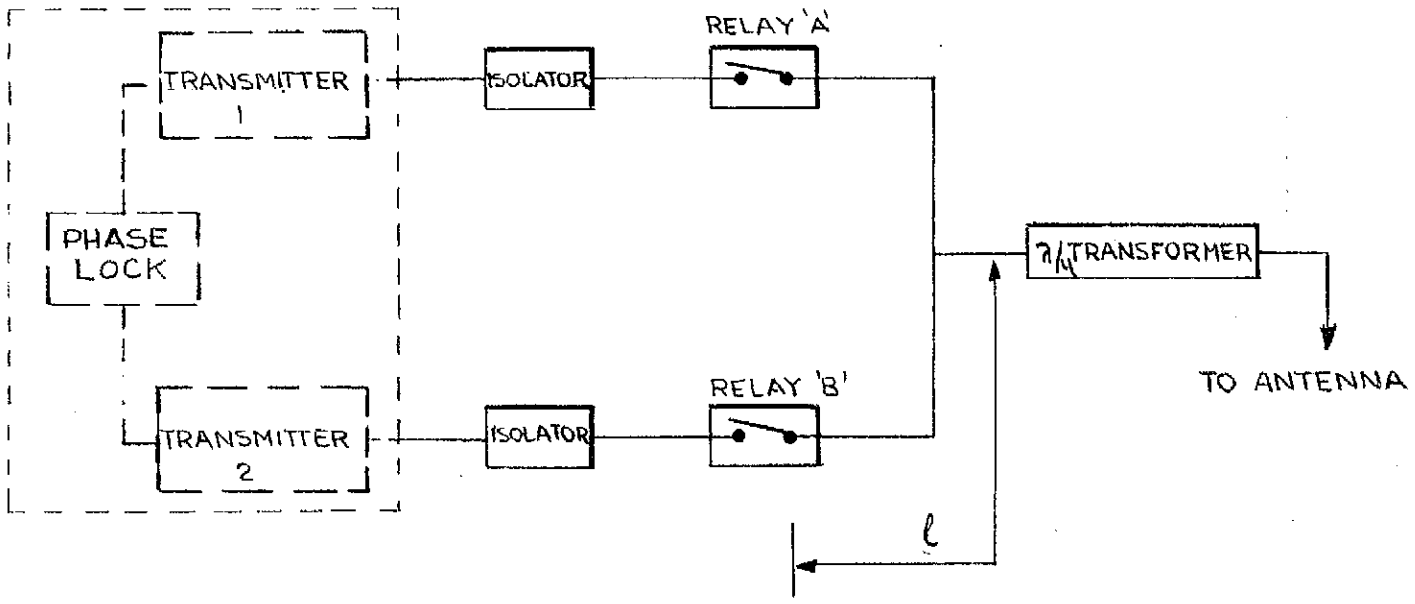

Figure 3–13 Power Combiner Configuration

Power Combiner loss	0.4 dB
Power combiner to 4 GHz filter feeder	0.1 dB
4 GHz filter	1.3 dB
Circulator to antenna port	0.5 dB
Rotary joint loss	0.3 dB
Total passive losses (4 GHz)	2.6 dB

Table 3.8

c) 136 MHz Beacon System

The total estimated 136 MHz Beacon System Losses are given in table 3.9.

Transmitter to rotary joint link	0.5 dB
Rotary joint	1.0 dB
Rotary joint to antenna input	0.5 dB
Total Passive losses (136 MHz)	2.0 dB

Table 3.9

3.4.3 COMMAND RECEIVER ASSEMBLY

Introduction

The command receiver assembly is defined as the assembly consisting of two separate but identical receivers and the power divider. A sketch of the assembly configuration is given in figure 3.14. In the discussion which follows we describe primarily one of the receivers. The power divider has been already discussed in the antenna system.

6 GHz Command Receiver

The commandreceiver would be a conventional double conversion superheterodyne type designed for high reliability of operation with minimum weight, complexity and power requirement. All components would be thoroughly stabilized to minimize aging effects.

A block diagram of the receiver is shown in Figure 3.15.

WEIGHTS (EST'D)	
RECEIVER 1	1 1/2 Lbs.
RECEIVER 2	1 1/2 Lbs.
POWER DIVIDER	1 Lbs.
MISCELLANEOUS	1/4 Lbs.

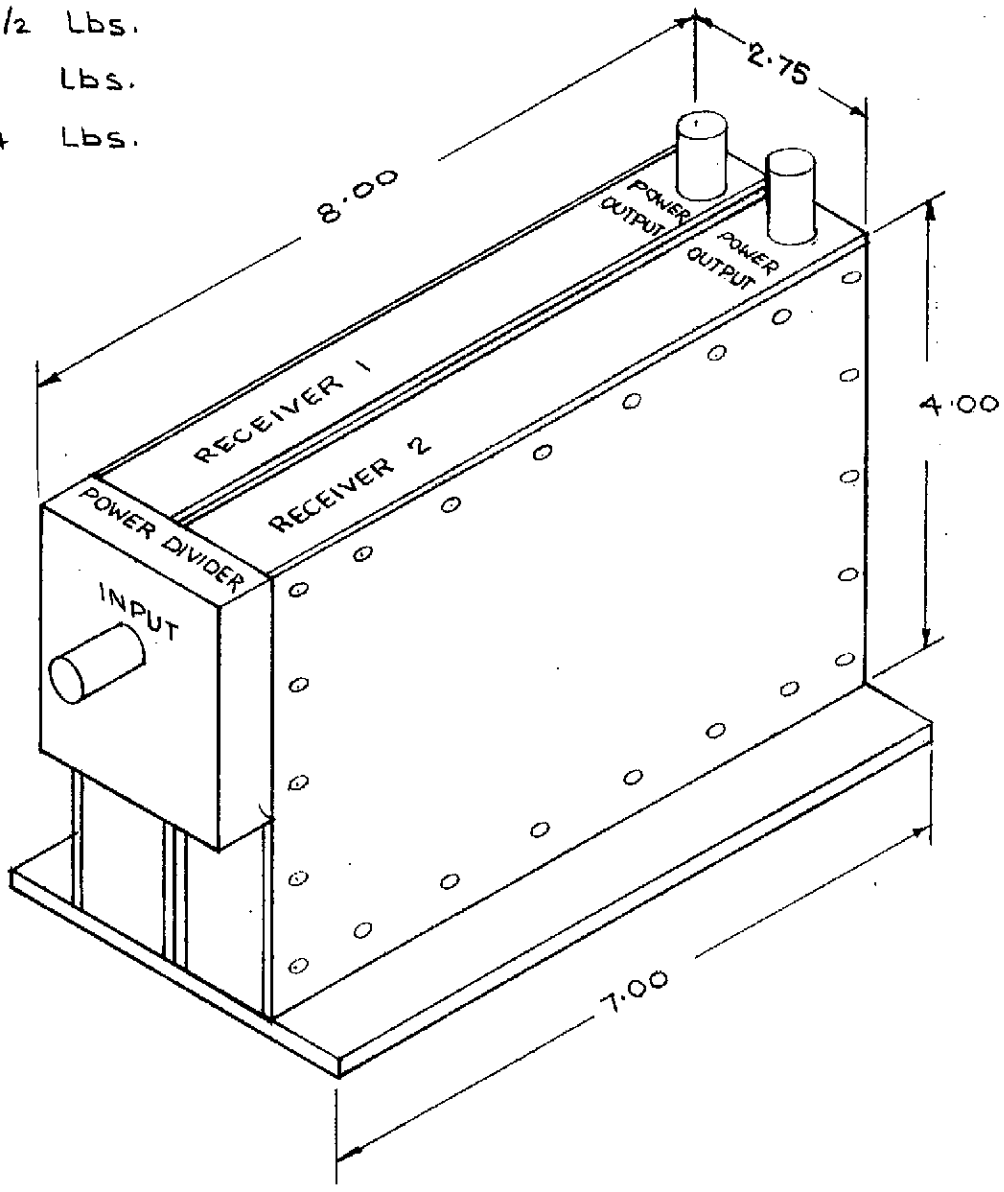

Figure 3-14 Outline of Command Receiver Assembly (Typical)

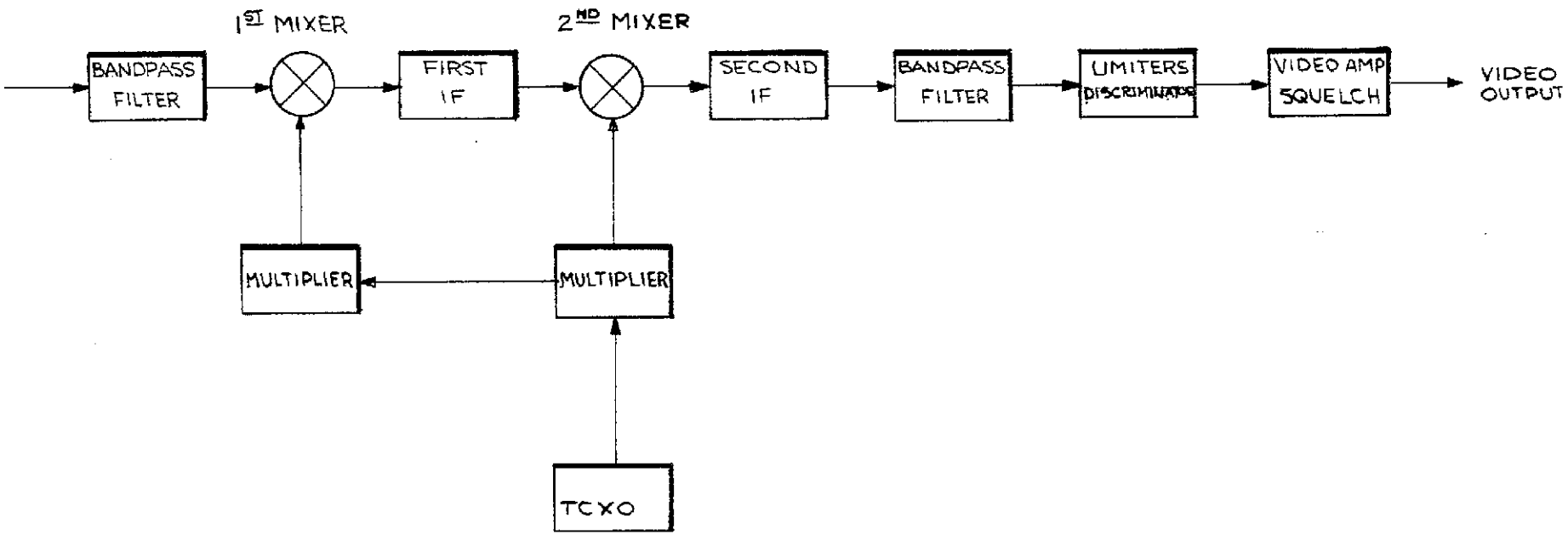

Figure 3-15 Block Diagram Command Receiver

Input Bandpass Filter

This bandpass filter located ahead of the 1st mixer would be a cavity type designed to provide sufficient attenuation to adjacent communication carriers in order to prevent receiver desensitization as well as to eliminate receiver responses at the image frequency. It would also attenuate local oscillator leakage from the receiver.

Frequency Conversion

Double conversion adds circuit complexity over single conversion. It is, however, decidedly advantageous when one considers frequency stability and the resulting effect on the local oscillator.

To illustrate this fact, let us compare a single conversion system using an I.F. of 70 MHz with a dual conversion system with a first IF of 300 MHz and a second IF of 10 MHz.

We know that the input sensitivity of a receiver for a given output carrier to noise ratio depends on the noise figure and the noise bandwidth of that receiver. First we must define the IF bandwidth required to take care of variation of the local oscillator frequency and also the variation of the IF center frequency.

The local oscillator variation could be estimated at ± 5 ppm for temperature effects plus ± 7.5 ppm for aging effects in 5 years. Therefore a peak to peak drift of 25 ppm at 6 GHz (approx.) could be 150 kHz. The variation of the IF center frequency could be estimated at approximately $\pm 0.3\%$ for 5 years providing all components are well stabilized before being used.

Table 3.10 shows the required bandwidth for single or dual conversion.

Required Bandwidth for Single or Dual Conversion Receivers		
	1 conversion IF 70 MHz	2 conversion IF 10 MHz *
Local oscillator drift peak to peak	150 kHz	150 kHz
If center freq. drift peak to peak	420 kHz	60 kHz
Tolerance and other variation peak to peak	30 kHz	10 kHz
Signal bandwidth requirements peak to peak	200 kHz	200 kHz
Total	800 kHz	420 kHz

*Note: In the dual conversion system the effective noise bandwidth is governed by the second IF of 10 MHz.

A reasonable noise figure for a Schottky diode mixer working in an IF of 70 MHz could be 6.5 dB at 6 GHz; the same mixer diode working into an IF of 300 MHz would have 8.0 dB because of the higher contribution of the first transistor amplifying at 300 MHz.

In addition, we should add 3.0 dB to allow for production tolerance plus 5 years aging effects.

Knowing the bandwidth and the noise figures we can compute receiver sensitivity for a given input carrier to noise ratio.

$$S = KT + 10 \log B + F_o + 10 \log (C/N)$$

where S = sensitivity of the receiver in dBm
KT = Thermal noise power in one cycle B. W.
B = Effective noise bandwidth
F = noise figure of mixer plus the first IF stage

Substituting for KT, B, and F_o, we have for a single conversion system:

$$S = -174 + 59.0 + 9.5 + 10 \log (C/N)$$
$$S = -105.5 + 10 \log (C/N)$$

and for a dual conversion:

$$S = -174 + 56.2 + 11.0 + 10 \log (C/N)$$
$$S = -106.8 \text{ dBm} + 10 \log (C/N)$$

Therefore to achieve the same input C/N ratio the dual conversion offers a net gain of 1.3 dB in the receiver sensitivity for the same output signal to noise ratio.

IF Amplifiers

The first stages of the IF are particularly important as these stages define the overall noise figure of the IF. Generally, transistors with very high F_T would have the best noise figure. Shot noise in transistors is approximately constant at mid frequencies until an upper cut off $F_C = F_T \sqrt{1 - \alpha}$ is reached, above which the noise figure increases 6 dB per octave of increasing frequency. At the present time the best low noise transistor starts to have a rising noise characteristic at approximately 100 MHz.

Amplifying stages should be designed with bandwidth wide enough to eliminate the effects of temperature and aging. Passive filters would limit the band to the required value. These filters would have to be designed to achieve very high stability regarding both temperature and aging effects.

AGC

It would be advantageous to use PIN diodes attenuators as automatic gain control in the IF strips. These diodes provide a wide range of gain without disturbing the optimum operating bias point of transistor; they also minimize change in output and input impedance, phase shift and tuning.

The location of these PIN diodes attenuators in the circuit is critical. They are preferably used at low levels to minimize AM to PM conversion in the receiver but if located too near the input of the receiver the signal power level at the following stage could be lower than the signal power level at the input for normal operation. Under these conditions the later stages could contribute significantly to the noise figure of the receiver.

Discriminator, video amplifiers and squelch

The discriminator and the video amplifiers would demodulate the frequency modulated signal and amplify it to 1 volt peak to peak in a 600 ohms balanced output with a typical distortion characteristic less than 5%*.

The baseband frequency response would be within 2 dB up to 50 kHz. This represents a practical value for the command signal. A squelch circuit would be provided to prevent unwanted operation of the decoder from high noise level due to poor or no carrier condition.

Receiver Specifications

A summary of the tentative specifications for the command receiver is given in table 3.11 below.

Table 3.11

Tentative Command Receiver Performance Specification	
Frequency	5925 to 6425 (Crystal and input circuit change
Type of reception	FM required)
Noise Figure	8 dB max.
	10 dB max. after 5 years
Input impedance	50 ohms
IF Frequency	approximately 300 MHz and 10 MHz
IF Bandwidth	431 kHz
IF Rejection	60 dB minimum
Image rejection	60 dB minimum
L.O. leakage to the input	25 microvolts
Power Requirement	1.5 W per receiver
Power Supply	28V regulated
Estimated Assembly Volume	77 cubic inches
Estimated Assembly Dimensions	4" x 7" x 2 3/4"
Estimated Assembly Weight	4 1/4 lbs.

* All parameter values are suggested as typical only. They are based on considerations of standardization, power consumption and so forth, and represent practical compromises.

3.4.4 Command Decoder Assembly

The command decoder must accept a twelve bit command code, five bits of which consist of a spacecraft address and seven bits define the command. As a safeguard against false commands, the command decoder requires that the twelve bit command code be sent twice as a twenty four bit code, preceded by a synchronization tone. The command as received by the command decoder is relayed to ground control via the telemetry system of the spacecraft, and the decision is then made to execute the command or not. Execution of the command is achieved by the transmission of a synchronization tone followed by the spacecraft address and an execute tone.

The spacecraft system uses the commands from the command decoder to control three typically different groups of functions.

The simplest group of functions are the "set" functions, wherein the command sequence consists of the twenty four bit redundant command code, preceded by a synchronization tone, and followed by ground verification and execution by the synchronization tone, spacecraft address, and execute tone. The "set" functions are used for setting relays, flip flops, and other such toggles, and the command decoder is "reset" after the execute tone.

The real time functions, for example thruster firing and control, differ from simple toggle functions in that they must be frequently repeated with precise control of timing and duration. The command decoder treats the "real time" command by producing a command output to the indicated device in the same way as for a "set" command, except that every execute tone subsequent to the first one produces an output for the duration of the execute tone. The data sequence to accomplish this is exactly that associated with the "set" command, save that subsequent execute tones operate the command decoder, which is "reset" by the next command received.

The "adjust" functions of the command decoder consist of entering numerical information into the adjust stores. The numerical information is in seven bit words. The data sequence for entering the information is as follows:

An ordinary "set" command specifies which store is to be adjusted, and prepares the store for the receipt of information. Another "set" command following the first, is so modified that rather than act as a command, its binary pattern is transferred to the previously prepared store upon execution, and the execution also "resets" the command decoder.

In order to save power, one "set" command is reserved for a switching off the power relay which feeds the logic of the command decoder. This relay is always turned on by the reception of the synchronization tone.

The reliability of the command decoder is enhanced by doubling the command decoder and taking advantage of the parallel redundancy so provided. An assembly sketch is shown in Figure 3.16.

Command Decoder Design

The principal components of the command decoder as shown in the block diagram Figure 3.17 are the "filter and synchronization block", the "shift register and comparator", the "counter", the "address check logic", the "command store", "decoder matrix", and the "select adjust store". These names denote functional entities, of course, and do not refer to physically identifiable assemblies.

The filter and bit synchronization block consists of four adaptive filters, an oscillator and some digital logic. The filters pick out the tones denoting execute, synchronize "zero" and "one" from the impressed audio signal, and adapt to noise to prevent spurious response. The oscillator locks onto the "zero", "one", and "synchronization" information and provides a two phase clock for the reset of the decoder. The digital logic in this block provides four mutually exclusive logic lead outputs, "one", "zero", "sync", "execute", and the two phase clock.

The shift register and comparator are made up of a twelve bit shift register and a one bit comparator with a flip flop memory. The shift register and comparator are reset by the synchronization pulse that precedes the command code, and the shift register provides a twelve bit delay, so that the two consecutive command words can be compared by the comparator.

The counter is a zero to twenty four counter, reset by the synchronization pulse and driven by the clock. The counter inhibits operation of the comparator until the first twelve bits of data have been shifted into the shift register, and interrogates the comparator after reception of the twenty fourth bit.

The address check logic is simply an "and" gate giving a signal whenever it is presented with the five bit address code corresponding to the spacecraft in question.

The command store is a flip flop register into which the contents of the shift register are transferred when the twenty fourth data bit has been received, the comparator agrees, and the correct address appears at the input of the address check logic.

The decode matrix in effect is a collection of "and" gates, corresponding to each command, which provides an output by channeling the execute signal to the output line corresponding to the command in the command store.

WEIGHT (EST'D) 8 lbs.

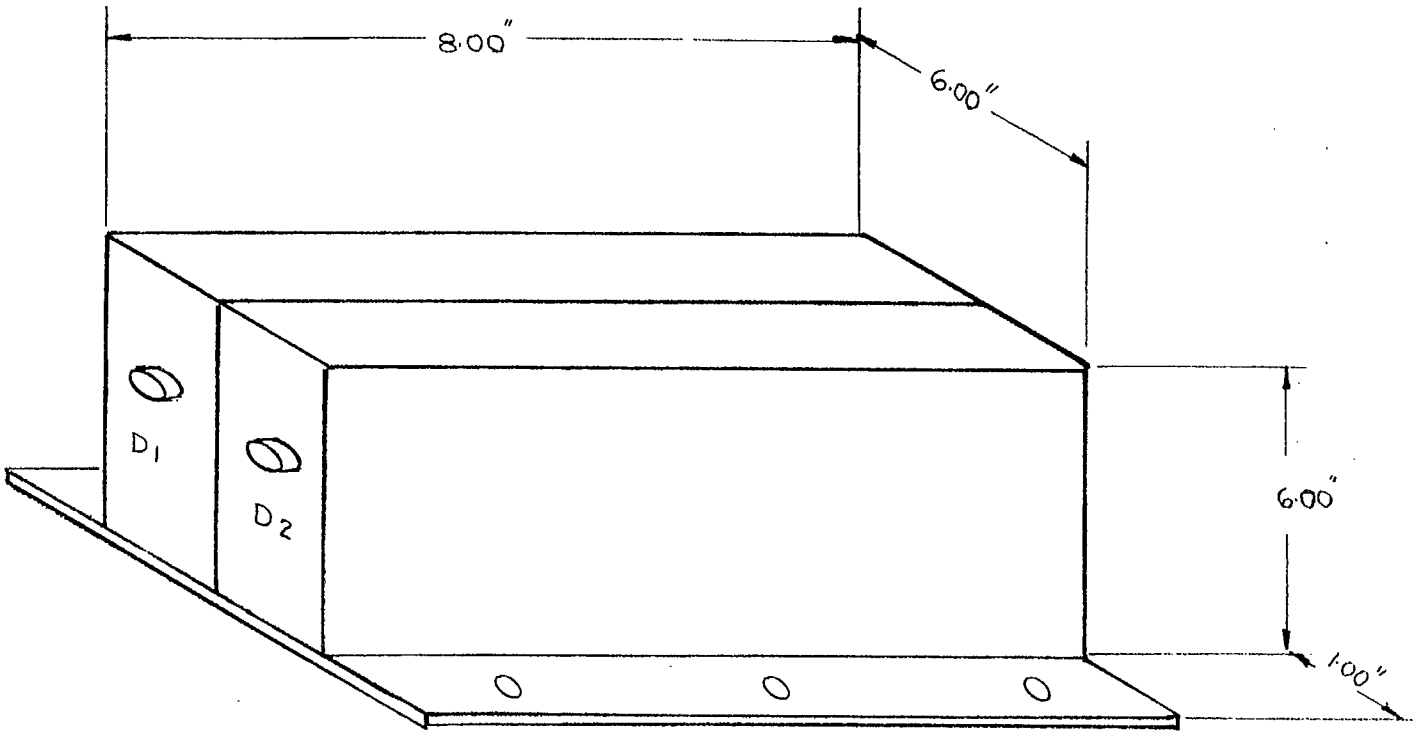

Figure 3-16 Typical Decoder Assembly

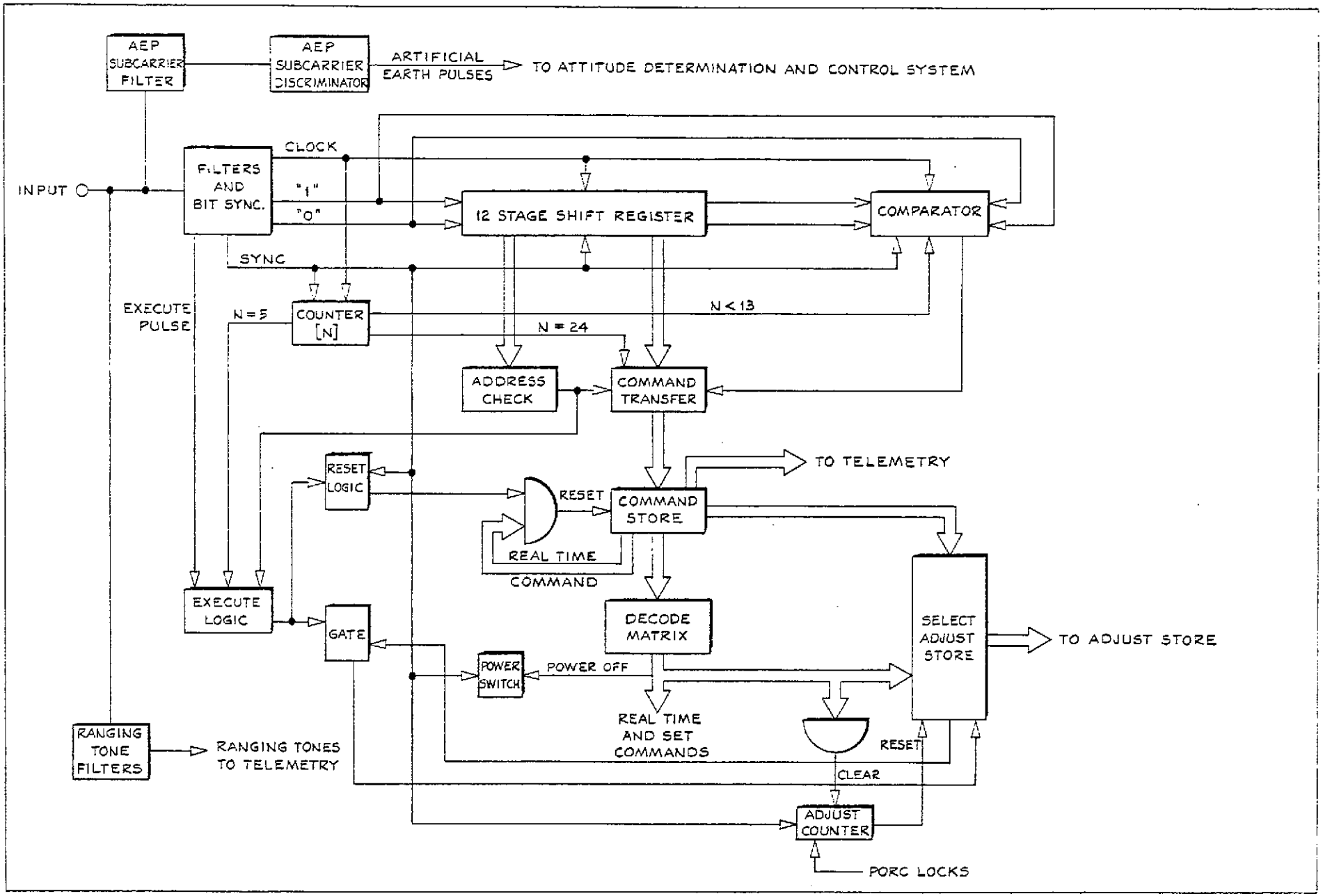

Figure 3–17 Block Diagram Command Decoder

The "select adjust store" consists of a flip flop and gate corresponding to each adjust store. Each flip flop is associated with a "set" command by which it may be set. When any flip flop is set, execute pulses are prevented from entering the decode matrix, and are sent to the "select adjust store" instead. The execute pulses arriving at the select adjust store are channeled through the gate associated with the previously set flip flop, and cause the corresponding adjust store to take up whatever binary number is found in the command store. The next synchronization pulse resets all the flip flops in the select adjust store.

The execute pulse is inhibited by the "execute logic" if the address check logic is not satisfied or if the counter has detected any number of data pulses other than five.

The dropping edge of the execute pulse clears the command store when the contents of the command store are anything other than a real time command.

The adjust counter is a two flip flop counter whose code is such that it has four valid states, and lock-loops on one of them (e.g. 0, 1, 2, 3, 3, 3, ...). The set commands which set the flip flops in the select adjust store are "ord" and used to set the adjust counter to "zero". The counter is then advanced one place by each subsequent synchronization pulse. The "three" state of the counter forces a reset on all the flip flops in the adjust store. The synchronization pulse preceding the code intended for the adjustment store advances the adjust counter to "one", that preceding the execute tone for this sequence advances the counter to "two," and that preceding the next command advances the counter to "three" and consequently resets the "select adjust store".

Tentative Command Decoder Performance Specifications	
Command Format: 5 bits address 7 bits command repeated.	
Input data rate:	128 p.p.s.
Execute tone length:	address followed by tone 47 msec.
Command tone "1" frequency:	13kHz
Command tone "0" frequency:	17 kHz
Execute tone Frequency:	14.5 kHz
Sync tone Length:	$2\frac{1}{2}$ bit
Sync tone frequency:	13kHz
Output pulse length:	30 ms
Verification:	verify before execute

Table 3.12

A summary of the tentative performance specifications of the command decoder is given in Table 3.12.

3.4.5 Encoder

General

The telemetry encoder (Figure 3-18) samples analog and digital data from spacecraft sources. Ninety-six channels of analog information are sampled and digitized to a "six bit" accuracy, at a rate of three channels per second. Twenty four words of digital data are sampled, each word consisting of six bits. Four words are sampled at a once per second rate, and twenty are sampled at a once per four second rate. This results in a bit stream output of seventy-two bits per second. A timing diagram is given in Figure 3-19.

The sampling sequence takes one analogue sample and three digital samples in turn, each digital sample being made up of six flags. This three and one sampling scheme provides for each analog channel to be sampled every thirty-two seconds, and each digital word to be sampled every one second or every four seconds depending on whether or not is super-commutated.

Analogue Commutator

The analog commutator consists of ninety-six analog gates, driven by two input "and" gates arranged in an eight by twelve matrix. The eight by twelve matrix is further divided into groups of six gates, whose command output line passes through a redundant switch, thus there are sixteen redundant switches. These redundant switches are further "ganged" into groups of four, with the common output line again passing through redundant switches, of which there are four at this level. The common output line of this level constitutes the commutator output. This "treeing" form of course changes its optimal configuration as the reliability numbers for the components change, so the number of command gates at each level of the tree is finally decided at the circuit design stage. Figure 3-20 shows the analog commutator.

The analog to digital converter which follows the analog commutator converts the signal in a serial fashion, making use of two sample and hold circuits and a comparator to perform the following operation on the sampled analog voltage V.

If $(V - K) < 0$, transmit 0 and repeat using $2V$

If $(V - K) > 0$, transmit 1 and repeat using $2(V - K)$
where K is the analog value of the most significant bit.

This provides analog to digital conversion and parallel to serial conversion at the same time.

WEIGHT (EST'D) 8lbs.

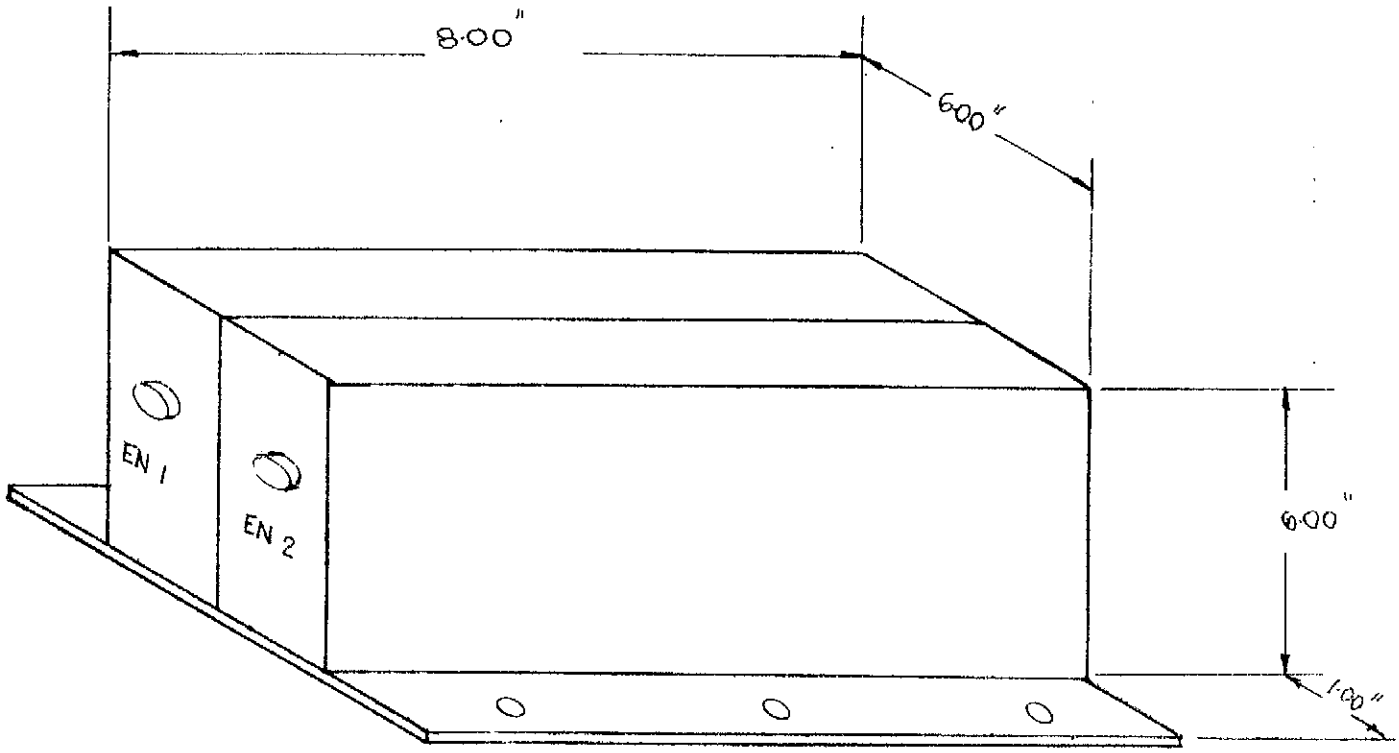

Figure 3-18 Typical Encoder Assembly

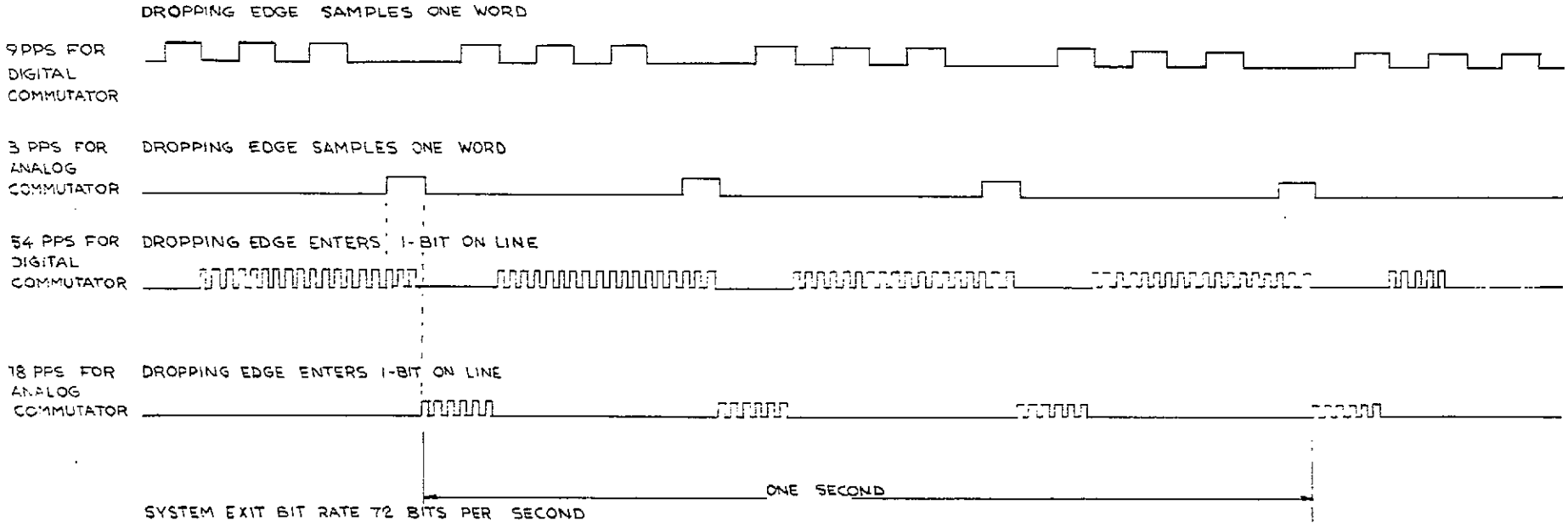

Figure 3–19 Encoding System Timing

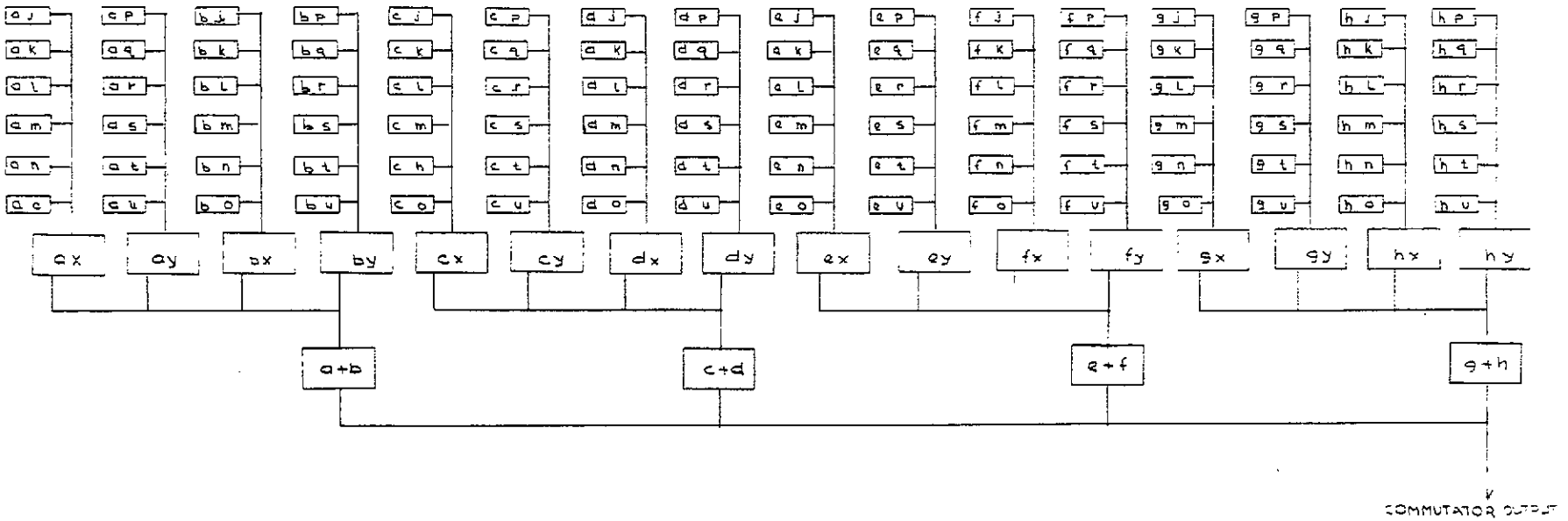

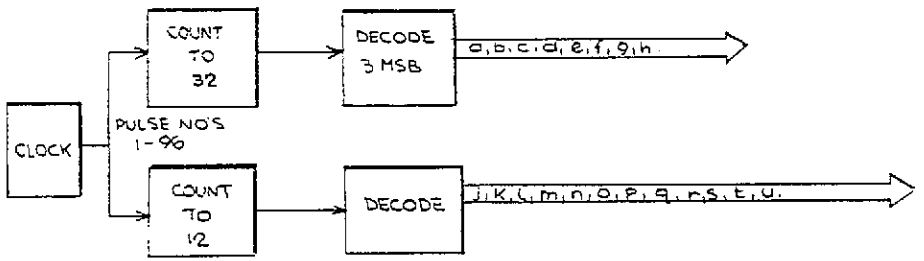

$j+k+l+m+n+o+p+q+r+s+t+u = x$

$a+b+c+d+e+f+g+h = y$

a	1	2	3	4	65	66	67	68	33	34	35	36
b	37	38	39	40	5	6	7	8	69	70	71	72
c	73	74	75	76	41	42	43	44	9	10	11	12
d	13	14	15	16	77	78	79	80	45	46	47	48
e	49	50	51	52	17	18	19	20	81	82	83	84
f	85	86	87	88	53	54	55	56	21	22	23	24
g	25	26	27	28	89	90	91	92	57	58	59	60
h	61	62	63	64	29	30	31	32	93	94	95	96
	j	k	l	m	n	o	p	q	r	s	t	u

PULSE NO'S AGAINST CHANNELS.

Figure 3–20 Analog Commutator

Digital Commutator

The twenty-four channel digital commutator consists of two hundred and sixteen "and" gates arranged in groups of six, making twenty-four groups or words. The words are selected in turn by means of two counters which are fed by the same clock. One counter has nine states, the other four. The first four states of the nine state counter select the four supercommutated channels, while the next five states "anded" in matrix with the four states of the four counter, select the other twenty channels. (See Figure 3-21).

The selected channel at any time consists of six digital flags, which are transferred in parallel to a shift register, from which they are shifted out in serial. This shift register is in parallel to serial converter.

System

To satisfy reliability requirements, two analog commutators, two digital commutators, and two telemetry transmitters are provided to provide the required degree of redundancy. Each analog commutator is associated with a telemetry transmitter, giving a redundant pair of commutator transmitter combinations. The digital commutator outputs are combined by command switching, and the output of the commutator so selected is mixed with the analog commutator outputs and transmitted. The system is shown in Figure 3-22.

The combining of the analog and digital commutator outputs is done by an adder which provides some clipping action so that a failure of one commutator or the other which results in a constant bias output, will not invalidate the data produced by the other. Table 3.13 summarizes the tentative performance.

Table 3.13

Tentative Telemetry Encoder Performance Specification	
Digital	
Analogue Inputs	96
Analogue channel sample rate	32 seconds/ 1 sample
Analogue digital resolution	6 bits /analogue sample
Digital flag inputs	120
Digital flag rate	4 seconds /1 flag
Digital flag resolution	1 bit /flag
Digital Verification Inputs	24 bits
Digital Verification Rate	1 second/ bit
Subframe Rate	4 seconds / subframe
Main Frame Rate	32 seconds / frame
Subframe/Main Frame	8

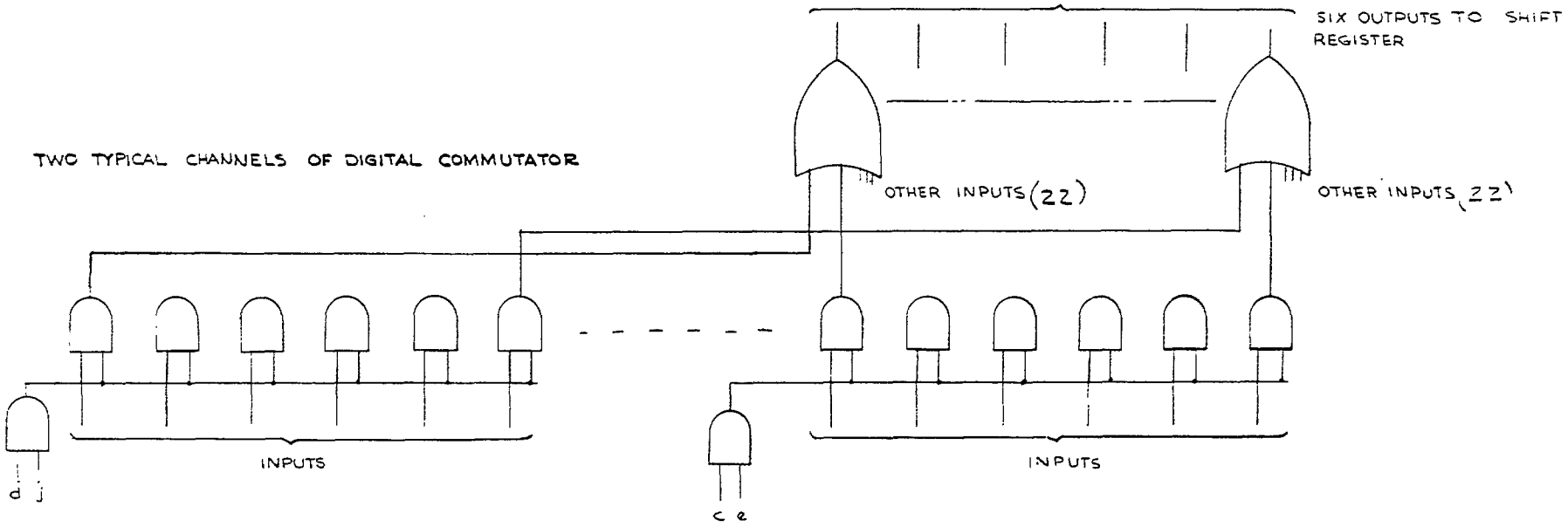

VERTICAL AND HORIZONTAL CHANNEL SELECTION GENERATION

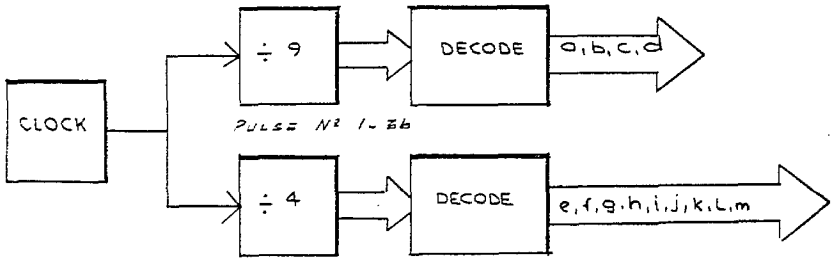

MATRIX OF CHANNEL SELECTION SEQUENCE FOR CHANNELS DESIGNATE e,f,g,h

aL, bL, cL, dL,
aj, bj, cj, dj.
aK, bK, cK, dK,
aL, bL, cL dL
am, bm, cm, cm

PULSE NO'S AGAINST CHANNELS

d				22,31 4,13	32	24	16	8	36
c			21,30 3,12		23	15	7	35	27
b		20,29 2,11			14	6	34	26	18
a	19,28 1,10				5	33	25	17	9
	e	f	g	h	i	j	k	L	m

Figure 3–21 Digital Commutator

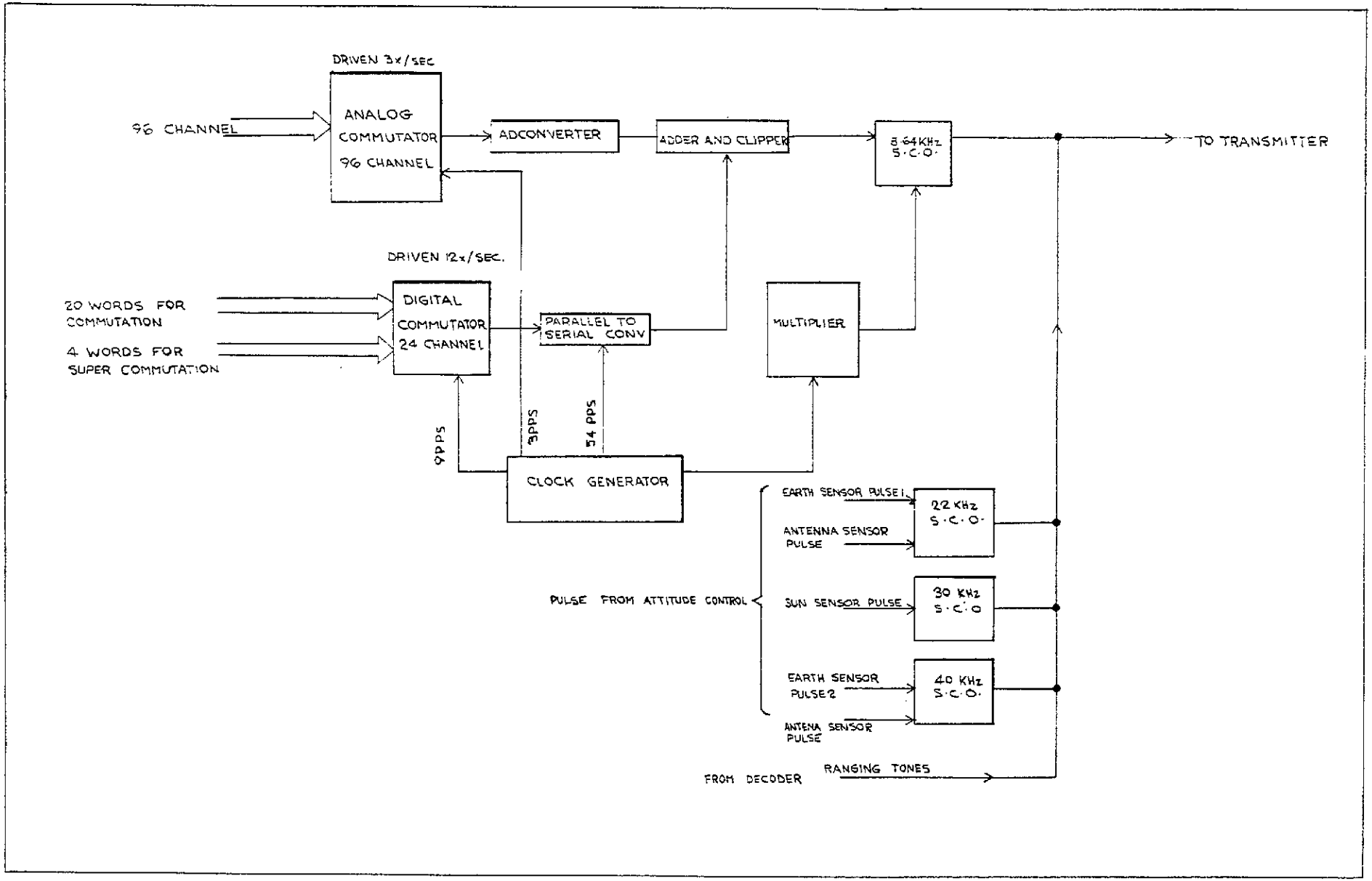

Figure 3–22 Block Diagram Encoder System (One Channel)

Table 3.13 continued

Output Data Rate	72 bits / 1 second
Output Signal	PSK subcarrier
Subcarrier Frequency	8.640 kHz
Real Time	
Earth Sensor, 1 subcarrier	1 RIG Channel 22 kHz
Earth Sensor, 2 subcarrier	1 RIG Channel 40 kHz
Sun Sensor, Subcarrier	1 RIG Channel 30 kHz
Execute Monitor	14.5 kHz

3.4.6 Telemetry Transmitter Assembly

Introduction

The telemetry transmitter assembly is defined as the assembly consisting of two separate but identical transmitters and a power combiner. A sketch of the assembly configuration is given in Figure 3.23. In the discussion which follows we describe primarily one of the transmitters. The power combiner has been already discussed in the antenna system.

General

The general approach to arrive at the output frequency is by multiplying up the frequency of an oscillator operating at a low frequency. This should be achieved with maximum simplicity and the highest efficiency.

The first aspect to consider is the multiplying ratio between the output frequency and the modulator. Limiting factors for this ratio could be the phase modulator and the frequency of the oscillator. Phase modulation is normally obtained by using a reactive network located between a stable frequency oscillator and an amplifying circuit. The modulation is achieved by using a variable capacitance diode as one element of the reactive network. Because of the naturally limited phase deviation possible from any simple reactive circuit, phase modulation is invariably performed at a small submultiple of the output frequency of the transmitters.

An adequate deviation is then obtained since it is multiplied by the same ratio as the frequency multiplication. A typical value of 1 radian peak to peak can be achieved with good linearity at the modulation frequency.

If we assume an operating frequency of approximately 100 MHz and an output frequency of 4 GHz the oscillator frequency and the phase deviation would be multiplied by 40.

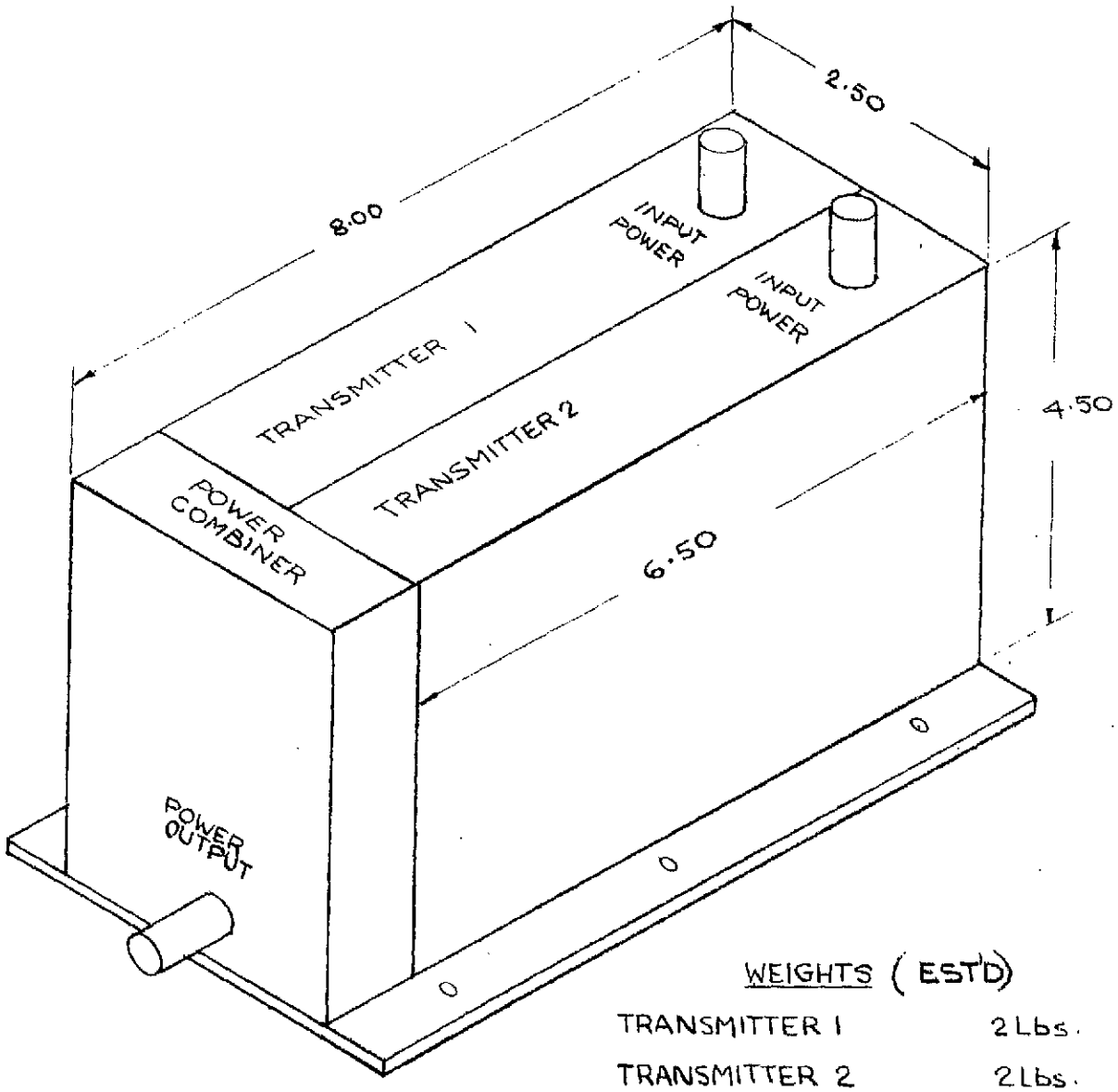

WEIGHTS (EST'D)

TRANSMITTER 1	2 Lbs.
TRANSMITTER 2	2 Lbs.
POWER COMBINER	1 Lbs.
MISCELLANEOUS	1/4 Lbs

Figure 3–23 Outline of Telemetry Transmitter Assembly

Although the location of the phase modulator is not the critical factor for the selection of the multiplying factor, it still would be located close to the oscillator. Then reasonable size discrete components would be used and the high multiplication of the phase deviation would permit operating the modulator well below its deviation limit, thereby improving its linearity.

The other factor which could determine the multiplying ratio of input vs output frequency is the oscillator frequency.

The best way to achieve the frequency stability requirement is by crystal controlled oscillator. In general crystal elements are more stable when operated in their fundamental mode which is up to approximately 25 MHz. However, it is now possible with the latest techniques in crystal cut, to have very good stability even when the crystal is operated in 5th or 7th overtone mode.

A well designed oscillator with its frequency controlled by a crystal element operating in the 5th or 7th overtone could operate at approximately 100 MHz with a frequency stability of ± 5 ppm for temperature effects and ± 7.5 ppm for aging effects in 5 years.

If a better stability is required then the crystal oscillator would operate at the fundamental mode at approximately 20 MHz. Further multiplication of 5 times would be required with some loss of efficiency and extra circuit complexity. A typical figure for a fundamental mode crystal with temperature compensation could be as low as 1 ppm for temperature effects and 7.5 ppm for aging effects.

At this point in time, it seems that the first system with a temperature stability of 5 ppm would be sufficient and there would be no justification to the extra complexity and loss of efficiency necessary to improve that frequency stability figure.

Now that the overall multiplication factor is defined we may evaluate different ways to reach the output frequency, assuming that an RF output of 0.54 watts is required at approximately 4 GHz.

Many combinations of amplifiers and multipliers can be used. In the 4 block diagrams shown below we have typical combinations with information concerning the power gain, output power and efficiencies.

In figure 3.24 we have a system offering simplicity and low weight as discrete components would be used right up to the X10 multiplier. Only the last X10 multiplier would be using cavity type circuitry. All these blocks use proven and reliable components in circuits which are commonly used. Unfortunately the overall efficiency is only 8.3% although recent and near future development could improve the gain and the efficiency of the 400

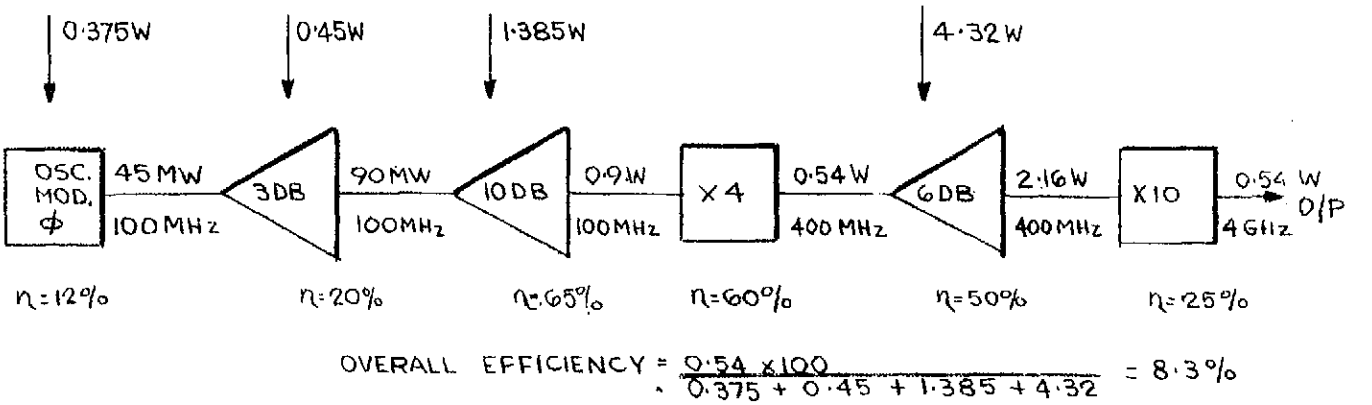

Figure 3–24 Block Diagram Transmitter System No. 1

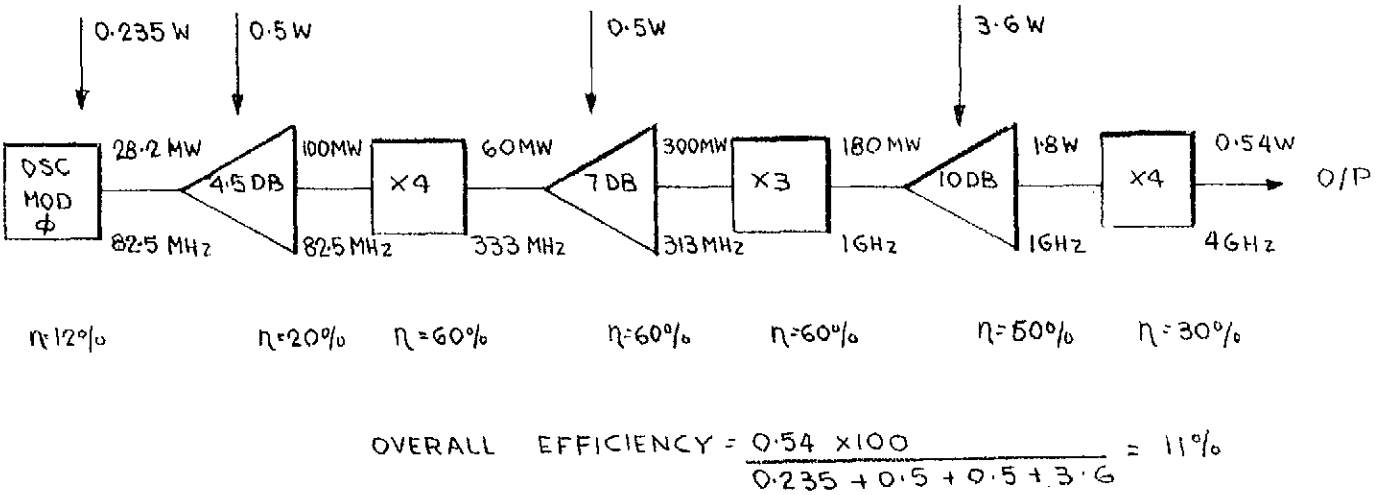

Figure 3–25 Block Diagram Transmitter System No. 2

MHz amplifier. This could improve the overall efficiency to approximately 11%.

The power output of this system can be increased very easily as all the transistors and diode multipliers are working well below their rated output and their maximum voltage ratings.

In Figure 3.25 the system uses discrete components up to the frequency of 333 MHz. The output of the tripler, the 1 GHz amplifier and the last quadrupler all use cavity type circuitry with its weight penalty. The 1 GHz amplifier is a state -of-the-art development. The over-all efficiency is the highest at 11%. The power output of this system can be increased and the limit would be set by the 1 GHz amplifier. All the other components are operated well below their maximum rated value.

Figure 3-26 shows a variance of system 2 where the carrier is amplified only at 100 and 1000 MHz. The efficiency is slightly less at 10% but otherwise the same comments as in system #2 are applicable.

In Figure 3.27 are amplifiers at 100, 1000 and 2000 MHz. The efficiency is very low and many cavity type circuits would be required. The weight and size would be large.

From the brief evaluation of these various block diagrams we conclude that the system of Figure 3.25 and Figure 3.26 is most promising. However, further evaluations would have to be made considering efficiency, simplicity, weight, and other parameters, before a final selection could be made.

Phase Locking System

As described in the power combiner section it is advantageous under certain conditions to parallel the operation of the 2 telemetry transmitters. This if feasible providing the outputs of each transmitter are and remain in phase. This is achieved by mixing the output carrier of each transmitter in a phase discriminator. The correction signal derived from the phase discriminator will be amplified and applied to a variable capacitor located in the reactive network used to adjust the center frequency of one of the transmitters. The correction signal will be a DC bias superimposed on the normal design bias for the varactor; therefore in the absence of a correcting bias the transmitter will resume its normal function at the adjusted center frequency.

In order to have identical transmitters, each one would contain a phase discriminator and an amplifier. The sample output would be received from the other transmitter through a short external connection.

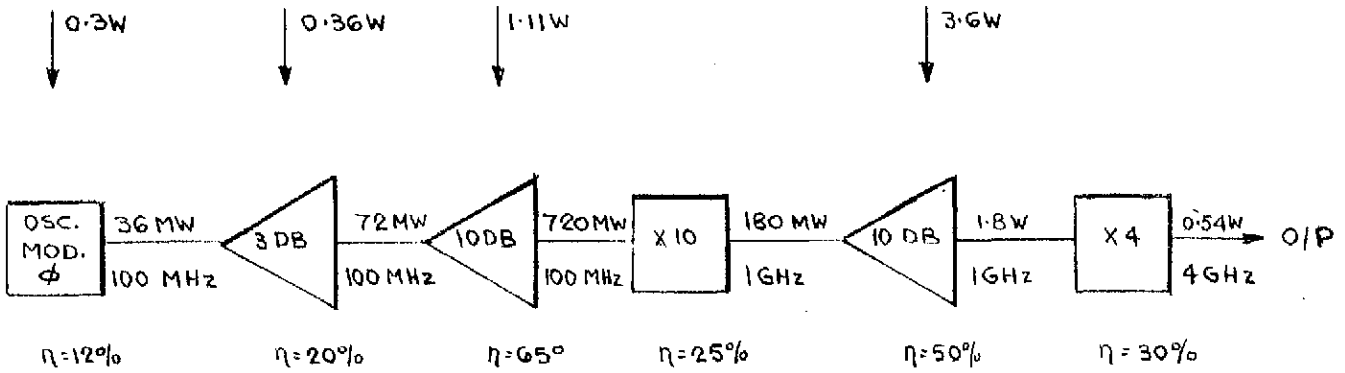

$$\text{OVERALL EFFICIENCY } \frac{0.54 \times 100}{0.3 + 0.36 + 1.11 + 3.6} = 10\%$$

Figure 3–26 Block Diagram Transmitter System No. 3

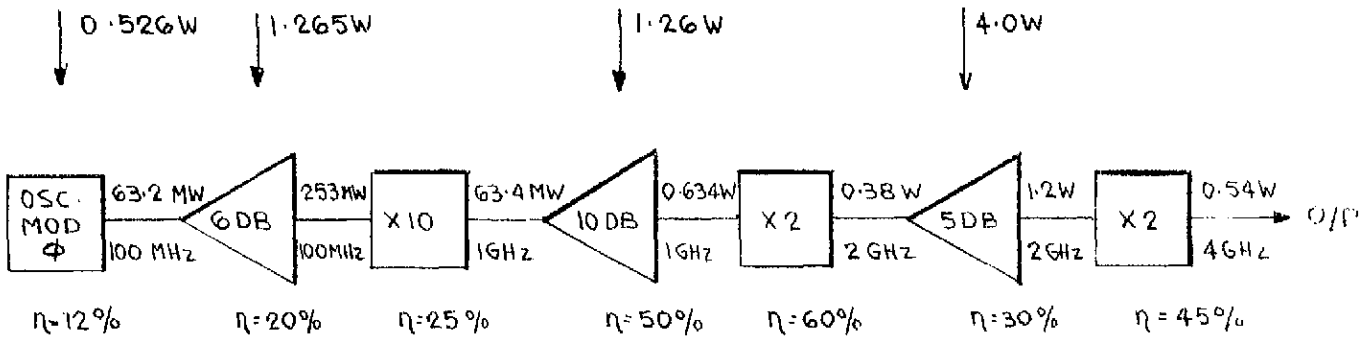

$$\text{OVERALL EFFICIENCY } \frac{0.54 \times 100}{0.526 + 1.265 + 1.26 + 4.0} = 7.7\%$$

Figure 3–27 Block Diagram Transmitter System No. 4

As a result of all the above considerations we could establish a tentative performance specification:

Tentative Telemetry Transmitter Performance Specification	
Frequency:	3700 to 4200 MHz (crystal and circuit value modifications)
Frequency Stability:	± 10 ppm with temperature ± 12.5 ppm for temperature and aging in 5 years
Output power:	Min. 0.54 W in 50 ohms
Power Requirement:	6.48 watts
Power Supply Voltage:	28V
Assembly Volume:	90 cu. in.
Assembly Dimensions:	8 x 4 1/2 x 4 1/2 inches
Assembly Weight:	5 1/4 lbs.

Table 3.14

3.4.7. Beacon Transmitter

Introduction

The Beacon transmitter operates in the 136 MHz band with an output of 5 watts. With minor modifications the telemetry transmitters developed for ISIS A and B would be suitable. The transmitter is an improved version of earlier models used in Alouette I and II. These transmitters are still performing successfully after many years of operation. An outline sketch is given in Figure 3.28.

Configuration

Figure 3.29 shows the block diagram of the transmitter. The frequency of the oscillator is controlled by a crystal element operating in the fundamental mode. The oscillator is followed by a buffer amplifier to minimize the effects of the subsequent stages on the stability of the oscillator. The output frequency is reached by multiplying the basic crystal frequencies by three varactor doublers properly separated by amplifiers to achieve maximum stability. The last block is a bandpass filter which reduces all spurious outputs to an acceptable level.

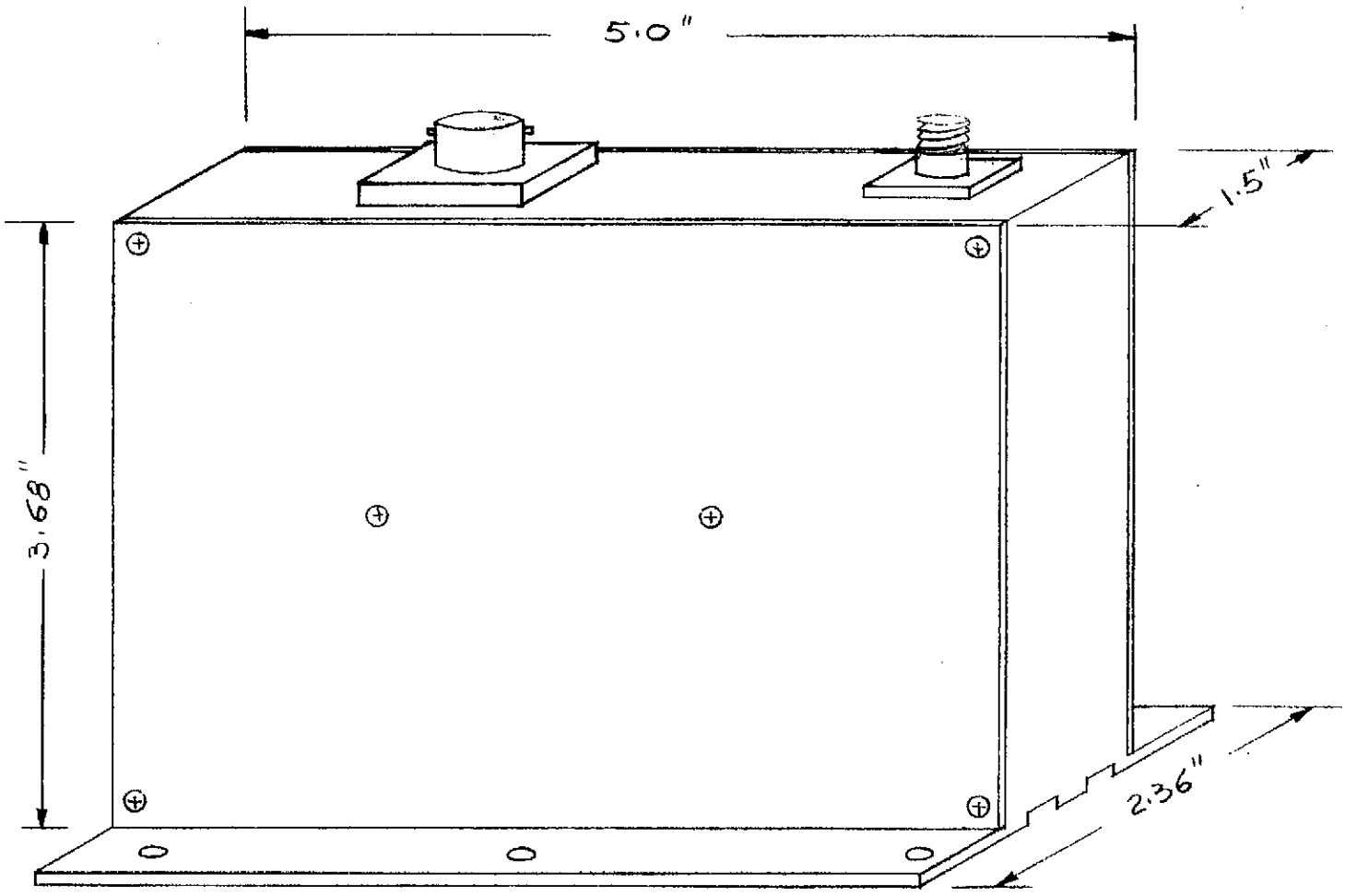

WEIGHT (EST'D) 14 oz.

Figure 3-28 Outline of 136 MHz Beacon Transmitter

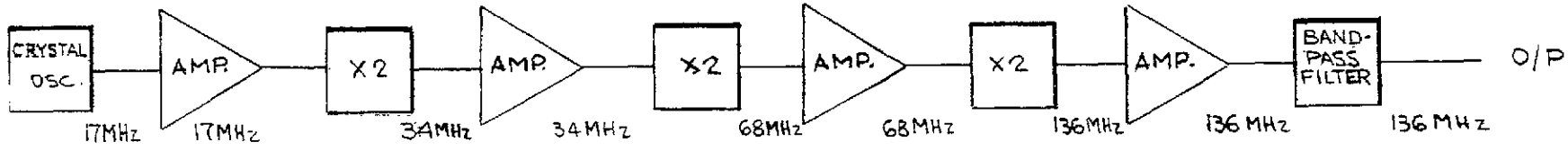

Figure 3–29 Block Diagram Beacon Transmitter

Tentative Beacon Transmitter Performance Specifications	
Frequency:	Approximately 136 MHz
Frequency stability:	+ 35 ppm with temperature
Output power:	5 watts nominal in 50 ohms
Power requirement:	13.5 watts nominal 25°C
Volume:	25 cu. in.
Dimensions:	2.68 x 1.5 x 4.5 inches

Table 3.15

4.0 POSITIONING AND ORIENTATION SUBSYSTEM

4.1 FUNCTIONAL DESCRIPTION

The Spacecraft Positioning and Orientation Subsystem provides the following functions:

- Initial orbital corrections resulting from off-nominal apogee motor performance and launch vehicle injection errors
- Attitude maneuvers and spin axis adjustments
- Station keeping corrections at periodic intervals over the satellite lifetime to maintain a synchronous, equatorial orbit

Initial orbital corrections and station keeping are accomplished by firing the axial thrusters in a continuous mode and firing the radial thrusters in a pulsed mode, thus providing the necessary velocity increment for orbit inclination and longitudinal drift corrections. Attitude maneuvers and spin axis corrections are accomplished by firing the axial thrusters in a pulsed mode of approximately 80 ms. per pulse. By this means the Positioning and Orientation Subsystem furnishes the necessary propulsive forces to position and maintain the satellite spin axis normal to the orbit plane during the period of communications performance.

Figure 4-1 presents a summary specification for the P and O Subsystem.

4.2 DESIGN CONCEPT

The design concept for the P and O Subsystem is identical to that currently used for the Intelsat III communications satellite system. A schematic of this subsystem is presented by Figure 4-2. The propellant is monopropellant hydrazine, which is catalytically decomposed by Shell 405 catalyst.

FUNCTION:

To provide a velocity increment capability to the satellite for orbit and altitude corrections during initial positioning and station keeping throughout a 5 year operational lifetime.

SUBSYSTEM PERFORMANCE AND OPERATIONAL REQUIREMENTS:

Minimum total velocity increment capability: 1144 ft/sec.

Minimum total impulse capability 16,700 lb-sec.

Duty cycle:

Total cold starts during operational lifetime = 500

Continuous mode firing time = 3,640 sec.

Total number of pulses = 21,100.

Satellite nominal spin speed: 100 rpm

Operational temperature range: + 40 to + 120 ° F

Storability: Capability of dry storage for 3 years when pressurized to 120 ± 10 psig with GN_2 while exposed to storage temperature of -25 to + 140° F.

Leakage: Not to exceed the equivalent of a 5 percent pressure loss over the operational lifetime.

RELIABILITY: .98 for 5 years

Figure 4-1(a) Summary Specification, Positioning and Orientation Subsystem

PHYSICAL CHARACTERISTICS:

Configuration: Total propellant to be equally divided between two independent subassemblies, each having a satellite maneuvering capability. Redundancy to be provided by normally-closed squib valve and plumbing. Propellant and pressurant fill and drain capability to be provided for ground operations prior to launch.

Propellant: Monopropellant hydrazine ($N_2 H_4$)

Pressurant: Gaseous nitrogen (GN_2)

Maximum Weight:

Dry weight	= 16.7 lb
Loaded weight (Including propellant and pressurant)	= 94.9 lb

THRUSTER PERFORMANCE CHARACTERISTICS:

Feed pressure range:	600 psia to 200 psia
Nominal thrust level:	4.0 lb 1.7 lb
Continuous mode nominal specific impulse:	229 sec. 217 sec.
Pulse mode nominal impulse bit (80 ms pulse width):	0.37 lb-sec to - 0.17 lb-sec

Reproducibility: Continuous mode firings to demonstrate at total impulse reproducibility of ± 4%. Pulse mode firings to demonstrate a total impulse reproducibility of ± 20% for the first 5 pulses, after which the total impulse reproducibility per pulse shall be ± 7%.

Figure 4–1(b) Summary Specification, Positioning and Orientation Subsystem

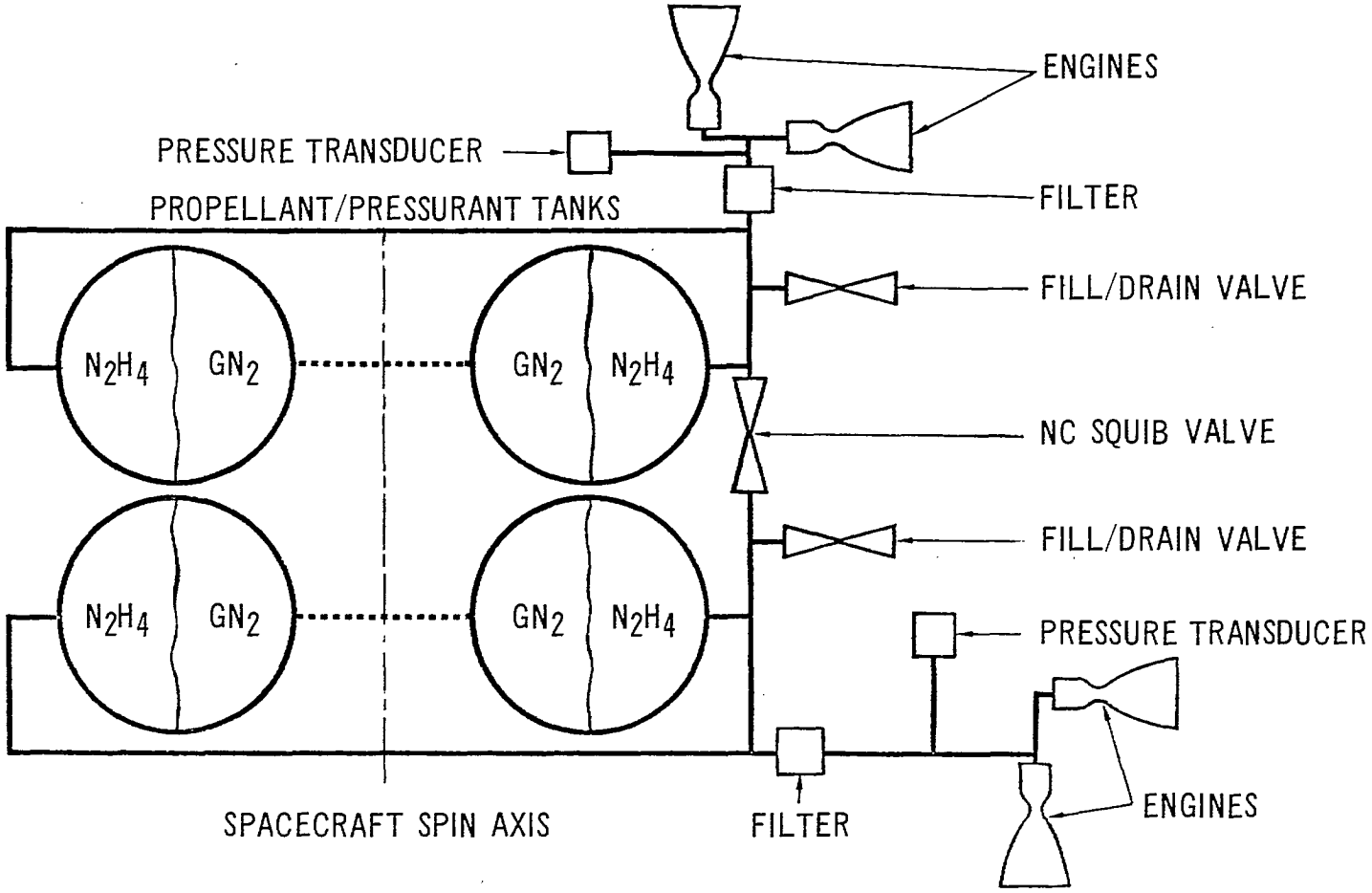

Figure 4–2 Positioning and Orientation System Schematic

The subsystem consists of two separate subassemblies each with its own fill and drain, instrumentation, and radial and axial thrusters supplied from an opposed pair of fuel tanks. The subassembly fuel feed lines are interconnected by a normally closed pyrotechnic valve. Actuation of this valve in the event of the failure of a thruster propellant valve in the closed position makes available all the remaining propellant to any of the remaining operable thrusters, thus maintaining both a radial and an axial thrusting capability.

Orientation of the propellant-to-pressurant interface is maintained by the centrifugal forces caused by the spinning satellite, and expulsion is accomplished by blowdown of the nitrogen gas in the pre-pressurized ullage space. Gaseous nitrogen is selected as the pressurant due to its negligible solubility in hydrazine and its reduced leakage potential when compared to helium. Pressure transducers in the propellant feed lines provide on indication of tank pressure.

Each subassembly has a fill and drain provision for fueling, pressurizing and, if necessary, draining the subassembly, and the routing of the propellant and pressurant lines and tank configuration and orientation is such as to permit complete draining of the system on the ground without the necessity of spinning the satellite. Also, it is anticipated that an all-welded construction will be provided to eliminate any possible sources of leakage which would exist with mechanical joints.

4.3 OPERATIONAL CHARACTERISTICS

The P and O Subsystem will be controlled by a ground station, which transmits commands for selection of the thruster to fired, firing mode (whether continuous or pulsed), and pulse duration. Initial tank pressures will be approximately 600 psia, with final expulsion pressures approximately 200 psia, which correspond to thrust levels of approximately 4.1 to 1.7 pounds. Thus, measurement of tank pressure provides a means for predetermining the firing duration required to achieve the desired total impulse, and for monitoring the propellant quantity remaining in the tanks.

The design feature of dividing the subsystem into two completely independent assemblies ensures flexibility in operation. Either of the two subassemblies can be used to perform any desired attitude, velocity, or latitude correction. Since the radial engines are located to provide thrust through the center of gravity of the satellite, either can be fired once per revolution to effect a longitudinal correction in either direction. Spin axis attitude corrections can be performed by either of the two axial engines by selecting the appropriate portion of the arc to fire the thruster.

Latitude corrections (and initial positioning prior to initial reorientation of the satellite) are obtained by continuous firing of the appropriate axial engine. Because of this flexibility, either system may normally be selected to perform a given correction maneuver and propellant utilization may therefore be managed to assure that total capacity for velocity correction will be available throughout the operational life of the satellite. Additional flexibility is provided by the backup mode of operation, in which the normally closed squib-actuated valve separating the two subassemblies is opened by ground command, permitting propellant from one system to feed the other in the event of failure of one propellant valve in a closed position. Therefore, the axial and radial thrusters of each subassembly is capable of burning the total propellant of both subassemblies.

4.4 THRUSTER PERFORMANCE AND PROPELLANT QUANTITY

INTELSAT III development, qualification, and acceptance test data records provide thorough documentation of the thruster performance characteristics. Delivered specific impulse for both steady state operation and minimum impulse bit for pulse mode (80 msec) operation as a function of feed pressure is presented in Figure 4-3. Figure 4-4 shows the variation of nominal thrust level as function of feed pressure for the first eight Intelsat III flight engines.

Based on a preliminary requirement for a total velocity increment capability of 1144 ft/sec, a total hydrazine propellant quantity of 76.4 pounds was determined to be required, for a spacecraft total weight in the transfer orbit of 965 pounds. This propellant weight was based on an average specific impulse of 225 seconds and includes a 3 percent allowance for expulsion efficiency, cold starts, and cosine losses due to radial thruster operation during initial positioning maneuvers.

4.5 COMPONENT DESCRIPTION

With the exception of the propellant tanks, plumbing, and possibly filters, the P and O subsystem for the satellite will consist of components which have been developed and qualified for the Intelsat III system. The approach will assure compliance with design and performance requirements and gives maximum assurance of meeting schedule and cost committments. Figure 4-5 shows the components of the Intelsat III Positioning and Orientation Subsystem.

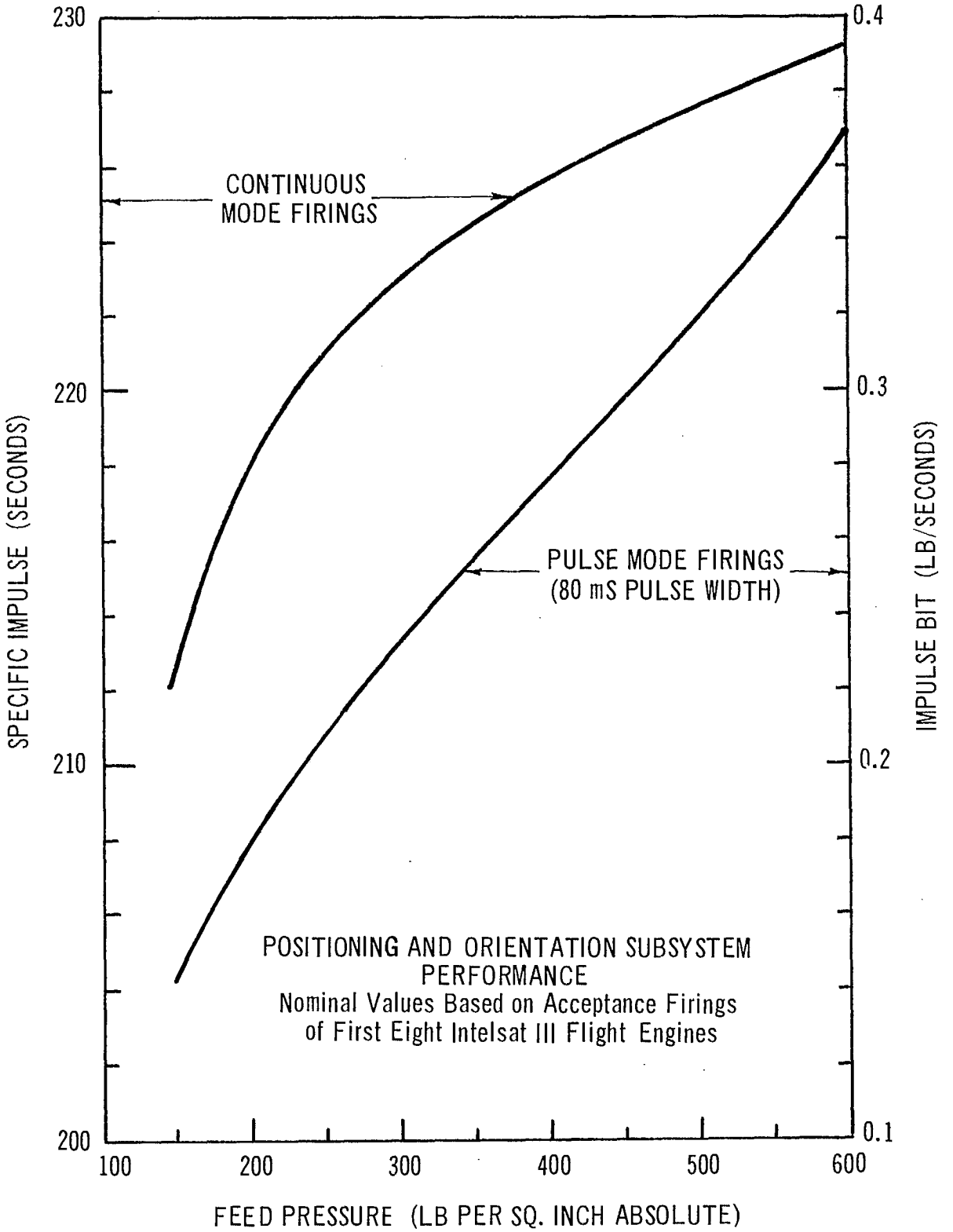

Figure 4-3 Specific Impulse and Impulse Bit versus Feed Pressure

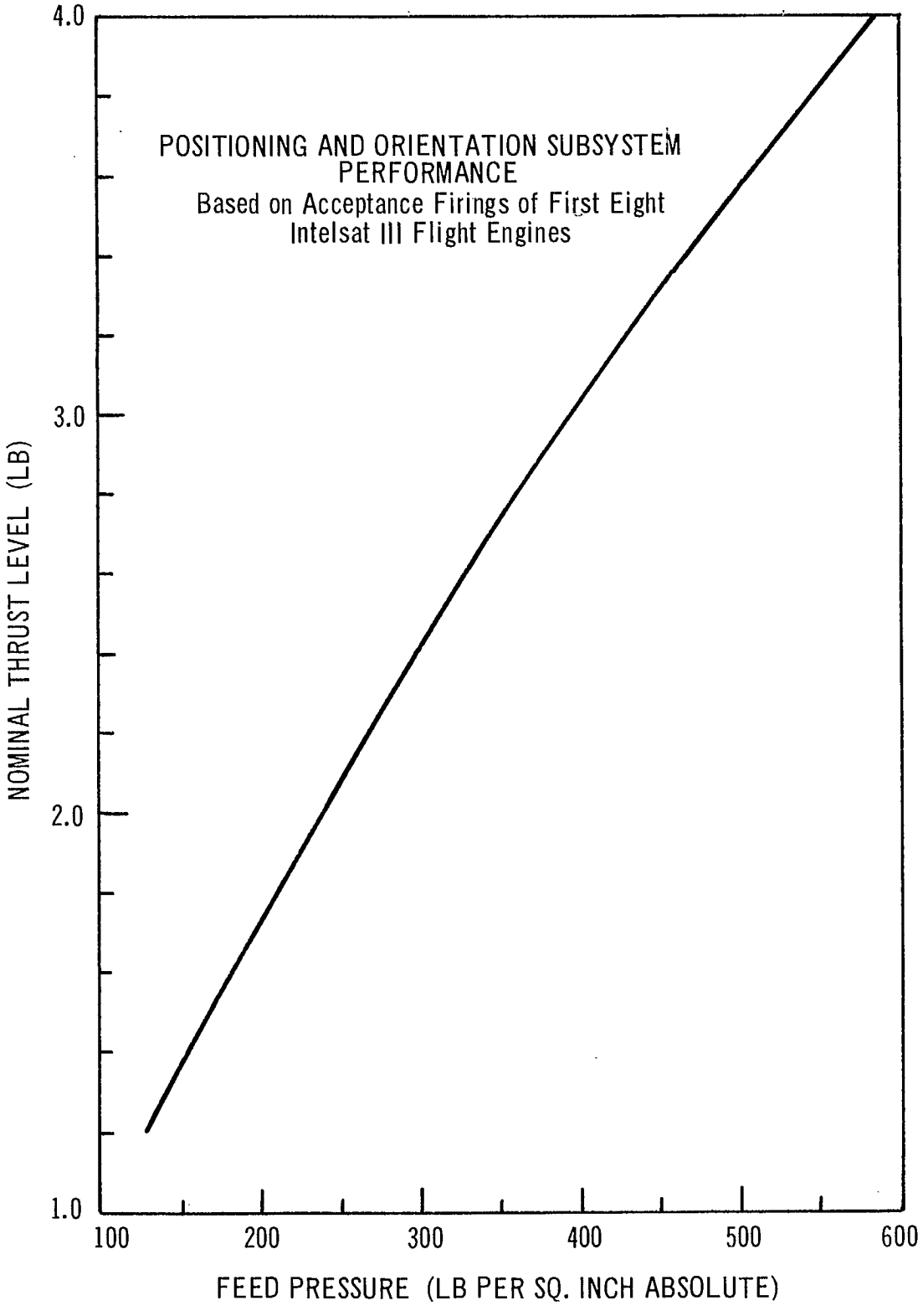

Figure 4–4 Thrust Level versus Feed Pressure

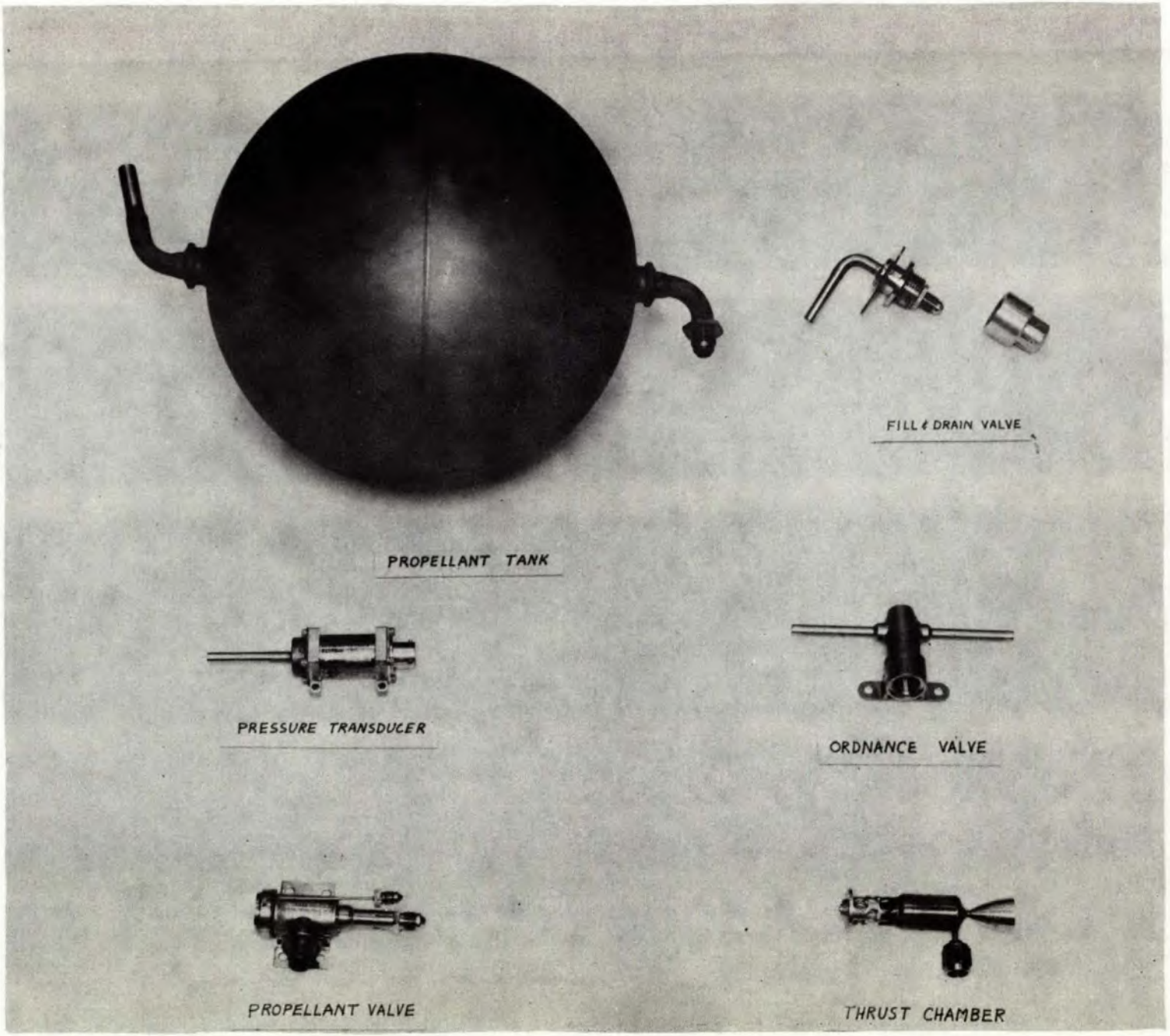

Figure 4–5 Components of the Positioning and Orientation Subsystem

4.5.1 Thruster Assembly

The thruster assembly is identical to that used for INTELSAT III, except that the mechanical connection at the propellant valve interface will be replaced by a welded connection, minimizing a potential source of leakage at this joint. (Experience with the INTELSAT III positioning and orientation subsystem has shown that provisions for replacement of thruster assemblies will not be necessary.)

The thrust chamber assembly consists of a capillary tube injector, a cylindrical reactor chamber filled with a catalyst, and a nozzle. A perforated, lightweight structural element connects the thrust chamber to the solenoid-actuated valve and minimizes heat transfer from thrust chamber to valve. The Shell 405 catalyst is held in the thrust chamber by stainless steel screens at both ends. A fitting is provided to enable chamber pressure measurements during acceptance testing of each engine, which is removed prior to installation in the flight spacecraft.

Maximum reliability is assured by the welded and brazed construction of the thrust chamber assembly. The chamber, nozzle, cap, sleeve, screen, and screen supports are all machined from Haynes Alloy No. 25 bar stock. The capillary tube injector is a piece of drawn tubing. The stainless steel screen assembly, previously assembled and resistance welded, is positioned with the reaction chamber and nozzle. When the chamber has been electron-beam welded to the nozzle, it is filled with catalyst, and electron-beam welded to the head-end assembly.

4.5.2 Propellant Valve

Design of this unit is such that solenoid valves initiate and terminate propellant flow to close tolerances of accuracy and repeatability. The dual, in-series seal design of the valve provides some unique redundancy features, contributing to the reliability of the system, without the added complexity normally associated with redundancy.

This series seating configuration is arranged to prevent the exposure of the solenoid armature to a hard vacuum and to provide a redundant seal against internal leakage when the valve is in the closed position. Redundancy is also provided in the dual-coil solenoid; either winding will actuate the valve. The integral inlet filter provides 25 micron absolute filtration and is oversized to preclude excessive pressure drop. Qualification test data on this valve show extremely good sealing characteristics. After approximately 60,000 cycles of testing while exposed to temperatures ranging from 25° F to + 120° F, the valve leakage did not exceed acceptance specification limits.

4.5.3 Propellant Tank

The propellant tank consists of hemisperical and conical sections which are electron-beam welded. The conical section permits complete drainage of the system while in the vertical position and complete expulsion of hydrazine while in the spinning mode, as shown in Figure 4-6 below. Titanium alloy Ti 6 Al 4 V, the same material used for the INTELSAT III tanks, will be used.

Although the tank configuration is slightly heavier than a spherical configuration with an additional outlet port for draining the propellant, a possible leakage source is eliminated. The drainage feature not only provides a safety feature for launch operations but also facilitates testing of the system when a referee propellant is used to simulate the mass properties.

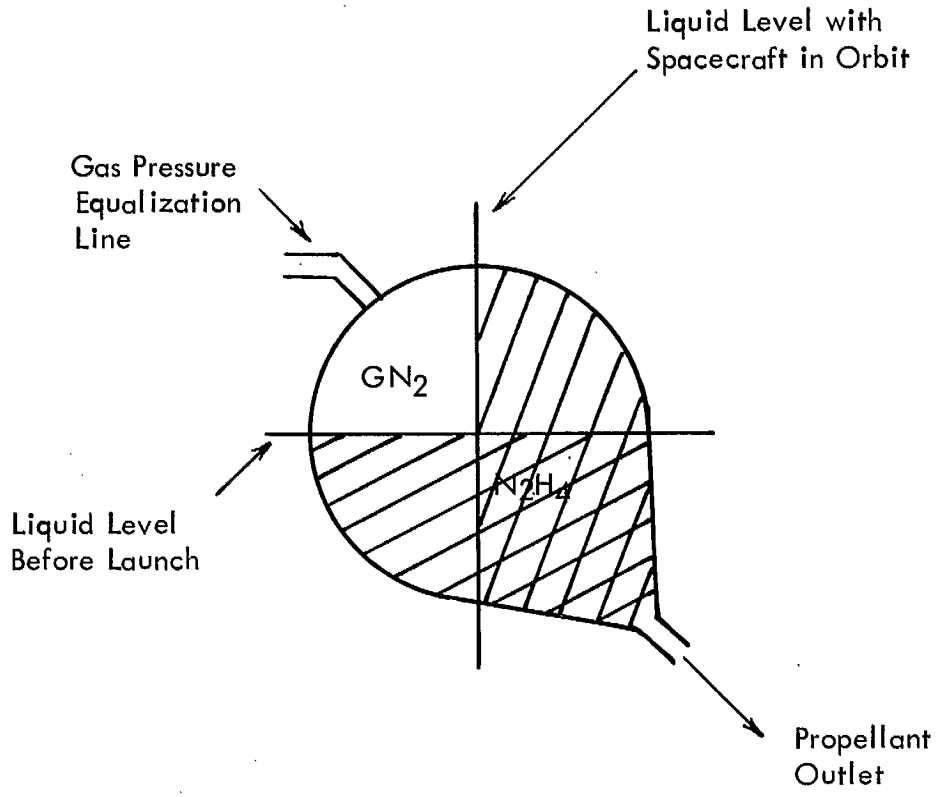

Figure 4-6 Propellant Tank Design Concept

4.5.4 Ordnance Valve

A normally closed ordnance valve interconnects the two assemblies in the event of a failure of one of the propellant valves in the closed position. High reliability of operation is assured by a dual bridgewire cartridge.

When the explosive train is ignited, it drives a plunger across two sealed end caps, which are pushed out of the flow path. The plunger stops when a cross port in it is lined up with the flow path, providing straight-through full flow.

4.5.5 Fill and Drain Valve

The fill and drain valve is used for both propellant and pressurant loading and unloading. It is manually operated, with redundant seals for positive sealing. When loading is completed, the entire valve is capped for final protection against leakage.

4.5.6 Pressure Transducer

The pressure transducer is a high output type (0 to 5 volts) and is calibrated to provide accurate measurement of tank pressure in the range of 0 to 600 psia.

4.5.7 Heatshield

The axial thrusters are enclosed in heatshields to prevent excessive heat rejection to the spacecraft during thruster firings of extended duration. These units consist of a low conductivity, nonevaporative insulation contained in a gold-plated outer shell.

4.5.8 Filter

The 15 micron absolute filter provides assurance that the propellant valves and thrusters will not be exposed to contaminents which could cause a malfunction.

4.5.9 Plumbing

Standard sizes of stainless steel and titanium plumbing are welded to the various components prior to final leak checks and installations of the P and O subsystem in the satellite.

5 ATTITUDE CONTROL AND ANTENNA DESPIN SUBSYSTEMS

5.1 INTRODUCTION

The Attitude Control and Antenna Despin Subsystem provides capabilities for performing the following functions:

- o Spin-axis attitude determination in both transfer and synchronous orbits.
- o Initial positioning, stationkeeping and spin-axis attitude control.
- o Antenna despin and pointing.

These functions involve on-board as well as ground station equipment. The design employs techniques similar to the ones developed for Intelsat III, which provide maximum degrees of simplicity and reliability. The overall block diagram of the Attitude Control and Antenna Despin Subsystems showing the corresponding functional organizations is given in Figure 5-1.

Spin-axis attitude determination is made using sun and earth sensors, the outputs of which are telemetered to the ground. The function counter processes the sensor information and provides indication of spin-axis attitude. The satellite is equipped with two radial and two axial thrusters. These thrusters are actuated by ground command to control the satellite as follows:

- o Reorientation and Attitude Control

  Pulsed operation of axial thrusters; pulses are timed to precess the satellite spin axis in the proper direction.

- o Correction of Orbital Inclination

  Continuous operation of axial thrusters.

- o Initial Positioning and Stationkeeping

  Initial positioning may be performed by continuous operation of the axial thrusters prior to satellite reorientation, or by pulsed operation of the radial thrusters after reorientation. Stationkeeping is performed by pulsed operation of the radial thrusters.

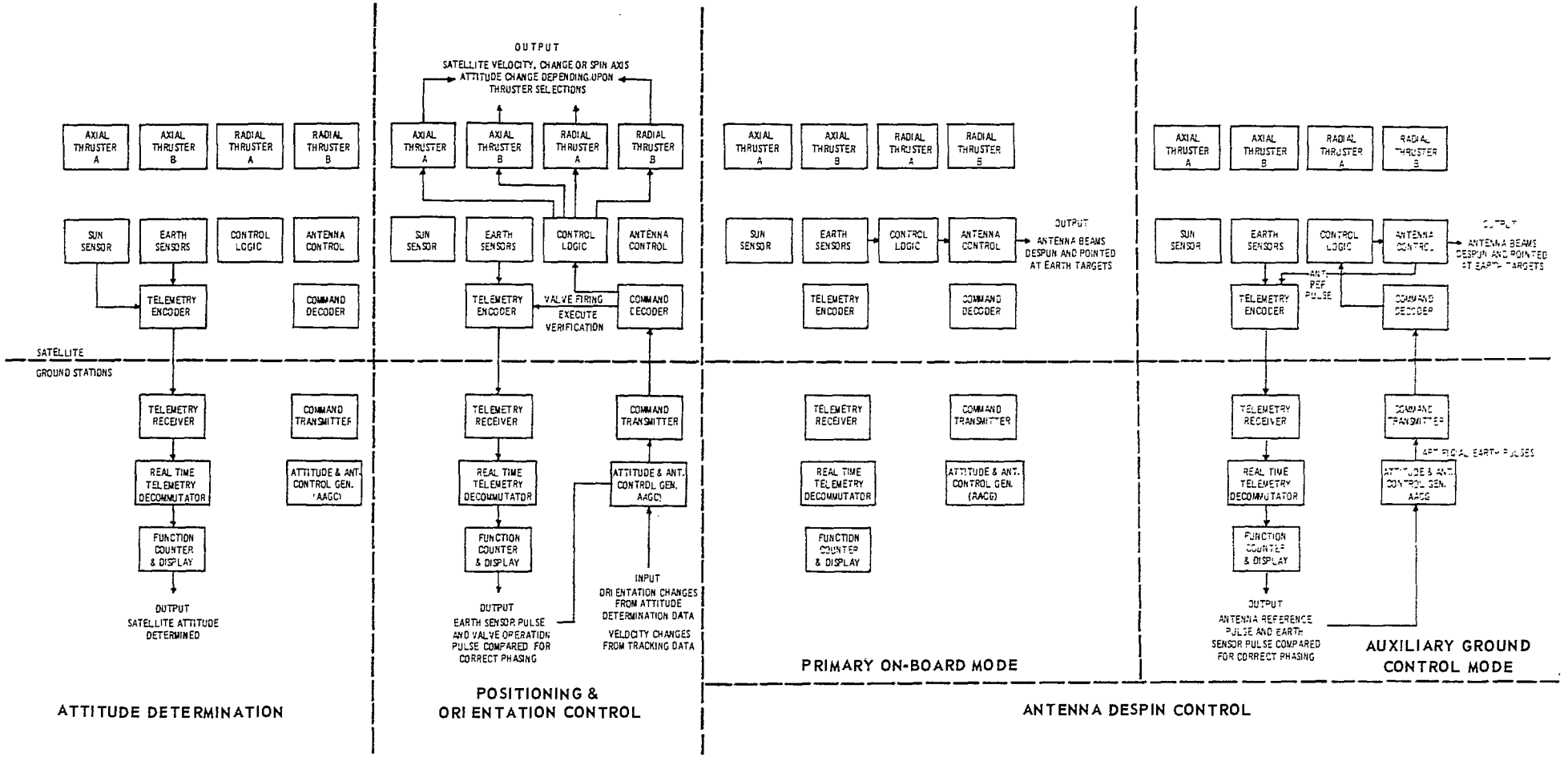

Figure 5–1 Functional Diagram of Positioning and Control Operations

The ground station attitude and antenna control generator (AACG) provides pulses at the proper time to the command encoder and transmitter which transmit the thruster valve commands to the satelite. Selection of the proper valve is accomplished by the command link. The AACG generates the pulses at the precise time required by measuring the time interval between reception of earth sensor pulses and telemetered valve operate pulses and by adjusting the transmission time of the valve operate pulses to obtain the desired interval.

Both on-board and ground antenna despin control alternatives are provided. On-board control is achieved by providing an earth reference pulse at the satellite rotational rate to the antenna control electronics. This once-per-revolution pulse synchronizes the generation of antenna waveforms to point the antenna beam at the earth target.

Ground antenna control is accomplished by first selecting the ground control mode using the command system and then transmitting artificial earth pulses (AEP) to the satellite at the satellite's rotational rate. The AEP's control the antenna beam in the same manner as the on-board control.

The timing of the AEP transmissions must, of course, be controlled to point the antenna beam at the earth. This is accomplished by comparing and adjusting the time interval between reception of an antenna reference pulse (ARP) and earth sensor (ES) pulse and adjusting the AEP transmission time for the proper ARP-ES interval. This latter function is performed by the attitude and antenna control generator (AACG) at the ground station. The desired ARP-ES pulse time interval is a manual input to the AACG unit, which then generates AEP pulses at the correct time and sends these pulses to the command encoder for transmission to the spacecraft.

Ground control will be required only when one earth sensor has failed and the sun or full moon are in the other earth sensor field-of-view and very close to the edge of the earth.

Preliminary specification for the attitude control and despin subsystems are given in Table 5-1.

Table 5-1 Preliminary Attitude Control and Despin Subsystem Specifications

Antenna Beam Pointing Accuracy	± 0.383 Degrees east-west ± 0.343 Degrees north-south
Despin Control Electronics Weight	9.0 Pounds
Despin Mechanism Weight	13.0 Pounds
Despin Control Prime Power	12.3 Watts
Reliability of Despin Subsystem	0.948 (5 years)

5.2 ANTENNA POINTING REQUIREMENTS

Antenna pointing requirements are 0.5 degrees (3σ) in both the E-W (pitch) and N-S (roll) directions. The spacecraft attitude must be controlled by the despin controller and the attitude control subsystem to maintain the above antenna pointing accuracy. As the antenna boresight is not coincident with local vertical, spacecraft yaw errors must also be considered in addition to the dominant pitch and roll error components. Specifically the antenna offset angles will be 7.4 degrees in roll (to point the antenna boresight at 51 degrees north latitude) and 5 degrees in pitch (to yield the proper ground coverage).

5.2.1 Antenna Pointing Error Budget

The predicted antenna pointing accuracies for on-station performance are

East-west accuracy: ± 0.383 degrees

North-south accuracy: ± 0.343 degrees

The estimate of accuracy is based on the predicted peak deterministic error added to the RSS 3σ statistical errors. The approach is conservative since the peak errors will seldom occur and will occur simultaneously even less often. The error analysis deals with first and second order statistics, and assumes uncorrelated statistical error sources.

The sources of east-west (E-W) antenna pointing inaccuracy include sensor errors, control loop accuracy (including the effect of sensor noice), spacecraft positioning errors, alignment of the antenna to the reference axes, alignment of the electrical boresight of the antenna to its mechanical axes, and antenna thermal deformation. Additional potential alignment error sources arise at the mechanical interface between the rotor and the antenna supporting structure. However, since the magnetic pick off in the despin mechanical assembly can be adjusted to remove these misalignments, the only pertinent alignment tolerance relates to the pipper adjustment, which can be made to an accuracy of 0.05 degree. Several factors of significance in N-S pointing (particularly rotor mass imbalance) are of second-order significance in E-W inaccuracy. Table 5-2 summarizes the E-W antenna pointing errors.

Many of the factors affecting E-W accuracy have a counterpart in the N-S error budget. Significant statistical contributors include attitude determination errors, mounting errors (tilt) at the interfaces of the despun mechanical assembly and the despun and spinning sections, rotor dynamic imbalance, antenna alignments, and sensor misalignments. Deterministic error sources arise from antenna thermal deformation and the attitude correction deadband. The results of their analysis are given in Table 5-2.

Sensor error sources include spin rate variation, mounting and internal alignment errors, electronic gain changes and bolometer time constant changes. For these sensors (identical to those in Intelsat III) the total long-term earth sensor error (excluding sensor mounting) will be maintained below 0.10 degrees (3σ) in despin error computation by in-orbit biasing: the same effects contribute a long-term error of less than 0.10 degree (3σ) in attitude determination including sensor misalignments. The mounting error in rotation is specified to be no greater than 0.05 degrees (3σ).

Inaccuracies in despin (E-W) control arise mainly from sensor noise, bearing noise, and noise in the tachometer circuit. The total for these effects is 0.300 degree (3σ) and represents the dominant error source for E-W pointing.

Table 5-2 Error Budgets for Antenna Pointing

Despin Pointing (E-W)	Mean	3σ
Sensor and processing (1)	0	.100
Control loop accuracy (1), (2)	0	.300
Sensor alignment (static and thermal)	0	.050
Magnetic Pipper alignment	0	.050
East-West positioning error (peak)	.02	0
Antenna alignment (static)	0	.050
Antenna boresight	0	.050
Antenna thermal deformation (5)	.03	.030

Expected value (peak) = .050
RSS of 3σ errors = .333
Mean plus 3σ error - .383 degrees

Attitude Pointing (N-S)		
Attitude determination (3)	0	.100
N-S positioning error	.020	0
DMA-bearing assembly	0	.020
DMA-Rotor alignment	0	.050
DMA-Antenna support structure alignment	0	.050
Rotor dynamic imbalance (static and thermal) (4)	0	.050
Antenna alignment to DMA hub (static)	0	.050
Antenna electrical boresight alignment	0	.050
Antenna thermal deformation (5)	.020	.020
Attitude correction deadband	.150	.010

Expected value (peak) = .190
RSS of 3σ errors = .153
Mean plus 3σ error = .343 degrees

(1) Assumes in-orbit biasing of long-term instability errors.
(2) Includes jitter due to sensor noise from electronic sources.
(3) Includes sensor misalignment.
(4) Equivalent to (100) (.001) = 0.1 slug-ft^2 imbalance for $I_R - I_T$ slug-ft^2.
(5) Mean value is peak predicted (deterministic) deformation; includes deformation in antenna and supporting structure.

Errors in the spacecraft longitude and orbital inclination contribute antenna pointing errors. Assuming positioning deadzones of 0.1 degree the resulting pointing errors are 0.02 degree in E-W pointing and 0.02 degree in N-S pointing.

Antenna wobble resulting from dynamic imbalance of the rotor will be maintained less than 0.05 degree by balancing the rotor on the ground. The rotor balance must be maintained throughout the mission; thus the design provides for accurately uniform depletion of hydrazine from its tanks.

Similar wobble is produced by bearing runout in the despin mechanical assembly, no greater than 0.02 degree, and tilt alignment errors at its interfaces with the rotor and antenna supporting structure, no greater than 0.05 degree.

Antenna alignment errors can be resolved into three components: static alignment of the antenna mechanical structure; alignment of the electrical antenna boresight to its mechanical reference axes; and deflection of the antenna boresight by thermal distortion in the antenna, its feedand supporting structure. The static alignments are statistical and apportioned at 0.05 degree (3σ) each. The thermal deflections are predictable with some accuracy. A detailed analysis in Section 8.0 indicates an error of 0.03 degree (peak) $\pm$ 0.03 degree (3σ) for east-west pointing and 0.02 degree (peak) $\pm$ 0.02 degree (3σ) for north-south pointing.

5.2.2. Total Antenna Pointing Error

The total antenna pointing error is primarily determined by the roll, pitch, and yaw spacecraft attitude errors as well as the roll and pitch offset angles of the antenna boresight. In general, the RSS radial antenna pointing error (ε) is:

$$\varepsilon = \left[\overline{\Delta\phi^2}\ (\cos^2\alpha + \sin^2\alpha\ \sin^2\beta) + \overline{\Delta\theta^2}\ \cos^2\beta + \overline{\Delta\psi^2}\ (\sin^2\alpha + \cos^2\alpha\ \sin^2\beta)\right]^{\frac{1}{2}}$$

where:

$\overline{\Delta\phi^2}$ = sum square roll error

$\overline{\Delta\theta^2}$ = sum square pitch error

$\overline{\Delta\psi^2}$ = sum square yaw error

α = pitch offset angle

β = roll offset angle

For roll and pitch offsets of 7.4 and 5 degrees respectively, the radial antenna pointing error is:

$$\varepsilon = \left[1.02\ \overline{\Delta\phi^2} + .985\ \overline{\Delta\theta^2} + .0241\ \overline{\Delta\psi^2} \right]^{\frac{1}{2}}$$

As the roll and yaw errors will be 90 degrees out of phase (a characteristic of attitude control systems with a pitch momentum bias), a conservative estimate of the radial pointing error is:

$$\varepsilon = \left[1.02\ \overline{\Delta\phi^2} + .985\ \overline{\Delta\theta^2} \right]^{\frac{1}{2}}$$

Employing the predicted east-west (pitch) and north-south (roll) errors of Table 5-2 yields a total radial antenna pointing error of 0.515 degree. The antenna pointing requirements of 0.5 degree in both the east-west and north-south directions is equivalent to a radial pointing requirement of 0.707 degree. Hence the proposed attitude control subsystem will provide the required antenna pointing accuracy with a substantial margin.

5.3 ATTITUDE CONTROL SUBSYSTEM

The Attitude Control Subsystem consists of a sun aspect sensor, two passive earth sensors, and valve driver electronics. With these elements the subsystem provides:

- Sensor information to ground stations from which the satellite's attitude and rotational position can be determined during transfer and final orbits.
- An earth reference pulse to the antenna for use as a position reference in pointing the antenna beam toward the center of the earth.
- Electronic power amplification for energizing the propulsion solenoid valves in response to ground commands for positioning and orientation.

A block diagram illustrating the subsystem configuration is shown in Figure 5-2.

5.3.1. Subsystem Description

A dual earth sensor and sun sensor system provides ground determination of spin-axis orientation. An accuracy of at least $\pm$ 1.2 degrees after no more than $\frac{1}{2}$ hour of continuous observation, and $\pm$ 0.6 degree after no more than 2 hours of observation during transfer and final orbits,

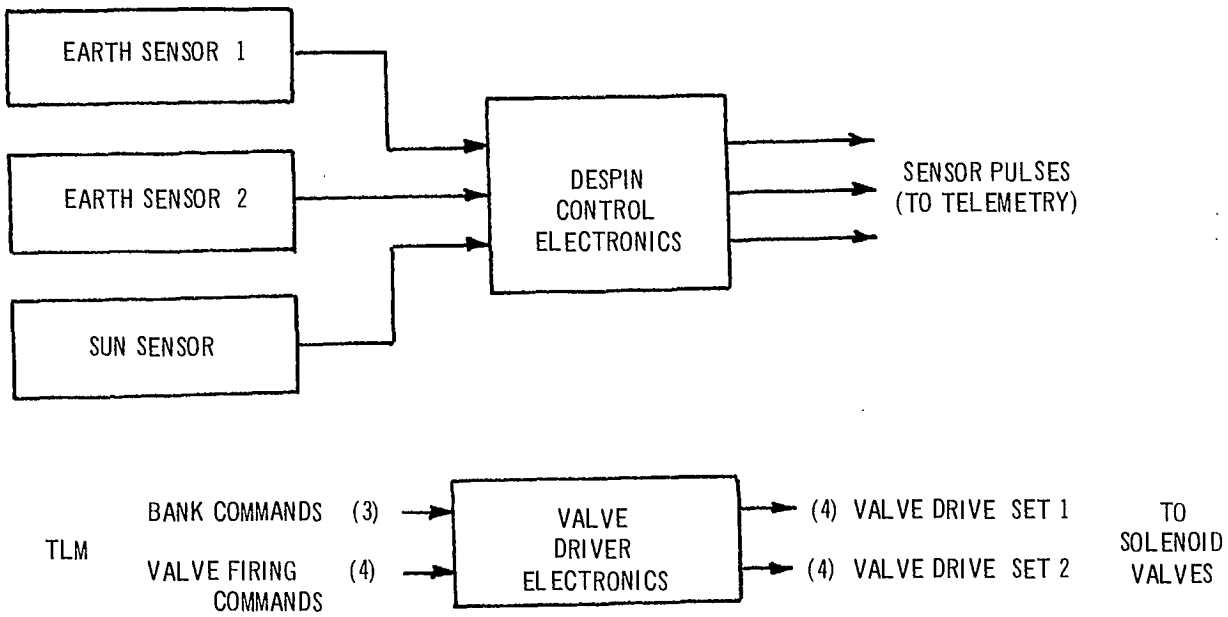

Figure 5-2 Attitude Control Subsystem Block Diagram

can be readily achieved. Two redundant earth horizon sensors and a sun aspect sensor permit satellite attitude and rotational position to be determined on the ground to an accuracy of ± 0.34 degree (3σ) with respect to the local vertical and the sun line. This accuracy is achieved within an observation period of 10 minutes on either the transfer or final orbits.

The earth sensors are the primary source of spin-axis attitude information. The optical axes of these two sensors are arranged in a "V" configuration with the plane of the "V" containing the spin axis (Figure 5-3). Each earth sensor sweeps across the earch once per satellite revolution and produces two pulses coincident with each earth horizon crossing. Under normal conditions, spin-axis attitude with respect to the local vertical can be determined accurately and rapidly on the ground by measuring the interval between the leading edge horizon contacts of the two earth sensor beams. When such contact times fail to coincide, spin-axis displacement can be computed and then corrected by ground command. In the unlikely case that one of the earth sensors should fail, the same attitude information can be obtained by measuring the interval between leading and trailing horizon pulses from the operating earth sensor. This interval, which affords a measure of the earth's chord scanned by the sensor, is then compared with a nominal value based on the accurately known fixed orbital altitude. The earth sensor data will not be degraded during eclipses.

The leading edge horizon pulses from the earth sensors are fed directly to the despin control electronics. Rotational speed of the antenna beam with respect to the satellite is then controlled by the frequency of earth pulses. Beam position is controlled to a fixed offset angle with respect to the earth sensor optical axis in phase with the earth horizon reference pulse. This angle is mechanically preset for the earth's chord length as scanned by the sensor at orbital altitude. Ground control of antenna beam rotation position and speed is also provided by substituting artificial earth reference pulses transmitted from the ground in place of the onboard earth sensor pulses for antenna despin control. Position bias capability is provided in the Despin Control System for offsetting the antenna up to a maximum of $+1$ degree (in 0.2 - degree steps) upon command. Provision for biasing of the long-term earth sensor error is also included. Bias steps of 0.03 degrees are employeed with the bias range being between -0.25 and $+0.25$ degrees.

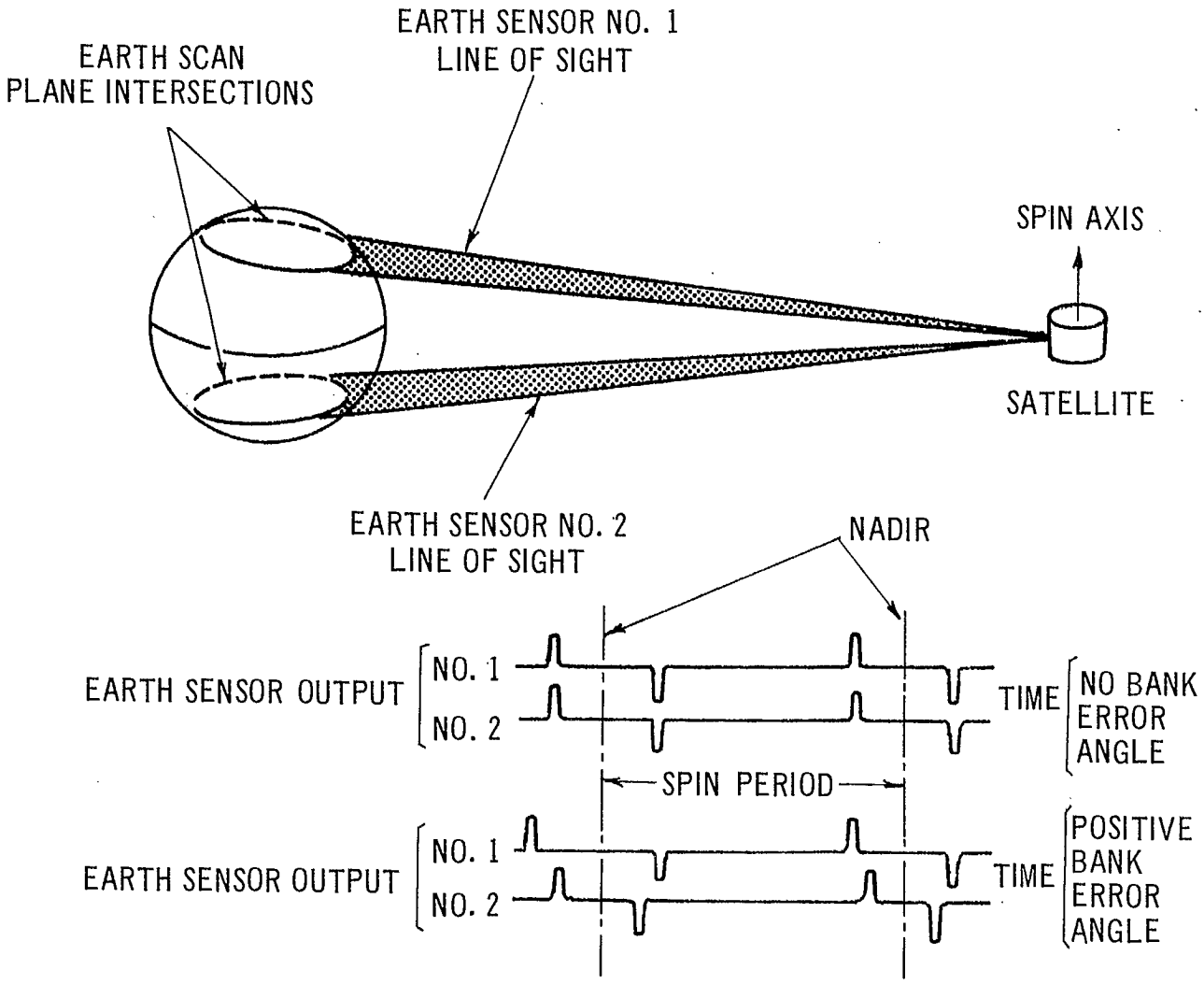

Figure 5–3 Earth Sensor

5.3.2. Component Descriptions

5.3.2.1 Earth Sensor

Each of the redundant earth sensors consists of a telescope with a thermistor bolometer mounted at the focal point. The sensor operates in the CO_2 (14 to 16μ) infrared spectral region to increase accuracy and avoid triggering on cold cloud gradients within the earth's atmosphere. The selected sensor is the same sensor as that which is being used in the Intelsat III satellite.

As the spacecraft spins, the telescope field-of-view scans across the earth, producing a pulse from the bolometer (Figure 5-3). After differentiation and amplification in the self-contained earth sensor electronics, a narrow pulse is produced at the output each time the telescope's 1-degree field-of-view crosses each earth horizon.

5.3.2.2. Sun Sensor

The sun sensor consists of a photovoltaic detector mounted at the bottom of a quartz substrate that is covered by a flat mask at its top. The function of the mask is to transmit light through narrow slits. As the satellite spins, the sun's image traverses each slit in sequence, producing detector pulses whose time separation varies monotonically with elevation angle of the sun line with respect to the spin axis. The quartz substrate medium, with its 1.46 refraction, aids in extending the sun sensor's field-of-view to $\pm$ 65 degrees. The selected sensor is the same sensor as that which is being used for the Intelsat III satellite.

5.3.2.3. Valve Driver Assembly

The valve driver assembly (VDA) is identical to that being used in Intelsat III. It contains all the logic and amplification needed to operate a valve solenoid when the proper command sequence has been received. A block diagram of the VDA is shown in Figure 5-4. The VDA operates in the following modes:

- o Bank 1 Operation

  After a SELECT VALVE DRIVER SET 1 command is received, and until a VALVE DRIVERS OFF command is received, the VDA applies power to coil 1 of any solenoid valve if and only if the corresponding valve command is being received.

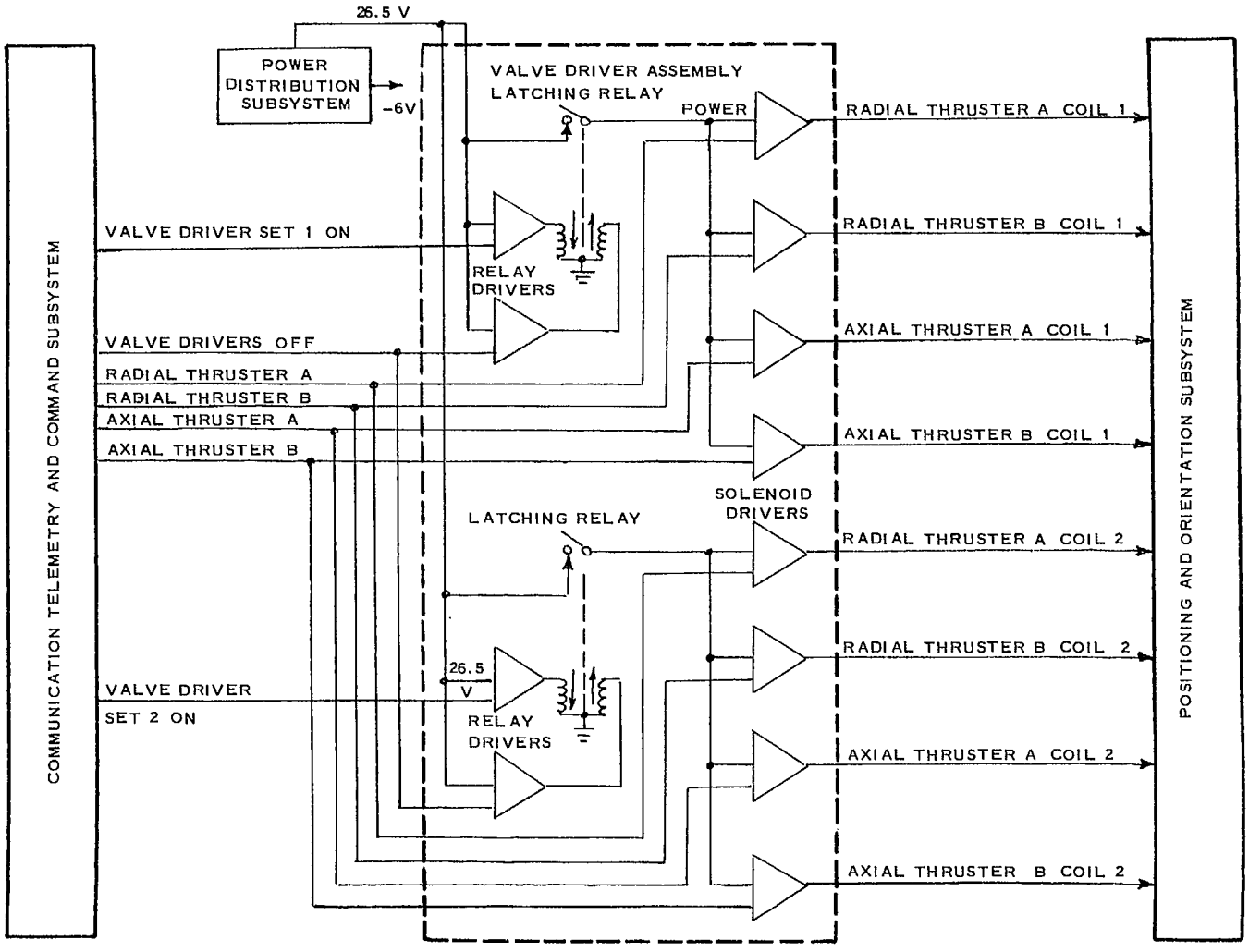

Figure 5–4 Valve Driver Assembly

- o Bank 2 Operation

  After a SELECT VALVE DRIVER SET 2 command is received, and until a VALVE DRIVERS OFF command is received, the VDA applies power to coil 2 of any solenoid valve if and only if the corresponding valve command is being received.

- o Standby Operation

  After a VALVE DRIVERS OFF command, and until a SELECT VALVE DRIVER SET 1 or SELECT VALVE DRIVER SET 2 command, the VDA will not apply power to any solenoid valve coil.

- o Failure Mode Operation

  If either latching relay fails in closed position, the VDA will not apply power to any solenoid valve coil unless a valve command is being received.

5.4 ANTENNA DESPIN SUBSYSTEM

The Antenna Despin Subsystem supports and positions the antenna system in order to point the beams at a specific point on the earth. Its main components are a motor drive assembly and its associated control electronics.

5.4.1 Motor Drive Assembly

The motor drive assembly is illustrated in Figure 5-5. The basic bearing ID is dictated by the required shaft ID (to allow for coaxial RF feed cable clearance) and torsional stiffness. It is desired to keep the torsional resonant frequency of the drive system above 40 Hz to avoid any undesirable interaction between the control system and the drive mechanism. The actual bearing size is chosen to withstand the launch load. The outer race of the antenna and bearing is fitted in the housing and preloaded axially outward by a light spring. The spring is installed in a manner which will allow sufficient axial play on the shaft to compensate for differential contraction between the housing and shaft when the assembly cools down to the minimum expected ambient. The spring preload is sufficient to locate the shaft firmly and is well below the minimum thrust capacity of the bearing for 5 years operation at 115 rev/min and maximum achievable reliability.

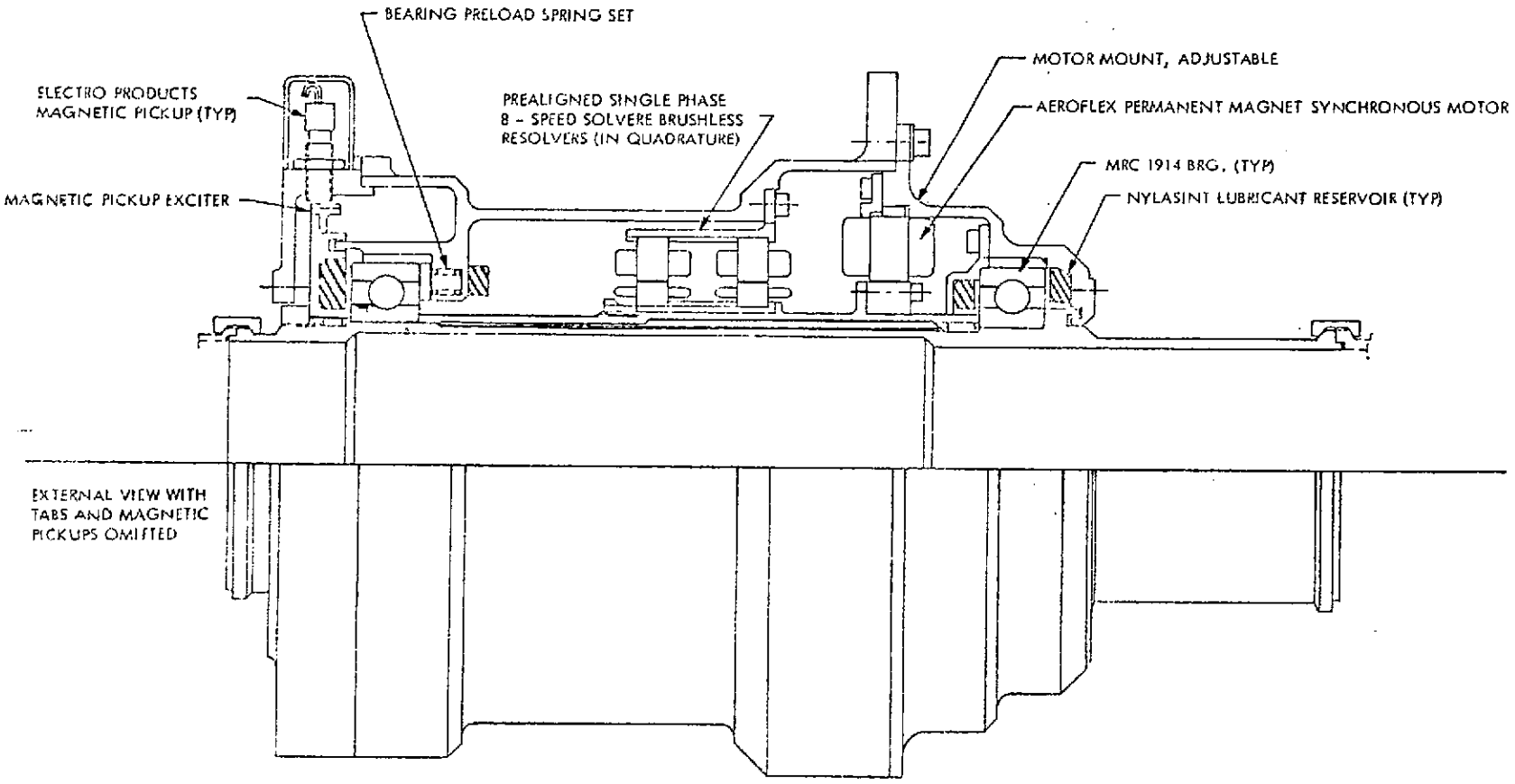

Figure 5–5 Motor Drive Assembly

The lubricant is a low vapor pressure organic liquid with metallorganic additives. It is applied in a thin film on all bearing surfaces and is impregnated into the ball separator, which has a specified 25 percent porosity in order to provide it with the necessary lubricant capacity. The lubricant and application method bear the designation Vac-Kote by Ball Brothers Research Corporation who developed the process for use on the Orbiting Solar Observatory series of satellites.

Lubricant replenishment is accomplished by oil stored in porous nylon reservoirs located on both sides of each bearing. Oil in the reservoirs out-gasses slowly until equilibrium is reached between the oil-coated surfaces of the assembly and the oil vapor in the closed compartment. As an oil molecule is lost by evaporation from any surface, it is replaced by one striking and being captured by the temporarily depleted area. At equilibrium there is a continuous interchange of lubricant molecules between the bearing surfaces, the space around them, and the oil-coated internal walls of the assembly. Oil molecules finding their way through the labyrinth seals are replaced by molecules from the reservoirs. The thin lubricant films which this system employs have been proven capable of lubricating lightly loaded ball bearings at moderate speeds and temperatures by hundreds of space-rated components operating successfully for many thousands of hours.

The drive motor in the despin assembly is a two-phase, 16-pole, permanent magnet synchronous motor. The magnet on the motor is made of Alnico 9 with a magnetization force of 1600 oersteds at the peak energy point and a flux density of 8000 gauss. This magnetization is inherently very stable with time as a function of ambient temperature variations and external demagnetizing fields.

The resolver required to drive the motor consists of two independent resolvers, one for the sine output and one for the cosine input. Each resolver has its own excitation winding. This configuration allows a better output wave shape and more accurate angular relationships between the nulls than the use of a single resolver for both sine and cosine outputs. In the resolver subassembly the two resolvers which are identical in all respects are mechanically rotated through an angle which will give an accurate 90 degree electrical phase shift between the two outputs (11.25 degree mechanical). The resolvers used have no slip rings or brushes but have rotary transformers on their rotors. The resolver assembly is positioned with respect to the motor to obtain a 90 degree electrical phase shift relationship between resolver magnetic field structure and the motor magnetic field; thus, the rotating magnetic

field in the stator of the motor will always lead by 90 electrical degrees the permanent magnet rotor. This, in effect, provides the commutation commonly associated with a conventional brush and commutator-type dc motor.

The assembly also provides the once-per-revolution signal for antenna pointing and a reset signal from a magnetic pickup operating in conjunction with a single steel tooth on the rotor. Rate feedback is provided from a third magnetic pickoff which operates with 180 precision machined teeth on the rotor.

In addition to providing the despin capability for the antenna system the DMA must also provide its structural support. The major structural items of the DMA are a high strength steel shaft and two roller bearings (Marlin-Rockwell Corporation, No. 1914 S). The critical design condition is boost lateral vibration at a maximum level of 23 g. This load produces a peak bending moment of 13,600 in.-lbs. in the shaft and a radial load of 2240 lbs. at the outboard bearing. Thrust loads on the bearings are small due to the low weight of the despun equipment.

Under the above loads the shaft will have a margin of safety in excess of 2.8. The large margin is a consequence of the shaft being designed to give a torsional resonant frequency above 40 Hz for the drive system. This will avoid any undesirable interaction between the control system and drive mechanism.

The bearings selected for the DMA are single row, deep groove bearings each containing seventeen, 11/32 inch balls. Each bearing is an AFBMA Class 7 which is next to the highest or most tightly toleranced class available. This will ensure minimum runout for the system and maximum bearing reliability. The no-visible Brinnell load for the 1914 S bearing is 7750 lbs. This is better than 3 times the maximum load (2240 lbs.) the bearing will be subjected to during launch. Based on experiments by various bearing manufacturers this margin is adequate to ensure extreme quietness of operation throughout the length of the mission.

5.4.2. Control Electronics

The control circuitry for despinning and stabilizing the antenna with respect to the earth is shown in the functional block diagram of Figure 5-6. The system comprises the following major functional blocks.

- o Earth sensors and earth reference select switches
- o Phase detector
- o Tachometer network
- o Acquisition network
- o Auxiliary despin mode control
- o Brushless motor resolver combination

5.4.2.1 Earth Reference Select Logic

Either of two earth sensors mounted on the spinning satellite body provides the basic pointing reference for the despun antenna. An alternate mode of antenna control uses an artificial earth pulse supplied by ground command. The earth reference select switches permit the selection of an earth reference pulse from either earth sensor of from the real-time command output identified as the artificial earth pulse (AEP). Two commands are required to control the selection: the earth sensor select and the AEP select.

Also, this block contains the circuitry required to threshold the raw earth sensor output signals and provide a square wave output pulse suitable for use by the phase detector.

5.4.2.2. Phase Detector

The phase detector compares the time phasing of the earth sensor output with that of the antenna position output as sensed by a magnetic pickup. The operation of the phase detector is illustrated in Figure 5-7 and its output is a sample-and-hold indication of the relative phase of the two signals.

The phase detector has provision for rejecting signals generated when the IR sensor views the moon. Rejection is accomplished on the basis that the earth sensor output pulse from the moon is shorter than from the earth. The phase detector output is inhibited unless the pulse from the earth sensor is at least as long as one-half the length of the normal earth pulse.

During those periods when the sun or the moon will appear in the field of view of the primary sensor, normal operation is achieved by switching to the output of the alternate, identical earth sensor. If one of the sensors fails, normal operation can be obtained with the other sensor and the use of the AEP mode during times of visibility of the sun or moon.

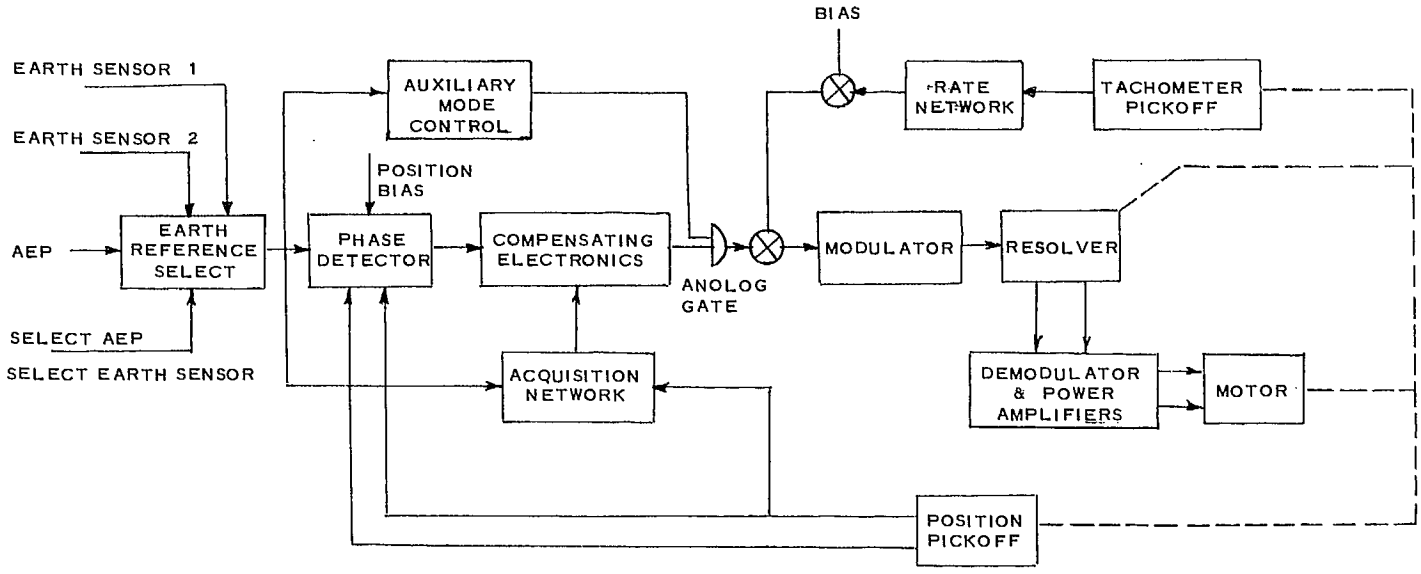

Figure 5–6 Block Diagram Control Electronics

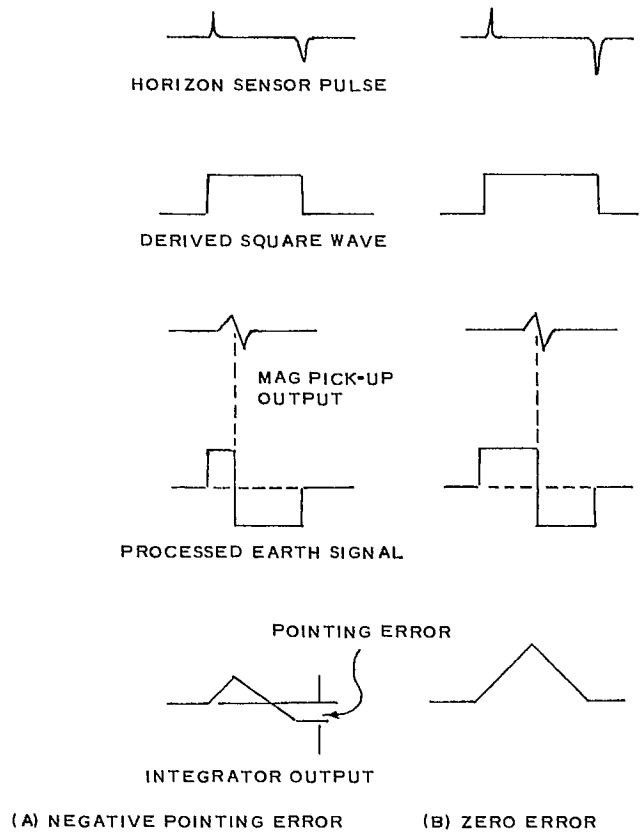

Figure 5–7 Phase Detector Operation

The phase detector also provides capability for biasing the antenna position upon ground command. This is accomplished by introducing an initial condition voltage on the integrator used to sample and hold the modified sensor pulses.

5.4.2.3. Tachometer and Position Feedback

Antenna position with respect to the spinning spacecraft is referenced through the use of two magnetic pickoff units and a ferromagnetic tooth attached to the antenna shaft. The first pickoff unit operates as a prime reference while the second unit is mounted 180 degrees from the prime to accomplish sign inversion for the control circuitry. Antenna relative rate information is derived from a third magnetic pickoff mounted on the drive housing adjacent to a multiple tooth ferromagnetic disk.

It was found that for high precision applications tachometer feedback was required to eliminate the effect of drag friction. In the development of the mathematical model of the dc torque motor and the rotating element, it was established that bearing friction varied by as much as $\pm$ 100 percent of the average friction level, with frequency components related to motor speed and the number of balls in the bearings. The use of the resolver introduced additional disturbances due to anomalies in the sine and cosine outputs. Several tachometer schemes were investigated.

In the selection of a tachometer feedback loop, both analog resolvers and incremental digital encoders were considered. It was concluded that the incremental digital encoder represented a lighter mechanical assembly, and, by using a magnetic pickup transducer with a slotted disk encoder, the weight, power, mechanical tolerance, sensitivity, and volume requirements could be minimized.

The slotted wheel encoder and magnetic pickup (MPU) combination output is in the form of a pulse train, the frequency of which is related directly to rotor speed. To avoid the need for a digital frequency lock loop and phase detector, the processing technique adopted converts the pulse train to a speed proportional signal with a form analogous to the output of a tachometer. This method is simple in principle and design. Operation is described in conjunction with the timing diagram in Figure 5-8.

Figure 5-8A shows a nominal output from the MPU. Each zero crossing is made to initiate a monostable multivibrator resulting in the output waveform as shown in Figure 5-8B. This latter waveform contains speed information in its average value. The rate network serves the dual purpose of filtering the tachometer ripple and providing adequate compensation for the rate loop.

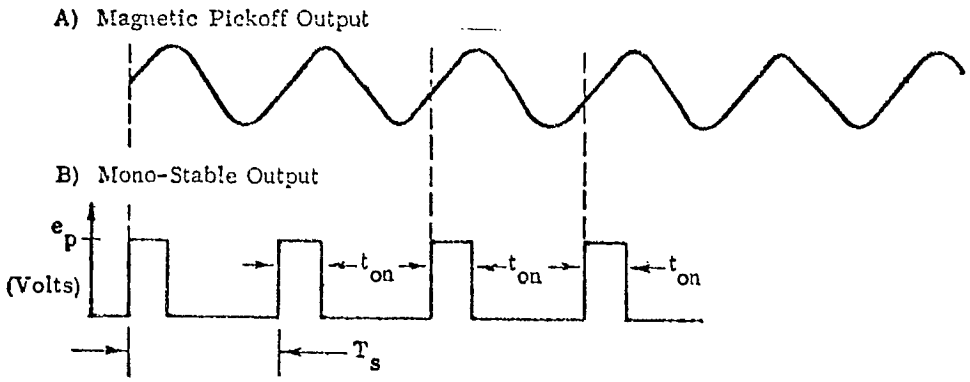

Figure 5-8 Tachometer Signal Processing, Timing Diagram

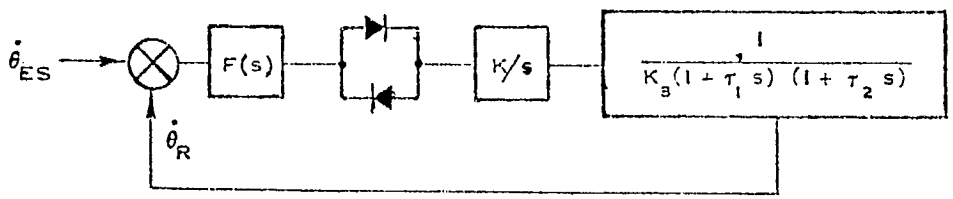

Figure 5-9 Acquisition Network Block Diagram

5.4.2.4. Acquisition Network

In the system used for normal mode despin control the output of the phase detector is ambiguous during acquisition. Therefore a velocity loop is synthesized which when connected to an integrator drives the system to the correct relative speed. The position loop becomes unambiguous and aids the velocity loop once the relative speed differential is within the capability of the phase detector. In the actual implementation, the acquisition network is disconnected whenever the error output is below a silicon diode threshold to accomplish a lower drift sensitivity to the acquisition network.

The acquisition network consists of a speed differential indication circuit which is as shown in Figure 5-9. The earth sensor output triggers a monostable multivibrator to generate a speed dependent signal as described earlier for the tachometer operation. This signal is compared to the output from a similar circuit operated by the reference MPU. The output error is proportional to the speed differential, after filtering. The linearized transfer function is shown in Figure 5-9.

5.4.2.5 Motor Resolver

The dc brushless torque motor used to drive the despin mechanism employs a rotary transformer type resolver which, when properly aligned, acts to commutate the synchronous permanent magnet motor. This effect is obtained by the use of an integrally mounted motor, resolver and rotary transformer. The resolver and rotary transformer are actually combined into a single unit. The resolver has an input winding which is excited at 1000 Hz and two output windings which have an output proportional to the input at the input carrier frequency modulated with a trigonometric function of the angular position of the rotor. The rotor is a variable reluctance element with shorted windings, whose turns and winding distribution are controlled to obtain an optimum modulation wave shape on the output winding and a desired phase relationship between the two windings. Schematically, the resolver is shown in Figure 5-10. This figure also shows the relationship between input and output signals where ϕ is an electrical phase shift between the carrier frequency input and output and θ is the angular position of the rotor. The motor, whose rotor is on the same shaft as the resolver rotor, is a permanent magnet two-phase synchronous motor having 8 pole pairs. The magnet is of Alnico 9 which has the highest energy product of the common magnet materials and has a coercive force of 1600 oersteds, thus exhibiting extremely good stability which ensures minimum degradation during satellite life. The motor is energized from the demodulated resolver outputs as shown in Figure 5-11.

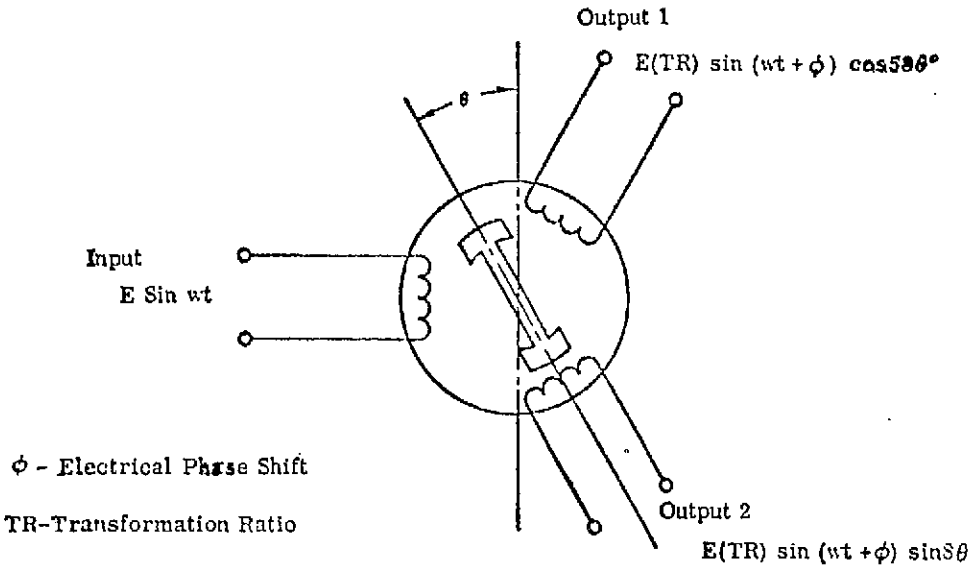

Figure 5-10 Resolver Diagram

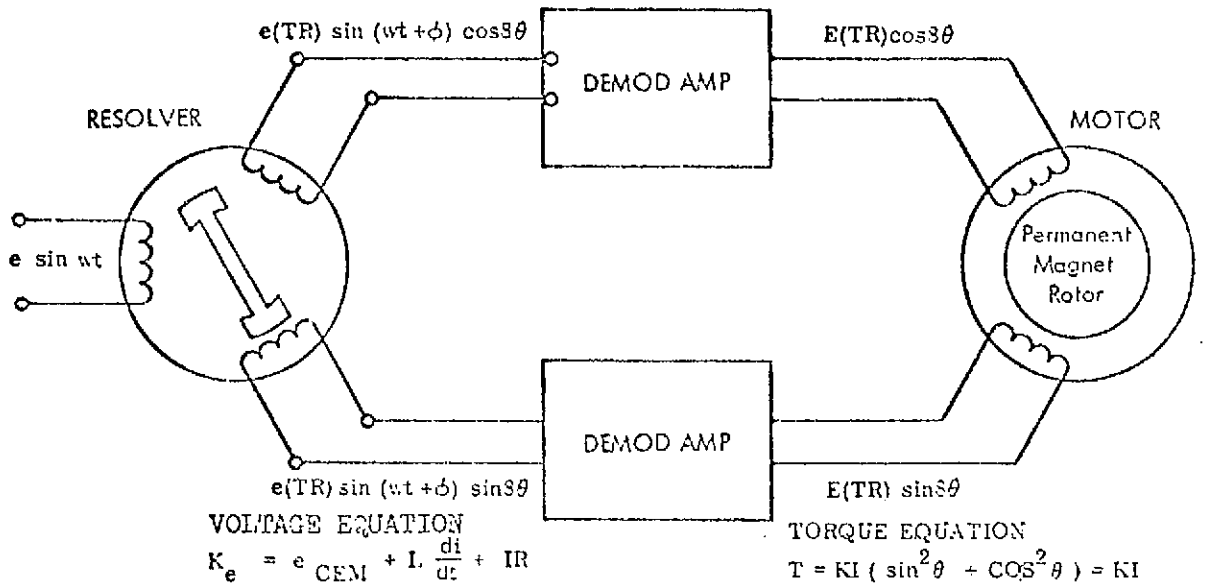

Figure 5-11 Motor-Resolver Block Diagram

The direction of rotation and peak torque per unit power is controlled by the relative positions of the resolver and motor stators. This position is mechanically fixed such that the stator rotating field in the motor always leads the rotor rotating field by $\pi/2$ electrical radians.

The output from the resolver is demodulated and power amplified to drive the corresponding motor sine and cosine windings. The torque speed curves for this combination very closely approximate those of a dc torquer. This motor offers the same advantages in starting and controlling as well as in electrical efficiency, mechanical size, and weight.

5.5 STABILITY ANALYSIS

5.5.1 Antenna Despin Subsystem

Pitch attitude errors of the antenna are controlled by a sampled-data control system employing position and rate feedback. Angular position errors are measured with an earth sensor and rate information is obtained via a tachometer. Control torques are generated by a motor in response to a modulator whose output is governed by the pitch angular error and error rate. A linear model of the sampled-data system (Figure 5-12) will be employed to assess the stability of the baseline system. The analysis also includes the effect of major spacecraft anomalies on the system stability margins; inertia cross-products of the despun antenna, offset of the antenna mass center, and spin rate variations comprise the unavoidable spacecraft anomalies investigated.

From the dynamics presented in Appendix B, the transfer function G(s) was evaluated as

$$G(s) = \Delta(s)^{-1} \begin{vmatrix} L_{11}s^2 & (-L_{13}s^2 - I_R \Omega_s s) & -L_{14}s^2 \\ (-L_{13}s^2 + I_R \Omega_s s) & L_{33}s^2 & 0 \\ -L_{14}s^2 & 0 & (L_{44}s^2 + Bs + K) \end{vmatrix}$$

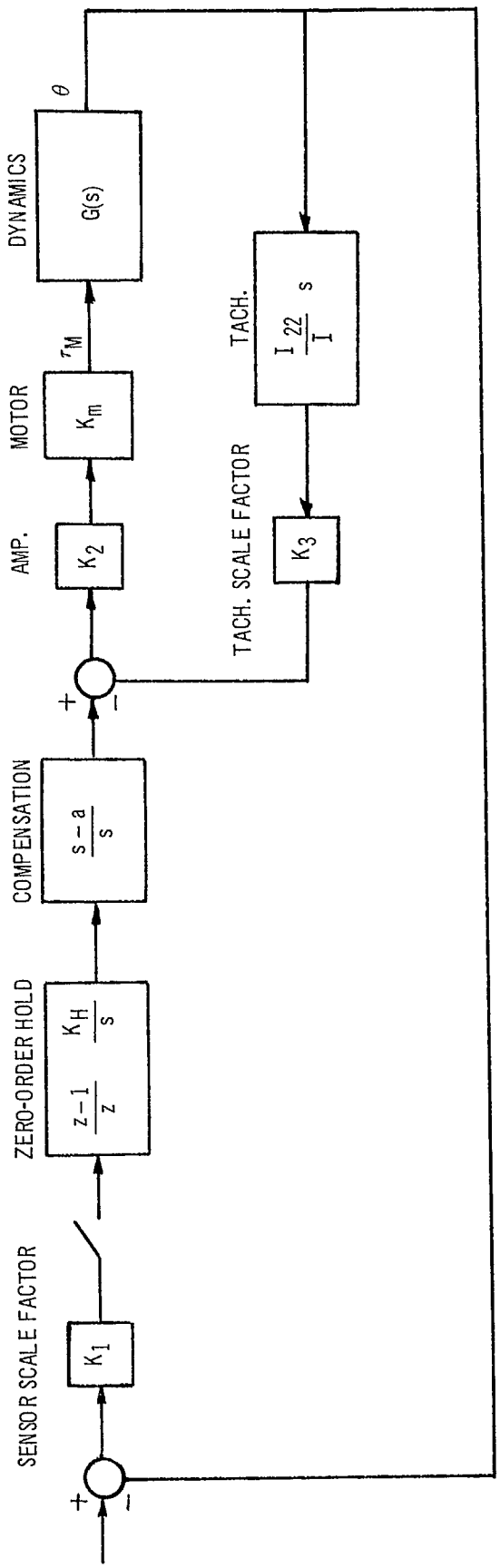

Figure 5–12 Linear Model of the Despin Control System

where:

$$\Delta(s) = \begin{vmatrix} L_{11}s^2 & -L_{12}s^2 & (-L_{13}s^2 - I_R \Omega_s s) & -L_{14}s^2 \\ -L_{12}s^2 & L_{22}s^2 & -L_{23}s^2 & -L_{24}s^2 \\ (-L_{13}s^2 + I_R \Omega_s s) & -L_{23}s^2 & L_{33}s^2 & 0 \\ -L_{14}s^2 & -L_{24}s^2 & 0 & (L_{44}s^2 + Bs + K) \end{vmatrix}$$

The nominal spacecraft mass properties (after the apogee burn) are listed in Table 5-3.

Table 5-3 Spacecraft Mass Properties

I_{11} = 1.51 slug-ft^2	a = b = 0
I_{22} = 0.093 "	c = 5.26 feet
I_{33} = 1.54 "	d = 0.333 feet
I_T = 71.0 "	e = -0.025 feet
I_R = 33.7 "	B = 0.0227 $\frac{lb}{ft/sec}$
m_1 = 0.565 slugs	
m_2 = 14.5 slugs	K = 0.113 $\frac{lb}{ft}$
m_3 = 0.00931 slugs	

The baseline control system parameters are shown in Table 5-4.

Table 5-4 Control System Parameters

Ω_s	= 100 RPM
T	= 0.6 sec
K_1	= 0.300 $\frac{\text{volts}}{\text{deg}}$
K_2	= 219
K_3	= 0.022 $\frac{\text{volts}}{\text{deg/sec}}$
K_H	= 0.0469
K_m	= 0.0227 $\frac{\text{ft-lb}}{\text{volt}}$
a	= 0.25 $\frac{\text{rad}}{\text{sec}}$
I	= 0.0927 slug-ft^2

where:

$$I = \frac{I_R \quad I_{22}}{I_R + I_{22}}$$

A high speed digital computer routine was employed to determine the phase and amplitude of the system open loop transfer function as a function of frequency. Figure 5-13 is a phase-amplitude plot for the nominal case. The nominal phase margin of 58.1 degrees and the gain margin of 14.6 DB represent adequate stability margins. System sensitivity to mass center offsets (of the despun antenna), inertia cross-products, and spin speed variations were next evaluated. As shown in Table 5-5, a mass offset of 0.5 inch (a conservative estimate) does not have an appreciable effect on the stability margins. The corresponding phase-amplitude plot (for a = b = + 0.5 inch) is shown in Figure 5-14. Inertia cross products of 0.302 slug-ft^2 (20% of I_{11}) also have a negligible effect on the stability margins as indicated in Table 5-5. Present balancing procedures can easily reduce the inertia cross-products to well below 0.302 slug-ft^2. Figure 5-15 illustrates the phase-amplitude characteristics for $I_{12} = I_{13} = I_{23} = 0.302$ slug-ft^2. Finally, the system spin speed was varied by $\pm$ 50% (normal expected variations are approximately $\pm$ 15%). Decreasing the spin speed by 50% decreases the phase margin by 10.6

Table 5-5 Effect of Anomalies on Stability Margins

System Anomaly	Ω_s	a	b	I_{12}	I_{13}	I_{23}	Phase Margin	Gain Margin
Nominal	100 RPM	0	0	0	0	0	58.14 deg	14.62 DB
Center of Mass Offset	100	0.5 in.	0.5 in.	0	0	0	58.09	14.64
"	100	-0.5	-0.5	0	0	0	58.14	14.62
Inertia Cross-products	100	0	0	$.302s-f^2$	$.302s-f^2$	$.302s-f^2$	57.60	14.22
"	100	0	0	-.302	-.302	-.302	58.28	14.57
"	100	0	0	-.302	.302	-.302	58.16	14.62
"	100	0	0	.302	0	0	58.14	14.62
"	100	0	0	0	.302	0	58.14	14.61
"	100	0	0	0	0	.302	58.14	14.62
Spin Speed Variation	50	0	0	0	0	0	47.54	8.48
"	150	0	0	0	0	0	61.77	18.60

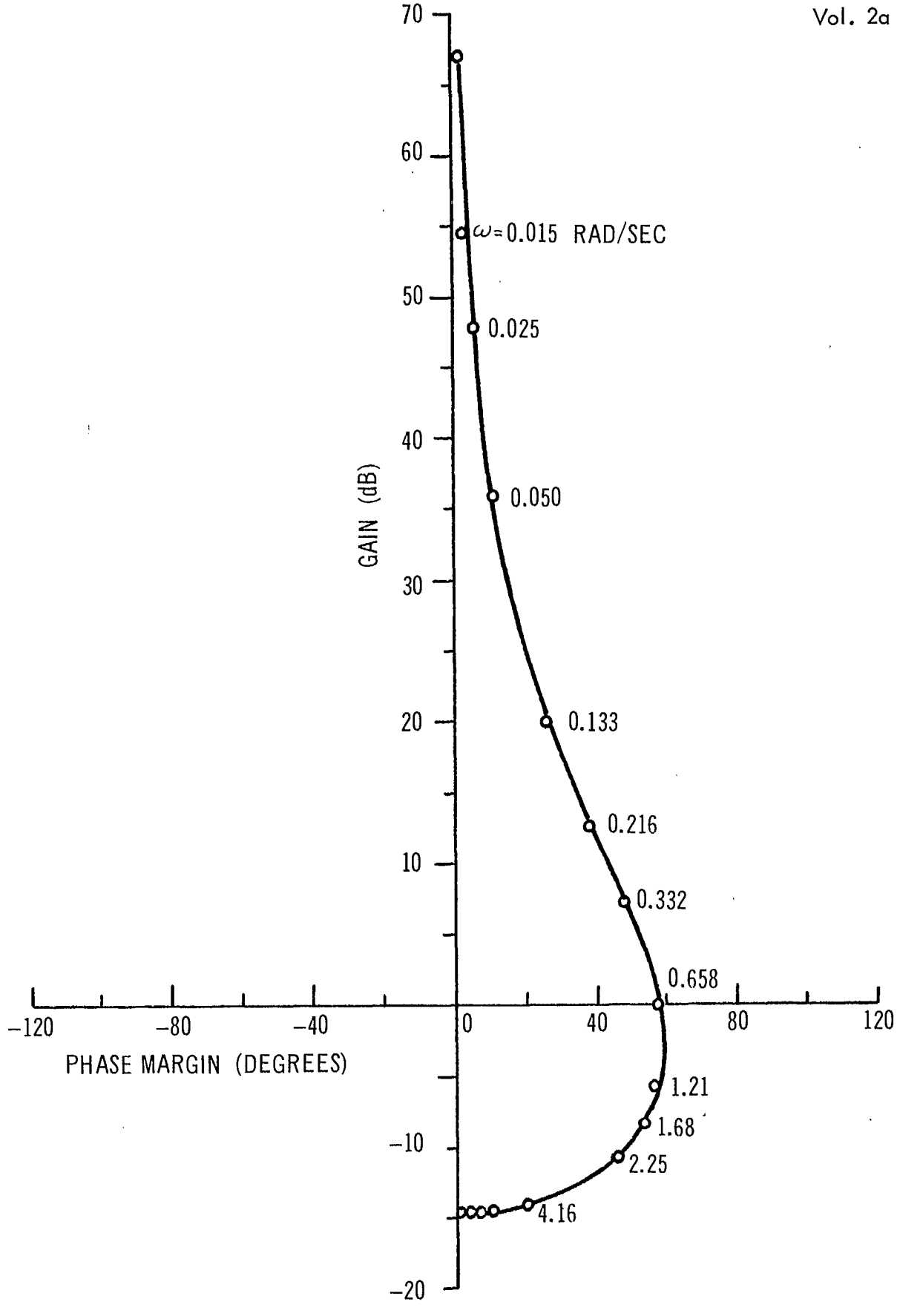

Figure 5–13 Nominal Phase – Amplitude Plot

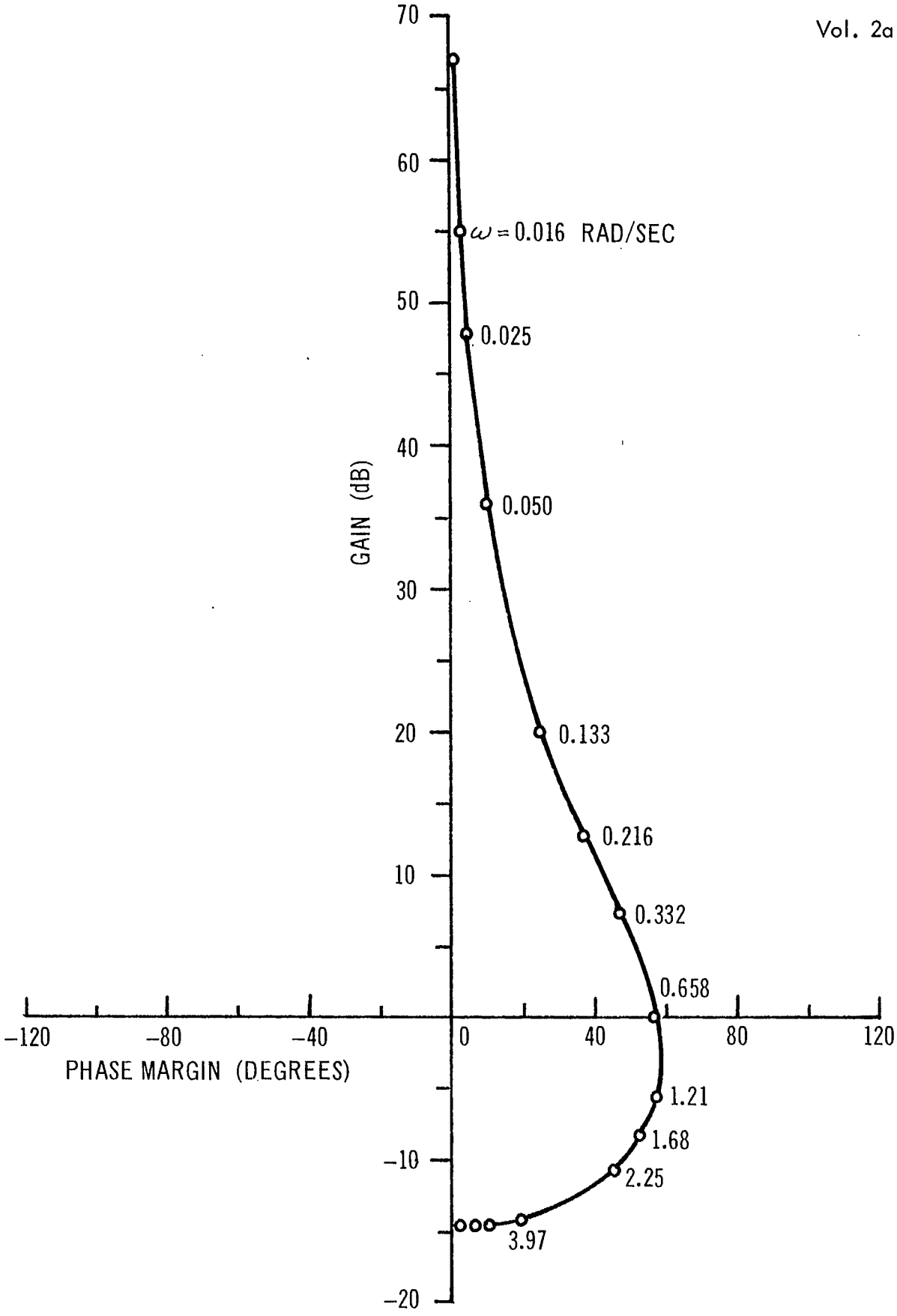

Figure 5–14 Phase-Amplitude Plot for mass center offset of + 0.5 inch

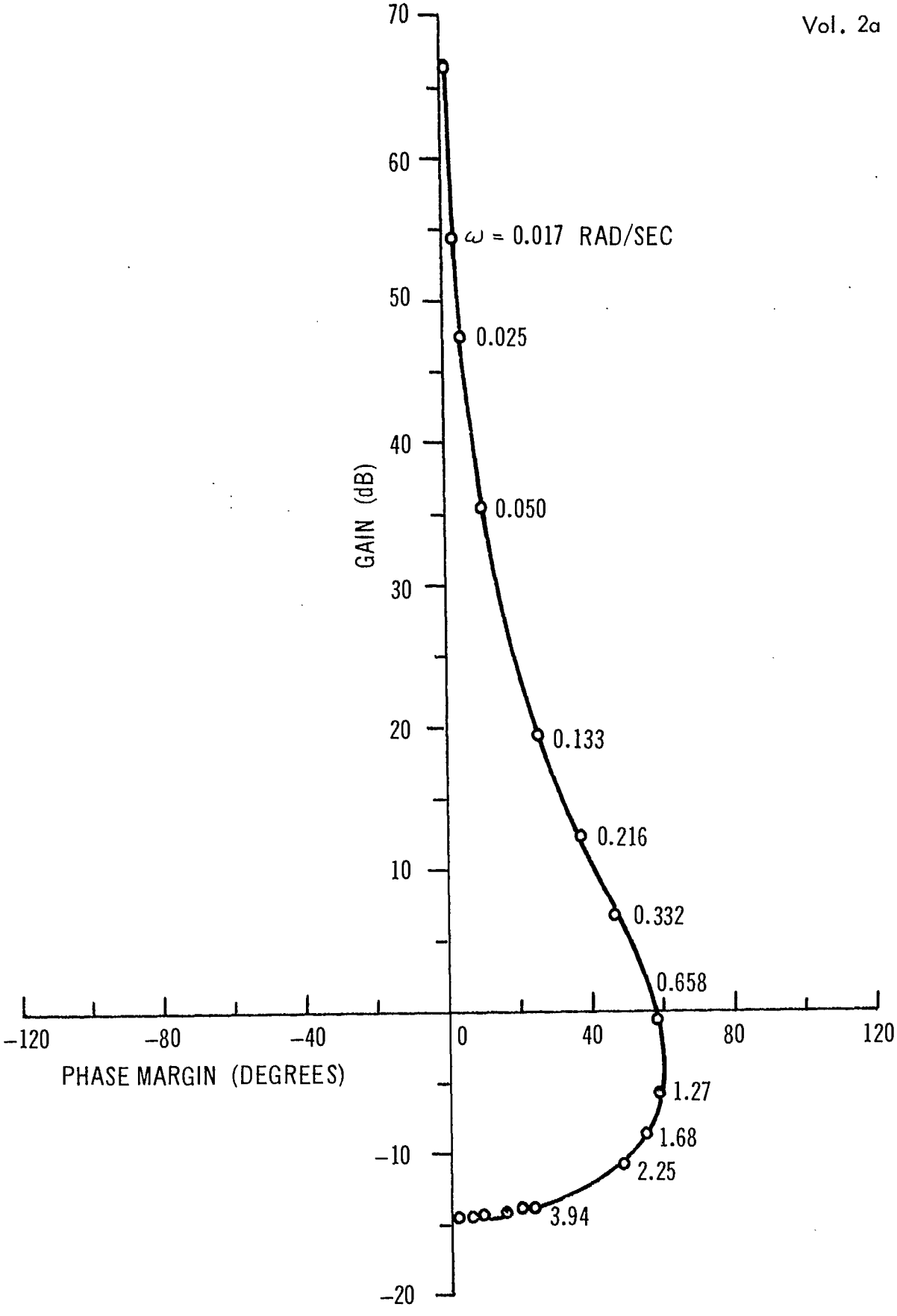

Figure 5–15 Phase-Amplitude Plot for inertia cross products of 20%

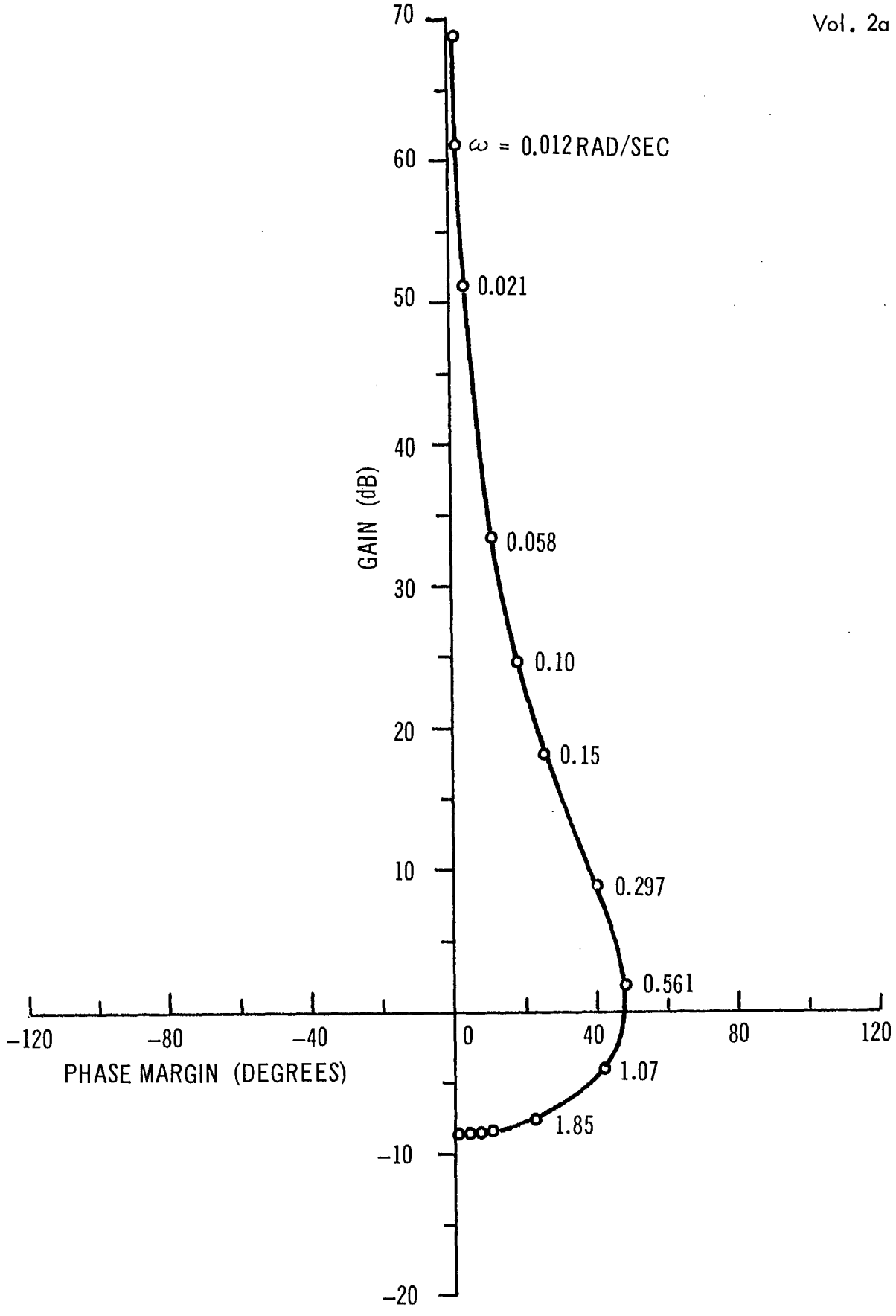

Figure 6–16 Phase-Amplitude Plot for spin speed 50% low

degrees (a large but inconsequential amount) and the gain margin by 6.14 DB. The phase-amplitude plot for this case is shown in Figure 5-16. Increasing the spin speed by 50% increases both stability margins as shown in Table 5-5 and hence produces a beneficial effect.

The above analysis indicates the antenna despin subsystem is relatively insensitive to mass center offsets, inertia cross-products, and spin speed variations. Satisfactory system performance will be realized if the system anomalies are constrained to the values evaluated above.

5.5.2 Attitude Control Subsystem

Using the dual-spin attitude stabilization concept with an energy removal mechanism mounted on the despun communication antenna, it is no longer required that the spin axis inertia be greater than the tranverse axis for stability. The damper required to ensure stability is relatively light (1.8 lb) and is extremely reliable (.997 for 5 years).

Dynamically, the spacecraft consists of two bodies in (non-uniform) relative angular motion, with energy dissipation on both members, intentionally (the nutation damper assembly) in the case of the antenna and unitentionally (e.g., structural damping and propellant slosh) on the rotor. In general, neither body is symmetrical nor has its mass centered along the drive assembly shaft; thus the dynamical equations are quite complex, containing periodic coefficients.

The small-perturbation stability criterion for a dual-spin spacecraft with a symmetric rotor and an asymmetric platform can be derived by an energy-sink analysis* as

$$\frac{P_R}{\lambda_R} + \frac{P_P}{\lambda_P} < 0$$

where P_R and P_P are the energy dissipation rates (negative) on the rotor and platform respectively, and

---

* P.W. Likens, "Attitude Stability Criteria for Dual-Spin Spacecraft," J. Spacecraft and Rockets, Vol. 4, No. 12, December 1967

$$\lambda_R = \lambda_o - \omega_R$$

$$\lambda_P = \lambda_o - \omega_P$$

$$\lambda_o = \frac{H_s}{I_T}\left[\frac{H_s - I_P\,\omega_P}{Hs - \frac{I_1 I_2}{I_T}\,\omega_P}\right]$$

$$H_s = I_R\,\omega_R + I_P\,\omega_P$$

$$I_T = \frac{I_1 + I_2}{2}$$

with ω_R the rotor spin rate, ω_p the antenna spin rate, Ip the antenna spin-axis inertia, I_R the rotor spin-axis inertia and I_1 and I_2 the transverse inertias of the composite configuration; I_T is the mean transverse inertia. In general, the energy dissipation rate on the antenna greatly exceeds that on the rotor. That is $k << 1$, where:

$$P_R = k\,P_P$$

This reduces the stability requirement to:

$$\frac{1}{\lambda_P} + \frac{k}{\lambda_R} > 0$$

For this configuration, the vehicle transverse inertias are approximately equal. Assuming inertia equivalence for this preliminary analysis permits simplification of the parameter λ_o to:

$$\lambda_o = \frac{H_s}{I_T}$$

Stability criteria for two particular cases of interest are:

- No damping on rotor, ω_p general

$$\omega_p < \frac{I_R \omega_R}{I_T - I_p}$$

- Damping on both bodies, ω_p zero

$$k > \frac{I_T - I_R}{I_R}$$

where $I_T > I_R > I_P$ and $\omega_R > 0$ are assumed. Table 5-6 lists the spacecraft inertias and the corresponding stability criteria for various times in the mission.

Table 5-6
Spacecraft Inertias (Slug-ft^2) and Stability Criteria

CONDITION	I_P	I_R	I_T	STABILITY CRITERIA
At Booster Separation	0.1	41.4	127.6	$\omega_p < .324\,\omega_R$ $k > 2.08$
After Apogee Motor Burn	0.1	33.7	90.3	$\omega_p < .374\,\omega_R$ $k > 1.68$
At End of Mission	0.1	30.4	88.6	$\omega_p < .343\,\omega_R$ $k > 1.91$

The first stability criterion indicates the speed below which the antenna must be despun to ensure stability while the second criterion specifies the factor by which the nutation damper energy dissipation rate must exceed that of the rotor. The proposed antenna rates and the nutation damper energy dissipation are well within the stability requirements of Table 5-6.

6. ELECTRICAL POWER SUBSYSTEM

6.1 INTRODUCTION

This section of the report presents the results of the studies which have been made of the power subsystem requirements and of the variety of configurations, techniques and hardware which could be used in designing a system to meet these requirements.

The load requirements are described in section 6.2. Section 6.3 contains a general description of the recommended design, defining the key subsystem elements and performance parameters. The recommended design is based on the trade-off studies presented in section 6.4. The battery, power conditioning equipment and power control equipment are described in detail in section 6.5.

The system and interface requirements of the solar cell array are derived in section 6.4 but a detailed description of the array design is deferred till section 7 of this volume.

6.2 POWER REQUIREMENTS

A summary of the total electrical power required by each subsystem during normal orbital operations in both sunlit and eclipse conditions is given in Table 6.1.

The loads given in this table are for the condition where six 8-watt TWT's are operating during sunlit periods and three are operating during eclipse periods. These load requirements include all cable losses, converter losses and power conditioning losses.

A detailed listing of the electrical power required by each unit on the spacecraft is shown in Table 6.2. The power required by each unit is tabulated by primary power (main bus power), secondary power (regulated power from central converter), and transient or peak power. The final two columns of the table show the nominal steady state power for all units (including redundant units) which could be operating simultaneously when six TWT's are active and when three TWT's are active.

All regulated power other than that required by the high and low level TWT's is to be supplied by a central equipment converter. Three secondary voltages (+ 28 VDC, +5 VDC, -5 VDC) are required, all having a total line and load regulation of $\pm$ 3%. A detailed listing

Table 6.1

Summary of Spacecraft Orbit Power Requirements

Subsystem	Nominal Orbital Sunlit Operations (6 Transponders)	Nominal Orbital Eclipse Operations (3 Transponders)
Communications	179.2 watts	94.6 watts
Attitude Determination and Control	14.5 watts	14.5 watts
Position and Orientation	.5 watts	.5 watts
Tracking, Telemetry, and Command	14.3 watts	14.3 watts
Electrical Integration	4.7 watts	2.4 watts
Electrical Power	12.1 watts	12.1 watts
Thermal Control (Multiplexer Heaters)		5.0 watts
Total S/S Load	225.3 watts	143.4 watts
Battery Trickle Charge	9.3 watts	-
Total Array Load (Solstice)	234.6 watts	-
Total Battery Load (Eclipse)		143.4 watts

Table 6.2 DETAILED POWER BUDGET

Subsystem	Unit	Per Unit Power: Primary Watts@ 28 vdc	Per Unit Power: Secondary Watts@ ___vdc	Per Unit Power: Transient Power Per Unit Watts@ ___vdc	Per Unit Power: Transient Power Per Unit Duration	Number of Units operating and Nominal Steady State Power Requirements. Orbit Operations. Six Transponders Active: No. of Units Oper.	Six Transponders Active: Nominal Power Watts	Three Transponders Active: No. of Units Oper.	Three Transponders Active: Nominal Power Watts	Remarks
Communications	Hi Level TWTA Power Supply (8w RF Power Output, 28.4% efficiency)	28.2w	-	-		6	169.2	3	84.6	
	Driver TWTA Power Supply	5.0w				1	5	1	5	
	Receiver (TDA's, Local Oscillators)		2.5w@ 28 vdc							
			2.5w@ 5 vdc			1	5	1	5	
Attitude Determination Control	Earth Sensar	0.70w								
	Valve Driver Assembly		0.30@ -5 vdc	.220w@ 28 vdc	50 msec. to 11 min.	1	.30	1	.30	
	Mechonical Despin Antenna Mechanism	12.3w	0.25w@ +15vdc	15.3w@ 28 vdc	Motor start up time	1	12.8	1	12.8	
			0.25w@ 24vdc							
Position of Orientation	Axial Thruster			5w @ 28 vdc	50 msec. to 11 min.	2	-	2	-	
	Radial Thruster			5w @ 28 vdc	50 msec. to 11 min.	2	-	2	-	
	Propellant Tank Pressure Transducer	0.25w				2	.5	2	.5	
	Propellant Tank Cross Connect Valve			164w@ 28 vdc	50 msec. Once per flight	1		1		
Apogee Motor	Safe & Arm Device			360w@ 28 vdc	50 msec. Once per flight	1	-	1	-	
Tracking, Telemetry & Command	Dual Receiver Unit		4.3w@ 28 vdc			1	4.3	1	4.3	
	Dual Decoder Unit		1w@+5vdc			1	2	1	2	
			1w@-5vdc							
	Encoder		.8w@+5vdc			1	1.6	1	1.6	2 encoders & 2 transmitters operation until spacecraft has reached desired station in synchronous orbit.
			.8w@-5vdc							
	Transmitter		6.4w@28vdc			1	6.4	1	6.4	
	Beacon Transmitter		6.0w @ 28 vdc			1	6.0	1	6.0	Used only during initial orbit attachment period.
Electrical Integration	E IA	.2w	.2w@5vdc	1.55w@ 28 vdc	50 msec to 750 msec twice per flight	1	.4	1	.4	
	Cable losses (Estimated at 2%)	4.48w				1	4.48	1	2.12	
Electrical Power	Power Control Unit	4w				1	4	1	4	
	Converter losses					1		1		20.3w, load, 72% efficient
	Shunt Element Assemblies			3w @ 28 vdc	Required only when excess array power is being dissipated	1	-	1	-	
Thermal Control	Transponder TDA Heaters			5w @ 28 vdc		1	5		5	

of the individual unit secondary power requirements is given in Table 6.3. The maximum load on the central converter occurs during the period from separation until the spacecraft is on station in synchronous orbit. During this period both redundant telemetry encoders and transmitters are on, as well as the 136 MHz beacon transmitter. The total central converter load at this time is 34.9 watts. After the spacecraft is on station and operating, the beacon transmitter and the redundant telemetry encoders and transmitters are turned off. The total load on the central converter then falls to 20.4 watts, at which level it will remain throughout the remainder of the mission.

6.3 RECOMMENDED POWER SUBSYSTEM

6.3.1 Functional Description

Figure 6-1 shows a functional block diagram of the electric power subsystem. The electric power subsystem contains four major components. The solar array is the primary source of power, converting sunlight to electric energy at an efficiency of approximately 10 percent. The electric power from the solar array is fed directly through the power control unit to the consuming loads without intervening loss elements (except for the solar array isolation diodes). Any excess power is diverted to the 20-cell, 12 A-Hr Ni-Cd battery and stored for use during the occulted periods. The power control unit controls the quality of power distributed to the loads and battery, controls battery charge and discharge, and rejects excess power which cannot be stored in the battery to the shunt element assemblies and to the solar array where it is dissipated as heat.

The solar array power is divided between the loads and the battery in parallel until the third electrodes in two of the three battery cells indicate the development of oxygen pressure. At this time the trickle relay opens, allowing the batteries to trickle charge. In the event that the battery oxygen pressure reduces to a low level, the trickle relay will close again, allowing an additional burst of current into the battery for complete charging. In normal operation the trickle current will maintain oxygen pressure high enough to prevent cycling.

When the solar array output voltage at a current equal to the sum of the battery current and the load current exceeds the voltage limit, the error amplifier develops an output causing current to flow through the shunt, and clamping the bus voltage at the preset voltage limit.

Table 6.3

Secondary Power Requirements
(from central converter)

Unit & Subsystem	Orbit Operational Power Requirement			Transfer Orbit Power Requirements		
	+28VDC	+5VDC	-5VDC	+28 VDC	+5VDC	-5VDC
Communication Subsystem Receiver	2.5w	2.5w	-	2.5w	2.5w	-
Attitude Determination and Control						
Valve Driver Assembly	-	-	.3w	-	-	.3w
Mechanical Despun Antenna	-	.25w	.25w	-	.25w	.25w
Telemetry, Tracking and Command						
Dual Receiver	4.3w	-	-	4.3w	-	-
Dual Decoder	-	1.0w	1.0w	-	1.0w	1.0w
Encoder	-	.8w	.8w	-	1.6w	1.6w
Transmitter	6.4w	-	-	12.8w	-	-
Beacon Transmitter	-	-	-	6.0w	-	-
Electrical Integration EIA		.2w			.2w	
TOTAL	13.2w	4.8w	2.4w	25.6w	5.6w	3.2w

Total Converter Load: 20.4 watts during normal synchronous orbit operations.

Total Converter Load: 34.9 watts during transfer orbit until final one orbit station is reached.

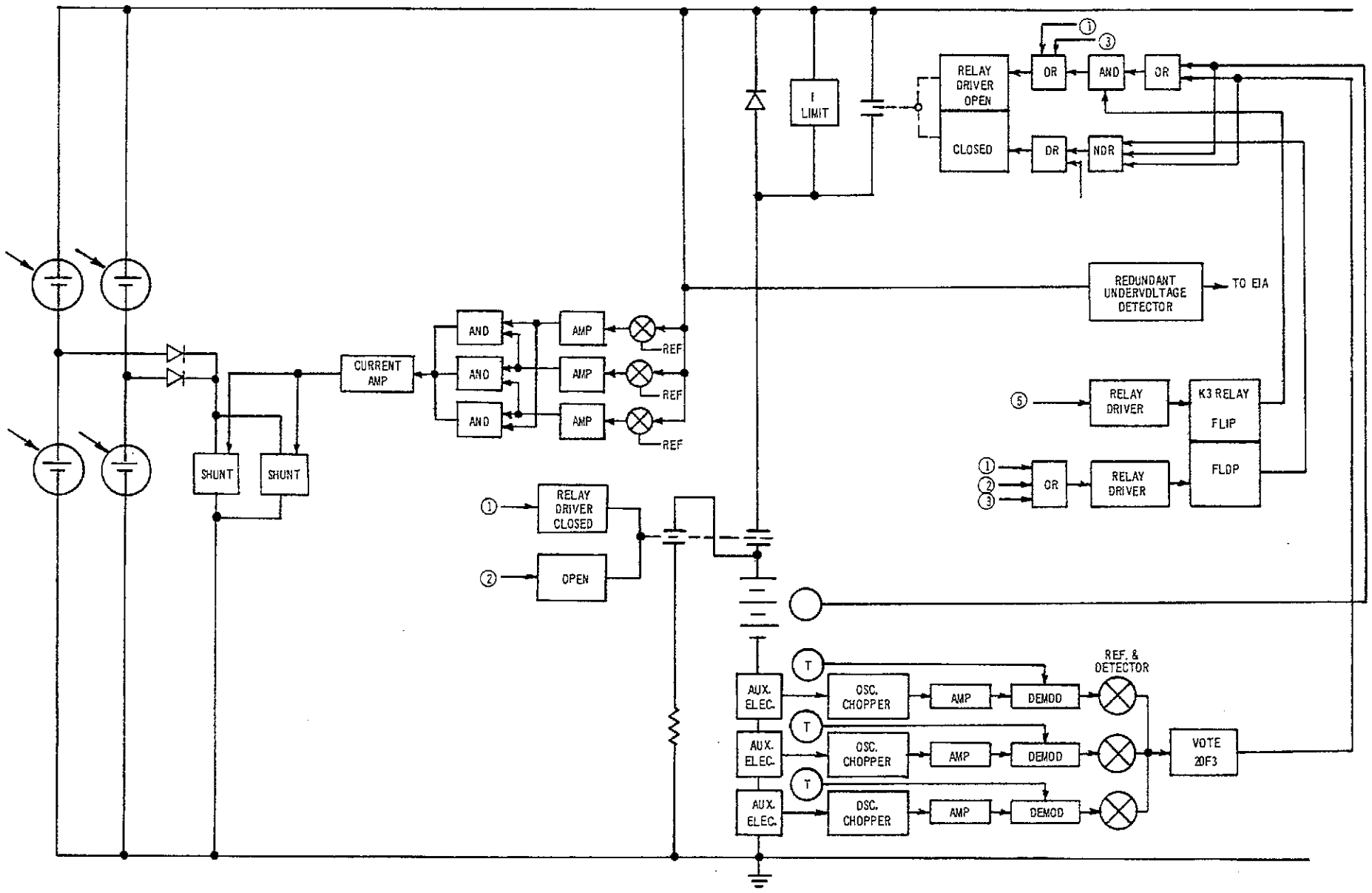

Figure 6—1 Recommended Electrical Power Subsystem

The system is totally commandable. Any command other than "auto" automatically disables the automatic controls and locks the system in the commanded mode until a final "auto" command is given to restore the automatic mode of operation.

All portions of the electric power subsystem electronics except for the battery and cell bypass electronics are fully redundant, so that no single part failure can cause system failure or performance degradation outside of specifications.

Battery cells and their associated bypass electronics are binomially redundant, in the sense that any one cell or its bypass circuit can fail short-circuited without causing system failure, although this will result in a reduction in minimum system voltage.

6.3.2 System Voltage Range

Under normal operating conditions, the system operating voltage will fall within the following ranges:

Normal system operation	25-29.4 volts
Battery Exhausted	20-29.4 volts
One battery cell failed	23-29.4 volts
One cell failed and battery exhausted	18-29.4 volts

6.3.3 Power Margins

The power required from the solar array for the operation of the spacecraft and communications loads at the critical design point (summer solstice) is 234.6 watts. A minimum power of 240 watts is delivered by the solar array at summer solstice after 5 years. This leaves a power margin of 5.4 watts, or 2.2%. Should power become critical at this stage, an additional margin of 9.3 watts can be made available by commanding the battery to recondition discharge, thus freeing the battery trickle charge power for use by the loads at 29 volts, rather than allowing the voltage to fall to 26 volts (the zero current potential of the battery) before the additional power becomes available. This step can be taken with minor risk to the battery because the battery bypass electronics will protect the cells from excessive reversal due to overdischarge of the battery. When the solar array output has increased from the summer solstice minimum, the battery may then be restored to the line and recharged.

The electric power subsystem is capable of operation without a battery without loss of power quality. However, this is only possible if the design of the converters which supply power to the communications equipment is so constrained as to prevent surge currents in excess of the solar array capability.

Figure 6-2 shows a typical turn-on current-voltage characteristic of a converter, assuming that no capacitor charging surges occur which tend to raise the output load line. At some low voltage the converter oscillator begins to operate and the current rises to point 0. Current and voltage increase resistively to point P, at which the regulation loop takes over and controls the converter output along the constant power line P-A-B. Normally the battery will supply the excess current required to drive the converter across the peak, F-P-A. However, in the absence of a battery, the converter will tend to lock stably at the false operating point, F, and since this is below the minimum allowable voltage of the system, the undervoltage circuit will operate to turn the loads off. This situation is aggravated by the presence of additional turn-on surges due to charging of input and output capacitors.

As a consequence of this, surge currents should be limited in the communications converters. The housekeeping converter does not require this limiting since it is on long before the communications converters are turned on and a large excess of solar array power is available for turn-on surges.

6.4 POWER SUBSYSTEM TRADEOFF STUDIES

6.4.1 Subsystem Configurations

Three basic types of sub-system were studied:-

a) Configuration 1 - The Straight Through Power system in which energy is taken directly from the source to the load without intervening series lossy elements such as regulators (see Figure 6-3.)

b) Configuration 2 - The Isolated Battery Charge system in which power is fed to the load directly from one section of the array and to the battery from a separate section (see Figure 6-4).

c) Configuration 3 - The Series Regulator System which employs a series regulator for control of main bus voltage (see Figure 6-5).

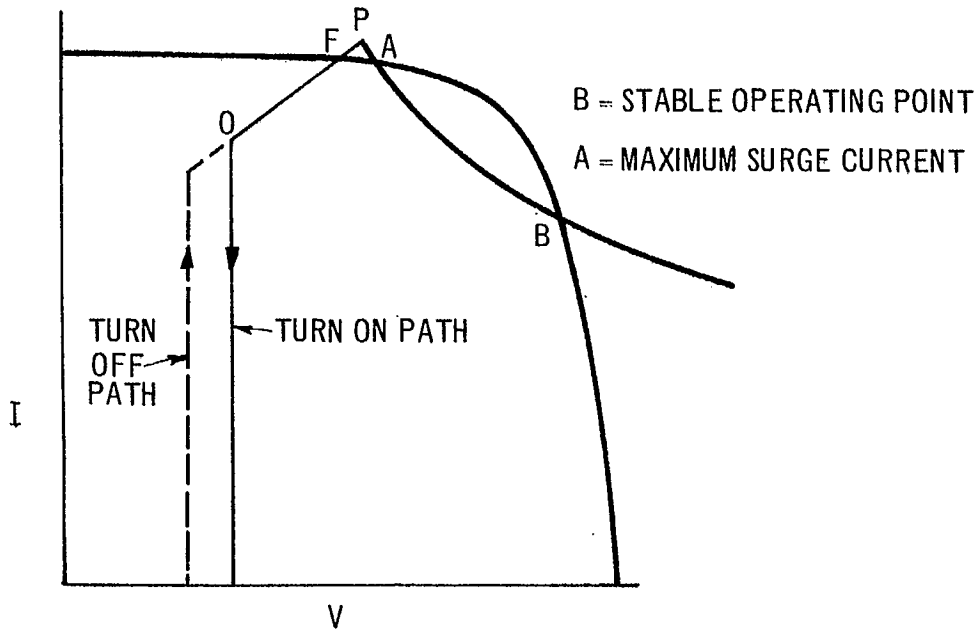

Figure 6–2 Converter Turn-On Characteristic

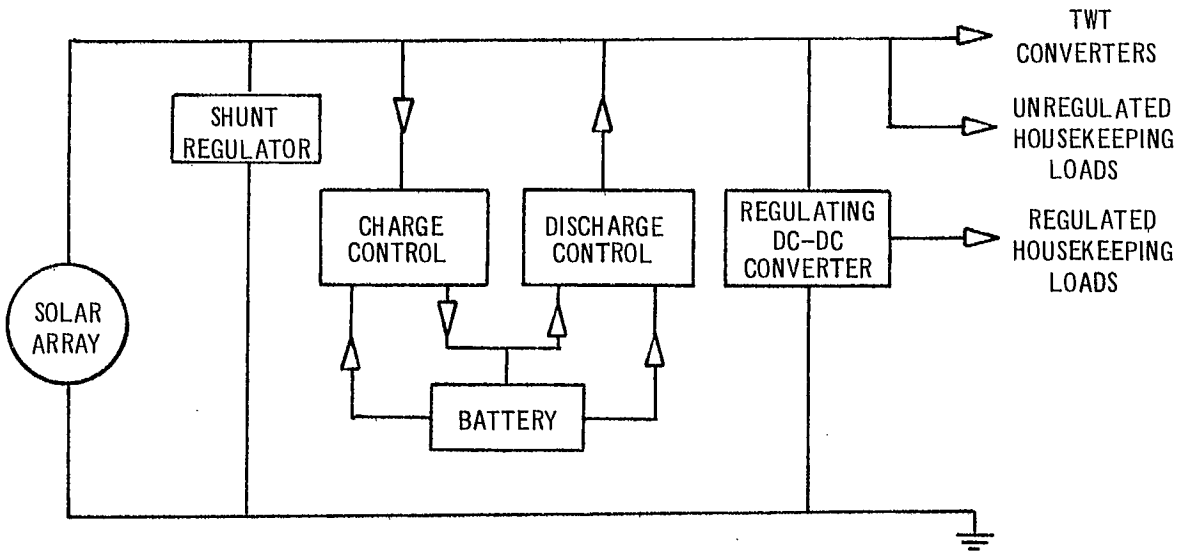

Figure 6–3 Basic Power System, Configuration 1

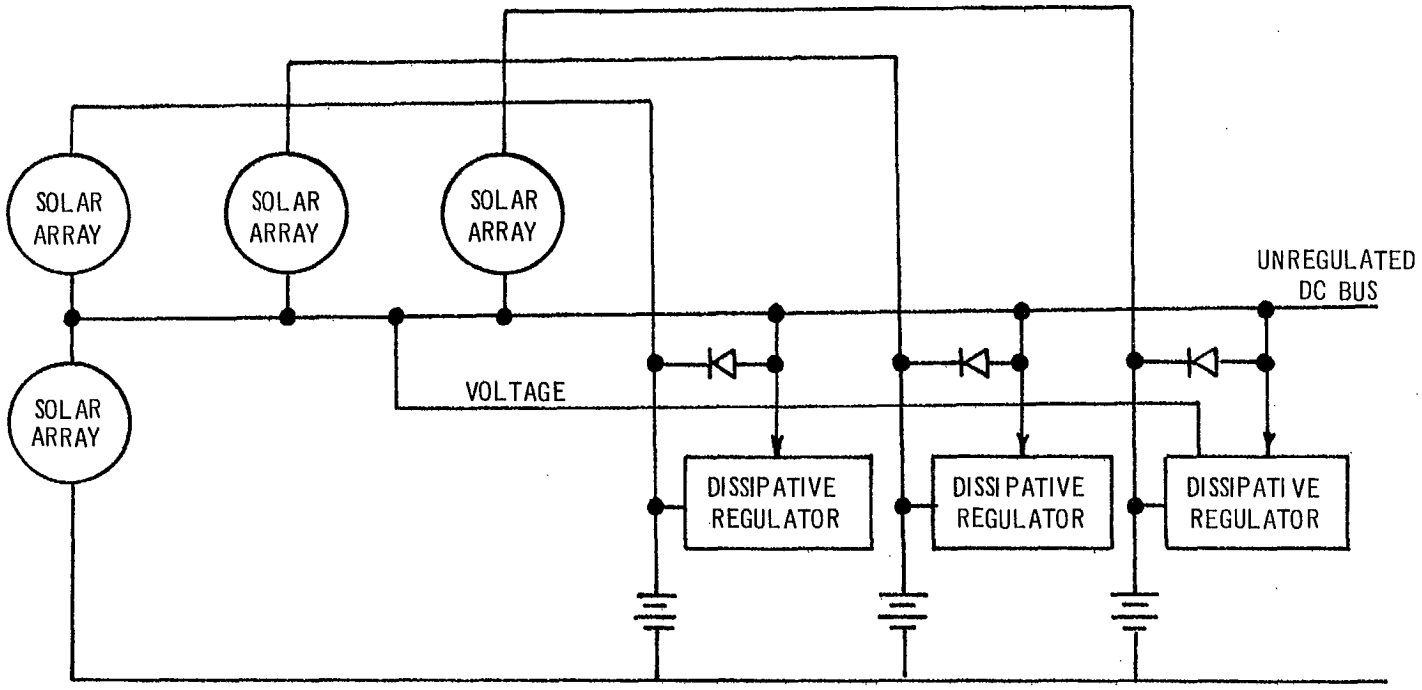

Figure 6–4 Configuration 2 – Batteries and loads are fed from separate portions of the solar array

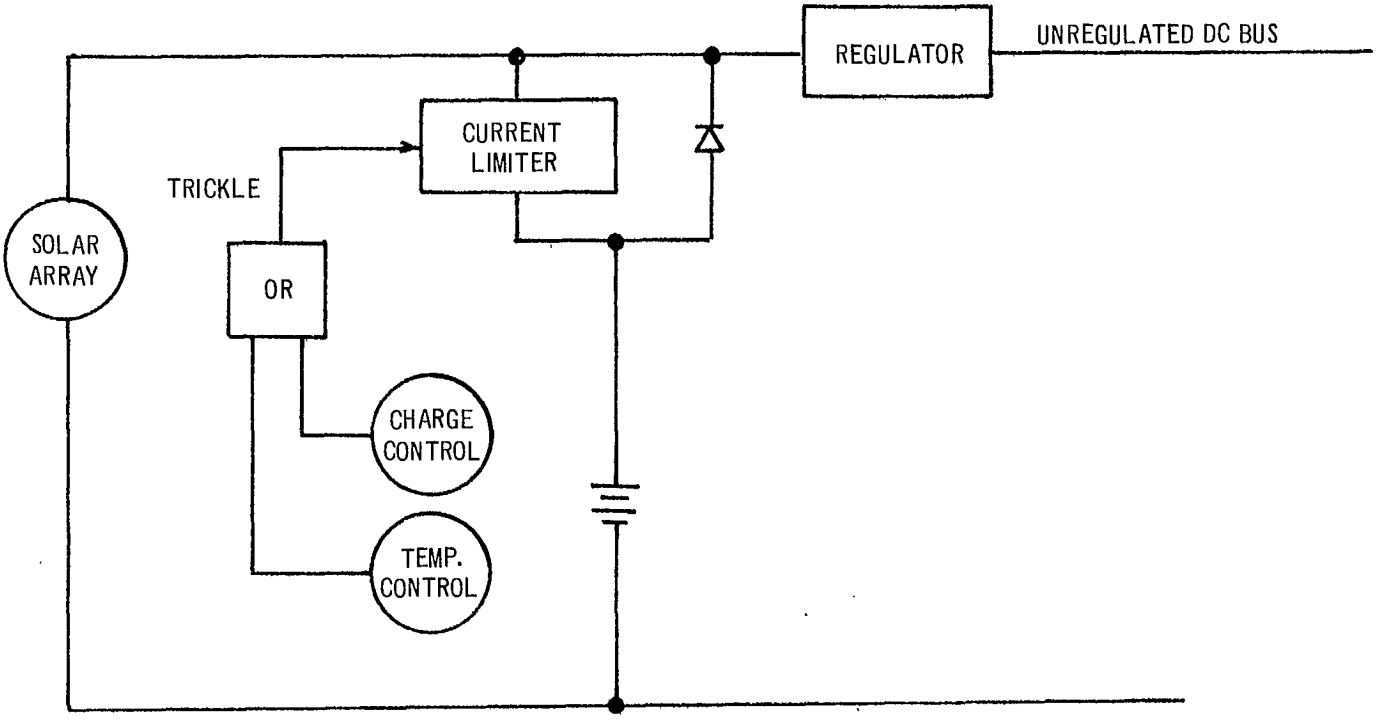

Figure 6–5 Configuration 3 – A series regulator is employed to regulate the main bus

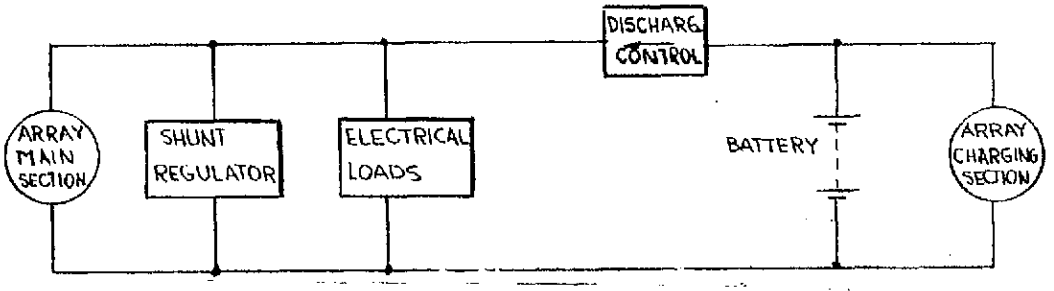

(a) Configuration 2A – Continuous Charging Current

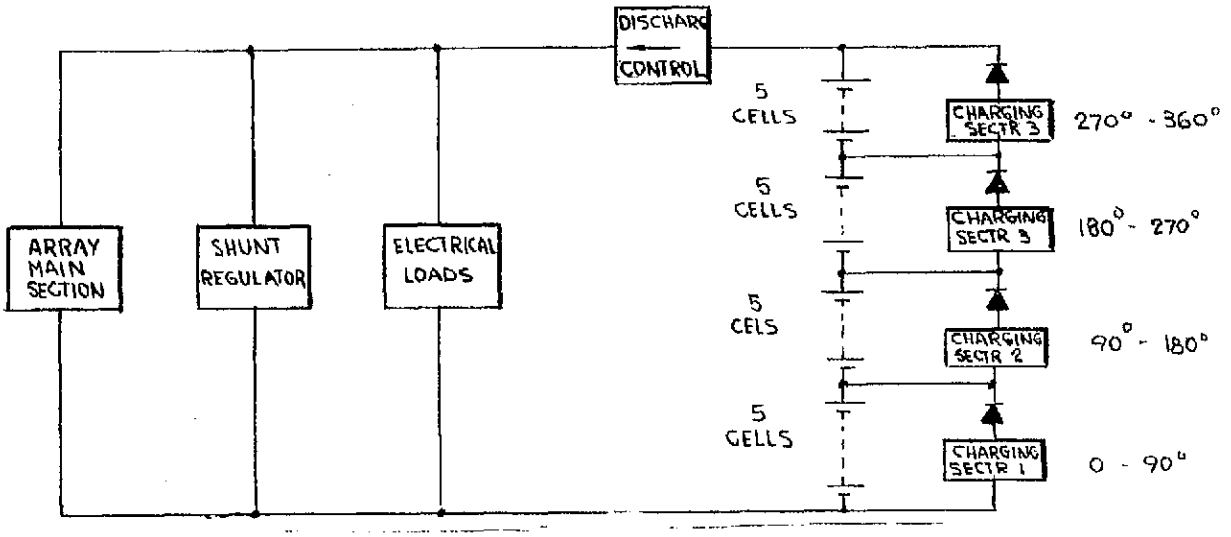

(b) Configuration 2B – Pulsed Charge, Modular Battery

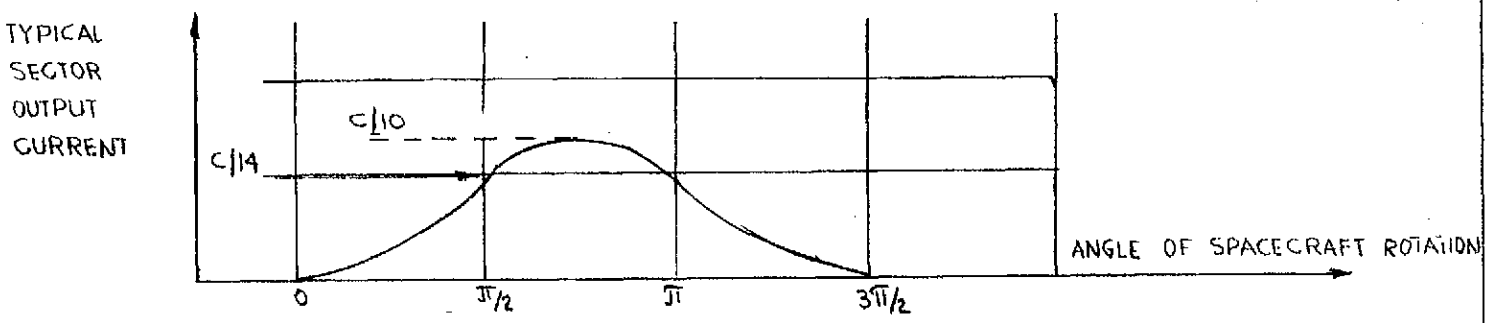

(c) Charging Current from One Sector of Configuration 2B as Spacecraft Rotates

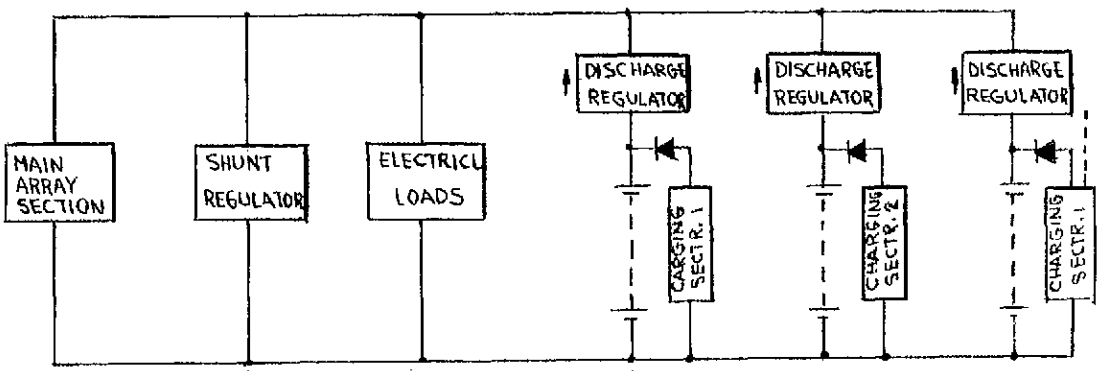

(d) Configuration 2C – Pulsed Charge, Multiple Battery

Figure 6–4 Isolated Battery Charge System

Each of the configurations is modeled by a set of equations which expresses the performance of the subsystem in terms of the size of the solar array required to support the satellite loads. The type of charge control used in configurations 1 and 3 may be thought of as a coulometer or third electrode, but the exact type has no significant bearing on the trade-offs at this level. Charge control will be discussed separately in section 6.4.2. Note that the trade-offs are concerned only with configurations in which silicon solar cells are the primary energy source and nickel-cadmium batteries provide energy storage. The size, weight, power level, geometry and mission requirements of the satellite preclude the use of alternative power systems such as RTG, nuclear reactors, solar thermoelectric or cadmium sulfide arrays.

6.4.1.1 General Expressions for System Parameters

In this section the concepts of the trade-off study are explained by deriving general expressions for the main system parameters. The general expressions are used in section 6.4.1.2 through 6.4.1.4 to compute these parameters for each candidate configuration.

Let W_E = power drain (watts) from the battery during eclipse

W_S = power drain (watts) from the solar array during sunlight, excluding battery power

W_C = power drain (watts) from the solar array to recharge the battery

W_T = power drain (watts) from the solar array to trickle charge the battery.

The distinction between W_C and W_T is that W_C is directly related to the eclipse load, being the power level at which recharge must occur to restore the battery within the sunlit period (22.8 hours minimum) of the shadowed orbits, whereas W_T is a compromise value chosen to maintain the battery at a reasonable temperature and state of charge during solstice seasons as well as to "top-off" the main recharge at a safe overcharge level during equinox seasons.

Except when otherwise indicated, W_T will be chosen to correspond with a charge rate of C/35.

Let t_E = maximum eclipse time = 1.20 hours

t_D = minimum sunlit time at equinox = 22.80 hours.

During peak eclipse the battery has to supply $W_E \cdot t_E$ watt-hours which corresponds to the maximum permissible depth of discharge, k (dimensionless). Thus

$$C_R = \frac{W_E \ t_E}{k \ V_D} \qquad (1)$$

where C_R = required battery capacity in ampere-hours and V_D = average battery discharge voltage. For the present, k will be taken somewhat arbitrarily as 0.60.

Neither C_R nor V_D is truly a continuous variable. However, it is convenient for the comparison to choose a fixed value of V_D and regard C_R as a variable. V_D is therefore chosen to correspond to a 20-cell battery, V_D = 25 volts. By definition

$$W_C = \frac{W_E \ t_E}{\eta_b \ t_D \ \eta_c} \qquad (2)$$

and

$$W_T = \frac{C_R}{T} \cdot \frac{1}{\eta_T} \cdot V_C$$

where η_b = battery watt-hour efficiency = 0.65

η_c = efficiency of recharge control element

η_T = efficiency of trickle charge control element

V_C = average battery voltage during trickle charge

and T = 35 hours

Let W_{SS} = power required from array at summer solstice

W_{EQ} = power required from array at equinox

P_{SS} = power supplied by array at summer solstice

P_{EQ} = power supplied by array at equinox

By orbit geometry $P_{EQ} = \frac{P_{SS} \times (1.0167)^2}{\text{COS } 23.5^\circ}$

$$= 1.127 \ P_{SS}$$

If $W_{EQ} > 1.127\ W_{SS}$, the array size is determined by the equinox requirement and $W_{EQ} = P_{EQ}$. If $W_{EQ} < 1.127\ W_{SS}$, the array size is determined by the summer solstice requirement and $W_{SS} = P_{SS}$. In the latter case (solstice limited array) the power available for recharging the battery (during sunlight at the peak eclipse season) is

$$P_{EQ} - (W_{EQ} - W_C) \quad \text{watts.}$$

By definition, $W_{SS} = W_S + W_T$

and $W_{EQ} = W_S + W_C$

It is convenient to define symbols for the load power requirements at this point:-

P_1 = Power required by 6 high level TWTs = 145.4 watts

P_2 = Bus power required by housekeeping equipment = 27.9 watts

P_3 = Regulated power required from central equipment converter = 20.4 watts

P_4 = Heater power (from battery during eclipse) = 5 watts

η_1 = Efficiency of TWT converters

η_2 = Efficiency of central equipment converter

6.4.1.2 Straight Through System

This configuration is further divided into three alternatives of varying efficiency and complexity by varying the nature of the charge and discharge control elements.

a) Configuration 1A (Figure 6-6)

In this version the charge control sensor opens relay K1 upon attainment of full charge. K1 is closed when the battery is on discharge. It remains closed throughout discharge and during the early stages of charge when it is not desired to limit charging current.

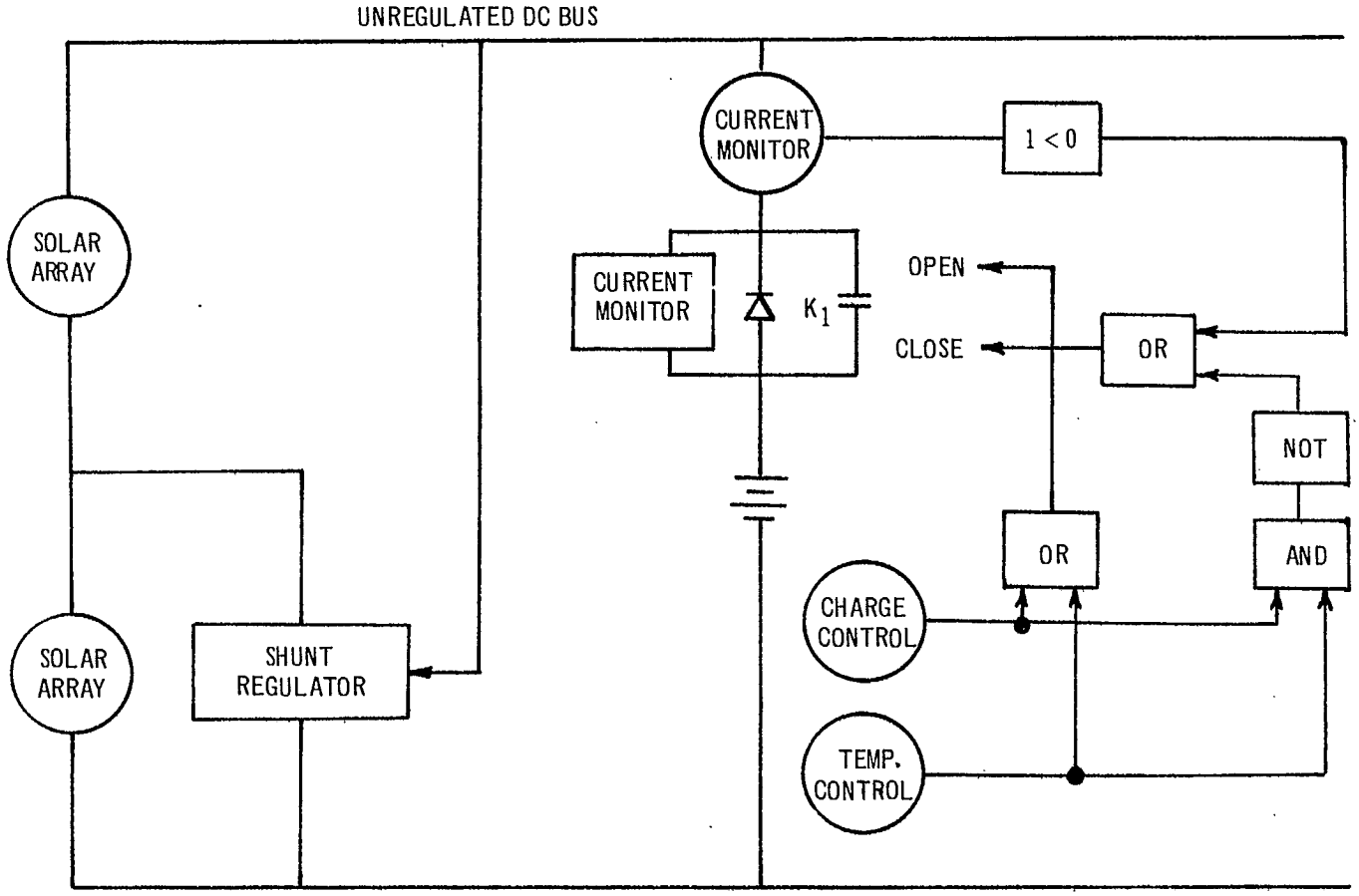

Figure 6-6 Configuration 1A

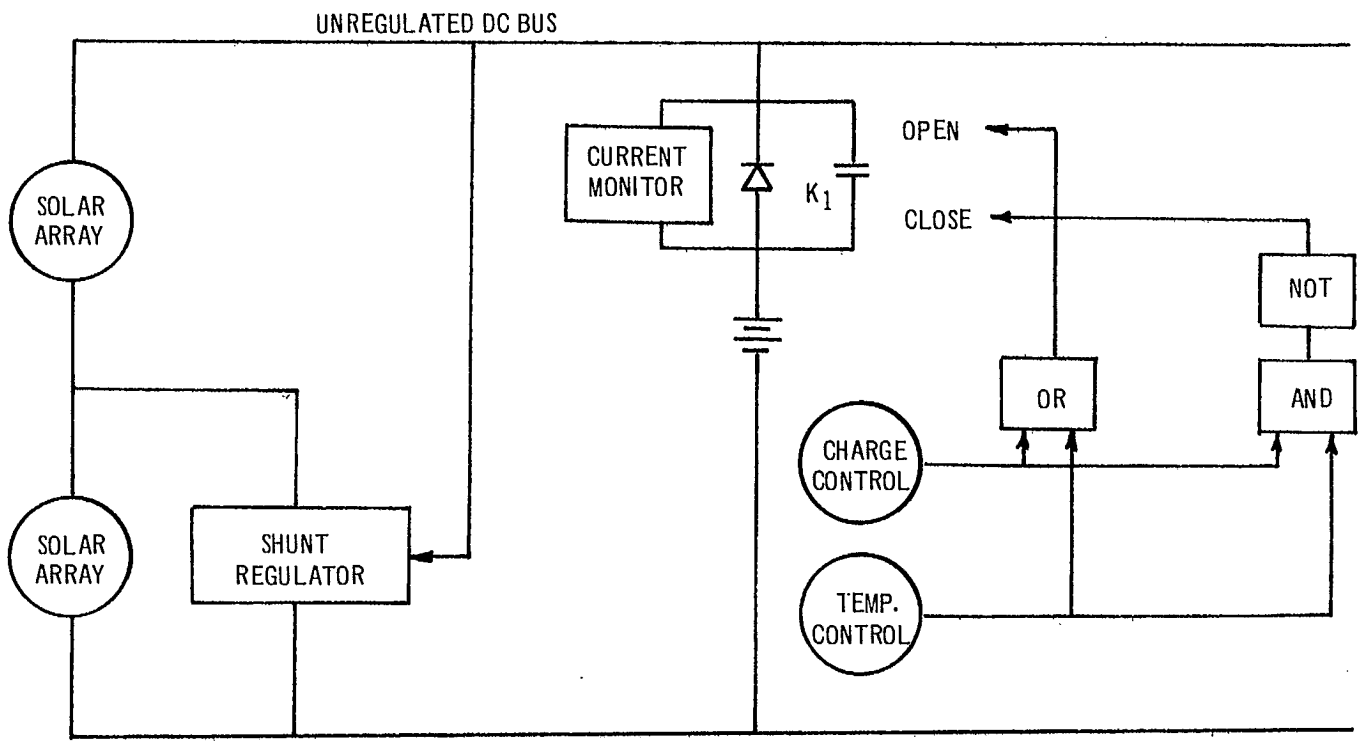

Figure 6-7 Configuration 1B

As the battery is connected directly to the bus during recharge and discharge, $\eta_c = 1$. During trickle charge the battery can be expected to be about 2 volts below bus voltage, giving $\eta_T = 0.93$.

As the bus is not regulated, $\eta_1 = 0.86$ and $\eta_2 = 0.75$.

$$W_E = \frac{P_1}{2\eta_1} + P_2 + \frac{P_3}{\eta_2} + P_4 = 144.7 \text{ watts}$$

$$W_S = \frac{P_1}{\eta_1} + P_2 + \frac{P_3}{\eta_2} = 224.3 \text{ watts}$$

Applying the relations derived earlier gives:-

$C_R = 11.6$ AH

$W_C = 11.7$ watts

$W_T = 9.05$ watts

$W_{SS} = 234$ watts

$W_{EQ} = 236$ watts

As $W_{EQ} < W_{SS} \times 1.127$, array size is solstice limited and

$P_{SS} = 234$ watts

$P_{EQ} = 264$ watts

Minimum power available for recharge is 264 watts - 224.3 watts
= 39.7 watts (C/8.75)

b) Configuration 1B (Figure 6-7)

This is identical to configuration 1A except that the discharge diode is not bypassed by a relay when the battery discharges. The battery discharge power is then increased by 3%. This difference in discharge power can be accomodated with a slight increase in depth of discharge and the same battery weight. As the difference in recharge power is a small proportion of the total array power and as the array of configuration 1A had a considerable excess recharge capability because the array was solstice limited, it is evident that the same array size can be used here. All system parameters are therefore essentially identical to those of configuration 1A.

c) Configuration 1C (Figure 6-8)

Configuration 1C is a much more complex power subsystem which has potential advantages in overall efficiency and consequently in solar array dimensions and weight. In this concept the charge control is designed to control charging current at the magnitude required to maintain the bus voltage at a constant level. When the battery is fully charged, the charging current is reduced further and the bus is then controlled by diverting current through the shunt regulator.

The discharge control consists of a boost converter which regulates the bus during battery discharge. The result is a continuously regulated bus, allowing operation of the housekeeping converter without pre-regulation and of the TWT converters over a narrower input voltage range, thus improving the efficiency of all converters. The following values are applicable:-

$\eta_1 = 0.89$

$\eta_2 = 0.78$

$\eta_C = 0.93 = \eta_T$

η_D = efficiency of discharge control = 0.88

Therefore

$$W_E = \frac{1}{\eta_D}\left(\frac{P_1}{2\eta_1} + P_2 + \frac{P_3}{\eta_2} + P_4\right) = 160 \text{ watts}$$

$$W_S = \frac{P_1}{\eta_1} + P_2 + \frac{P_3}{\eta_2} = 218.5 \text{ watts}$$

Applying the relations derived earlier:

C_R = 12.8 AH

W_C = 13.9 watts

W_T = 10.6 watts

W_{SS} = 228.1 watts

W_{EQ} = 231.4 watts

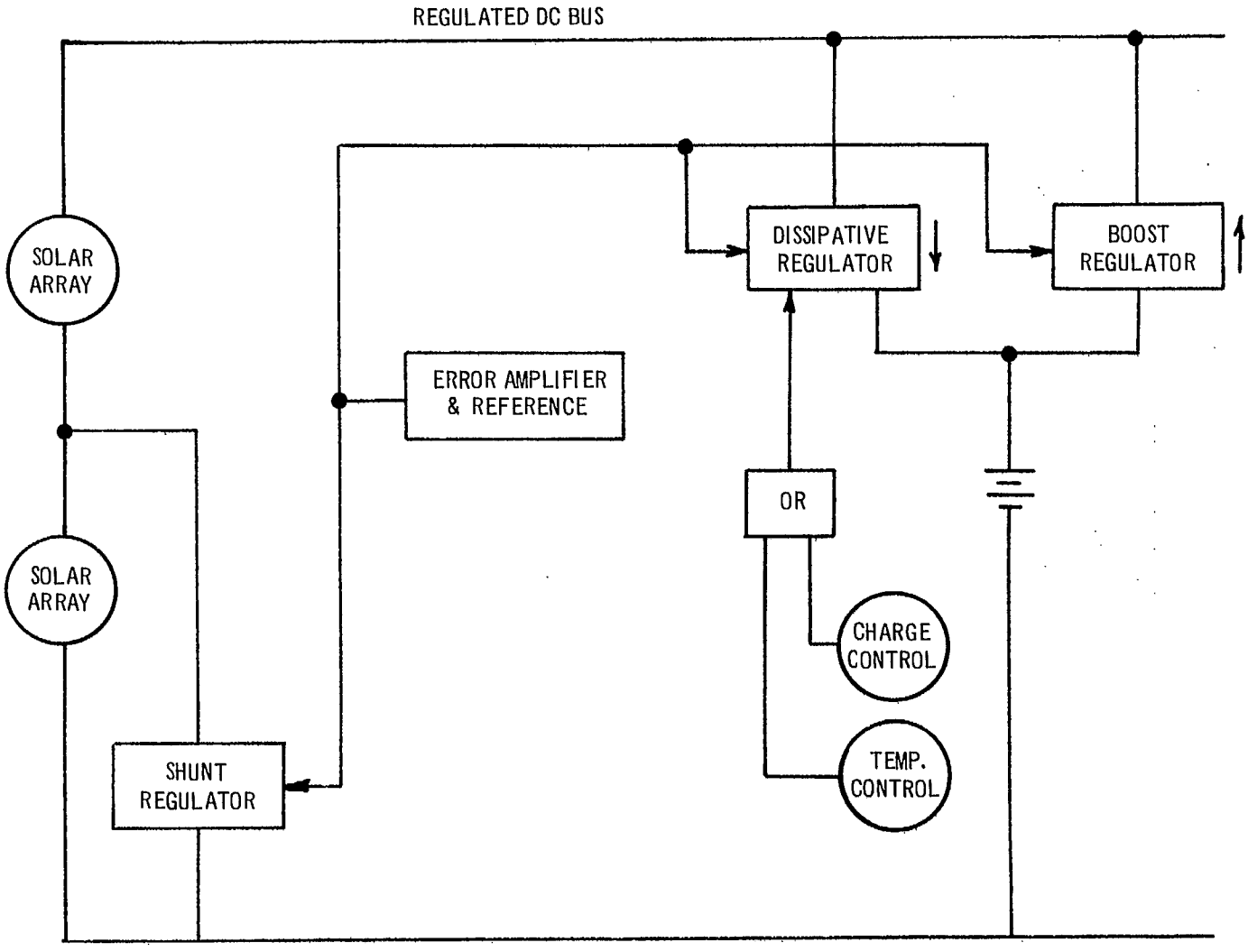

Figure 6–8 Configuration 1.C

As $W_{EQ} < 1.127\ W_{SS}$, the array size is solstice limited and

$$P_{SS} = W_{SS} = 228.1 \text{ watts}$$

$$P_{EQ} = 1.127\ P_{SS} = 257.2 \text{ watts}$$

The minimum power available for recharge is 39.7 watts (C/8.2).

6.4.1.3 Isolated Battery Charge System

This configuration seeks to simplify the power subsystem as much as possible by eliminating the charge regulator. This is accomplished by utilizing a separate section of solar array for charging the battery, relying on the inherent current-limiting characteristic of the solar cells to limit charging current to that which the battery can tolerate continuously.

Three variations of the system are examined to provide a full assessment of its capabilities. The variations have modified forms of the charging array section and/or the battery to improve efficiency.

a) Configuration 2A - Continuous Charging Current (Figure 6-4a)

In this configuration the charging section of the array provides a steady level of charging current to the battery throughout the spacecraft's rotation.

$$W_E = \frac{P_1}{2\eta_1} + P_2 + \frac{P_3}{\eta_2} + P_4 = 144.7 \text{ watts}$$

$$W_S = \frac{P_1}{\eta_1} + P_2 + \frac{P_3}{\eta_2} = 224.3 \text{ watts}$$

$$C_R = \frac{W_E\ t_E}{k\ V_D} = 11.6 \text{ AH}$$

These results are the same as in configuration 1A. In configuration 2A however, the main section of the array has to provide the same power at summer solstice as at equinox and is therefore solstice limited, whereas the charging section is sized by the equinox recharge requirements.

Main section $P_{SS} = W_{SS} = W_S = W_{EQ} = 224.3$ watts

$P_{EQ} = 1.127 \times P_{SS} = 253$ watts.

Charging Section

$$W_C = \frac{W_E \ t_E}{\eta_b \ t_D \ \eta_c}$$

= recharge power required during equinox season

= 11.7 watts, assuming $\eta_b = 0.65$ and $\eta_c = 1$.

The corresponding charge rate is C/27, a rate which is far too low for efficient recharge i.e. $\eta_b = 0.65$ is not valid at this rate. One solution to the difficulty is to boost the charge rate to a more practical value such as C/15 by increasing the size of the array charging section, with a consequent weight penalty, but this would cause excessive periods of overcharge, leading to shorter battery life, and would increase the difficulty of the thermal design.

b) Configuration 2B - Pulse Charge, Modular Battery (Figure 6-4b)

An alternative solution is to use a pulse charging approach. In this the array charging section is arranged to provide a number (typically 4) of independent low voltage high current pulses. The average power level is the same as in the previous layout (11.7 watts) but power is time shared to provide higher peak power. The 20-cell battery is grouped as 4 modules of 5 series cells. The modules discharge in series but are charged independently in sequence by the 4 array pulses.

In principle this increases the instantaneous charge rate from C/27 to C/7, a very efficient value for recharge. In practice this rate can only be achieved by a time-sharing scheme in which the total output of the charging section is switched electronically to each group of cells in turn. The complexity of switching defeats the main objective, system simplicity, of the isolated battery charge system.

A more practical method is to modify the connections of the c ircuits in the charging array to provide 4 independent charge pulse generators, each one being the total output of one 90° sector. The rotation of the spacecraft then provides time-sharing automatically. The shape of the charging current pulse with this arrangement is shown in Figure 6-4c. Some charging current is present in each pulse over 270° of rotation, but

the instantaneous level is only adequate for efficient recharge over approximately 90° of rotation. The average charge rate over this 90° angle is C/11. To ensure complete recharge this must be boosted to C/7 by increasing the size of the charging sectors by about 60%. This method also introduces a thermal design problem.

c) Configuration 2C - Pulse Charging, Multiple Battery (Figure 6-4d)

The pulse charging approach could also be implemented by splitting the 11.7 AH battery into several batteries (e.g. 3 of 4 AH) each with 20 cells. Such an arrangement was discussed in the interim report. It has the same disadvantages as the modular approach as far as array size is concerned. In addition, it requires discharge regulators to ensure that the load is shared equally among the batteries. These regulators are relatively heavy, complex and inefficient. As the bus voltage is closely regulated during discharge, it varies considerably less than in configurations 1A, 1B, 2A and 2B, permitting an improvement in the efficiency of the TWT converters and the central equipment converter. Regulation is not adequate to permit the central equipment converter to be unregulated. Estimated values for the efficiencies of the converters are $\eta_1 = 0.87$ and $\eta_2 = 0.76$. The efficiency of the discharge regulators is taken as 0.80.

6.4.1.4 Series Regulated System (Figure 6-5)

This configuration uses a series line regulator to regulate the bus voltage. It has the advantage of a relatively constant heat dissipation throughout its operating life, at a level much lower than the maximum possible heat dissipation of the shunt regulator. This simplifies the thermal interface design. The degree of regulation enables the central equipment converter to operate without internal regulation, but the communications converters still require regulation. An efficiency improvement is obtained ($\eta_1 = 0.89$, $\eta_2 = 0.78$). The battery requires a boost discharge regulator to maintain the bus regulated in eclipses. The efficiency of this regulator is $\eta_{br} = 0.88$. The efficiency of the series regulator is $\eta_R = 0.88$.

$$W_E = \left(\frac{P_1}{2\eta_1} + P_2 + \frac{P_3}{\eta_2} + P_4 \right) \frac{1}{\eta_{br}} = 160 \text{ watts}$$

$$W_S = \left(\frac{P_1}{\eta_1} + P_2 + \frac{P_3}{\eta_2} \right) \frac{1}{\eta_R} = 247 \text{ watts}$$

Applying the relations derived earlier gives:

C_R = 12.8 AH

W_C = 14.0 watts

W_T = 10.0 watts

W_{SS} = 257.6 watts

W_{EQ} = 261 watts

As $W_{EQ} < 1.127\ W_{SS}$, array size is solstice limited and $P_{SS} = W_{SS} = 257.6$ watts.

$P_{EQ} = 1.127\ P_{SS} = 290$ watts

Minimum power available for recharge is 43 watts (C/8.3).

6.4.1.5 Discussion of Configuration Analysis

The results of the preceding analysis are shown in Table 6.4. Configuration 2A is not included since it was shown to be impracticable without the pulse charge modification. In configurations 2B and 2C, total solstice and equinox power levels are shown as two parts, the larger number corresponding to the main section of the array and the smaller corresponding to the isolated battery charging section. The power available for recharge in configurations 2B and 2C is the total power produced by the charging section (18.4 watts and 22.8 watts). These figures include the increase in size of the charging section due to the fact that the pulse shape (derived from the rotation of the spacecraft) is only effective in recharging the battery over about 90° .

The values tabulated under "Relative Array Size" provide a provisional figure of merit for the configurations. A more complete assessment requires an examination of the charge control technique and all-up system weight. It is noted in passing, however, that

(a) the high charge rates available for configurations 1 and 3 place a heavy emphasis on the provision of a reliable means of charge control

(b) Provision of regulation in configurations 1C and 3 implies a penalty in battery weight and system complexity compared to the unregulated systems

Configuration	1A	1B	1C	2B	2C	3	Units	Symbol
TWT Converter Efficiency	86	86	89	86	87	89	%	η_1
Equipment Converter Efficiency	75	75	78	75	76	78	%	η_2
Power into TWT Converters								
Daylight (6 ON)	169.2	169.2	163.4	169.2	167	163.4	watts	P_1/η_1
Eclipse (3 ON)	84.6	84.6	81.7	84.6	83.5	81.7	watts	$P_1/2\eta_1$
Power into Equipment Converter	27.2	27.2	26.2	27.2	26.9	26.2	watts	P_3/η_2
Bus Power for Housekeeping Equipment	27.9	27.9	27.9	27.9	27.9	27.9	watts	P_2
Heater Power (eclipse only)	5	5	5	5	5	5	watts	P_4
Battery Capacity	11.6	11.6	12.8	11.6	14.3	12.8	ampere hours	C_R
Depth of Discharge	60	62	60	60	60	60	%	k
Power required for trickle charge @ C/35	9.05	9.05	10.6	9.05	11.0	10.6	watts	W_T
Power required for recharge over 22.8 hours	11.7	12.1	13.9	18.4	22.8	14.0	watts	W_C
Power required from array at summer solstice	234	234	228.1	(224.3 +9.05)	(221.8 +11.0)	257.6	watts	W_{SS}
at equinox	236	236.4	231.4	(224.3 +18.4)	(221.8 +22.8)	261	watts	W_{EQ}
Min. power available from array at summer solstice	234	234	228.1	(224.3 +16.3)	(221.8 +20.2)	257.6	watts	P_{SS}
At equinox	264	264	257.2	(253 +18.4)	(250 +22.8)	290	watts	P_{EQ}
Min. power available for recharge at equinox	39.7	39.7	39.7	18.4	22.8	43	watts	
Minimum charge rate	C/8.7	C/8.7	C/8.2	C/27	C/27	C/8.3		
Relative Array Size	1.03	1.03	1.00	1.06	1.06	1.13	-	

Table 6.4 Comparison of Candidate Configurations

(c) configuration 2C less efficient than configuration 2B in array size and battery weight

6.4.2 Charge Control Methods

Of the various methods of charge control available, four were selected as being sufficiently practical for further study.

- o Constant Current (Pulsed Charge Modification).
- o Limited voltage with a maximum temperature override.
- o Auxiliary electrode charge control.
- o Coulometric charge control.

Voltage switchdown methods were eliminated from consideration because of their extreme sensitivity to the relatively wide range of operating temperature to which the battery is expected to be exposed.

6.4.2.1 Constant Current Charge Control

Constant current charge control is the technique in which the battery charge current is limited only by the characteristics of the array which is charging it. No additional method is used to control overcharge current. The charging array is therefore sized to produce less current than the battery can accept continuously on overcharge.

This technique has been used successfully in many spacecraft, including the Canadian Alouette-ISIS series. In its simplest form it is particularly suitable for low power, low altitude, scientific satellites where the duty cycle involves frequent discharges of low depth and the battery undergoes a relatively wide range of operating temperatures. Its advantage in these cases is its simplicity and consequent reliability.

This reliability does not carry over automatically to the long life synchronous communications satellite because in this application the battery spends most of its time on overcharge. Qualitatively, battery life is improved if the overcharge current can be kept to a low level.

Only the pulsed charge modification can give a charging level which is high enough to permit efficient recharge within 22.8 hours and an average overcharge current which is low enough to maintain low internal pressures and provide a compatible thermal interface.

Constant current charge control can not be used with Configurations 1 or 3 but is a natural adjunct to configuration 2.

The main advantages of this method are:-

(a) No electronic or electrochemical charge controls are necessary.

(b) The pulse charge rate provides efficient recharge.

(c) The battery cannot be overcharged at too high a rate.

(d) The pulsed overcharge ensures a higher state of oxidation of the nickel plate than the steady low-rate trickle overcharge of competitive methods.

The disadvantages of this method are:-

(a) The thermal interface problem is more severe than in competitive methods because the battery dissipation is greater, and varies more over the 5 years of life, than with a steady, low-rate trickle overcharge.

(b) The array size is greater and cell layout less uniform than in competitive methods.

(c) The size of the charging array is not tolerant to variations in battery charging efficiency or load requirements, such as may be caused by deterioration of the battery or the loads. Additional charging array is required to allow for such changes, increasing the thermal problem. Competitive systems are less critical in this respect, except at the end of life.

6.4.2.2 Limited Voltage with Maximum Temperature Override

The method can be used conveniently with Configurations 1A, 1B and 1C, but not with Configurations 2 and 3. The main bus voltage, and consequently the charging voltage applied to the battery is limited to a level of approximately 1.46 volts/cell, which will not permit high rate overcharge of the battery at low temperatures, and consequently minimizes or prevents the irreversible evolution of hydrogen gas in the

cell at low temperatures. A constant voltage limit applied to the cell normally results in a condition of thermal runaway due to the negative voltage-temperature characteristic of the cell at any constant current. The system uses a thermal override switch to reduce the charging current to the C/40 level at a preset temperature, thus interrupting the thermal runaway. This technique of charge control provides an additional advantage, in that it permits independent control of battery temperatures, easing the thermal control problems of the spacecraft somewhat.

One disadvantage of this method is that the battery is exposed to brief periods of high overcharge current (if such high currents are available from the primary power source) during the latter stages of charge. The thermal controls for the battery must be designed to dissipate sufficient heat to permit cooling with C/40 trickle currents being applied to the battery. Another disadvantage is that the charge control becomes ineffective in the event of a metal-to-metal short-circuit in any one cell of the battery. It is not normally disturbed by the usual cell failure mode, in which the charging voltage across the defective cell is almost normal.

This charge control method is also disturbed by the effects of use and aging of the cells over long periods of time. This is manifested in an increasing variation from cell to cell of the charging characteristics, causing an unequal distribution of voltages between cells when the voltage limit is applied across the battery. A similar inequality of cell voltage is caused by unequal distribution of temperature throughout the battery pack. Should these inequalities in voltage distribution be additive, one or more cells could enter the high voltage region which permits generation of hydrogen gas, leading to progressive pressure buildup and eventual failure of the cell with the highest voltage.

6.4.2.3 Auxiliary Electrode Charge Control

Cells can be purchased containing auxiliary electrodes whose output voltage relative to the negative electrode is a function of the internal oxygen pressure of the cell and of the temperature. Since generation of oxygen within the nickel-cadmium cell occurs only near the end of charge, the electrode output voltage (or current through a fixed load) may be used as an indicator of approaching full charge. This signal can be used to initiate termination of charge or reduction of charge rate.

Because the oxygen pressure is a function of the generation rate and the recombination rate, both of which are non-linear functions of temperature, a more accurate estimate of the state of charge is obtained by compensating the switch-to-trickle point for variations in battery temperature. The output of the auxiliary electrode is of the order of 0.25 V.

The advantage of the auxiliary electrode charge control is that it measures directly a cell characteristic indicative of charge completion. The amount of charge energy restored to the cell may be varied by varying the operating point of the sensor with battery temperature, thus compensating for the lower efficiency and earlier start of gas evolution with increased temperature. The auxiliary electrode tends to terminate charge earlier than the temperature override of a voltage limited charge, leading to lower battery maximum temperatures, less overcharge at high rates, and generally longer life. It is relatively insensitive to cell aging and will still perform satisfactorily if one cell shorts.

The disadvantages of the auxiliary electrode charge control are as follows:

a) Electronic implementation is complex. The low output voltage of the auxiliary electrode makes a direct DC amplifier impracticable. The use of AC requires an excitation oscillator and amplifier, with resulting reliability and weight penalties. A block diagram of the auxiliary electrode charge control is shown in Figure 6-9. Figure 6-10 shows the required temperature compensation curve.

b) The auxiliary electrode gives a false full-charge signal for a brief period after switchover from discharge to charge. In a long charge-time application such as this, the impact of this disadvantage is negligible.

c) The auxiliary electrode is known to drift in sensitivity with aging, the rate of drift decreasing with increasing age.

d) Insufficient reliability data are available on auxiliary electrodes, although testing has not disclosed any significant change in failure rate due to the presence of the auxiliary electrode.

The auxiliary electrode can be used with any of the configurations discussed in section 6.4.1

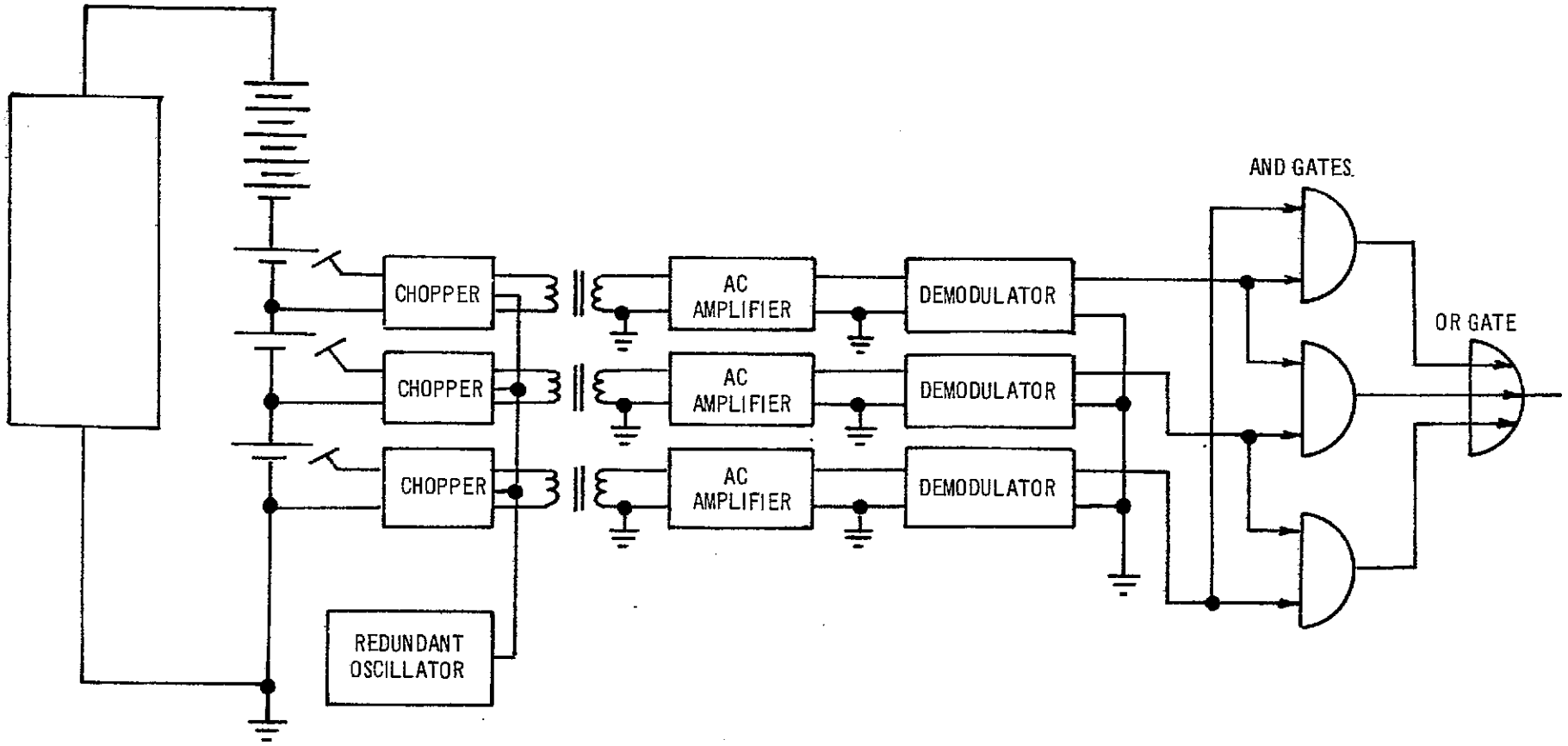

Figure 6-9 Auxiliary Electrode Control Circuit

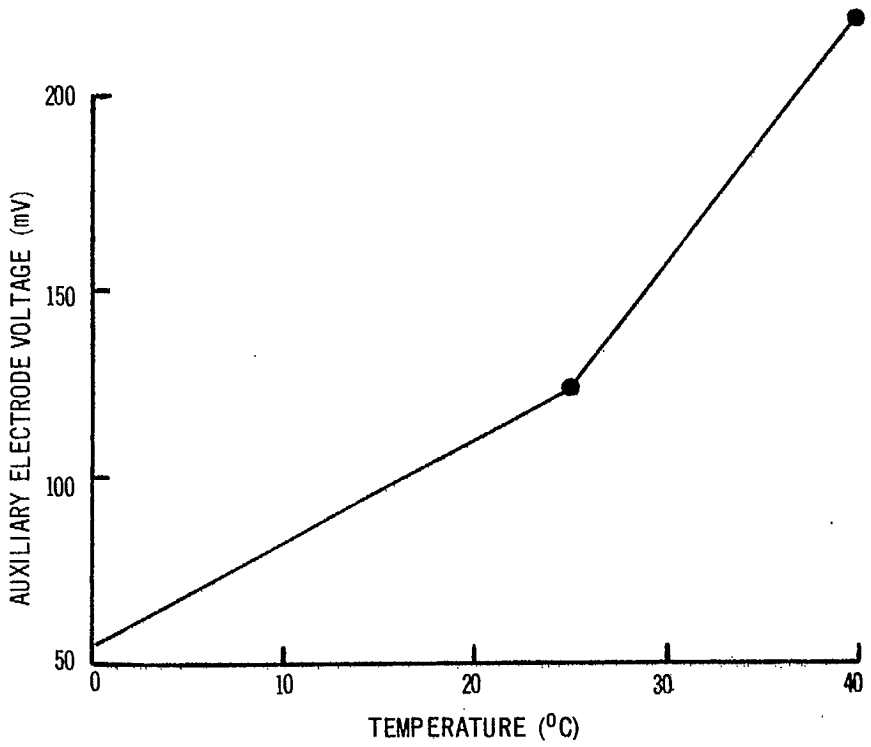

Figure 6-10 Auxiliary Electrode Temperature Compensation Curve

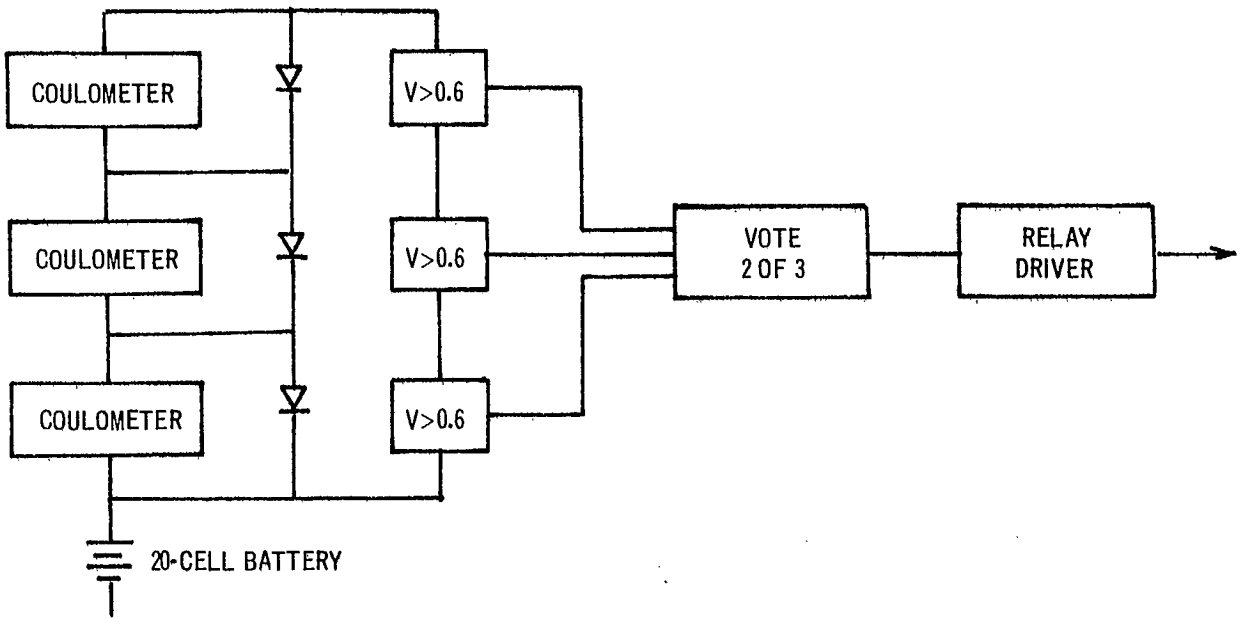

Figure 6-11 Coulometer Charge Control

Coulometric Charge Control

Cadmium-Cadmium Coulometers have been used in controlling the charge of nickel-cadmium cells. The coulometer consists of paired parallel sets of cadmium electrodes, which are charged and discharged as the battery current passes through the coulometer. As long as neither electrode set is exhausted (either fully charged or fully discharged), the voltage drop across the coulometer is of the order of 50 mv. When the coulometer cathode is fully charged, however, the voltage rises rapidly towards the hydrogen evolution potential of about 1.5 volts. It is necessary to limit the voltage which can be applied to the coulometer to approximately 0.8 volts by using a diode bypass. A block diagram of the coulometer charge control is shown in Figure 6-11.

The ampere-hour efficiency of the Cd-Cd coulometer is approximately 100%; consequently it forms an accurate analog of cell performance only when the cell efficiency is also 100%. The coulometer has been used to control cells on cycling at moderate depths of discharge and normal temperatures for several thousand cycles. However, at depths of discharge greater than 35%, results have not been uniformly successful. It is also probable that the coulometer will fail to control battery charge at high battery temperatures without some sort of current-temperature compensation for variation in battery efficiency. The weight of a coulometer is approximately that of a cell, and the addition of a coulometer requires provision in packaging for the addition of the coulometer cell, similar in size to one cell. The coulometer drifts in capacity with aging, the rate of drift falling to a negligible level after several hundred cycles. Insufficient test data are available on coulometers for accurate reliability assessment.

Coulometric charge control can be used with any of the candidate configurations.

6.4.3 System Weight

A realistic calculation of system weight requires that redundancy philosophy be included in the design. Preliminary evaluation suggests that acceptable system reliability is obtained if no single part failure can cause mission failure. This results in the use of quad or majority voting redundancy for the power control functions.

The ground rules used in each of the systems are as follows:-

a) Control circuits of all shunt regulators are of the majority voting logic type.

b) Shunt power elements are quad redundant.

c) All battery cells are equipped with electronic protection which bypasses the cell if it becomes overdischarged. This allows the battery to go on working if any cell develops an internal shunt, a failure mode in which the cell voltage on charge is almost normal but the discharge capacity is very low.

d) A metal-to-metal short circuit within a cell does not prevent correct system operation, except for those systems using the voltage-limited charge control method.

e) Charge control logic and components are majority voting redundant, including the auxiliary electrodes and coulometers. This results in a severe weight penalty for the coulometer charge control.

Table 6.5 shows the weight analysis of the candidate configurations, each considered with applicable versions of the four candidate charge control methods. Configurations 1 and 3 are considered only with auxiliary electrode, coulometric or voltage-limited charge control. Configuration 2 is considered only with constant current charge control.

System 2C is considered with cylindrical D size cells. The standard capacity matches the system requirement but a penalty is paid in packaging and heat sinking weight. All other systems use prismatic cells since space-qualified cylindrical cells do not have higher capacity than 9 AH.

6.4.4 Selected System Configuration

On the basis of the trade-off studies presented above, the recommended system configuration is 1B with auxiliary electrode charge control. Configuration 3 is rejected because the excessive weight does not appear to compensate adequately for the improved thermal control. Configuration 2C is similar in performance to 2B but much heavier. Configuration 2B has attractive weight and performance features but is rejected because its recharge capability provides a smaller performance margin than the selected system and because it imposes a greater thermal design problem. Configuration 1C provides little benefit for the extra weight and complexity as compared to 1A or 1B. Configurations 1A and 1B are almost equal in weight and performance. The coulometric charge control versions are rejected because of the weight penalty. The voltage-limited charge control versions are rejected despite the weight advantage because of the criticality of this technique as noted in section 6.4.2.2.

Table 6.5 Subsystem Weight Trade-offs

Subsystem Configuration	Array	Battery	PCU	Equip Conv.	Shunt	Syst. Status TLM	Total
1A	52.4	30.5	2.0	3.5	3.6	2.0	94.0
1A + 3rd Electrode	52.4	30.7	3.6	3.5	3.6	2.0	95.8
1A + coulometer	52.4	33.5	3.2	3.5	3.6	2.0	98.2
1B	52.4	30.5	1.9	3.5	3.6	2.0	93.9
1B + 3rd Electrode	52.4	30.7	3.5	3.5	3.6	2.0	95.7
1B + coulometer	52.4	33.5	3.1	3.5	3.6	2.0	98.1
1C	50.5	30.5	10.2	3.5	3.6	2.0	99.3
1C + 3rd Electrode	50.5	30.7	11.5	3.5	3.6	2.0	101.8
1C + coulometer	50.5	33.5	11.1	3.5	3.6	2.0	104.2
2B	54	30.5	2.5	3.5	3.6	2.0	96.1
2C	54	36	7.5	3.5	3.6	2.0	106.6
3 + 3rd electrode	57.4	30.7	12.8	3.5	-	2.0	106.4
3 + coulometer	57.4	33.7	12.4	3.5	-	2.0	109

6.5 DESCRIPTION OF HARDWARE

6.5.1 Power Control Unit (PCU) and Shunt Assemblies

The functions of the PCU and shunt assemblies are:

- Limit main bus voltage when the solar array capability exceeds connected load power.
- Provide acceptable battery charge rate; provide battery discharge during eclipse; provide automatic or command control of battery charge.
- Connect or disconnect the battery in response to ground command.
- Provide for reconditioning discharge and recharge of the battery upon receipt of ground commands.
- Condition electrical operating parameters for telemetry transmission.

The PCU and shunt assembly specification appear in Figure 6-12.

For maximum reliability, the PCU is designed to permit operation of the spacecraft in the event of a battery failure. The load bus limiter produces a stable, well-regulated output in conjunction with only the solar array. Load characteristics and controls are constrained to guarantee operation near the maximum power point of the array at the end of life after maximum array degradation. Each logic element contains adequate energy storage to assure assumption of its correct state when source power is removed during eclipse or transient load fault.

6.5.1.1 Load Bus Voltage Limiting

Voltage Limiting requirements are to:

- Limit main bus voltage to $(29.4) \pm 0.2$ vdc when array power exceeds load power.
- Provide a main bus impedance of 1 ohm maximum, DC to 100K Hz, under all operating conditions when the bus is not directly connected to the battery.
- Consume minimum power when load power exceeds array power.

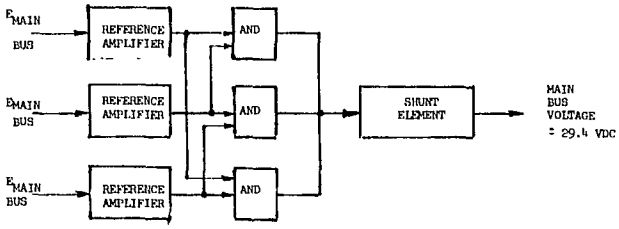

- Limit main bus voltage when array power exceeds load power.

$E_{main\ bus}$ = 29.4 ±0.2 VDC

Figure 6-12(a) Main Bus Voltage Limiter

- Permit full charge rate when solar array is illuminated and battery is not charged.
- Permit trickle charge rate when salar array is illuminated and battery is fully charged.
- Permit trickle charge rate when salar array is illuminated and battery temperature is greater than 90° F.
- Permit discharge into main bus when solar array is eclipsed.

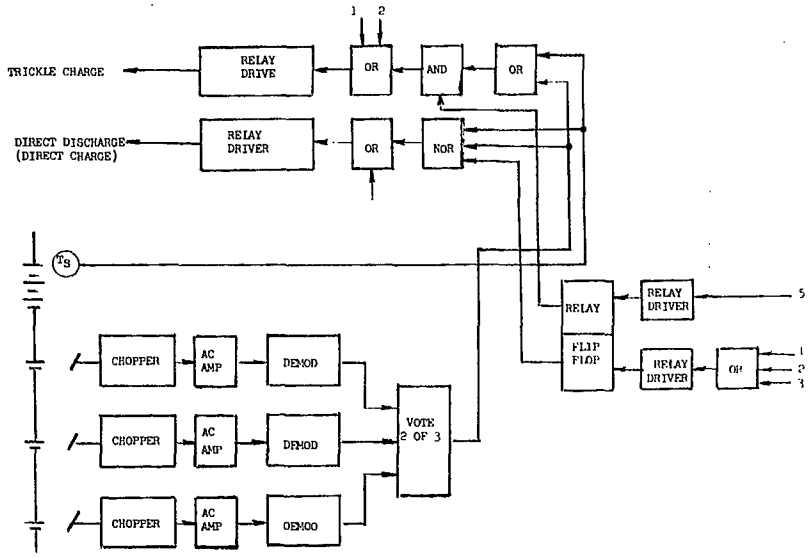

Figure 6-12(b) Battery Charge Control

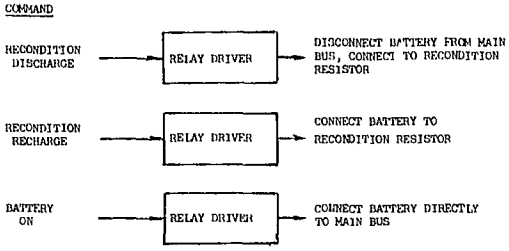

- Disconnect battery in response to ground command.
- Connect battery to recondition recharge resistor in response to ground command.
- Connect battery directly to main bus in response to ground command.

Figure 6-12(c) Battery Connect Control

- Provide under voltage signal when main bus voltage is less than 18 ±0.5 VDC for periods greater than 80 milliseconds.
- Provide signal after the main bus exceeds 20 ±0.5 VDC.

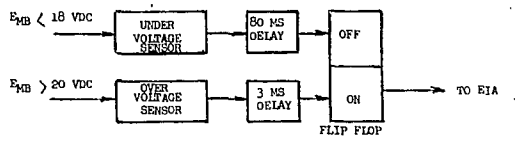

Figure 6-12(d) Undervoltage Signal Control

The partial shunt regulator was selected because it features minimum regulator power dissipation consistent with low output impedance in the presence of excess solar array capacity, and minimum dissipation where load power exceeds array power (as at end of life or during eclipse). The partial shunt regulator consists of a shunt element or class A power amplifier connected to a tap. The tap is located at the approximate midpoint of the solar array. The impedance of the shunt element is varied by a current amplifier which is controlled by an error amplifier which compares main bus voltage to a reference voltage. Shunt impedance is varied such that it shunts more or less array current, so that the main bus voltage remains constant when array power exceeds connected load power. Excess array power is dissipated partially in the shunt element and partially at the source (solar array). When array power excess is greatest, the shunt element is saturated and virtually all the power excess is dissipated in the array, the geometry of which is ideally suited.

6.5.1.2 Undervoltage Signal Control

Requirements are to:

- Initiate undervoltage control signal when main bus voltage falls to a level below 18 ± 0.5 vdc for periods in excess of 80 milliseconds.
- Reset when main bus voltage exceeds 20 ± 0.5 vdc.

Direct control of loads occurs in the electrical integration assembly in response to PCU undervoltage signal. The undervoltage signal is generated by a sensor which detects the critical bus voltage, 18 vdc. The detection of undervoltage causes the detector to generate an error signal which is amplified and produces an output to indicate that undervoltage has occurred. A short delay is incorporated into the undervoltage sensor to prevent false undervoltage signal generation in response to transient undervoltages. A hysteresis of two volts insures that a normal voltage level has been reached.

6.5.1.3 Battery Charge Control

The PCU determines the battery charge mode in response to battery state information supplied by battery auxiliary electrode sensors and battery temperature sensors. The design approach and control sequence take advantage of the low control power and low contact resistance of magnetic latching relays. The use of temperature and auxiliary electrode (also referred to as third electrode or signal) to control the charge of

nickel-cadmium batteries has been demonstrated to be effective. On overcharge, oxygen is produced from the nickel electrode. The auxiliary electrode produces an output signal proportional to oxygen pressure over a limited range. This signal voltage can be detected by the PCU and used to terminate or reduce overcharge current. Use of a few auxiliary electrode cells in the battery in conjunction with temperature sensors mounted on the selected cells provides signals to the PCU that can be used to maintain the capacity of the battery above the rated value and optimize overcharge. As the spacecraft exits from the eclipse, the discharged battery is placed on full charge through relay contacts. When the battery is fully charged and enters the overcharge region (as indicated by a signal from the auxiliary electrodes or by the temperature sensors) the relay is latched open and the battery is placed on trickle charge. The battery remains at a constant current trickle charge until either its temperature or auxiliary electrode signal drop below their threshold values at which time the battery will be returned to the bus for further charging. When the spacecraft enters an eclipse, the battery will discharge through diodes if it is in trickle charge or through relay contacts if either the temperature or auxiliary electrode signal are below their threshold values. By command this automatic charge or discharge can be disabled and controlled from the ground.

6.5.1.4 Battery Connection Control

Battery disconnect is accomplished in response to ground commands by operation of magnetic latching relays. One of the relays connects the battery to a resistive load for reconditioning-discharge. Reconnect occurs in response to another ground command which reconnects the battery for recharge through the current limiting resistors. A further command restores the battery to normal automatic battery charge and discharge control.

6.5.1.5 Hardware Implementation of PCU

a) Shunt Voltage Limiter

Figure 6-13 is a detailed block diagram of the shunt voltage limiter. The load bus is sensed, divided down and compared with three separate precision references. The net error voltage in each comparator is amplified by a separate amplifier and the resultant amplified error signals are summed in a majority voting network, from which an output can be obtained only if two of the three signals are correct.

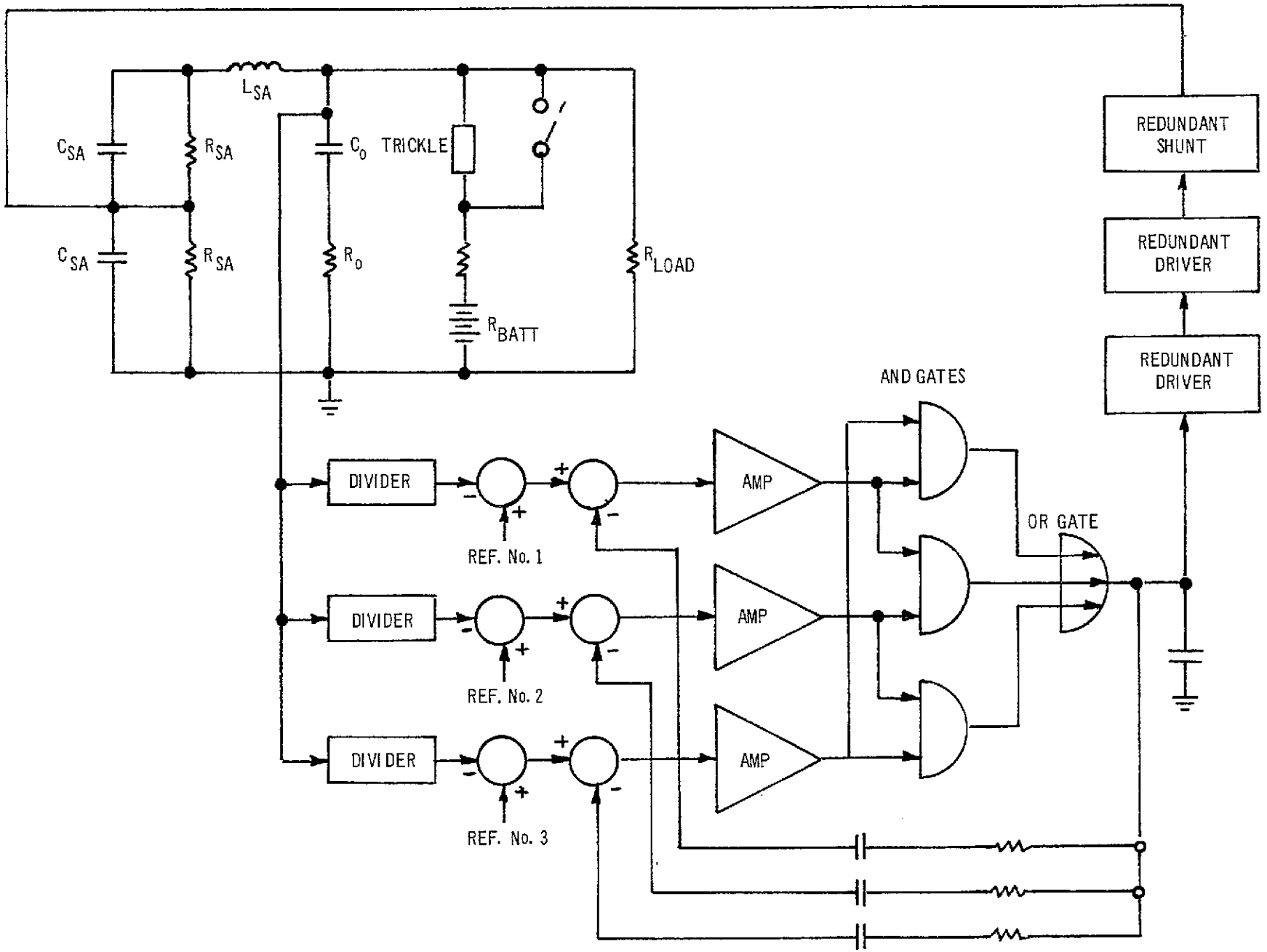

Figure 6-13 Block Diagram of PCU Shunt Regulator

The output signals are fed back through independent RC networks to reduce ac amplifier gain. The final output signal is then further amplified in two redundant stages of current amplification to provide sufficient power to drive the shunt transistors, which control the current bleed from the tapped solar array to maintain the correct output voltage. When the solar array output voltage is lower than the bus voltage limit, no error signal appears and all amplification stages beyond this point draw no current.

Normal in-tolerance operation continues in the event of a single part failure, and in some cases several parts can fail without affecting limiter performance.

b) Shunt Voltage Limiter Dynamic Analysis

Dynamic analyses have been performed on flight equipment using similar circuitry. The stability of the regulator is a function of the impedance of the system loads and interconnecting impedances.

The basic criteria for stability is that the phase margin be greater than zero degrees at an open loop gain of zero db. Good design practice provides a phase margin of 35 to 45 degrees to minimize voltage "ringing" which may be caused by load transients. In practice, typical margins in similar equipment have been found of approximately 76 - 77 degrees. The stability of the shunt regulator has been demonstrated in integration tests on other spacecraft using identical circuitry.

c) Battery Charge Control

Termination of high rate battery charging is accomplished by sensing the pressure of oxygen evolved within a cell during overcharge, by means of an auxiliary electrode within each of three cells.

Two alternative circuits appear to be attractive for implementation, of the auxiliary electrode sensing system; the chopper-amplifier, and the magnetic amplifier.

A trade-off was made between the chopper-amplifier approach and the magnetic amplifier approach:

In the chopper-amplifier approach, the signal from each auxiliary electrode is chopped and the resulting ac signal, isolated from the dc battery voltage by an isolation transformer, is amplified, rectified and integrated to give a dc output signal proportional to, but greater than, the input dc signal.

In the magnetic amplifier approach, the current from the auxiliary electrode of each cell is fed through the control winding of a square-wave excited saturable-core reactor, the width of whose output waveform is proportional to the magnitude of the current in the control winding. The output of the magnetic amplifier is rectified and integrated to form a dc signal proportional to the magnitude of the auxiliary electrode current.

The advantages of the magnetic amplifier approach when used with multiple cells are as follows:

- o Fewer parts and lighter weight, leading to an improvement in both reliability and weight over the chopper-amplifier approach.

The advantages of the chopper-amplifier are:

- o Availability of off-the-shelf circuit designs.

Since the chopper-amplifier represents a minimum design effort and probable lower cost, it is selected as the approach to be implemented (Figure 6-14).

The auxiliary electrode output signal is fed to a chopper-amplifier-demodulator circuit, whose output is proportional to electrode current output and isolated from the voltage of the cell whose electrode is being sensed. The amplified output from each auxiliary electrode is then compared with a reference threshold voltage which is compensated for the temperature of the battery cell associated with the sensed electrode. When the threshold is passed the detector delivers a digital output signal. The detector output signals are summed in a voting network. Two such signals must be present before the voting network will put out a signal.

The output of the voting network is fed to the battery control and command logic.

d) Trade-off of Passive and Active Trickle Current Limiting

Receipt of a third electrode signal or of an overtemperature signal from the battery will cause the power control unit to enter the "trickle charge" mode, by opening the K1 relay contacts which parallel the discharge diode and trickle current limiter.

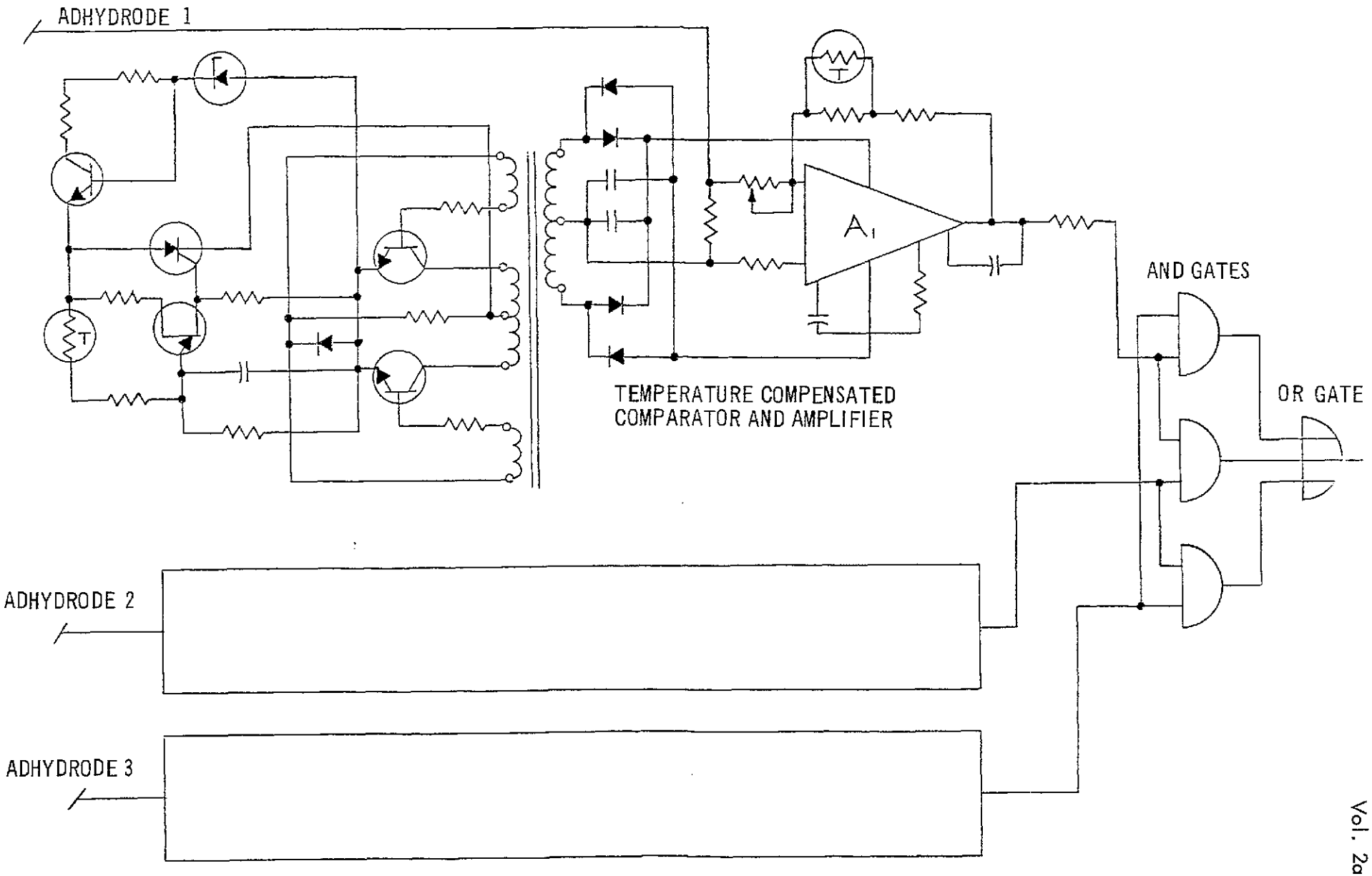

Figure 6-14 Adhydrode Charge Control Circuit

Trickle current may be limited either by the insertion of a resistance in series with the battery. The current will vary with the applied voltage and battery temperature, and will increase in the event of a single cell failure in the battery.

An active current limiter in place of the resistors will hold the current at an approximately constant level, regardless of variations in battery temperature or the number of unfailed cells, and has the following advantages:

- After reconditioning the battery to low voltages, the active current limiter prevents excessive current from flowing into the battery due to low battery voltages, thus preventing momentary undervoltage load dumping when the battery is returned to the line.

- The active current limiter has lower heat dissipation upon restoration of a low voltage reconditioned battery to the line than does the passive current limiter for a period of a few seconds.

- The active current limiter results in lower overcharge heat dissipation in the battery than does the passive limiter in the event of a single short-circuited cell.

The passive current limiter has the following advantages:

- It is lighter by approximately 0.6 lb. than the active limiter for a device of similar reliability.

- The increased overcharge current in the event of a cell failure (provided that it can be tolerated by the thermal control subsystem) tends to hold the remaining cells at a higher state of charge, at least partially compensating for the loss of stored energy. Heat dissipation on overcharge will increase from approximately .300 A x 28.2 v = 8.8 w to .500 A x 27.1 v = 12.5 watts. Neither overcharge current nor heat dissipation is excessive in the failed cell case.

- The current limiter is not essential to the charging or maintenance of charge on the batteries. An open circuit failure of the current limiter will not result directly in system failure, but will cause the trickle relay to cycle open and closed more frequently. The lack of a short-circuit failure mode in resistors therefore results in a very high reliability of the system using passive current limiting.

A comparison of the two methods leads to the conclusion that although the active limiter is more desirable from an automatic functioning standpoint, the system will function adequately with the lighter, lower cost passive limiter. Consequently the passive trickle current limiter is selected. All of the necessary commands exist for restoring loads after an undervoltage and the down time need be no longer than is required to react to an undervoltage upon returning the battery to the line. This need never occur if the batteries are not discharged below 10 volts on reconditioning. At worst, undervoltage for a period of 10 seconds twice a year will be the result.

e) Undervoltage Detector

Figure 6-15 illustrates the schematic of the undervoltage detector circuit. Functionally, the circuit provides an output to the majority voting AND Gate when bus voltage has dropped below the undervoltage level for a period of time exceeding approximately 100 milliseconds. When two of the three detectors provide a positive input, the gate provides an output.

Transistors Q1, Q2 and Q3 comprise a gain stabilized amplifier referenced to the voltage level set by reference diodes (VR1 and VR2). The output controls the complementary emitter follower transistors Q4 and Q5 which allow the time delay (C1 and R11) to operate. When the voltage on C1 forward biases Q7, the PNP-NPN bistable (Q7 and Q8) switches to the On state providing an output to the AND Gate.

6.5.2 Equipment Power Converter

The basic requirement of the equipment converter is to supply regulated 28 v and $\pm$ 5 v (both regulated to $\pm$ 3%) to a variety of equipment. Of the many possible converter designs, two were selected for a detailed tradeoff analysis. The two approaches are shown in Figures 6-16 and 6-17. The design shown in Figure 6-17 was selected since it offered the best compromise between performance, weight, size, efficiency, reliability, and producibility. It is similar to equipment already developed and space qualified.

6.5.2.1 Converter Tradeoffs

Figure 6-16 shows a dc-to-dc converter scheme where preregulation of the bus voltage is performed before inversion and output rectification. A synchronized or free-running clock oscillator can be utilized to provide drive for the inverter as well as the time base for modulating the input switching regulator. For a multiple output configuration, the sensing or control point can present disadvantages. If the highest rated load

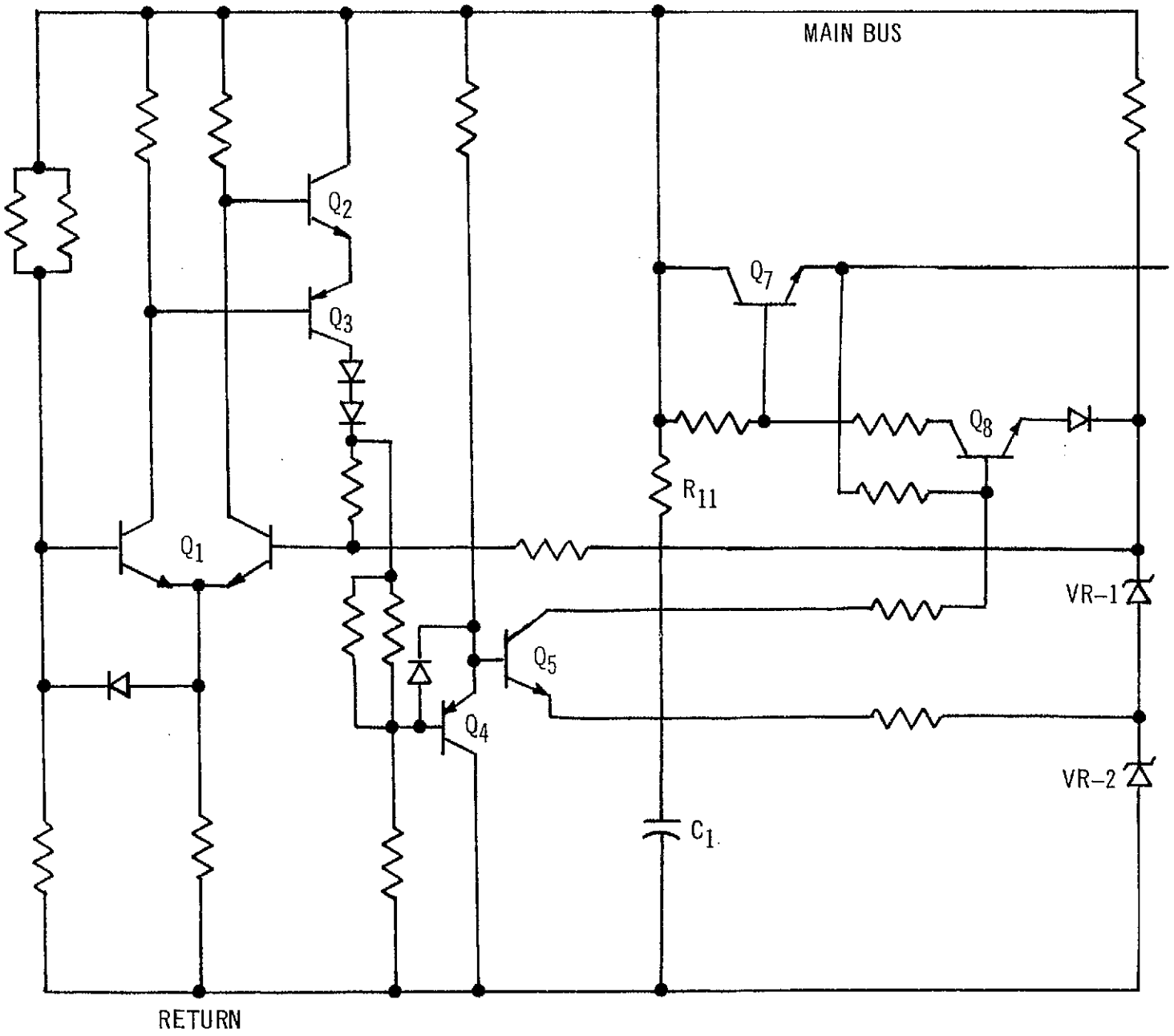

Figure 6-15 Undervoltage Detector Circuit

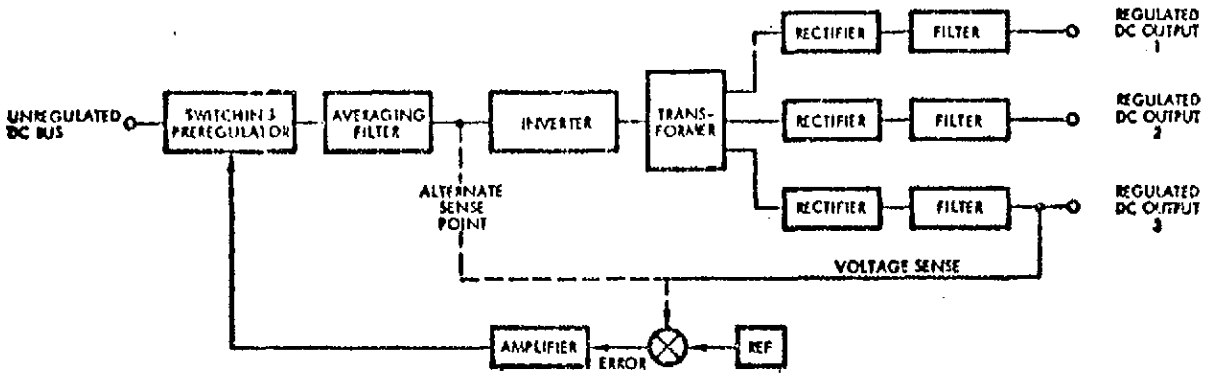

Figure 6-16 Power Conversion System, Preregulation Conversion

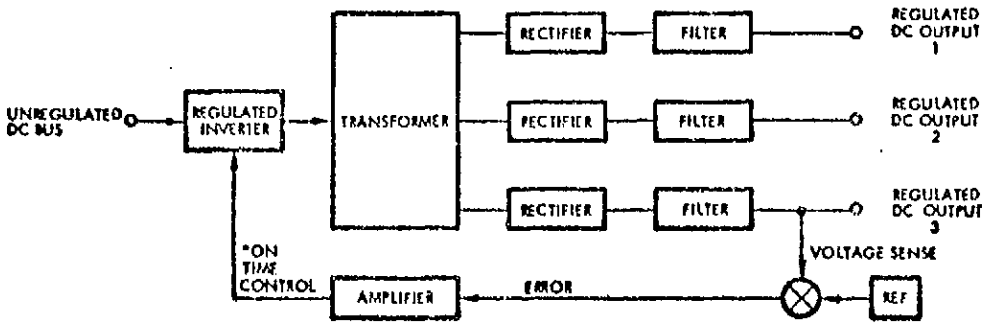

Figure 6-17 Power Conversion System, Combined Inversion and Regulation

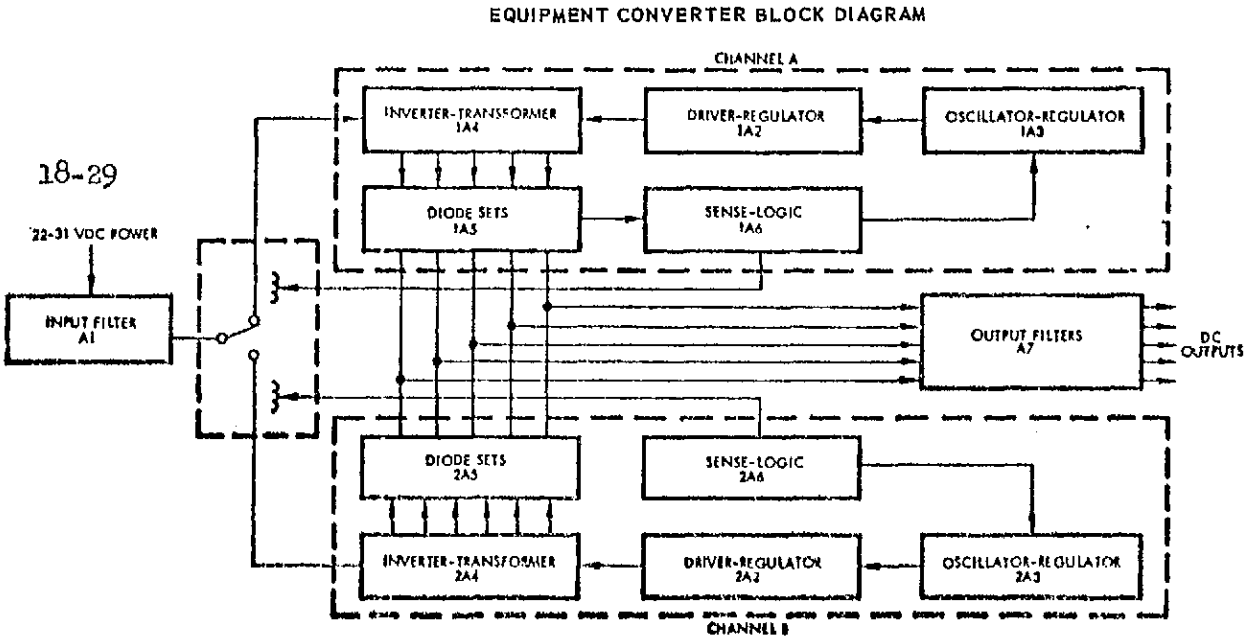

Figure 6-18 Selected Converter Design

voltage is sensed to drive the regulator error amplifier, the remaining outputs, while regulated against input line variations, will not be compensated for variations in output resulting from changing loads and temperature effects on output rectifier circuitry. An additional problem with the approach of Figure 6-16 is the loop stability compensation required because of the additional filter within the regulating loop. If the sense point is provided at the regulator output, load regulation is not provided at any dc output. A further disadvantage in this scheme, especially at high power levels, is that the preregulator must handle all the input power. Efficiency suffers in that power is lost in two series switching elements, the preregulator transistor switch and inverter switching element. The averaging filter requirements also become severe at higher power levels, with a consequent penalty in size, weight and efficiency.

Another scheme for multiple-output, dc-to-dc conversion, is shown in Figure 6-17. Regulation is accomplished within the inverter stage by means of pulse-width control of the inverter base drive. This arrangement has 15% higher efficiency than the configuration of Figure 6-16, primarily because the regulator is not an inline function in the power flow path. Other advantages are the relative circuit simplicity and easily controlled loop stability. Loop response again suffers in comparison with dissipative regulators. The disadvantages related to sensing with multiple outputs also apply in this case. Output rectifier filter requirements are increased in comparison to the previous cases because the inverter output is a variable-width chopped square wave. The worst case occurs with a high input line condition and light load.

6.5.2.2 Functional Description of Selected Converter

The converter consists of a high efficiency (93%) regulator-inverter system followed by the rectifier-filter functions with virtually all of the losses due to fixed silicon diode voltage drops associated with the low output voltage requirements.

Figure 6-18 illustrates the dual channel design of the converter. Part redundancy is maintained in the input filter module (A1) and the output filter module (A7). These are L-C type filters using small dissipative resistors and multiple tantalum capacitors. The resistors minimize surge currents, provide damping in the vicinity of cutoff frequency, and act as fuses in the event of a capacitor short-circuit failure. Inductors at low voltage levels are not used in a part redundant manner. The remainder of the converter has a simple high-efficiency arrangement. Regulation is achieved by maintaining a constant volt-second integral waveform into the multiple secondary output transformer (A4) supplying power to the conversion rectifiers (A5) and then to the output filters (A7).

The circuit operates as follows: The power relay contacts following the input filter (A1) favor one channel, say "1" as shown. A special winding on each output transformer (A4) produces a small amount of power to operate a differential amplifier in the oscillator-regulator module (A3). This power is filtered in the sense-logic module (A6) and also charges an energy storage capacitor associated with a unijunction transistor (in A6) and input power relay winding. The voltage from this special winding is proportional to the volt-second integral produced by the inverter output transformer.

The differential amplifier drives a series control transistor with the amplified error after comparison to a reference diode.

Excitation from the oscillator-regulator (A3) drives an amplifier in the driver-regulator (A2) which, in turn, drives the bases of the inverter (switching) transistors in (A4). A timing circuit in (A2) shuts off the drive to the bases of the inverter transistors. The regulating loop is then from the inverter-transformer (A4), through the sense-logic (A6), to the oscillator-regulator (A3), to the driver-regulator (A2) and back to the inverter-transformer (A4).

A failure in the operating channel will remove the power to the sense-logic module (A6), or at least lower it. A unijunction transistor in this module will then "fire", discharging the energy storage capacitors through a winding of a power switching relay. The impulse causes the latching relay to switch to the alternate position, thus energizing the remaining good channel.

A modularized packaging approach will be used in the equipment converter. Groups of parts are assembled in cordwood fashion with welded interconnections.

6.5.3 Battery

The battery assembly contains 20 nickel-cadmium cells of 12 ampere hour capacity and associated hardware. The battery will operate at a nominal 5.5 amperes (9 amperes maximum) while supplying 22 to 30 volts.

The battery probability of success has been based upon the following demonstrated life capabilities:

- Nickel-cadmium cells on test by TRW Systems have operated for more than six years. Over 200 cells have been in continuous laboratory use for over four years and more than 300 cells have

been in use for over three years without apparent degradation. Failures due to manufacturing defects on early cells have been eliminated through enforcement of rigid specifications in the vendor's facility during production and at TRW Systems. No failures have been observed on cells passing TRW acceptance tests.

- A total of 60 Vela and 33 OGO nickel-cadmium batteries have been built and tested to date at TRW. Batteries not flown are alternately cycled and trickle charged. The age of currently active batteries in the laboratory ranges from 1 to 5 years. One battery failure occurred early in life due to a divergent cell. As a result of this failure, cell matching procedures were improved and no failures have occurred since.

- Mission profile tests have been conducted at TRW Systems on nickel-cadmium cells and batteries at environmental and orbital extremes since 1962. No failures have occurred during these tests. Output capacity of properly reconditioned batteries has not decreased appreciably during life.

A separate resistive load is provided for reconditioning the battery in orbit. Reconditioning is needed to restore capacity lost during repeated cycling and to bring individual cells into balance. At least one reconditioning cycle is desirable before each eclipse season. The reconditioning resistor is located on the spacecraft central cylinder and is commanded "on" through the PCU.

The battery has a mechanical design identical to a battery presently in use on a military satellite program with electronic circuitry and cell protection circuits identical to those used on Intelsat III.

The battery assembly consists of the following major components:

- Cell Pack

  20 Nickel-Cadmium, 12 ampere-hour, hermetically sealed cells in an aluminum restraining structure.

- Battery Electronics

  Temperature sensing and logic circuitry which signals excessive battery temperature.

  Cell-reversal protection circuitry which shunts discharge current around a fully discharged cell.

- Thermistors

  Three thermistors used in conjunction with logic circuitry to compensate battery auxiliary electrode voltage limit; one thermistor used to provide telemetry.

- Recondition Resistor

  Mounted separate from the battery. Used to recover battery capability loss due to normal cycling.

The cell pack structure functions to restrain the cell under normal conditions of internal pressure and provides support against handling and launch vibration, shock and acceleration. It also conducts heat from the cells and electronics to the spacecraft equipment platform. By utilizing temperature-compensated charge control and cell-reversal protection, internal cell pressures can be kept well below 50 psi. This permits use of a lightweight restraining structure.

The temperature sensing and logic circuitry are mounted on circuit board assemblies on the battery and provide a signal to the power control unit (PCU) when battery temperature exceeds a preset limit. Temperature is sensed at the top of three cells (normally the hottest external portion of the cell). Signals from any two of the three sensors will cause a majority voting circuit to produce an output signal to the PCU. On receipt of a high temperature signal, the PCU reduces the charge level to a low rate, which in turn reduces the internal heat generation rate to a low level, resulting in battery cool-down.

Cell reversal protection is required to increase the probability of successful battery performance over a 5-year period. Protection of individual cells is necessary in applications requiring high reliability and long life because of the individual cell failure rate level and divergence of characteristics with age and cycling. The reversal protection circuit protects individual cells from being force-discharged because of low capacity. When an individual cell voltage falls below zero volts, the discharge current is shunted through a transistor circuit. Pressure build-up due to gas evolution on cell-voltage reversal is thus minimized. In addition, if a cell is open circuited, the reversal bypass circuit will permit current to flow during discharge.

7. SOLAR CELL ARRAY

7.1 INTRODUCTION

A solar array design study was performed to meet the power requirements defined in Section 6 for a mission life of 5 years. In order to produce an optimum design, a number of important parameters were examined such as:

- o Cell thickness
- o Cell base resistivity
- o Cover glass thickness
- o Charged particle degradation
- o Cost
- o Assembly methods
- o Total Array weight
- o Total Array area
- o Total Array power

In addition to these factors, the study considered the problems associated with operating in a low temperature environment during eclipse and array degradation due to low energy protons.

After trading off all these factors, an optimum solar array was designed, whose summary specification is contained in Table 7.1.

The following sections contain a discussion of the tradeoffs leading to the selected design.

7.1.1 Assumption and Limitations

The spacecraft is to be launched in late 1971. The 5 year, end of mission, equinox power requirement is 264 watts with the possibility of extending the mission to 7 years at a lower power level. The bus voltage of 29 volts dc is not to be exceeded during the mission. The array is to be body mounted to a cylindrical spinning spacecraft which is 56 inches in diameter and 79 inches long. At the solstice seasons the sun angle is 66.5°. No shadows are expected to fall on the array from the spacecraft or associated equipment.

7.2 TRADEOFF ANALYSIS

The tradeoff studies performed include:

- o Basic cell electrical parameters of candidate cells
- o Solar cell performance degradation due to time independent factors, time dependent factors, and temperature.

TABLE 7.1

SOLAR ARRAY SPECIFICATION

Cells:	
No. of cells	20,480
Cell Type	n/p
Cell Size	2 x 2 cm
Base resistivity	2 ohm-cm
Cell Thickness	.010"
Efficiency:	10.75% min. at AMO, 28°C
Covers:	
Thickness	.006 Silica
Filter	.410 micron blue
Coatings	Anti-reflective and UV reflective
Adhesive	XR6-3489 Dow Corning Silicone
Interconnects:	Thin solder
Material	Kovar
Redundancy	Triple
Module Design	2 parallel X 4 Series (2P x 4S)
Total Weight	52.4 lbs

Output Power (minimum)

	0 Years	5 Years
Equinox	329	263
Summer Solstice	313	252
Winter Solstice	294	240

- o Power-to-mass and power-to-area ratios for candidate cell and cover combinations.
- o Cost consideration

7.2.1 Basic Cell Electrical Parameters

Reference 1 establishes the parametric AMO, 28°C data for 2 x 2 cm, N on P, silicon solar cells of both 2 and 10 Ω-cm base resistivities and of various thicknesses. Candidate cell thicknesses for this analysis are 0.008, 0.010, and 0.012 inches. These data (average values) are tabulated in Table 7.2 and plotted in Figures 7.1 and 7.2. The 20°C operating temperature is the end of mission temperature predicted by thermal analysis for the equinox seasons. The time independent degradation factors shown in table 7.2 are based on extensive TRW Systems experience with Pioneer, Intelsat III and similar programs over the past several years. The module assembly losses are for assembly by resistance soldering techniques in use at TRW.

7.2.2 Performance Degradation Due to Environment and Equivalent 1 MEV Fluence

7.2.2.1 Radiation Environment

This section discusses the time dependent degradation factors and establishes the equivalent 1 Mev fluence levels for the mission.

Figures 7-3 and 7-4, from reference 3, show respectively:

7-3 The fact that a spacecraft launched after mid-1971 will have a 5 year mission during the minimum solar activity period.

7-4 The equivalent 1 Mev fluence levels for various cover slide thickness due to the trapped electron environment at synchronous altitude.

The various radiation environments considered are as follows:

Transfer Orbits. Based on a maximum of 12 transfer orbits, the total equivalent flux at the active surface of the cell is expected to be 0.18×10^{13} 1 Mev e/cm^2.

Synchronous Equatorial Orbit. The equivalent 1 Mev fluence which is expected during five years in orbit is 2.0×10^{14} 1 Mev e/cm^2, for cells with 0.006 inch covers. This number is based upon the environment shown below.

Cell	Unit Type	2 x 2 cm, N/P, 2 Ω - cm						2 x 2 cm, N/P, 10 Ω - cm					
Cell Thickness	Inches	0.008		0.010		0.012		0.008		0.010		0.012	
Cover thickness	"	bare	0.006	bare	0.006	bare	0.006	bare	0.006	bare	0.006	bare	0.006
Cell temperature	°C	28	20	28	20	28	20	28	20	28	20	28	20
V_{oc}	mV	578	589	582	593	587	598	542	554	550	562	553	565
V_{op}	mV	479	489	482	495	484	496	430	444	434	448	437	451
I_{op}	mA	120	110	122	112	124	115	124	114	129	119	131	121
I_{sc}	mA	125	115	128	118	131	121	133	123	138	128	110	129
P_{op}	mW	57.4	53.9	58.9	55.5	9.6	57.1	53.2	50.7	55.9	53.4	57.0	54.5
η	%	10.8	10.2	11.1	10.5	11.25	10.75	10.0	9.56	10.5	10.0	10.8	10.25
β	mV/°C	-2.2		-2.2		-2.2		-2.3		-2.3		-2.3	

Degradation factors (time-independent)

I_{sc}	Assembly	0.970
	Filter	0.975
	Mismatch	0.980
	Temp. cycling	0.985
	Total	0.923
V_{oc}	Assembly	0.99
	Temperature coefficients - β	

Table 7-2 - 2 x 2 cm, N on P, Silicon solar cell. AMO performance parameters for bare cells and for assembled cells which include current and voltage time-independent degradations

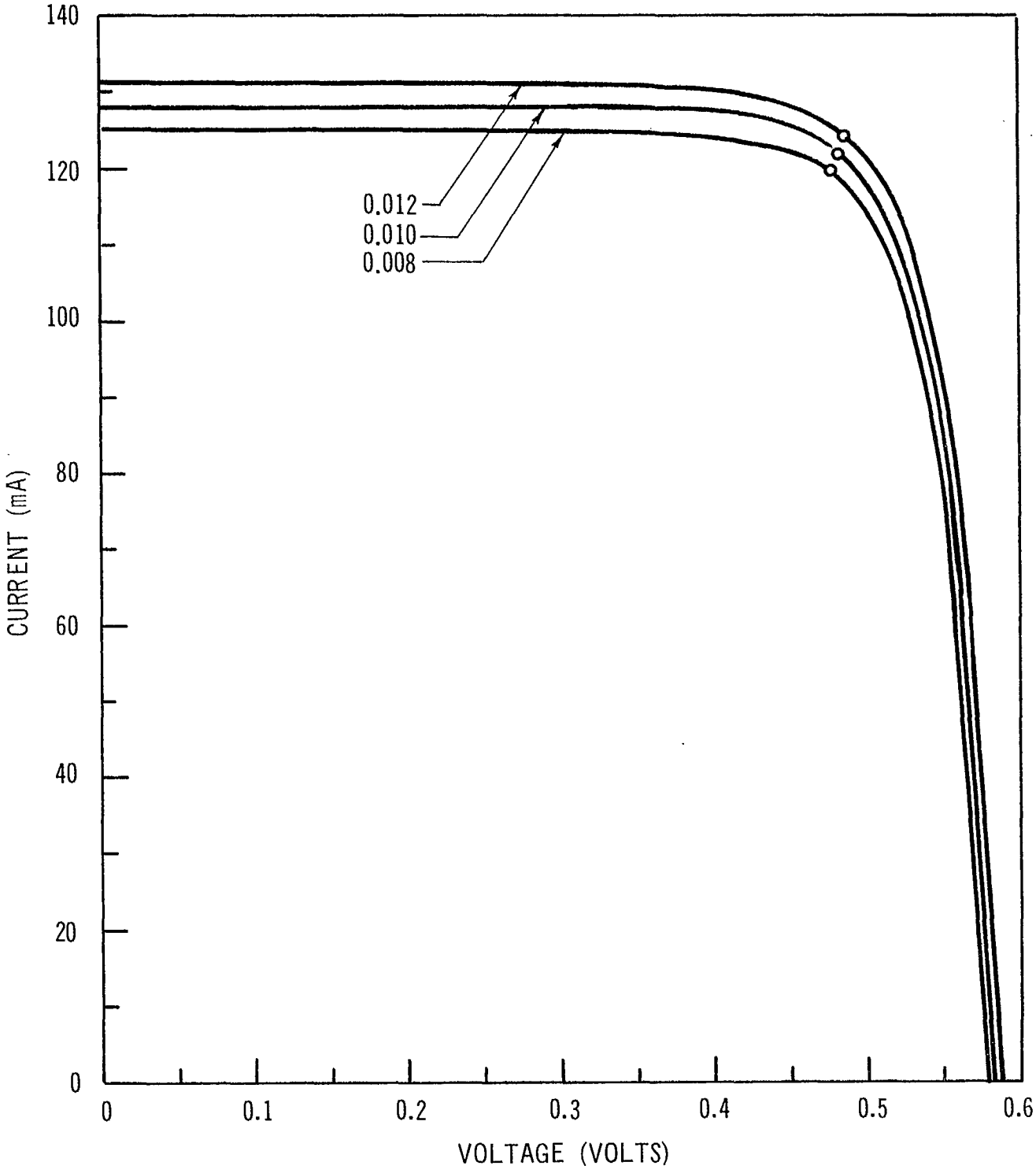

Figure 7-1 Initial (BARE) 2 x 2 cm, 2 Ohm/cm Solar Cell AMO, 28°C IV Characteristics. (Average)

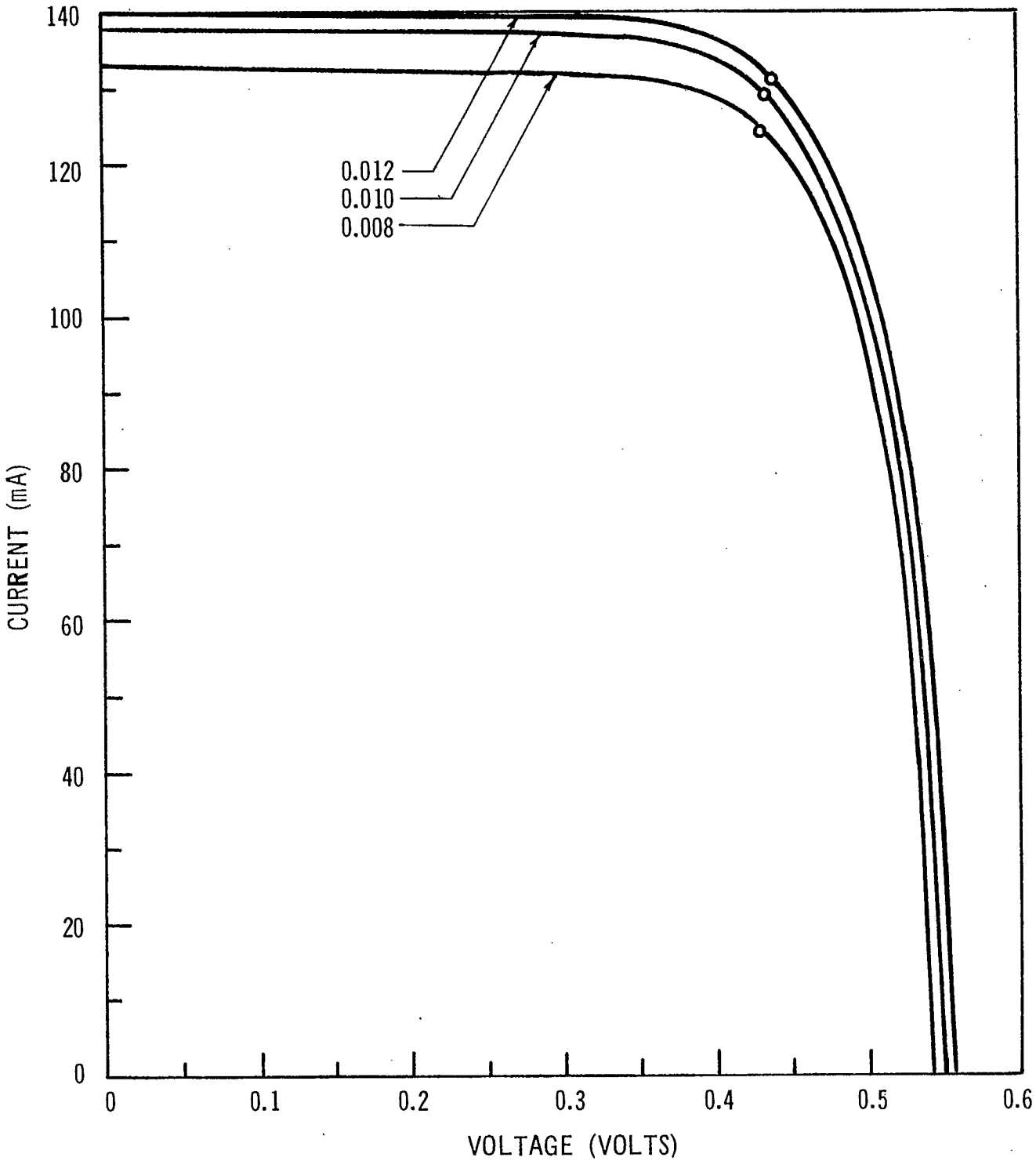

Figure 7-2 Initial (BARE) 2 x 2 cm, 10 Ohm/cm Solar Cell AMO, 28°C IV Characteristics. (Average)

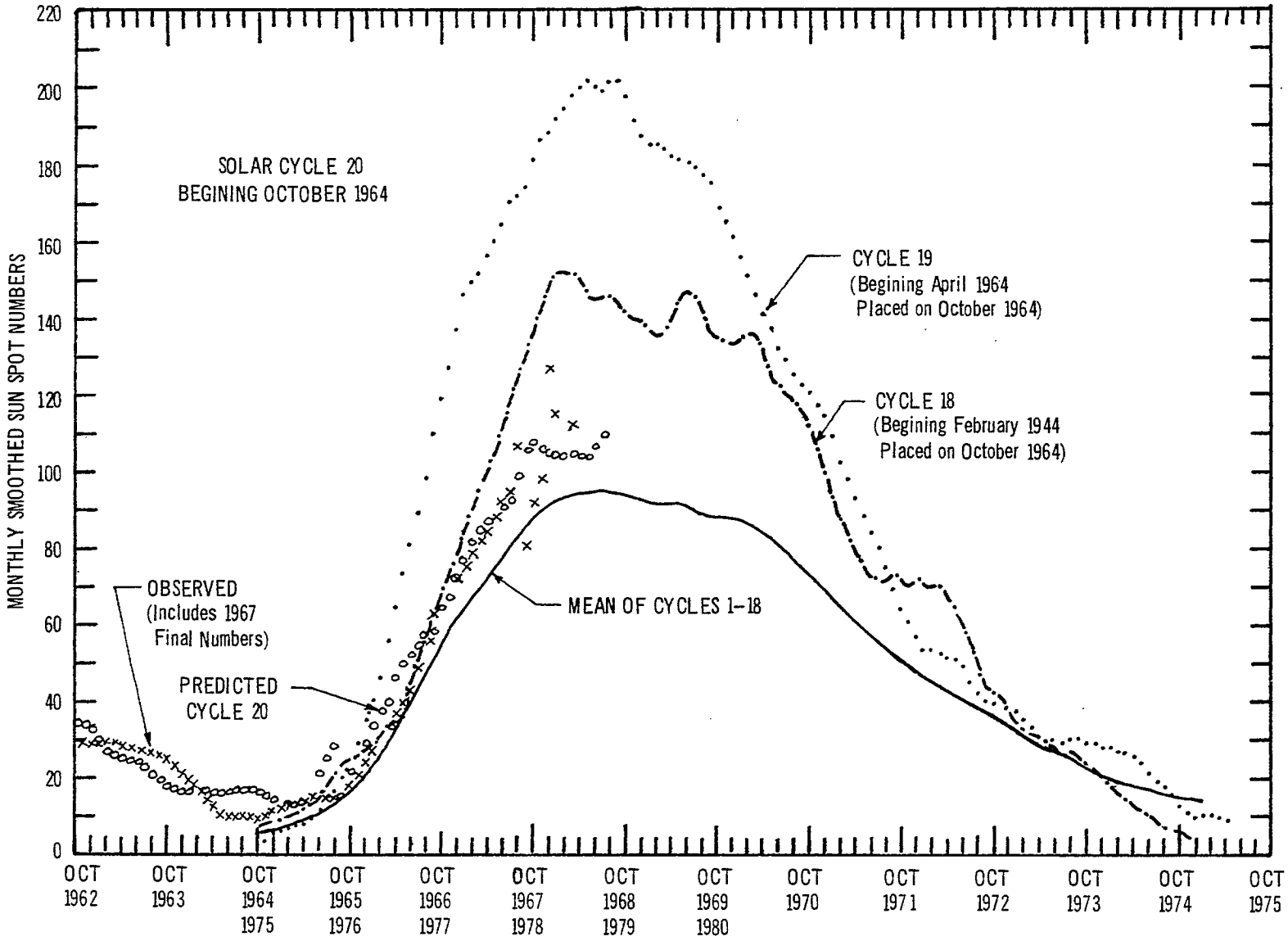

Figure 7-3 Sun Spot Numbers for Several Solar Cycles Based on Reference O

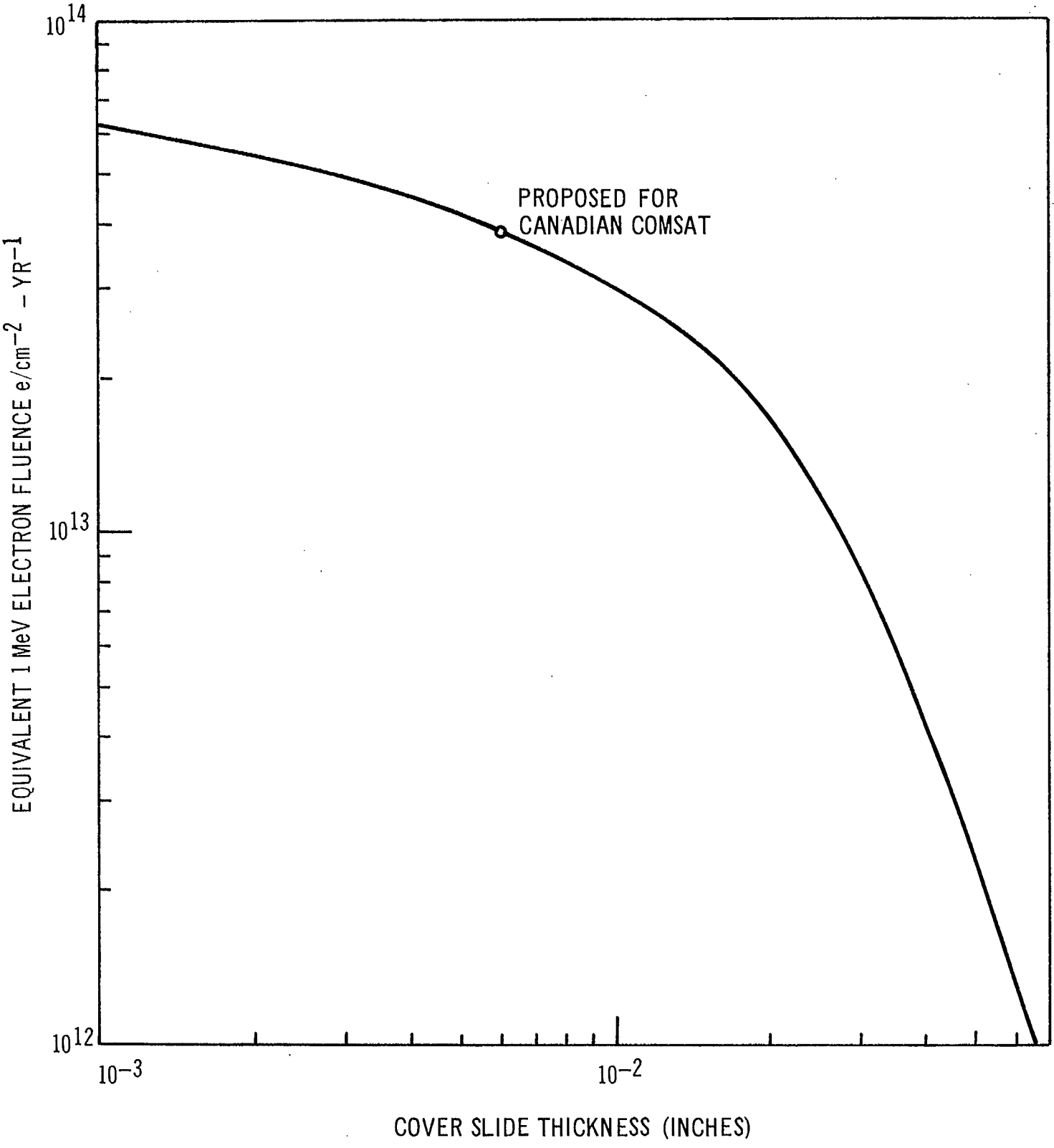

Figure 7-4 Equivalent 1 MeV electron fluence per year for solar cells, corresponding to the trapped electron environment at synchronous equatorial orbit as a function of cover thickness (Ref. 1)

Trapped Electrons - The trapped electron environment in a synchronous equatorial orbit has the following time-averaged integral flux spectrum:

$$0.05 \leq E \leq 0.5 \text{ Mev: } \phi_e\ (>E) = 7.96 \times 10^5 E^{-1.56} (e.cm^{-2}.sec^{-1})$$

$$0.5 \leq E \leq 4.0 \text{ Mev: } \phi_e\ (>E) = 1.02 \times 10^7 \exp(-2.9E)\ (e.cm^{-2}.sec^{-1})$$

The flux represents the number of electrons per cm^2 per sec above energy E where the units of E are Mev. The total flux is 2.0×10^8 $e.cm^{-2}.\ sec^{-1}$ (E>0). The equivalent 1 Mev flux at the cell is 4.0×10^{13} $e.cm^{-2}$ in one year, for cells covered by 0.006 inch thick quartz.

Trapped Protons - The trapped proton environment has the following time-average integral flux spectrum.

$$0.1 \leq E \leq 4.0 \text{ Mev: } \phi_p\ (>E) = 2.09 \times 10^7 \exp(-9.09E)\ p.cm^{-2}.sec^{-1}$$

The total flux is to be taken as 2.0×10^8 $p.cm^{-2}.sec^{-1}$ (E>0). The equivalent 1 Mev flux is negligible, provided that the entire solar cell is protected from low energy protons.

Solar Flare Particles - The total fluence of solar protons is considered to be negligible due to the 1971 launch date which as shown in Figure 7-3 corresponds to the minimum solar flare activity period of the cycle. (Reference 3)

The total equivalent 1 Mev fluence is therefore 4.18×10^{13} $e.cm^{-2}.yr^{-1}$ or 2.03×10^{14} $e.cm^{-2}$ for the five year mission when using 0.006 inch thick coverslides. This value reduces to 2.8×10^{13} $e.cm^{-2}.yr^{-1}$ if 0.012 inch covers are used.

7.2.2.2 Radiation Dependent Losses

Radiation damages the solar cell in such a way to cause both short-circuit current and open-circuit voltage degradation. The equivalent 1 Mev fluence values assume 0.006 inch thick fused silica cover glass protection for the entire active solar cell area.

a) Short-circuit Current and Open-circuit Voltage Degradation
The radiation loss factors for short-circuit current and open-circuit voltage considered to be most probable are based on data in Reference 1.

b) Angle of Incidence Effects due to Radiation

Because the solar array is cylindrical in shape, solar cells are simultaneously subjected to illumination at various angles of incidence. The short-circuit current from solar cells is not exactly proportional to the cosine of the angle of incidence. This relationship between short-circuit current and the angle of indicence is dependent on the cut on wavelength of the ultraviolet reflective filter on the cell coverslide and on the amount of charged particle radiation to which the cell has been subjected. The loss factor for this effect is 0.990 (approximately -1% of short-circuit current). The data upon which the angle of incidence factors are based are found in Reference 13.

The output current from the solar cells is reduced by the cover slide installation and is a function of the cut-off wavelength of the ultraviolet filter. In the calculation, an initial cover transmission factor of 0.975 has been used. For the type of solar cells to be used in the array, TRW Systems tests have shown that this factor corresponds to a filter cut-off wavelength of 0.410 micron. Charged particle irradiation causes the spectral response to shift to shorter wavelengths, causing a relative increase in the part of the cell response which is eliminated by the ultraviolet reflective filter. However, for the 24-hour orbit, this effect is negligible even after 5 years in orbit.

7.2.2.3 Micrometeorite Degradation

With respect to degradation to be anticipated from micrometeorites, experiments have been flown on various spacecrafts and measurements have been made of the particle momentum, kinetic energy, and mechanical impact damage, utilizing various sensors and detectors. Data accumulated from numerous experiments has allowed the plotting of particle mass versus influx rate. (W.M. Alexander, C.W. McCracken, L. Secretan, and O.E. Berg, "Review of Direct Measurements of Interplanetary Dust from Satellites and Probes," NASA Technical Note D-1669, May 1963.) Ninety percent of the meteorites are expected to be in the extremely low density range of 0.44 g/cm^3, 9 percent at about 3.5 g/cm^3 and 1 percent at approximately 8.0 g/cm^3. This distribution is for a meteorite mass of 10^{-9} or greater and of an average velocity of 99,000 ft. per second. Having obtained estimates from the micrometeorite flux, a common denominator is required to relate the damage of a glass-covered solar cell to a given flux, mass, diameter, and velocity of micrometeorites. To this end, some general guidelines have been derived from experimental data on particle bombardment of solar cells, which indicate a need to provide protection.

The results of bombarding Corning Glass Works fused silica Type 7940 and Microsheet Type 0211 with glass spheres 75 and 35 microns in diameter at velocities from 41,500 to 99,000 feet per second have been evaluated for over 250 impacts. (John A. Fager, "Effects of Hypervelocity Impact on Protected Solar Cells," AIAA Paper No. 65-289, July 1965.) The effects of this test were cratering at the impact points and crazing around the craters in the form of fissuring in the adjacent material. At the higher velocities, increased cover thickness appeared to reduce cratering, but increased the crasing. This test indicated that 0.006 inch covers could adequately protect cells for prolonged periods against micrometeorite impact with little effect.

In order to provide a design allowance for the reduction in solar cell power output due to cratering of the cover slides and erosion of the anti-reflective coatings of the exposed glass surface, an allowance for short-circuit current reduction has been made in the array performance calculations.

7.2.2.4 Additional Factors

The effect of the angle of incidence on the output characteristics of silicon solar cells and the change of this effect due to charged particle irradiation has been treated in detail (Luft, op.cit.). The relative short-circuit current values used in the array performance calculations are based on this previous work.

Allowances were made for loss in adhesive transparency due to charged particle irradiation and due to ultraviolet irradiation. An additional margin for random cell failure losses has been included. Each of these factors is shown in table 7.3 for four periods during the mission. For the effect of cover thickness and cell thickness, however, only the solar cell normal to the sun line has been considered. Spacecraft configuration has been included in the total array performance calculation presented later.

Figures 7-5 and 7-6 show how the various cell types, thicknesses and cover combinations are expected to perform at various times during the mission. The same charged particle fluence and degradation factors were assumed for both cell types for comparison purposes.

When reviewing the data of figure 7-5 and 7-6 it is shown that for both cover thicknesses there is no significant difference in cell power output at the end of the mission for either base resistivity or cell thickness. The 2 Ω -cm solar cell does, however, show a slightly (1%) higher output. The crossover point between 2 and 10 Ω cm cell performance superiority occurs between 7 and 10 years depending on cover thickness used.

Table 7-3 Total Solar Cell Performance Degradation (Including Time Dependent, Time Independent and Temperature Effects) for Time Periods During the Mission, for a Single Solar Cell at AMO, 20°C Covered with Either 6 or 12 Mil Covers

	Year	0		1		3		5	
	Fluence	0	0	4×10^3	2.8×10^{13}	1.2×10^{14}	8.4×10^{13}	2×10^{14}	1.4×10^{14}
	Cover Thickness (inches)	0.006	0.012	0.006	0.012	0.006	0.012	0.006	0.012
	Micrometeroids			0.990	0.990	0.987	0.987	0.984	0.984
	Adhesive and Cover (U.V.)			0.991	0.987	0.990	0.985	0.989	0.984
	Adhesive and Cover (Rad)			0.984	0.987	0.974	0.977	0.968	0.972
	Chromatic Shift (Rad)			0.9979	0.9982	0.996	0.9964	0.9950	0.9959
	Random Failure			0.997	0.997	0.991	0.991	0.983	0.983
	Subtotal			0.96	0.959	0.94	0.936	0.922	0.921
2 ohm-cm cells	I_{Sc} (Rad) 8 Mil	115	115	112.1	114.0	107.9	109.6	104.9	106.8
	MA 10 Mil	118	118	114.0	114.8	108.6	110.5	105.6	107.9
	(1) 12 Mil	121	121	114.8	116.4	109.3	111.3	105.6	108.3
	V_{oc} (Rad) 8 Mil	589	589	560	564	548	553	541	546
	(mV) 10 Mil	593	593	560	564	548	553	541	546
	(1) 12 Mil	598	598	560	564	548	553	541	546
	8 (mA) I_{sc}	115	115	107.5	109.5	101	103	96.6	98.3
	Mil (mV) V_{oc}	589	589	560	564	548	553	541	546
	(2) (mW) P_{op}	53.9	53.9	46.7	48.9	43.5	44.7	40.7	42.2
	10 (mA) I_{sc}	118	118	109.5	110	101.5	103.5	97.3	99.4
	Mil (mV) V_{oc}	593	593	560	564	548	553	541	546
	(2) (mW) P_{op}	55.5	55.5	48.5	48.7	43.5	44.6	41.1	42.4
	12 (mA) I_{sc}	121	121	110.0	111.5	102	104.5	97.3	99.2
	Mil (mV) V_{oc}	598	598	560	564	548	553	541	546
	(2) (mW) P_{op}	57.1	57.1	48.4	49.0	43.7	44.9	40.8	42.5
10 ohm-cm cells	I_{sc} (Rad) 8 Mil	123	123	120.8	121.2	117.0	118.9	115.1	117.0
	(MA) 10 Mil	128	128	122.7	123.1	119.7	120.8	116.7	118.9
	(1) 12 Mil	129	129	125.4	126.5	120.5	122.0	117.4	119.7
	V_{oc} (Rad) 8 Mil	554	554	532	535	524	528	519	523
	(mV) 10 Mil	562	562	535	537	525	530	520	525
	(1) 12 Mil	565	565	537	540	526	531	520	526
	8 I_{sc} (mA)	123	123	115	116	109.5	111.5	106	107.5
	Mil V_{oc} (mV)	554	554	532	535	529	528	519	523
	(2) P_{op} (mW)	50.7	50.7	45.7	45.8	43.0	43.8	40.5	41.5
	10 I_{sc} (mA)	128	128	118.0	118.5	112.0	113	107.5	109.0
	Mil V_{oc} (mV)	562	562	535	537	525	530	520	525
	(2) P_{op} (mW)	53.4	53.4	46.3	46.3	43.5	43.8	40.6	41.8
	12 I_{sc} (mA)	129	129	120	121.5	113	114	108	110.0
	Mil V_{oc} (mV)	565	565	537	540	526	521	520	526
	(2) P_{op} (mW)	54.5	54.5	47.4	46.8	43.4	44	40.5	42.2

(1) Includes only fluence and time independent degradation.

(2) Includes total degradation (product of (1) and subtotal above).

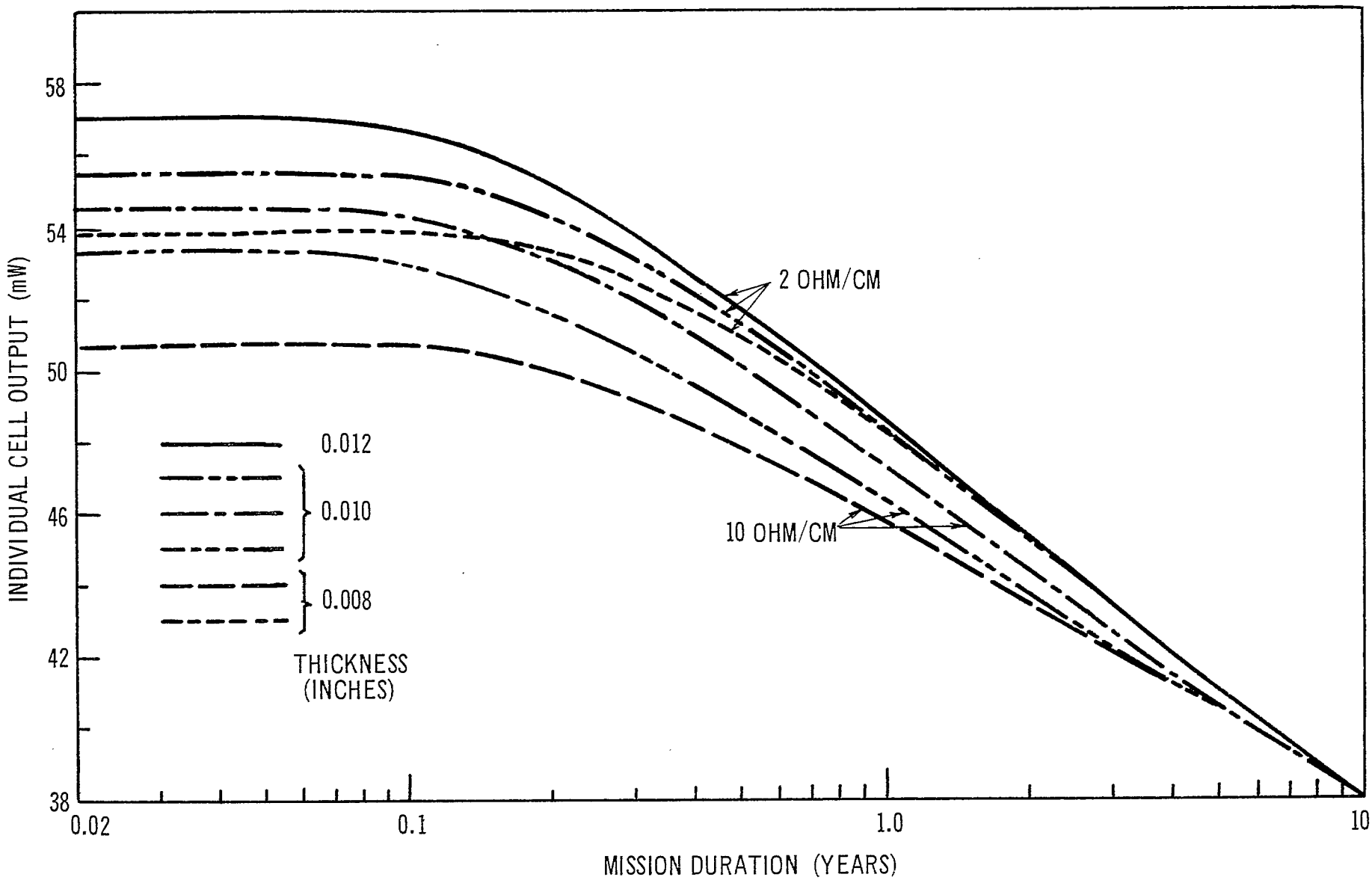

Figure 7-5 Solar cell output versus mission duration for 1 and 10 Ω/cm cells of various thicknesses having 0.006 inch covers and at AMO, 20°C (considers only the cell normal to sun line at equinox)

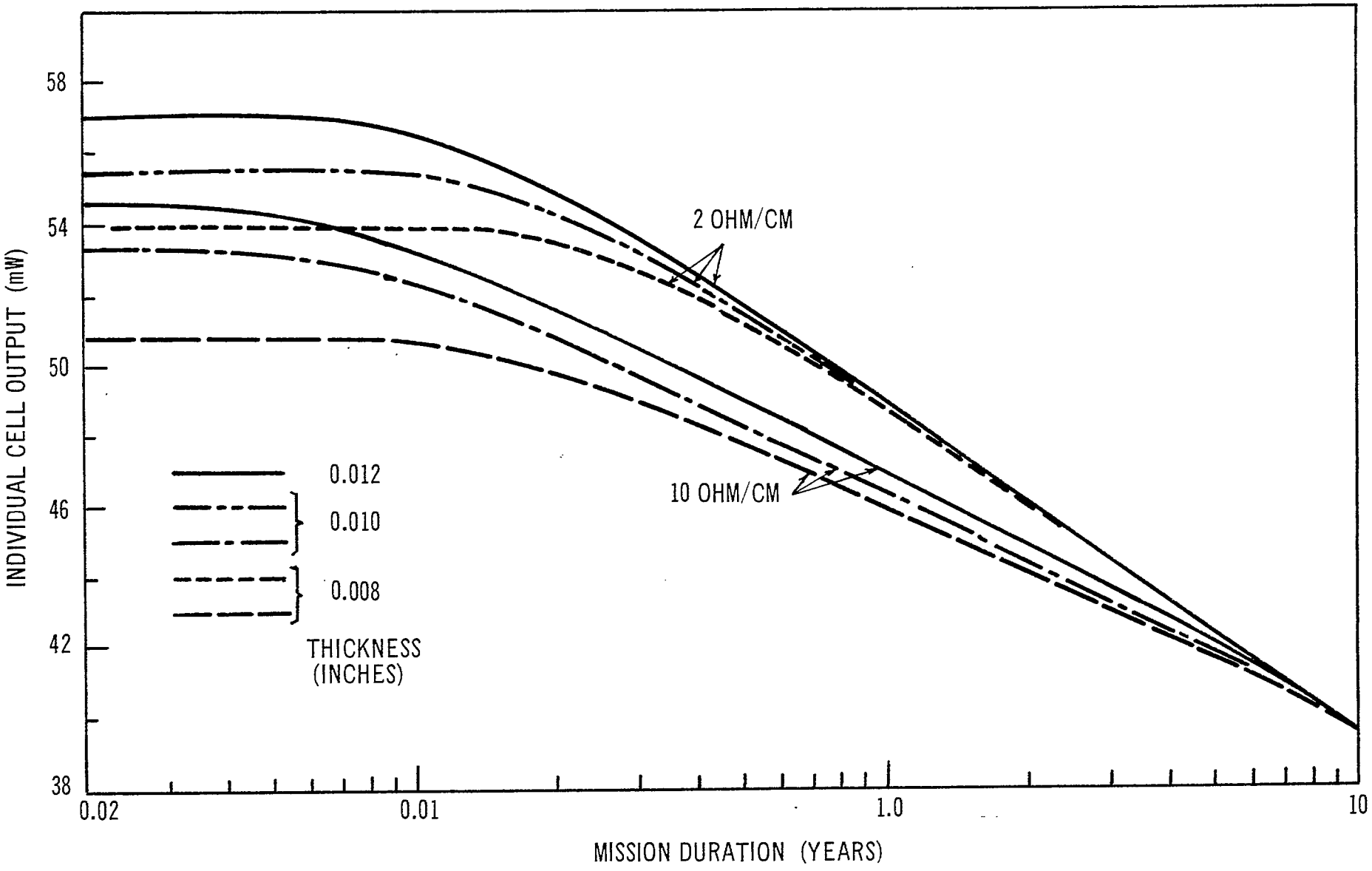

Figure 7-6 Solar cell output versus mission duration for 2 and 10Ω/cm cells of various thicknesses having 0.012 inch covers and at AMO, 20°C (considers only cells normal to the sun line at equinox½

7.2.3 Candidate Array Power to Mass and Power to Weight Ratios

One area of prime interest is the array weight. The array diameter is fixed and preliminary analysis established a realistic length as discussed earlier.

Figure 7-7 presents the average weight versus thickness for coverslides and solar cells of the type proposed for this mission. Other weight data considered includes those items in table 7-4. Table 7-5 summarizes the weight analysis for an array capable of supplying 264 watts at the end of mission. The voltage losses due to isolation diodes was not included here. However, these losses have been included in the detailed performance analysis described later and are the same for both cell types.

It can be seen in table 7-5 that power to mass ratios are, as might be expected, higher for cells covered with 0.006 inch thick covers rather than for 0.012 inch thick covers. There is also a net wieght savings of 6.5% (11% weight savings less 3.5% power loss) for 6 mil versus 12 mil covers. Figure 7-8 shows how the array weight changes with cover thickness for the end of mission conditions. Cover slides thinner than 0.006 inches are not considered cost effective at this time due to increased attrition from handling and assembly. Since there is no significant increase in power output at the end of mission with increase in cell thickness, initial preference is to select 0.008 inch thick cells (this thickness is considered the practical lower limit on cell thickness today for manufacturability of arrays). However, it should be noted that cell attrition (as with covers) increases with decrease in thickness. At this time, TRW Systems has considerable experience using 0.010 inch thick cells and considers their use desirable from a producibility view point.

7.2.4 Cost

From the cost aspect, a 2 Ω-cm solar cells allow a savings of 5%, for the same cell thickness as that of a 10 Ω-cm cell. For this mission which requires some 20,480 cells this is significant. Similarly, for coverslides, 0.012 inch thick covers are nearly double the cost of 0.006 inch covers for a very small increase in performance. Based on these two factors the 0.010 inch thick, 2 Ω-cm, solar cell covered by 0.006 inch fused silica appears to be the optimum selection for this mission. Cost estimates from one supplier indicate that, at this point in time, 0.008 inch thick solar cells to be 50% to 100% higher in cost than are 0.010 inch thick cells.

7.3 Solar Array Design Considerations

TRW Systems background and experience in the successful design and assembly of solar arrays is quite extensive. Programs using TRW designed arrays include:

Table 7 - 4. Prelinary Mass Breakdwon for Solar Array Electrical Components

Components	Qty.	Unit Mass (Grams)	Total Mass (Grams)
Cell	8	0.285	2.280
Cover glass	8	0.135	1.080
Cover glass adhesive	8	0.032	0.256
Substrate adhesive	8	0.030	0.240
Dual cell interconnector	9	0.012	0.108
Positive interconnector	3	0.016	0.048
Negative bus	1	0.016	0.016
Total			4.028
Module weight = 4.028 gm = .00888 lb.			

Array (excl. Substrate)			
Item	Qty.	Unit Mass (lb.)	Total Mass (lb.)
8 Cell Module	2,560	0.00888	22.73
Pos. Feedthrough	320	0.000124	0.04
Neg. Feedthrough	160	0.0000876	0.01
Diodes	320	0.000606	0.19
Connector	16	0.020	0.32
Terminals	880	0.00014	0.12
Terminal board	16	0.0135	0.22
Terminal board insulator	16	0.00225	0.04
No. 28 wire	1,680 ft.	0.00092 lb/ft	1.55
No. 24 wire	416	0.002 lb/ft	0.83
Feedthrough insulator	16	0.0056	0.09
RF shield	16	0.121	1.94
Misc. solder	16	0.100	1.60
Total			29.68

Total Elec. Pwr. = 29.68 lb.
Substrate = 27.7 lb.
Total Array = 52.4 lb.

Total (each panel) = 3.27 lb.

Table 7-5. Solar Array Weight Analysis Summary for 2 x 2 cm, N on P, 2 Ω - cm Solar Cells at AMO, 20°C 5 Year EOM Performance

Cell Thickness (Inches)	Cell Performance at EOM 20°C (MW)	Cells used per S/C (fixed)	Array Area ($ft.^2$ fixed)	Structure (lb) (fixed)	Misc. Elec. (lb) (fixed)	Adhesive & Pieceparts (lb)(fixed) 0.1069 in./cell	Covers (lb) 0.006 (inch)	Covers (lb) 0.012 (inch)	Cells (lb)
0.008	41	20480	104	22.7	6.95	4.77	6.1	12.2	10.6
0.010	41	20480	104	22.7	6.95	4.77	6.1	12.2	12.85
0.012	41	20480	104	22.7	6.95	4.77	6.1	12.2	15.0

Cell Thickness (Inches)	Total (lb) 0.006 (Inches)	Total (lb) 0.012 (Inches)	Power to Weight (W/lb) @ 264 W at EOM 0.006	Power to Weight (W/lb) @ 264 W at EOM 0.012	Power to Area (W/ft^2) @ 264 W at EOM	Weight Increase Over 0.006 in. for 0.012 in. covers (%)	Power Increase 6 to 12 mil Covers at EOM (%)
0.008	51.02	57.12	5.18	4.63	2.54	11	3.5
0.010	53.27	59.37	4.96	4.46	2.54	11	3.5
0.012	55.42	61.52	4.77	4.29	2.54	11	3.5

Note: From Figure 7 - 5 the 10 Ω - cm cell would require a 1% increase in array area for the same power at EOM

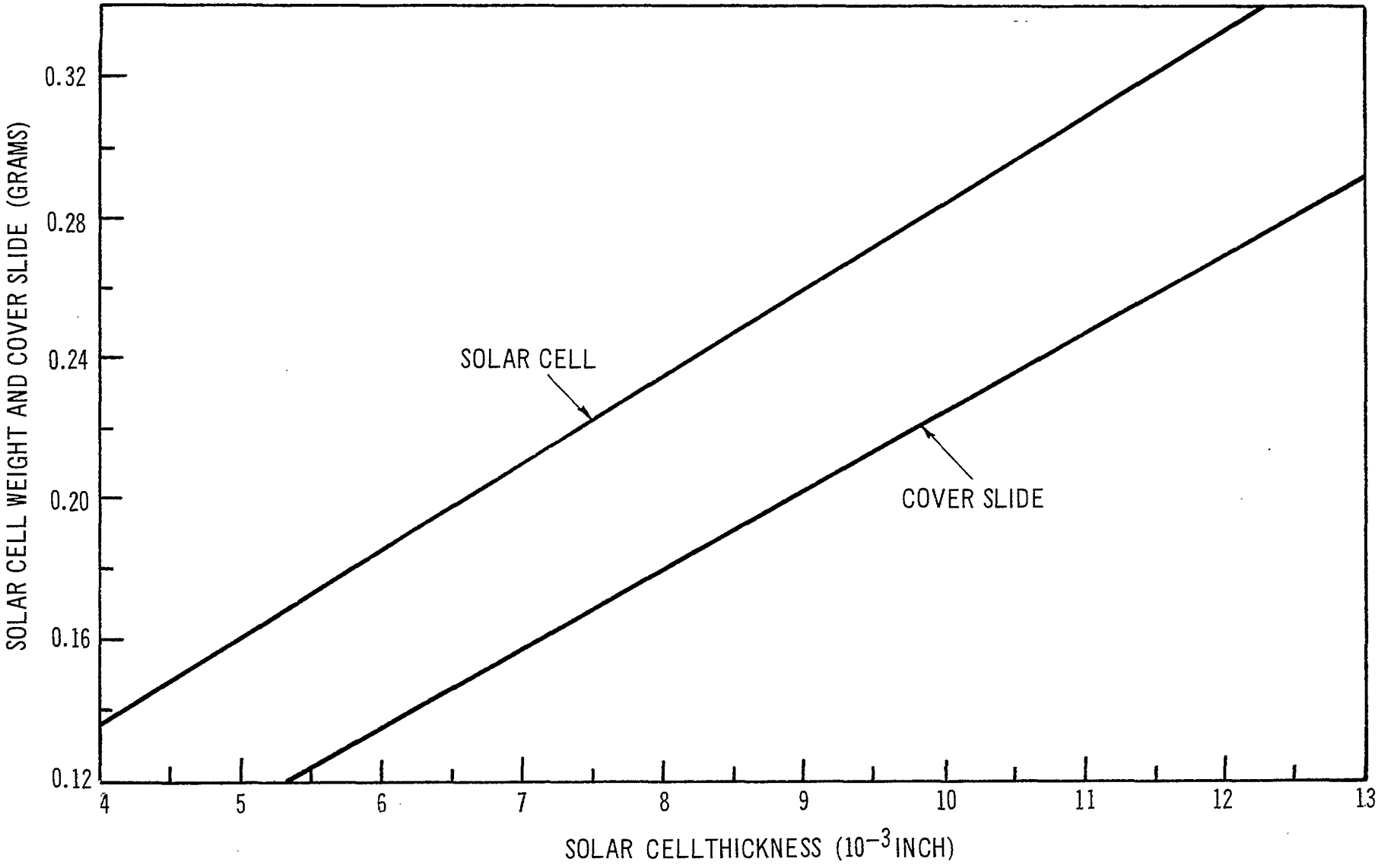

Figure 7-7 Solar cell and cover slide as a function of thickness for 2 x 2 cm cells, humidity resistant

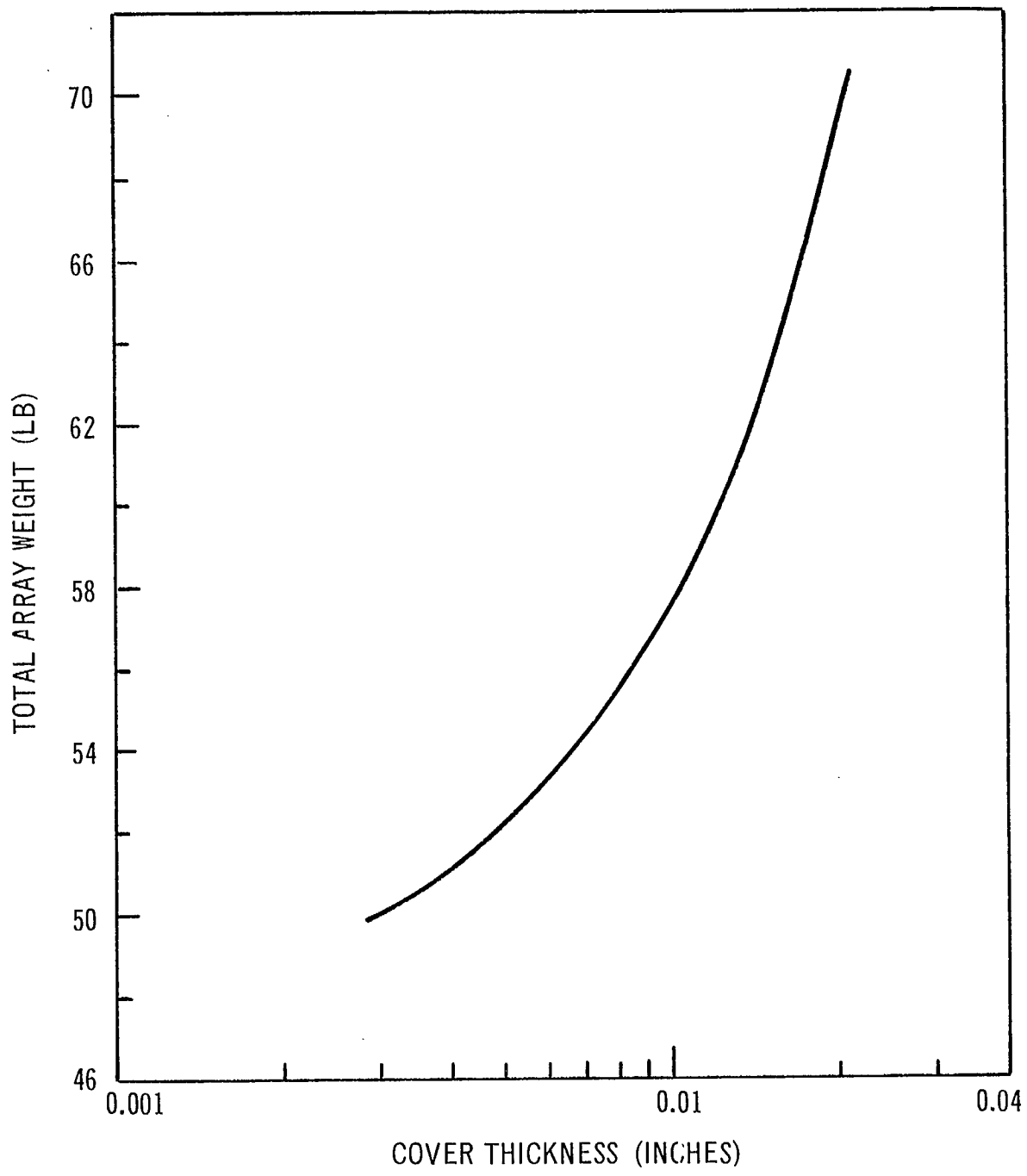

Figure 7-8 Effect of cover slide thickness on array weight for a 20, 480 cell array using 0.010 inch thick, 2 Ω/cm cells at AMO, 20°C. (Canadian Comsat Equinox EOM condition)

- Vela I through 5
- Pioneer 6 and 7
- 2029 Project
- OGO A through F
- Intelsat III
- Project 169
- Project M-35

Through the years, each of these programs has developed at TRW Systems the capability of selecting from their file of design data, those components, materials and techniques which can best satisfy the mission environment, life and reliability within the program budget.

7.3.1. Materials Considerations

In establishing the optimum solar array assembly components to be used for the mission environment and life the following has been considered:

- Cover glass material and thickness
- Cover glass to cell adhesive
- Cell interconnect material
- Solar cell type, thickness and base resistivity
- Solar cell to structure adhesive

7.3.1.1 Cover Glass

There are several alternate cover slide materials which are in use today. The list includes man-made saphire, fused silica (quartz) and micro-sheet. The most commonly used material is quartz, due to its relatively low cost and stability in the space environment over extended mission times.

As is shown in the trade off study, covers greater than 0.012 inches thick are not required for the subject mission. This figure also shows that a weight savings of nearly 14% may be realized by using 0.006 inch covers instead of 0.012 inch. The glass thickness suggested for this mission is 0.006 inches since tradeoffs clearly show that maximization of area rather than increasing cover slide thickness yields the optimum power to weight ratio.

7.3.1.2 Filters

The slides are coated with interference filters. One side contains an ultraviolet reflective filter and the other side an anti-reflective filter of MgF_2. The ultraviolet reflective filter is located on the cell side of the cover slide, and it provides protection of the cell-to-glass adhesive.

Two basic types of filters are available: blue and blue-red. While the use of blue-red filters is capable of reducing the array temperature by an estimated 5°C, the net result due to lower filter transmission efficiency is an overall reduction in power output of approximately 3 percent. This loss of output, as well as the higher cost of blue-red filters, makes them undesirable for this application. The use of blue filters is considered essential in order to prevent severe ultraviolet degradation of the adhesive used to attach the cover slides to the cells. Calculations show that a filter cut-off wavelength of 0.435 micron results in approximately 3 percent greater power loss than 0.410 micron cut-off filter. The effect on the adhesive due to the difference in cut-off wavelengths in this region is believed negligible on the basis of test results from the TRW Tetrahedral Research Satellite (TRS). Therefore, the filter selected is a blue reflective filter with a cut-off wavelength of 0.410 micron.

7.3.1.3 Glass-to-Cell Adhesive

Adhesives for bonding cover slides to solar cells are predominately organic, high-polymeric materials. The basic polymer resins are modified by the control of the molecular weight, degree of cross-linking, and the incorporation of additives to improve specific properties. Changes in the chemical balance of the adhesive may lead to drastic changes in the physical properties. In the case of optical adhesives, changes in the refrective index or spectral transmittance can considerably affect the solar cell output.

The principal adhesives of interest for space use are epoxies and silicones because of their superior ability to withstand ionizing radiation for long periods without structural changes or changes in the optical transmittance.

Photochemical decomposition results in changes in optical properties such as adhesive darkening and increased solar absorptance. A consequence of this darkening is a general increase in the solar array operating temperature with resulting reduction in the electrical output. By selecting an adhesive which has minimum absorption of ultraviolet photons, and distribution of this energy along the polymer chain, the ultraviolet degradation of optical properties can be minimized. Silicones have this property of minimum absorption and energy distribution and have thus been selected. Dow Corning's silicon type adhesive XR6-3489 has been selected since laboratory tests have shown this adhesive to have the least discoloration due to charged particle irradiation compared to other commonly used adhesives for solar arrays. Data from satellite experiments have shown that discoloration of adhesive due to charged particle irradiation has not occurred for time integrated fluxes corresponding to 3 to 5 years at communication satellite orbits.

7.3.1.4 Solar Cell

The solar cell considered as the optimum for this application is the N-on-P, 0.010 inch (nominal) thick, 2 ohm-cm type. The ohmic contacts are of TiAg covered by a thin solder layer.

a) Polarity - N-on-P cells are preferred to P-on-N cells due to the fact that they are more radiation resistant and the mission requires the use of the more radiation resistant solar cell type. A second reason for selection of N-on-P cells is their relative availability.

b) Thickness - Up to approximately 0.016 inch, increased thickness results in increased power output for non-irradiated cells. This condition is caused by the fact that electron-hole pairs generated in the bulk material away from the junction have a sufficient diffusion length to allow the minority carrier to reach the junction and thus contribute to power output. After having been subjected to charged particle irradiation, the diffusion length decreases. As a result, hole-electron pairs generated far from the junction will generally recombine before the minority carrier reaches the junction. Consequently, thinner cells which initially have a lower output than a thicker cell may have the same output after having been subjected to a certain amount of corpuscular radiation. This condition has led to the selection of a 0.010 inch thick cell for maximum power to weight effectiveness at end-of-life. In addition to the weight advantage gained, the selection of such cells results in an acceptable power output variation between the beginning and end-of-life and reasonable array manufacturability.

c) Base Resistivity - The relatively low resistivity was selected, after tradeoff studies against 10 ohm-cm cells, because of the higher end-of-life performance of the 2 ohm-cm ones. Whereas the 10 ohm-cm cells have a somewhat higher charged particle radiation degradation resistance than the 2 ohm-cm cells, the latter have higher power initially. It was found that, for the environment specified, the initial higher power output outweighed the advantage of higher radiation resistance for the 10 ohm-cm cells.

d) Area - Silicon solar cells can be obtained in 1 x 2, 2 x 2, 3 x 3 and 2 x 6 cm sizes. In general, cost per unit area of silicon solar cells decreases as the cell area increases. For the 3 x 3 cm and 2 x 6 cm cells, insufficient data, lack of experience and possible increased handling costs preclude their use at this time. 2 x 6 cm cells have been eliminated at this time due to the fact that they are not capable of being used satisfactorily with the bodymounted solar array concepts. 2 x 2 cm cells as well as 1 x 2 cm cells have been successfully used on several satellites and are expected to be the most

desirable cell for spacecraft use in the forseeable future. The cost advantage of the 2 x 2 cm cells relative to the 2 x 1 cm cells therefore dictates their use for this program. The cell is 0.788 x 0.788 inches in size and has an active area of 0.589 in ^{2} (3.80 cm^2).

e) Contact Type and Material - Many organizations have recently found that solderless cells having TiAg contacts show severe degradation when subjected to a combination of high temperature and humidity. Extensive tests (detailed in Reference 4) at TRW Systems on cells from various manufacturers have confirmed this condition to exist. Our tests also showed that completely soldered covered cells exhibit insignificant degradation as a result of such exposure.

Conventional solder covered cells are obtained by dipping the cells into solder. This approach results in unnecessarily heavy cells. The amount of solder required for the humidity protection is much less. Cells have been developed with only a thin coating of solder (but sufficient to make them humidity resistant). Such cells are considered acceptable for this mission. Array weights are based on use of these relatively lightweight, humidity resistant solar cells.

7.3.2 Interconnect Design for Temperature Cycling

An important consideration for any earth orbiting satellite solar array is the ability to survive the thermal cycling which occurs during the mission eclipse periods. Solar array reliability is affected by repeated low temperature exposure of the interconnection between cells.

There exists considerable test data on the effects of this environment on 0.003 inch thick copper, Kovar and molybdenum interconnect materials. With an expansion coeffieicnt 4 times that of silicon, copper severly stresses the point of attachment causing joint failure after relatively few temperature cycles.

Kovar, although magnetic and more expensive than copper, more closely matches the expansion coefficient of silicon. Molybdenum, with the best match with silicon, presents problems in forming and plating which is required for soldering. Molybdenum is non-magnetic but is also considerably more costly than Kovar.

The array temperatures range from 20°C during illuminated periods to -165°C during eclipse. Temperature cycling tests (reference 5) have been performed at TRW Systems to determine the optimum cell interconnect material and thickness for maximizing the life of solar arrays in this orbit. The interconnect geometry is a small U-shaped part with stress relief loops in the module series and parallel directions. The materials considered during the evaluation

program were copper, Kovar and molybdenum. Failure criteria was established as cracks, including microcracks, in the solder in the area of the interconnect joint. This criteria is based on the premise that these cracks will eventually propagate until complete separation of the silicon has occurred causing an open joint.

The number of failed joints varied greatly with material used (85% for copper versus 7% for Kovar and no failures for molybdenum after 100 cycles to -175°C). There was also a significant correlation between failure rate and temperature differential. An observation during the evaluation showed that it is very important to have oxide free surfaces which are to be joined by soldering to assure good joints. Also resulting from the program are the facts that proper interconnect plating is important and that temperature shock rate is not of great importance for the designs considered.

Specimens tested included those in a freely suspended state as well as those bonded to metallic substrates with silicon adhesives. The bonded specimens resulted in higher failure rates for those using 0.003 inch thick material due to the motion between modules and substrate. Figure 7-9 clearly shows that the percentage of failure is attributed to the fact that the stress level in the 60-40 tin-lead alloy solder is greatly reduced at the low temperature range by the extremely flexible thinner materials. It has been determined (Reference 5) that a stress reduction of 5% can reduce the failures by a factor of 5 times. This leads to the postulation that variations in solder composition may have major effects on fatigue rate. Detailed study of this area is beyond the scope of this effort.

These evaluation tests have established that Kovar interconnects of 0.001 inch thickness are capable of surviving up to 300 thermal cycles with an acceptably low failure rate. This material is suggested as the optimum for the mission.

It should be noted that for a module width of two 2 x 2 cm cells in parallel, there are six solder joints (three per cell, as shown in Figure 7-11). This triple redundancy assures that, statistically, there is a very low probability (at a high confidence level) that all three joints will fail on the same cell at the same time. Each joint is capable of carrying the full output from the cell and thus the use of the suggested interconnect design is highly reliable.

7.3.3 Low Energy Proton Protection

Recent data within the industry, from ATS-1, shows conclusively that uncovered solar cell areas are damaged by low-energy protons present in a synchronous equatorial orbit (Refs. 6 and 7). The damage is hypothesized as having a shorting effect on cells, thus causing an output degradation (23% in 1 year measured) far in excess of degradation proportional to the uncovered cell area (0.7%). The cells used were 1 x 2 cm (negative contact along the 2 cm dimension), N-on-P cells with solder covered contacts. They were covered by 0.030 inch thick fused silica cover slides. The cover application

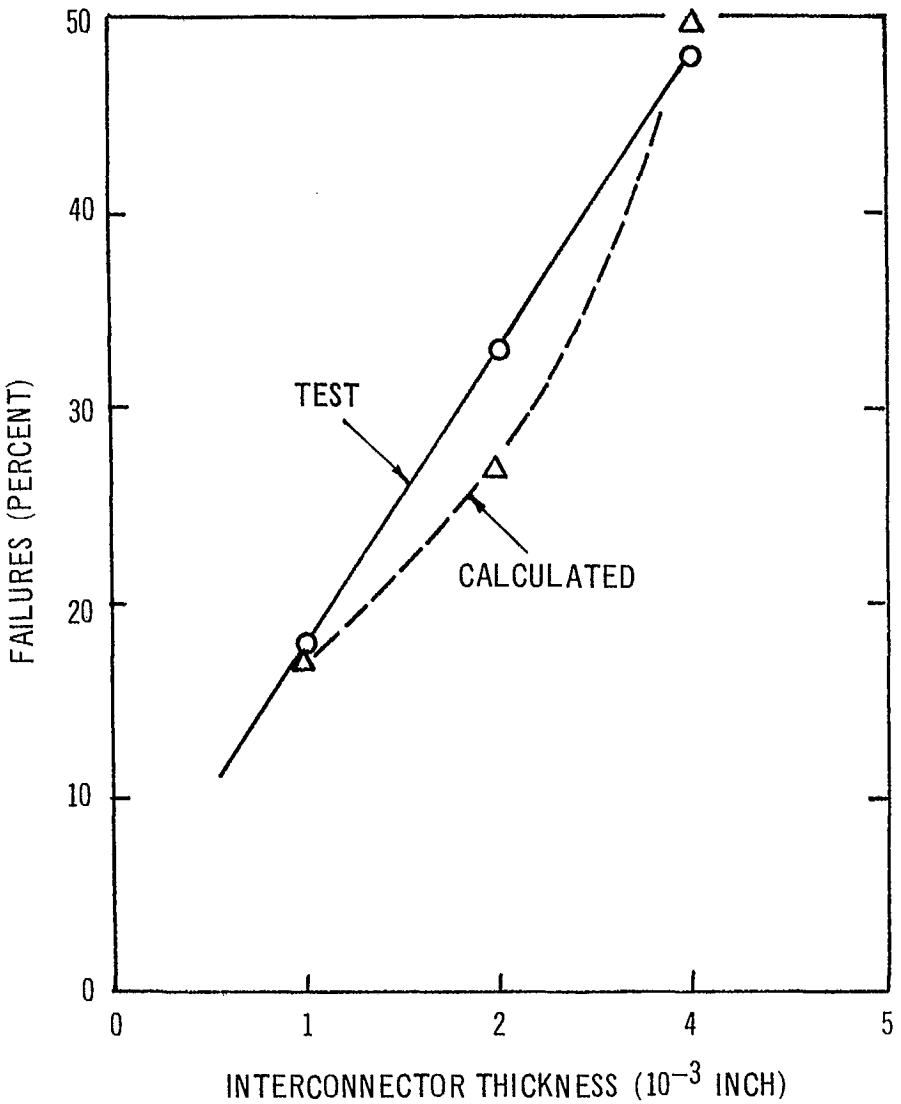

Figure 7-9 Solar cell joint failure level after 300 thermal cycles versus interconnector thickness as determined by tests and by calculations

(due to the use of conventional cover size and assembly tolerances)resulted in a 0.005 inch wide area along the 2 cm dimension remaining uncovered. Preflight degradation estimates were 2% per year. The unexpected damage was attributed to low energy (E<5 MEV) protons which damaged the exposed cell area. This assumption was confirmed by laboratory tests on similar assemblies. At 10^{13} p/cm^2 fluence levels, a softening of the I-V characteristic curve knee was observed resulting in a 25% decrease in maximum power output. This was obtained with an exposed strip only 0.003 inches wide. It was also determined that satisfactory protection from this degradation mechanism is accomplished by the application of a thin layer of material over the exposed area.

There are several methods by which the exposed cell area can be eliminated. TRW Systems has had experience with two of these methods of protection. One low cost technique is to apply at the completed panel level, a thin layer of the cover slide adhesive (selected because it will not block light from the area to which it is applied) to the area exposed when using covers having conventional dimensions. In this case the only cost is that for a small amount of adhesive and application time. The extent of UV darkening of the exposed adhesive has not been completly evaluated. However, assuming 100% darkening (no light transmission) less than 1% of the active cell area would be affected causing less than 1% reduction in output. Further evaluation of this method is considered warranted.

Another protection method is to use cover slides which are sized to cover all the active area of the cell completely, leaving no edge exposed for proton damage. Although this method gives a positive protection with no loss of active cell area it is also considerably more expensive than the first approach due to tighter tolerances on cover slides as well as possible increased attrition to these larger covers during array assembly and handling.

With cost and high confidence in the degree of protection as criteria for selecting a method, the optimum choice at this time is considered the addition of adhesive to the complete array exposed cell areas.

7.3.4 Alternative Module Design

The proposed module design satisfies completely the mission requirements, is flexible and is one with which TRW Systems has considerable experience. This overlapped cell concept gives additional protection to the solar cells from low energy protons in that the normally exposed solar cell area between the N contact and the cell edge is covered by the joining series cell.

There is one adverse factor in using this design which is eliminated by the use of the alternative flat module (no overlapped cells). This factor is the ease of cell replacement prior to launch and subsequent to being bonded to the structure. The overlapped design presently requires removal of the

complete 8-cell module for replacement of from one to eight cells and although experience has shown this requirement to be infrequent the fact that 8 cells are involved may have some program cost impact. Flat modules lend themselves readily to individual cell replacement at any stage of assembly. A complete cost tradeoff between the two module alternatives including replacement history, program delays, etc. is considered beyond the scope of this analysis, but may be an area which could be evaluated during the early design stages of the program. Use of the flat module design will cause, due to the relatively low packing efficiency of the cells, a weight penalty to the array by requiring a longer cylinder length for the same number of cells, to allow for the area now overlapping series cells. The spacecraft diameter would remain unchanged. No additional weight to the electrical components would be involved but the increased structure area could be prohibitive.

Unless a cost tradeoff shows significant cost savings for the flat design it is presently considered that the proposed design is the optimum for this mission.

7.4 DESCRIPTION OF THE SOLAR ARRAY

This section concludes the analysis by describing the design and construction of the array and discusses its electrical output for three seasons at the beginning and end of the 5 year mission.

7.4.1. Functional Description

The solar array consists of 20,480, 2 x 2 centimeter silicon solar cells, with 0.006 inch fused silica cover slides, body mounted on a cylinder 79.00 inch long by 56 inch in diameter. The entire cylinder is covered with cells except for two 2 inch slots running the length of the cylinder and located 180 degrees apart, and thirty spaces 0.68 inch by 1.58 inch reserved for structural and protective cover attachments. The cells are divided equally among sixteen panels (1280 cells each). Each panel is further divided into ten strings (five string-pairs) each string being 64 cells in series by 2 cells in parallel.

Blocking diodes are connected in series at the positive end and at the tap of each string-pair to isolate the string-pair from the output bus during the periods of darkness.

Each string is formed from sixteen eight-cell modules (4S x 2P), connected in series to form a 64-series-cell string. The combination of modules and their relative position for each string differs depending upon the position of the string relative to the holes for panel and protective cover-mounting provisions. All cell and module interconnections within a string are redundant.

The triple redundancy between series connected cells results in very high reliability. The manufacturing processes employed for assembly subjects the cells to minimum stresses and provides for 100 percent microscopic inspection by the operator. The above facts in conjunction with the high built-in interconnection redundancy account for the high reliability of the proposed solar array. An extensive statistically designed test program involving extended temperature cycling (discussed in section 7.3.2.) over a wide temperature range has shown the recommended assembly method to provide joints of high inherent strengths.

Negative, positive and tap connections are made with redundant feed-through connections at the back of the panel. The feedthrough connections are backwired to turret terminals on a pre-fabricated terminal board assembly bonded to the back of the panel near the equipment platform. For fabrication simplicity, the feedthroughs are soldered to the module during panel assembly, thus limiting the module configuration to one type.

Redundant isolation diodes are utilized to connect the positive output of each illuminated solar panel power bus and the tap point to the main control bus. These diodes provide low resistance paths for current flow from the illuminated strings of the solar array while preventing leakage currents through the non-illuminated panels. At the positive, negative and shunt tap terminals of each string, redundant feed-through connectors extend through the substrate to the panel back wiring.

TRW Systems has developed methods (discussed in Section 7.3.3.) to assure that the solar cells will have full protection from low energy proton radiation. These protective methods have been thoroughly evaluated by tests and the applicability to normal fabrication conditions have been proven on other production projects.

7.4.2 Schematic Diagram

The schematic diagram of each pair of solar cell strings is shown in Figure 7-10. Each solar panel has five such string-pairs, i.e., a total of ten strings per panel. All panels are identical.

The panel positive, tap and negative terminals are each wired in parallel with the other respective terminals within the spacecraft wiring harness to form positive, tap and negative spacecraft bus connections.

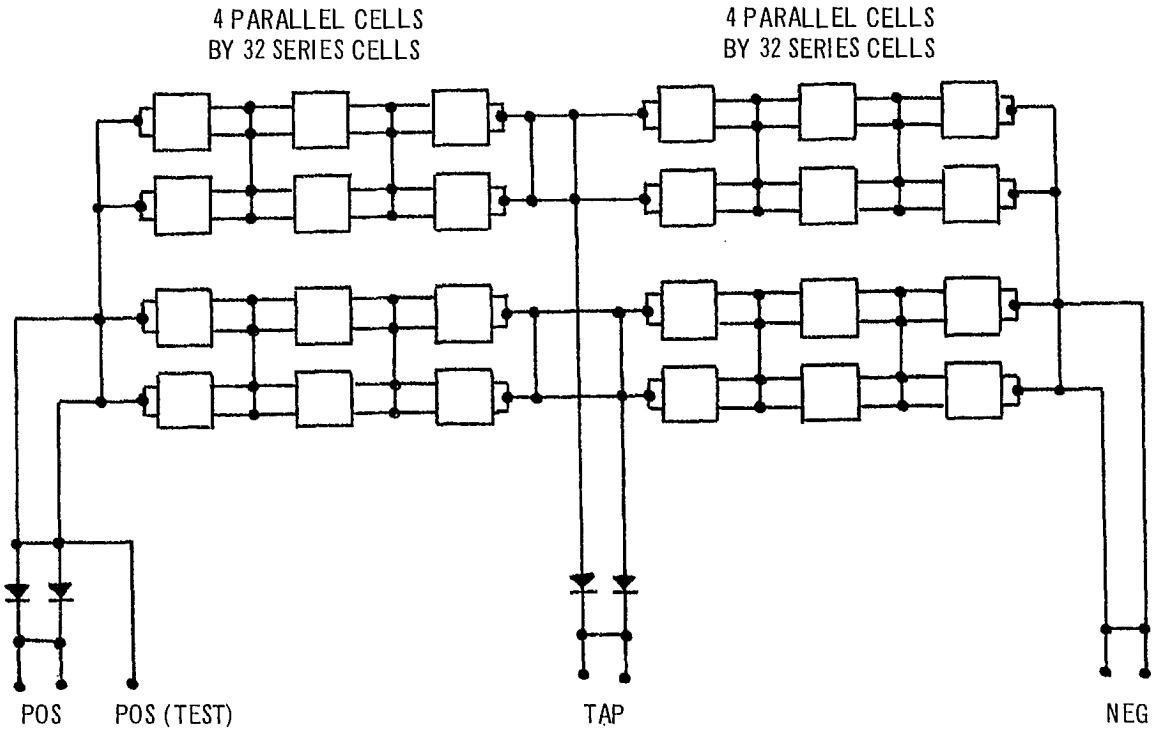

Figure 7-10 Schematic Diagram for Solar Cell String Pair

7.4.3. Description of Components

Solar panel components are as follows: -

Solar Cell

Type	N-on-P, silicon
Size	2 x 2 centimeters x 0.010 inch thick
Front contact	Solder covered, titanium silver
Back contact	Zone soldered, titanium silver
Grids	Six, solder-free
Resistivity	2 ohm-cm nominal
Electrical output	AMO efficiency = 10.75 percent minimum at 28°C (11% average)

Solar Cell Covers

Type	Fused silica, corning Glass No. 7940
Size	2 x 2 centimeters x 0.006 - inch thick
Cut-on wavelength	410 + 15 nanometer
Coatings	Anti-reflective and ultraviolet reflective

Temperature Sensor

Specification	PT4-14-1400
Temperature range capability	-150°C to +125°C

Other

Diodes	PT4-2276
Terminals	SPO-132-1
Connector	PT2-62
Wire	PT3 - 38

7.5 SOLAR PANEL CONSTRUCTION

The solar panel consists of solar cell modules cemented directly to panel substrates consisting of two face sheets bonded to aluminum honeycomb. The adhesive used to mount the solar cell modules to the solar panels is a room temperature vulcanizing silicone which allows for differential thermal expansion between modules and substrate. The solar panels will be subjected to temperature variations over the range of +20°C to -129°C.

The solar array utilizes one module configuration (2 parallel by 4 series cells as shown in Figure 6-22). The cells are overlapped as shown in this figure using interconnector strips of 0.001 inch Kovar. The interconnector strip provides interconnection between the two parallel connected cells as well as connection to the next pair of series connected cells. At the end of each module special interconnections are used. On the N terminal a formed ribbon is used and on the P terminal, a special interconnector with tabs designed to fit the N terminal, a ribbon of the adjacent module is used. This interconnection scheme provides highly flexible modules which may easily be attached to a curved surface and is similar to the design used on the Intelsat III and Pioneer Spacecraft solar cell modules.

Every two strings (64S x 2P) are bussed at each end and at the tap to form a string-pair. The panel specification provides for electrical output from each string-pair to meet a minimum output requirement. All wiring is made at the back of the panel except for the interconnection of modules at the end of each row. Such interconnections are short wires since the modules to be connected are adjacent. All sixteen panels are identical except two which are equipped with a temperature sensor located on the rear surface. The temperature sensors are located such that when used in conjunction with thermal analysis data, the array temperature can be ascertained during launch and orbital conditions. The output from each panel will terminate in a 37-pin approved connector located on the rear of the panel to plug into the spacecraft wiring harness. This harness will interconnect the positive, tap, and negative connections between the panels and power bus.

7.5.1. Module Design and Fabrication

The overlapping module design is recommended to achieve maximum power output per unit area, and because of its ability to withstand the temperature extremes.

Figure 7-11 shows a typical module with eight 2 x 2 cm cells in the overlapped configuration. The cells are interconnected with small U-shaped 0.001 inch thick, tin plated Kovar interconnectors. Therefore the module is flexible and self-supporting. A Kovar ribbon is soldered across the exposed

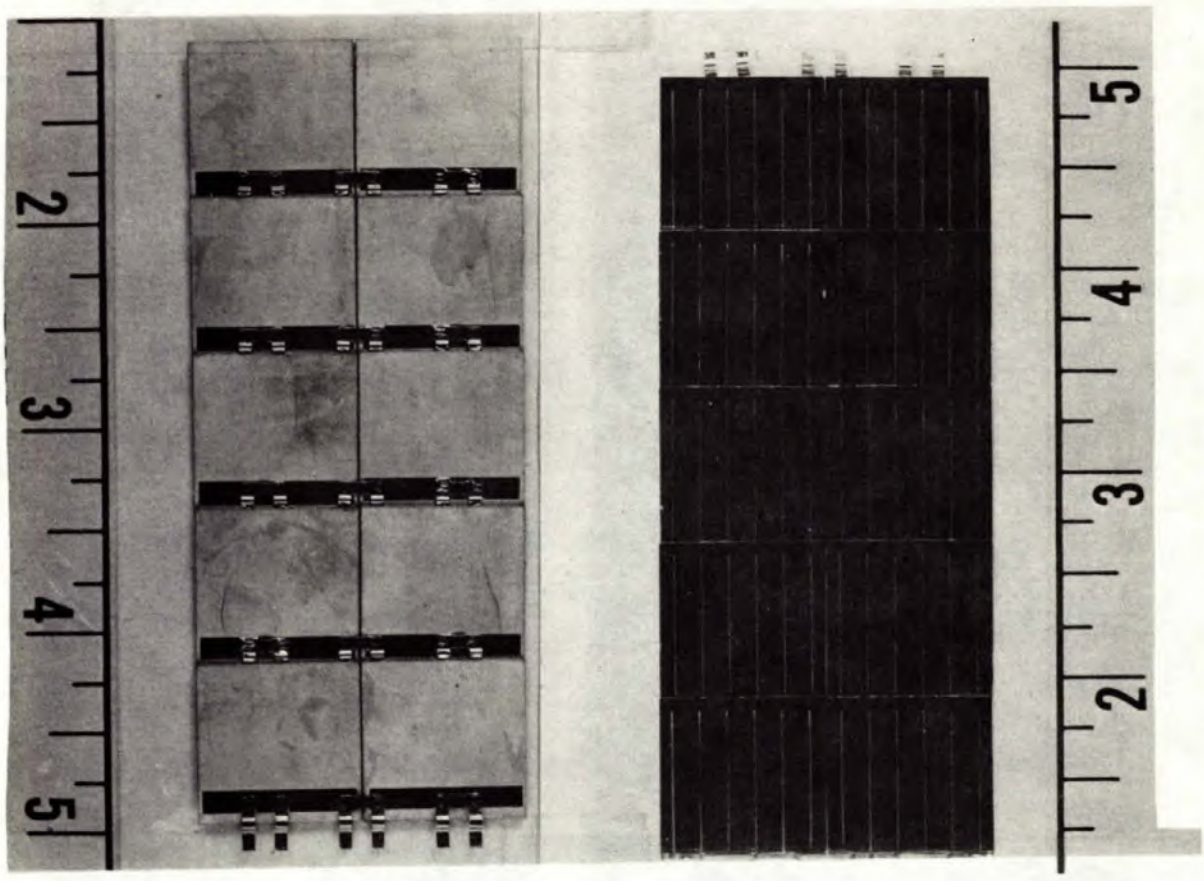

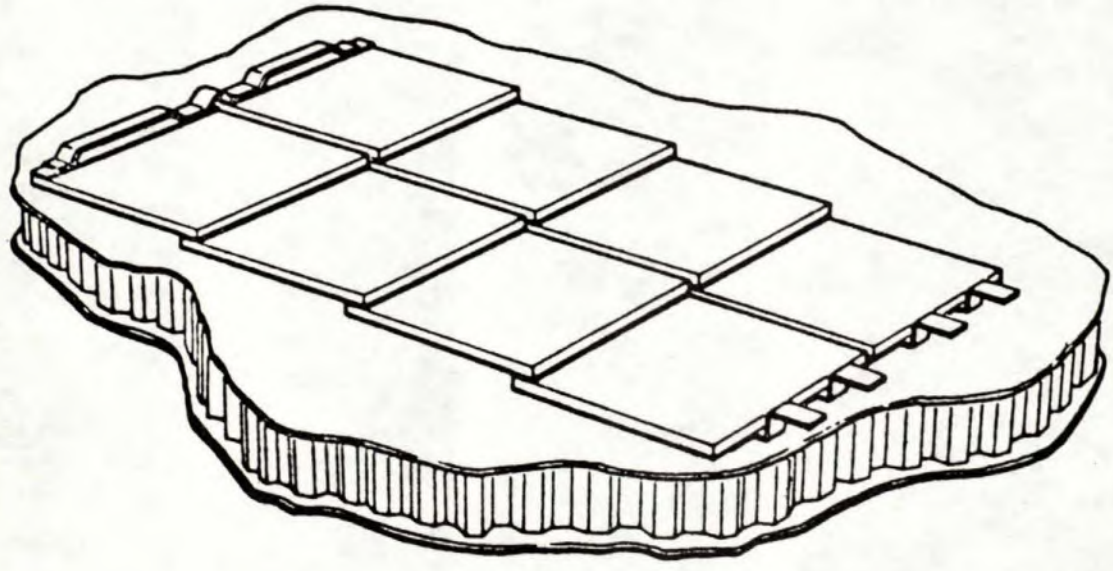

Figure 7-11 Solar Cell Module (for illustration purpose only)

top collectors of the first 2 cells and 4 small tabs extend from below the last 3 cells at the other end of the module, which provide for redundant interconnection between series modules.

The module is assembled in a special positioning fixture where the U-shaped tabs are soldered to the cells by applying pulse heating (resistance soldering). This assembly method not only allows the use of simple inexpensive fixtures but also reduces the solar cell electrical average assembly losses considerably, since the cell is locally heated only where the cell and interconnects are joined.

The equipment used to solder the cell interconnects is the Development Associates Company's VTC resistance soldering machine. A thermocouple located between the parallel electrodes in employed for temperature sensing. The heat applied to an assembled connection is controlled on the power supply by presetting the temperature current rise and fall time.

The solar cells and interconnects to be joined are held in a fixture which positions the parts in relation to each other. The electrodes are placed on the interconnect to be soldered to the cell by depressing a footswitch which activates the power supply after the pre-set electrode pressure is reached. The actual resistance soldering operation takes place under a 10 power stero microscope, where each individual solder joint is inspected during the solder operation. This makes it possible to perform any possible rework at the lowest assembly level.

The philosophy adopted in the module fabrication is to pre-glass the cells prior to the module assembly, in order to provide maximum protection of the solar cell i.e., allowing the cover slide to overlap the negative collector strip, as well as the three remaining edges of the cell.

7.6 SOLAR ARRAY ELECTRICAL CHARACTERISTICS

The predicted electrical characteristics of the array at the beginning and the end of life are stated in Table 7-6 for equinox, winter solstice, and summer solstice.

Figure 7-12 shows array power at 29 volt bus voltage for equinox, winter solstice and summer solstice, plotted as a function of operating time. The data presented in this figure are based upon the power averaged over a complete revolution of the spacecraft. Plots of minimum current and power versus voltage during equinox and summer solstice are presented in Figures 7-13 and 7-14 for year 0 and year 5.

Table 7.6
Electrical Characteristics of Solar Array at the Beginning and End of Mission

Condition	Equilibrium Temperature (°C)		Distance from Sun (Au)	Sun* Angle (Deg.)	Minimum Power at 29V		Minimum Short-Circ. Current		Open-Circuit Voltage		Current at 29 V Average	
	0 Yr. (Min)	5 Yr. (Max)			0 Yr. (W)	5 Yr. (W)	0 Yr. (amp)	5 Yr. (amp)	0 Yr. (V)	5 Yr. (V)	0 Yr. (amp)	5 Yr. (amp)
Equinox	10.0	19.5	1.0000	90	329	263	11.64	10.04	37.5	34.5	11.35	9.0
Winter Solstice	8.3	17.2	0.9837	66.5	313	252	11.04	9.48	37.5	35.0	10.79	8.68
Summer Solstice	1.5	12.2	1.0163	66.5	294	240	10.29	8.82	38.5	35.5	10.13	8.27

* From satellite spinaaxis

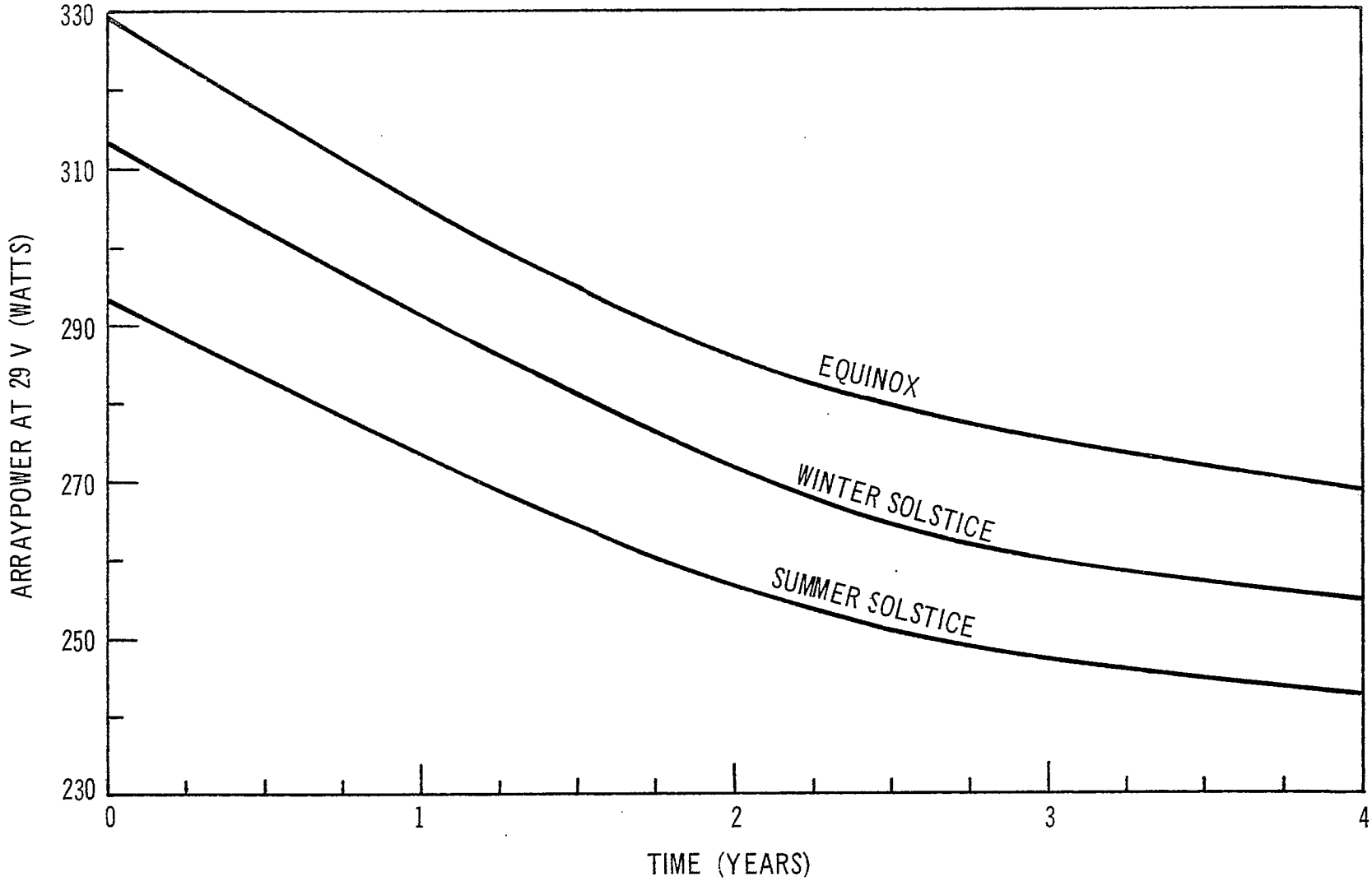

Figure 7-12 Solar Array Power at 29 V for Three Seasons

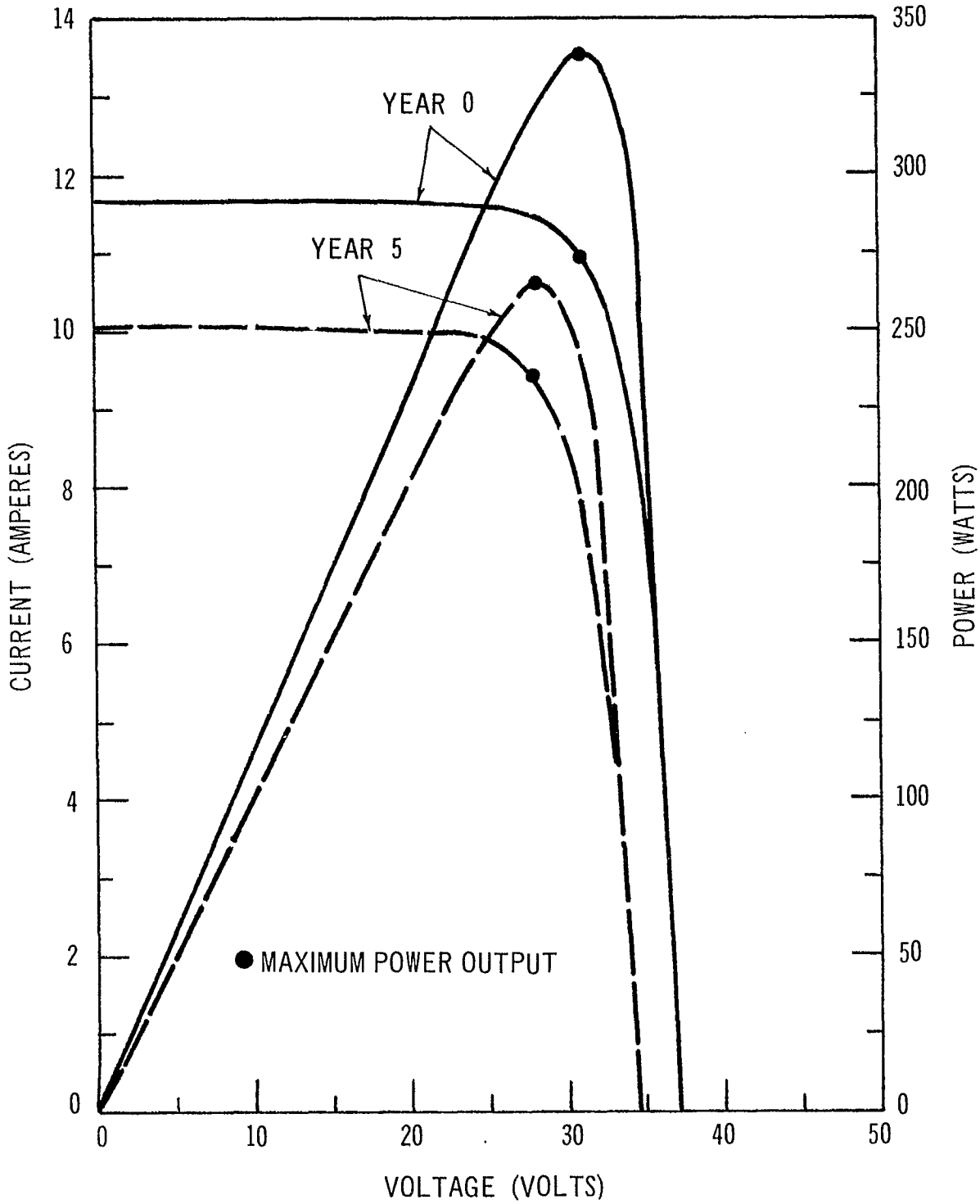

Figure 7–13 Solar Array Performance at Equinox for beginning of life and end of mission, using 2 Ω/cm cells. (Nominal case using minimum cell characteristic).

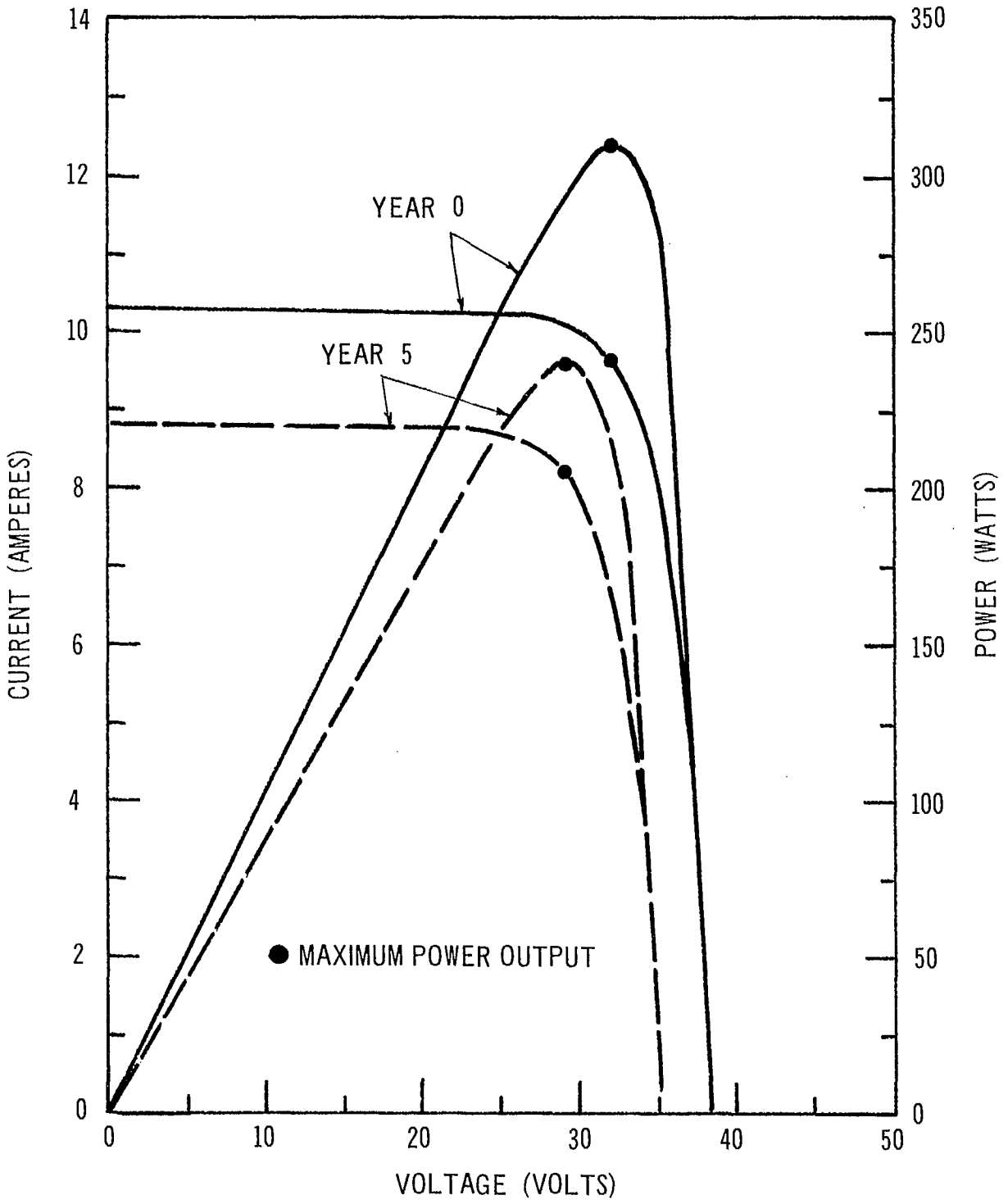

Figure 7-14 Solar Array Performance at Summer Solstice for beginning and end of mission, using 2 Ω cm cells. (Nominal case using minimum cell characteristics)

The solar array performance calculations were made with the aid of TRW Systems' computer program which allows the following factors to be taken into account:

a) Temperature of each illuminated solar cell string.
b) Solar cell short-circuit current degradation due to charged particles irradiation.
c) Open-circuit voltage degradation due to charged particle irradiation.
d) Effect of angle of incidence on solar cell output and the variation due to charged particle irradiation.
e) Temperature coefficient of solar cell short-circuit current and its variation due to charged particle irradiation.
f) Temperature coefficient of the solar cell open-circuit voltage and its variation due to cell temperature.
g) Adhesive transmittance degradation due to charged particle and ultraviolet irradiation.
h) Coverglass transmittance degradation due to charged particle and ultraviolet irradiation, and micro-meteorite erosion.
i) Chromatic response shift of solar cells due to charged particle irradiation.
j) Distance to sun.
k) Output losses of solar cells due to cover glass installation
l) Solar cell output losses due to soldering
m) Power losses due to isolation diodes
n) Operation time
o) Charged particle effects

The values for these factors, which include both time dependent and time independent variables, are those discussed in Section 7.2. These values are considered to be a realistic assessment of the degradation of a solar array from its assembly through the end of mission and are based on the latest information available.

7.6.1. Diode and Wiring Losses

Maximum series voltage drops between the photovoltaic array and the spacecraft are:

Blocking diode drop	0.82 volt
Panel wiring	0.18 volt
Array wiring	0.14 volt
	1.14 volt

7.6.2 Array Output Characteristic.

The array output characteristic is based on the minimum cell output characteristic as presented in Table 7-7. Actual array output is expected to be 2% higher when the average cell characteristic is considered.

Table 7-7-Minimum Electrical Characteristic of Solar Cell (AMO, 28°C)

Voltage (v)	Current (mA)
0	128
0.1	127.99
0.2	127.99
0.3	127.93
0.40	127.04
0.42	126.4
0.44	125.1
0.46	122.9
0.475	120
0.48	118.1
0.50	111.9
0.52	99.4
0.54	79.3
0.56	43.35
0.5715	0

7.6.3 Array Output Probability Prediction

The solar array output calculations have been made for the nominal level. This means that the median value of each degradation factor was used, resulting in a 50% probability that the predicted output will actually be achieved.

Reference 8 describes in detail a technique by which the power output at any desired probability may be determined. This technique utilizes the Monte Carlo method of selecting the magnitude of the degradation factors. The output is then calculated at the particular operating voltage being considered.

Referring to figure 7-15, the value of K (K=Vop/Voc=29/34.5) is approximately 0.85 for this array at equinox after 5 years. The array output at 90% probability is therefore 0.925 times the nominal value.

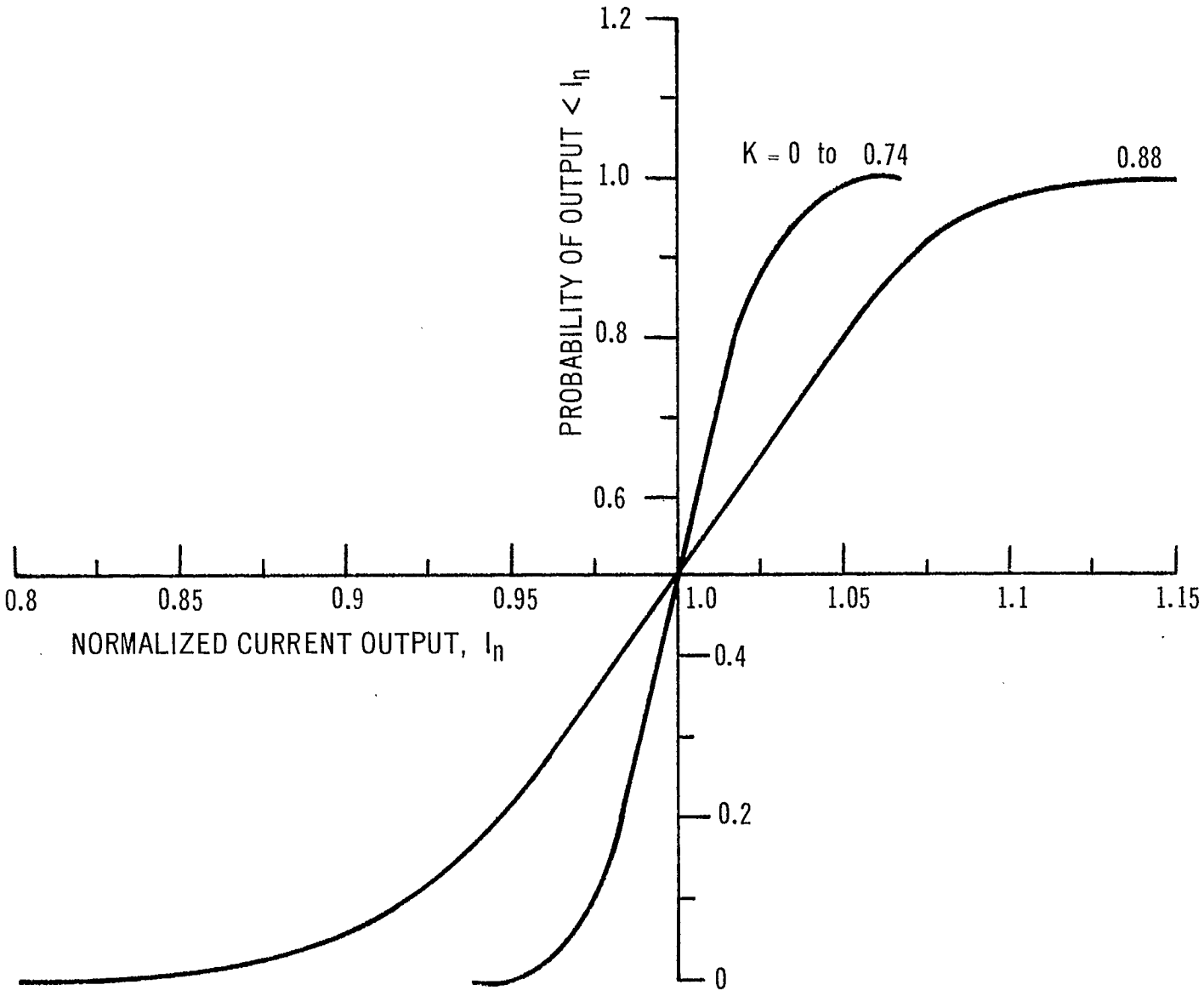

Figure 7-15 Dimensionless current output distribution over a range of normalized voltages

8. ELECTRICAL INTEGRATION SUBSYSTEM

The Electrical Integration Subsystem serves as an integrating element for all other electrical subsystems of the spacecraft and provides a common interface for subcontractors' black-box equipment. The Electrical Integration Subsystem is designed to:

- Condition and distribute a portion of the commands.
- Condition and distribute a portion of the telemetry.
- Control Ordnance.
- Control and distribute electrical power.

The Electrical Integration Subsystem consists of two major parts:

- The Electrical Integration Assembly (EIA).
- The Interconnection Harness Assembly.

8.1 ELECTRICAL INTEGRATION ASSEMBLY

The Electrical Integration Assembly (EIA) integrates the electrical subsystem equipment located on the two spacecraft platforms. The functional requirements to be met by the EIA are:

- Command implementation of power switching and ordnance commands.
- Functional control of spacecraft ordnance devices.
- Test Point access for a portion of the command functions, spacecraft power monitoring, and ordnance circuit testing.
- Conditioning of internal command status for diagonistic telemetry.
- Signal conditioning for thermal and pressure transducers.

A functional block diagram of the EIA is shown in Figure 8-1.

8.1.1 Mechanical Characteristics

The EIA is designed as a modular, unit slice package. The circuitry is divided into five logic slices that are six inches wide by seven inches high by one inch thick. Overall dimensions of the EIA are 7 x 7 x 5 inches. The weight of the EIA is approximately six pounds. Each slice houses a double sided etched circuit board used to interconnect discrete components and cordwood welded modules.

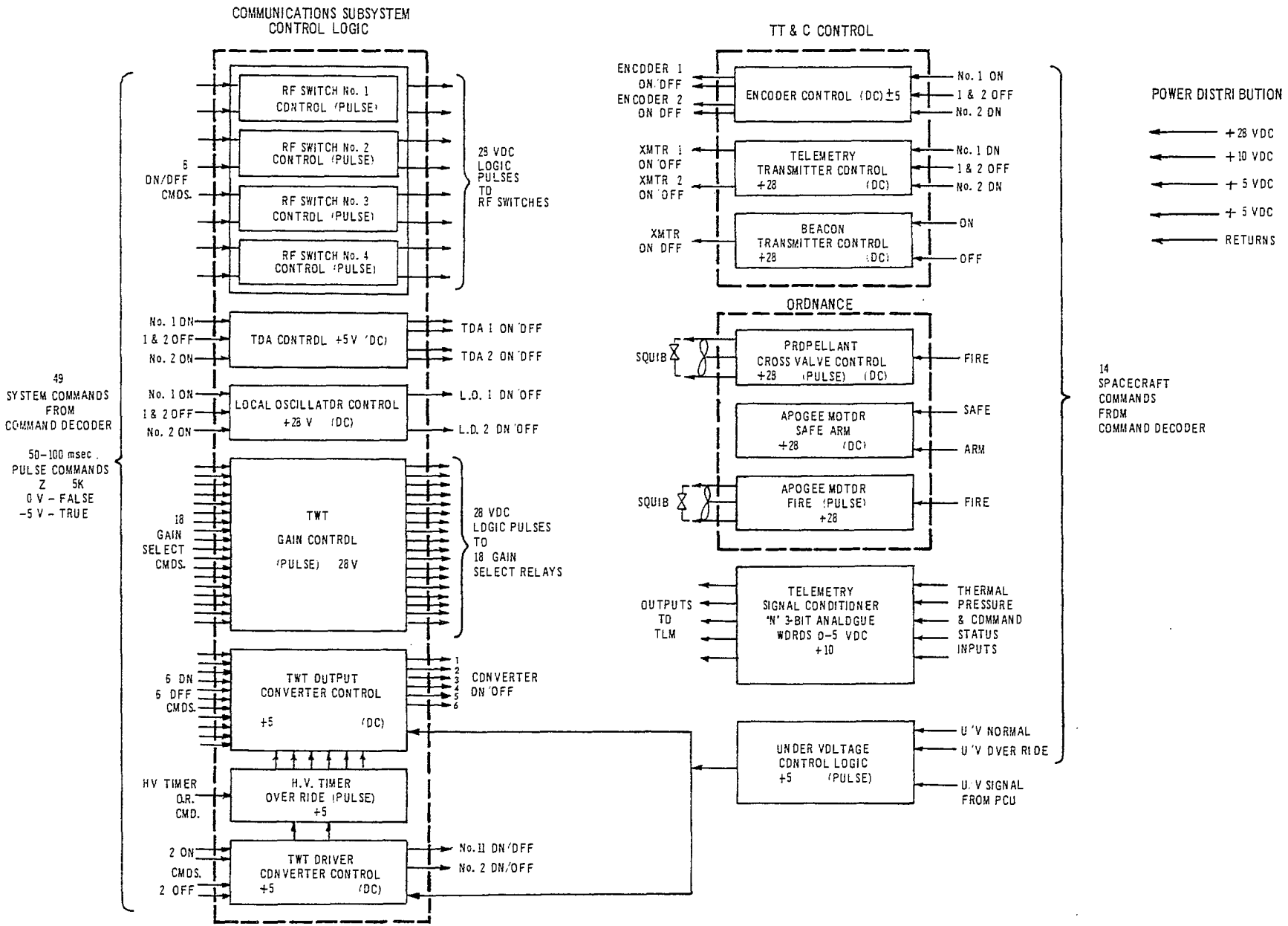

Figure 8–1 Functional Block Diagram of EIA

8.1.2 Electrical Characteristics

All command implementation takes place in response to a discrete impulse received from the Command Decoder. The discrete pulses, 50 to 100 milliseconds wide with a 5 volt amplitude, are used to provide the necessary command format, either an impluse for a required duration or a DC static command.

Cross strapping of the redundant Command Decoders takes place within the EIA input circuitry. Diode or gates are used to prevent total system loss due to the failure of one Decoder. The Command Decoder/EIA interface is performed with T^2L integrated circuits selected from high reliability families of available devices.

Command outputs are designed around discrete transistor circuits to preclude interface failure caused by capacitive surge currents or transient voltage spikes appearing on an interface line. Discrete transistors used in the EIA have been selected from high reliability silicon transistor families.

Electromagnetic interference (EMI) shielding is provided for in the EIA by EMI shield enclosures in each slice on an "as required" basis. The ordnance functions, for example, are contained in one slice that has all necessary power and RFI filtering. Electrical power used by the EIA is received in one slice, filtered to meet electromagnetic compatibility (EMC) requirements and distributed to the balance of the slices. Power ground is treated in a similar fashion so that the EIA structure is not relied upon for power returns.

8.1.2 Design

Wherever possible, command switching has been implemented by solid state switches rather than relays. Solid state switches have the advantage of not being vibration sensitive and interface with the Command Decoder outputs directly. Buffered interfaces are not required. An integrated circuit, type SH2002, has been selected as the basic logic block for all solid state switches. This IC, a 10 lead 3/8 inch square flat package, is compatible with T^2L Logic and is constructed of chips demonstrated to be reliable for use in a five year program.

The output switches have been designed to consume no power in the standby or non-command mode. Ordnance devices are controlled with electro-mechanical relays to satisfy range safety requirements for Safe/Arm functions.

8.2 INTERCONNECTION HARNESS ASSEMBLY

The spacecraft interconnecting harness distributes electrical power and signals to all subsystem electronic equipment. The harness will consist of multiple-strand insulated wires soldered or crimped to rectangular subminiature connectors. The routing of the harness will be developed on the spacecraft engineering model.

All harness connectors are potted with semi-flexible compounds to provide wire-to-wire insulation resistance, to protect against entry of contaminants which can cause shorting or arcing, to retain contact float characteristics and to provice increased reliability and stress relief. The cable uses solder type and crimp type "D" series subminiature and circular miniature connectors throughout.

Shield ground terminations at cabling connectors will utilize the following processes:

- Terminate short shield pigtails to a grounding bracket (halo-ring) that is attached to the "D" series subminiature connector.
- Terminate exposed shields to a connector RFI back shell with conductive epoxy.
- Terminate exposed shields to the connector shell or standard back shell by the use of conductive epoxy.

8.2.1 Interface Description

The function of the harness assembly is to interconnect the various spacecraft subsystems electrically. The major cabling functional interfaces are described below.

8.2.1.1 In-Flight Jumper

The in-flight jumper connector allows opening of the lines between the battery and the Power Control Unit (PCU) to provide power to the main power bus from the spacecraft electrical test equipment during ground operations. A second function is to open the lines between the power shunt and the PCU during ground operations.

The connector is also removed when the spacecraft bus must be de-energized. During system test, bus power measurements are made at this connector interface. The in-flight jumper connector consists of a mated pair of D subminiature connectors.

8.2.1.2 Ordnance Connector

The ordnance connector is designed to meet ETR range safety requirements and will enable testing of the ordnance circuitry up to the ordnance device. One mating connector will provide a short circuit of the ordnance firing circuit and a point to simulate an ordnance load for system testing of the ordnance commands during ground operations. A second mating connector will be used for flight and will connect the EIA to the ordnance devices to allow arming. A sketch illustrating the ordnance test connector concept is shown in Figure 8-2.

8.2.1.3 Umbilical Launch Vehicle Connector

Additional electrical interfaces with the power subsystem and launch vehicle will be accomplished by means of an umbilical launch vehicle connector. The umbilical connector is a "zero entry" quick release type connector and provides electrical access to the spacecraft from the launch vehicle and launch facility. Among the functions to be accomplished through the connector are battery charging during launch operations. This connector is the only electrical interface between the spacecraft and the launch vehicle.

8.2.1.4 Ordnance

The Ordnance Harness will utilize twisted shielded wire to maintain electrical balance and minimize inductive pick-up. Continuous circumferential shielding will be used, grounded to the structure at both ends and containing no electrical discontinuities.

8.2.2 Separation Switches

Separation switches are located on the spacecraft side of the separation interface with the Booster. The normally closed switches are held in the open position when the spacecraft is mated to the adapter by an angles tab on the adapter section. The two switches are wired in parallel and are used to initiate the separation sequence. The redundant switches will be located 180° from each other at the separation plane.

8.2.3 Wiring Integration Design Engineering (WIDE)

The interconnection of the spacecraft systems will be controlled by a computer technique called WIDE (Wiring Integration Design Engineering). This technique provides the continuity of control needed from interface definition through design, fabrication, and test to ensure that all equipment operates with complete compatibility.

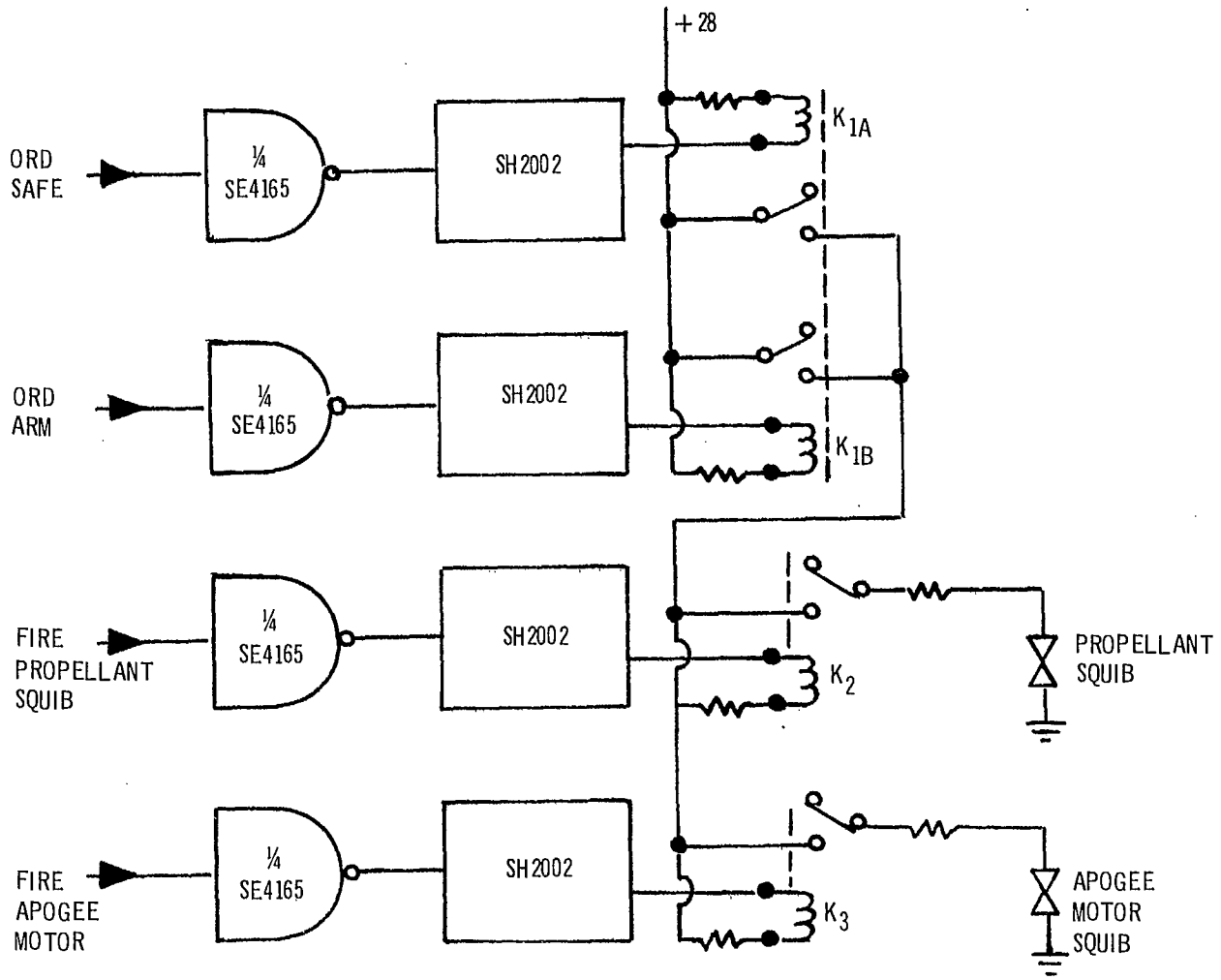

Figure 8–2 Ordnance Implementation

In using this concept, each designer fills out a standard interface definition for which lists every external electrical signal to his equipment with its characteristics. This information is then used as input data to a computer. The computer automatically performs error detection operations which ensure that the characteristics and wiring of interfacing signals between any two units are compatible. Any errors detected are listed on computer printouts, which are then studied in detail and resolved.

A second type of computer printout is generated and this is used directly in the fabrication of the harness. The computer also uses this information to provide input data to an automatic circuit tester for acceptance testing of the harness.

8.2.4 Fabrication and Test

The fabrication of the spacecraft harnesses will be accomplished utilizing a full size, three-dimensional fabrication fixture. The use of this fixture will ensure proper routing and fit of a completed harness assembly into the spacecraft.

Electrical acceptance testing of the completed harness assemblies will be accomplished using the flexible automatic circuit tester (FACT). FACT is a pre-programmed data card controlled means of automatically testing cabling. The WIDE data card format has been developed to be compatible with FACT requirements.

Environmental acceptance testing of the harness assemblies will be accomplished during the spacecraft testing.